Role of the ribosomal DNA repeats on chromosome segregation of *Saccharomyces cerevisiae*

A dissertation presented in fulfillment of the requirements for the degree of

Doctor of Philosophy
in
Genetics

at Massey University, Albany
New Zealand

Daniela M Quintana Rincon

2016

[blank page]

ABSTRACT

Chromosome segregation is a highly conserved process that progresses with great accuracy. Failure of proper segregation can lead to genetic disorders, such as Down syndrome in humans. Interestingly, segregation errors found in human genetic disorders and associated with spontaneous abortions or stillbirths are frequent in the chromosomes containing the ribosomal RNA gene repeats (rDNA). The rDNA is essential for cell viability and growth as it encodes ribosomal RNA, a major component of ribosomes. In yeast, the rDNA locus has a unique cohesin-independent cohesion mechanism to hold sister chromatids together before separation, and behaves in unique ways with respect to replication, recombination and transcription. These rDNA-specific features may promote a chromosome segregation mechanism distinct from the rest of the genome. Therefore, the aim of this thesis was to test the hypothesis that the rDNA affects chromosome segregation.

To test this hypothesis I focused on mitotic chromosome segregation, and used the model genetic organism, *Saccharomyces cerevisiae*. *S. cerevisiae* offers many advantages for testing this hypothesis, including its tolerance to aneuploidy and systems that have been developed to genetically manipulate the rDNA. I developed and optimized a chromosome loss assay (CLA) that measures the rate of chromosome loss during mitosis in *S. cerevisiae*. I modified a number of strains that had alterations associated with the rDNA, including strains deleted for the chromosomal rDNA repeats, with a reduction in rDNA copies, and with the rDNA translocated to a different chromosome, with specific phenotypic markers for detection of chromosome loss events. I then tested the chromosome loss rates of these strains using the CLA. My results demonstrate that the rDNA affects mitotic chromosome segregation fidelity at two levels. First, the rDNA increases the segregation fidelity of the rDNA-containing chromosome, defining a local chromosome segregation role for the rDNA. I found that this local effect is mediated by the rDNA binding protein Fob1, and I propose three potential mechanisms for how Fob1 mediates this role: (1) through establishment of rDNA recombination-intermediates that may help to stabilize the long rDNA locus; (2) through recruitment of condensin to establish intra-chromatid linkages that promote timely condensation of sister chromatids; or (3) through recruitment of a silencing complex to achieve an appropriate rDNA chromatin state for chromosome segregation. Second, I show that the rDNA has

a global effect on chromosome segregation fidelity, with rDNA deletion or reduction in rDNA copies influencing the segregation of many or all chromosomes. Curiously, heterozygosity of rDNA state, regardless of what states are present, confers wild type missegregation rates. I rule out trivial explanations for this global effect, and instead propose that the rDNA affects segregation through changes in nucleolar structure and overall nuclear organization that impact spindle polarity and thus the fidelity of chromosome segregation. Together, these results define a new role for the rDNA in facilitating chromosome segregation, and one that acts at two different levels. This work provides insights into a novel beneficial role of the rDNA in chromosome segregation of *S. cerevisiae,* and the conserved mechanism of chromosome segregation across eukaryotes suggests the rDNA may play similar roles in more complex organisms. It will be interesting to determine if the rDNA also has beneficial role in meiosis, where the rDNA has been associated with missegregation.

ACKNOWLEDGEMENTS

First and foremost I would like to dedicate my thesis to two special women whom I have lost but have made a huge impact in my life: **Abu y Tía Ruth**. Abu: Hasta en tus últimos días, pedias mas por tu familia que por ti misma. Siempre admire tu altruismo, tu capacidad de querer sin fin y tu fe. Te adoro Abu! Tía Ruth: Fuiste siempre una persona y mujer ejemplar, y encarnabas empatía y justicia. Me enseñaste mucho con tus monitos y trato de vivir siguiendo tu filosofía. Te quiero más de lo que siempre imaginaste y que cuando debí, no supe expresar.

An enormous GRACIAS to my family, I love you all. As a PhD student, a solid emotional support was crucial so I could stay sane through-out the degree, and despite a geographical and time zone barrier, my family has gone far and beyond to show me their support in endless ways.

- **Masa**, thanks for being my best friend and an amazing inspiration. You showed me how to step out of my comfort zone and encouraged me to try new things that helped me make one of my biggest dreams a reality. You stood by me through some very hard times and supported the path I chose despite the difficulties it conveyed. I am truly lucky for having you in my life, and I am thankful that it is you I get to share all my dreams with. I love you!

- **Ma y Pa**. Thanks for always being encouraging of my career and my passion for learning, and for your financial support. Gracias Ma por las largas conversaciones y por siempre, siempre estar ahí para mí. Gracias por estar pendiente de que estuviera viva en mis momentos de retracción social y por tu larga visita durante el doctorado que me lleno el corazón de felicidad y amor maternal. Thanks Pa for being the perfect example of hard work and for pushing me so I could do better than I ever thought possible. You taught me to work hard for what I want and to not let geography ever be a problem! Gracias a los dos por su amor incondicional, por sus consejos y por apoyarme siempre. Ustedes son mis mejores ejemplos a seguir y los mejores padres que cualquier persona puede desear tener. Ustedes me dieron las alas que me han llevado a donde estoy y también los primeros empujoncitos que necesitaba para aprender a volar. You are, have always been and always will be, my hero's.

- **Pichu y Ricky**, con sus combos. You are amazing! Pichu, my partner in crime, thanks for taking time off work to fly out to NZ from LA for a weekend of wedding dress shopping, eating, sightseeing, and meeting people. It was one of the best trips ever! Thanks for being my express imaging expert all this years. Thanks for giving me time when you barely had any for yourself, and

thanks for listening to my bickering when I needed to unload. Thank you Winrich for your tech support and for all the great burgers we had during my visits. Ricky, thanks for your endless tech support, your remote data recoveries after my goofs and your help and encouragement to learn to not hate statistics! It really got me through a hard writing phase. Thank you also for your visit to NZ when Alex wasn't even a year old! Having you there gave me a huge and highly needed emotional boost. Thank you Mary for the countless skypes, phone calls, messages and pictures to keep in touch and to keep me connected to family. And thank you Alex! Your innocence and happiness kept me balanced and gave me the happiness I needed on some difficult days. Love you Pichurulos y tribilines!

- Claudia, Jereme, Masa D, Natalia, Chandler. Thanks for letting me and Masa crash at your place almost unannounced countless times. Thanks for your support all these years and for understanding whenever I forgot to call or do something in my busy PhD times.

- A mis abuelos: Abu, Alexio, Pansy, Ricardo, Chepa; and to Gpa and Gma. I love you all dearly!

- A mis tías y tíos: tío Ricardo, tía Mary, tía Mirian, tío Alberto, tía Aura, tía Chaby, y a todos mis primos y primas (Mayi, Oscar y Ma Andreina; Pala; Gaby y Tavo; Ricardo A., Yoalida y Elena; Francia y Michelle; Isabel Cristina e Isabel de los Angeles), primitos y primitas. Los adoro a todos. Cada llamada, texto, foto, video y abrazo, lo aprecie más de lo que pueden entender.

Thank you also to my best friend outside the lab: **Julia**! My sister from another mister. I still wonder sometimes how I got lucky enough to find such a great friend. I have to leave written evidence of the fact that you scanned my lab books when I was running around like a headless chicken about to leave NZ. I still cannot believe some of the things you did for me! Your meals on wheels, late hour lab visits with snacks, hanging out with lab people just for moral support (that must have been torture with all the geek talk going on, LOL), flat-sitting and cleaning, dragging me out when I needed time away from lab, and these are only a few things. You honestly did too much, and all of it with a smile on your face. Thanks immensely!

A big thanks to my best lab friend **Saumya**. Thanks for being such a great friend, for your support, for pushing me to keep going and for listening when I needed to talk. Thanks for being my shoulder to cry on and for sharing your PhD difficulties, they made me feel like I wasn't alone in my PhD journey. As a senior PhD student in the lab, you left big shoes to fill in, but you also helped me get there! Because we were only a few years apart in our degrees, you truly understood me, and you were a fantastic example of hard work and determination. You will always be my PhD hero ☺

A HUGE thanks to my supervisor, **Austen**. You have been a great PhD supervisor and mentor, and have become through the years also a friend. I learned so much from you, and I only hope my PhD and future research work reflect that. I am extremely thankful for your flexibility and for allowing me to finish my write up from abroad due to my personal circumstances. Thanks for the express meeting in the US to talk about my discussion and for the countless corrections, ideas, discussion and suggestions, especially through email and skype. I know you put a great deal of trust in me, and I hope my contributions to the chromosome segregation project fulfilled your expectations. I can only hope we will work together again in the future.

Matt: post-doc, co-supervisor, cloning guru and friend! I believe those designations summarize the impact you had on my PhD student life, and yet they don't make justice to the level of support you gave me. Thank you so much! I hope many publications come out of our work together and that our friendship prevails through time and distance.

Megan and Ilog, thanks immensely. You helped with so many colony counts, lab experiments, scanning plates. So much! Besides that, you were wonderful students. It was an absolute pleasure to teach you both during my PhD and I am glad that you helped push the project forward! Megan, you gave it all a fresh perspective and found the most petty tasks fun! You truly boosted my motivation and my love for the lab on so many occasions. Aida, gracias por ser siempre tan especial. El apoyo que me has brindado todos estos años y a pesar de la distancia ha sido invaluable. Gracias por tu amistad condicional! Elizabeth, thanks for your patience with me and your invaluable help in the lab during my first few months as a PhD student. Your clever suggestions made arduous and bulk technical tasks much easier to handle. Thanks Naz, Naomi, GengGeng, Mark, and other Ganley lab members that haven't mentioned. You all made lab times, especially late nights and weekends so much more fun than they should have been! And I have fantastic memories of you all. Laura: I am thankful for your great friendship while it lasted and for all your help in the lab. You were a good friend and a patient flatmate.

Thank you Ninin for all our help with qPCR and the wonderful meals you always prepared. Thanks for your friendship. Thanks also to Tatyana and Yuri, Ralph (thanks for the *S.pombe*!), Justin, Lutz, Mack, and all other members of the **O'Sullivan lab**. You all contributed to many long and meaningful scientific discussions and you have all been great friends. A special thanks to the **Sattlegger lab** members: Evelyn, Rashmi, Su, Renuka, Michael, Richard. Thanks for your endless help with the detection machine, for the swap marker plasmids, for letting me borrow restriction

enzymes, and especially for the company during many late nights and weekends! Also special thanks to the **Hendrickson lab**: Heather, Richard, Akarsh. Random food outings, volunteering events and endless (even not so useful) discussions made the office a fun place to be! Thanks also to Wayne (my first co-supervisor) with, and to Paulina, Gaby, Eric, Matteo, Matilda. Thanks also to **Sebastian** for supervising and co-supervising my thesis and for tips on using R, and to **Nikki** for co-supervising on such short notice. Thanks also Sylvie for your help with RNA extractions. Colleen, Muharram and Vesna, thanks for all the admin support. Colleen, besides being fantastic at your job and providing students with such strong support, walking to building 11 to greet your smiling face everyday truly made an impact. Thanks for being so wonderful EVERY single day!

I also want to thank all the members of the Jordan lab, the latest tamoxifen team at the Department of Breast Medical Oncology at MD Anderson in Houston, TX. Dr Jordan, Ping, Amit, Niru, Smitha, Poulomi, Philipp, Yousef and Balkees. Thanks for your patience! A special thanks to Niru for help with references and strain names, to Ping for qPCR analysis suggestions, to Amit for random discussions. Thanks to Philipp for your flexibility during busy work times, and to PB, SY and NP for your constant encouragement and help with endnote. Thanks also to the Atascocita public library for providing me with a quiet and peaceful place to work on my writing.

It's also necessary to thank my yeasties: my beautiful microscopic friends that were there every step of the way and helped me learn how to use genetic tools on them and taught me to be patient. There is an anonymous quote that reads "hard work is the yeast that raises the dough". In my case it was hard work AND the yeast which raised the growing dough that was my PhD.

Thanks to the Marsden Fund and INMS for my PhD scholarship and financial support.

Four pages of thanks later, and there are still many things I have not given thanks for and many people I haven't mentioned… But if I keep going my acknowledgements will be even longer than this thesis!! So, I want to close this section by thanking those of you that I have not mentioned but helped me in one way or another. Even the smallest things like saying hello and smiling! You all made a difference in my PhD life**.** So, to all of you present during my struggles, I dedicate to you my success!

Finally I'd like to end with a short quote that I feel summarizes well my PhD: **"Success is the sum of small efforts, repeated day in and day out" -Robert Collier**

TABLE OF CONTENTS

LIST OF FIGURES

LIST OF TABLES

[blank page]

APPENDIX LIST

LIST OF ABBREVIATIONS

5FOA: 5-Fluoroorotic Acid

APC: anaphase promoting complex

CAR: cohesin association region

Chr: chromosome

CEN: centromere

CF: core factor

CHEF: contour-clamped homogeneous electrophoresis

CIN: chromosome instability

CLA: chromosome loss assay

Cp: Cross point cycle

DF: dense fibrillar component

EDTA: ethylenediaminetetraacetic acid

FC: fibrillar center

fdr: false discovery rate (p-value adjustment)

G418: geneticin, an aminoglycoside antibiotic

GC: granular component

gDNA: genomic DNA

GFP: green fluorescent protein

HP: helper plasmid

IGS: intergenic spacer

INMS: Institute of Natural and Mathematical Sciences (Massey University)

KU: CLA tags *kanMX2* and *URA3*

lacI-GFP: *lac* operator/ *lac* repressor system coupled to GFP

lacO: *lac* operator

MCS: multiple cloning site

nm: nanometer (wavelength unit for OD measurements)

NOR: nucleolar organizer region

OD: optical density

O/N: overnight

pGAL-*FOB1*: galactose inducible *FOB1* plasmid

PIC: pre-initiation complex

Pol I: RNA Polymerase I

Pol II: RNA Polymerase II

Pol III: RNA Polymerase III

rARS: rDNA origin of replication

RDN1: ribosomal DNA gene

rDNA: ribosomal RNA gene repeats

RENT complex: regulator of nucleolar silencing and telophase complex

RFB: replication fork block

rRNA: ribosomal RNA

RT: room temperature

SD: synthetic dextrose medium

SGal: synthetic galactose medium

SM: starvation medium

SMC: structural maintenance of chromosome

Sp*ADE6*: *ADE6* gene from *S. pombe*

SPB: spindle pole body

t_0: CLA time 0

t_1: CLA time 1

UAF: upstream activation factor

WT: wild type

YPD: yeast peptone dextrose

YPGal: yeast peptone galactose

YPGly: yeast peptone glycerol

CHAPTER ONE: INTRODUCTION

[blank page]

1.1 MITOTIC CHROMOSOME SEGREGATION

Mitotic cell division involves replication of each chromosome to yield two sister chromatids, followed by their separation through the process of chromosome segregation, so that all the chromosomal genetic information can be fully inherited by both daughter cells. Chromosome segregation is a crucial part of the cell cycle, and is extremely accurate, with around one error in every 10^5 divisions in *Saccharomyces cerevisiae* cells (Hartwell et al. 1982; Murray and Szostak 1985).

1.1.1 Important features of chromosome segregation

1.1.1.1 Sister chromatid cohesion

During S-phase, each chromosome is replicated to produce a pair of two identical chromosome copies (sister chromatids) (Yanagida 2009), and these are tightly held together (cohere) through linkages established by a multi-protein complex called cohesin (Strunnikov et al. 1993; Guacci et al. 1997; Klein et al. 1999; Uhlmann et al. 1999). Cohesin consists of a heterodimer of two members of the structural maintenance of chromosome (SMC) protein family, Smc1 and Smc3, in a complex with two non-SMC proteins Scc1 (also known as Mcd1 or Rad21) and Scc3 (also known as Irr1), that together form a large protein ring structure (Haering et al. 2002). To provide cohesion, cohesin must first be loaded onto chromosomes and this requires a loader complex composed of Scc2 and Scc4 proteins (Kogut et al. 2009). The mechanism by which cohesin is able to topologically embrace DNA is not well understood, but one of the currently accepted models is that when docking occurs, cohesin is in an open hinge conformation, and ATP hydrolysis from the SMC heads after docking closes the hinge structure so that the cohesin complex physically entraps the two sister chromatids (reviewed in Marston 2014; Nasmyth, 2011).

Cohesin is partially removed from sister chromatids in early mitosis to allow the resolution of chromosome arms, with centromeres remaining associated until the onset of anaphase when centromere-enriched cohesin is removed (Guacci 2007). The bulk of cohesin removal occurs at the beginning of anaphase and requires activation of separase, a protease that cleaves the Scc1 unit, thus disrupting the entrapment and allowing separation of the sister chromatids (Uhlmann et al. 2000). Once all chromosomes are aligned properly, the anaphase

promoting complex (APC) targets securin, an inhibitor of separase, for degradation (reviewed in Queralt and Uhlmann 2005). This chain of events activates separase, which is then able to cleave cohesin and trigger the start of anaphase. Cohesin cleavage is irreversible and hence it is tightly controlled (Uhlmann 2003). A non-protease action of separase has also been shown to release the Cdc14 phosphatase from the nucleolus and activate it, which initiates exit from mitosis and ultimately results in cell division (Sullivan and Uhlmann 2003).

Cohesin has specific binding sites on chromosomal DNA, known as cohesin-associated regions (CAR). In yeast, cohesin binding has been shown to correlate with intergenic regions between convergent genes (Glynn et al. 2004), and to be enriched in large regions surrounding the small centromeres (Tanaka et al. 1999). Cohesin binding to silent chromatin has been shown to require the evolutionarily conserved silent information regulator 2 protein Sir2 (Guacci et al. 1997), a member of the sirtuin protein family of NAD^+-dependent protein deacetylases, and an essential silent chromatin component best known for its transcriptional silencing at the mating-type loci (Wu et al. 2011), telomeres (Rusche et al. 2003) and ribosomal RNA gene repeats (Wierman and Smith 2014).

1.1.1.2 Kinetochore attachments

During metaphase, the cohesin linkages enable sister chromatid attachment to microtubules from opposite poles of the mitotic spindle, while providing resistance against premature separation (Michaelis et al. 1997). Sister chromatids are directly attached to microtubules through their kinetochores, a structure that assembles in a unique chromosomal locus: the centromere (Westermann et al. 2007). In yeast, each kinetochore binds to just a single microtubule (Winey et al. 1995). Microtubules are the main structural element that forms the mitotic spindle, which is the macromolecular machine that separates chromosomes (Walczak and Heald 2008). Spindle microtubules are anchored to two centrosomes, or spindle pole bodies (SPB) in yeast, which define the mitotic poles in the dividing cell (Winey and Bloom 2012). In yeast, the nuclear envelope does not break down, so the SPBs remain embedded in the nuclear envelope throughout the duration of the cell cycle (Biggins 2013).

Proper kinetochore attachment allows biorientation of sister chromatids so that later on they can be pulled apart to opposite sides of the dividing nucleus for equal segregation of chromosomes into the daughter cells. It has been suggested that cohesin enrichment at the centromeres facilitates the proper biorientation of sister chromatids, as absence of this enrichment leads to increased chromosome loss (Tanaka et al. 2000; Ng et al. 2009). A surveillance mechanism, known as the spindle assembly checkpoint, monitors chromosome

attachment to microtubules. The spindle checkpoint has the ability to prevent cleavage of cohesin by separase and halt the cell cycle until any erroneous attachments are corrected and proper biorientation is achieved (reviewed in May and Hardwick 2006), and the APC is an established target of the spindle checkpoint.

1.1.1.3 Sister chromatid condensation

Following kinetochore attachment, each sister chromatid is compacted into a rigid structure through intra-chromatid linkages in preparation for sister chromatid resolution. These intra-chromatid linkages are established by the cohesin related multi-protein complex condensin (Strunnikov et al. 1995; Guacci et al. 1997; Hirano 2000), and require the help of topoisomerase II, an enzyme that resolves catenation entanglements generated as a result of replication (Gimenez-Abian et al. 2000). In mammals, there are two condensin complexes (I and II) that mediate condensation, but in yeast there is a single condensin complex: condensin I. Yeast condensin has two SMC subunits (Smc2 and Smc4) and three non-SMC subunits (Ycs4, Ycs5 and Brn1), all of which are essential for cell viability (Hirano 2002). In condensin defective mutants, the mitotic spindle is able to pull chromosomes apart, but these fail to separate and form what is known as anaphase bridges (Strunnikov et al. 1995). A similar phenotype is observed true for topoisomerase II defective mutants (Hirano 2000). Hence, it seems that condensin and topoisomerase function together to remove connections between sister chromatids (Freeman et al. 2000), and this process has been referred to as “sister chromatid compartmentalization” (Strunnikov 2003). Condensin has also been shown to contribute to the establishment of proper tension at the kinetochores (Yong-Gonzalez et al. 2007).

1.1.2 Monitoring chromosome segregation errors

Despite the high fidelity of chromosome segregation, it is not always a faultless process. Normal separation of chromosomes of sister chromatids is termed disjunction, and when there are errors in separation, these are called non-disjunctions. Non-disjunction results in aneuploidy, which is whole-chromosome gain or loss. Much of what is known about the molecular features of eukaryotic chromosome segregation is derived from research in the budding yeast, *S. cerevisiae* (reviewed in Yanagida 2009).

In yeast, aneuploidy can provide a fitness advantage over euploidy (normal number of chromosomes) under certain environmental conditions (Selmecki et al. 2015); but it can also be detrimental, leading to an imbalance of gene expression (affecting protein homeostasis), changes in genome stability (potentially leading to DNA damage), and altered growth characteristics (reviewed in Storchova 2012). Yeast studies have shown that the frequency of aneuploidy can increase with mutations of genes that affect regulation of the cell cycle, mitotic spindle, kinetochore attachments, or sister chromatid cohesion (Siegel and Amon 2012).

1.2 THE RIBOSOMAL RNA GENES

Ribosomal RNA (rRNA) is an essential component of ribosomes, the molecular complexes that carry out protein synthesis in the cell, and therefore is critical for life. In most species, ribosomes are made of four rRNA molecules that form a complex with up to 80 ribosomal proteins (Verschoor et al. 1998), and assemble into two subunits: the small and large subunits (figure 1.1). In eukaryotes, the small subunit (40S) contains the 18S rRNA together with over 30 ribosomal proteins, while the large subunit (60S) comprises 5S, 5.8S and 28S rRNAs that are associated with about 45 ribosomal proteins (reviewed in Henras et al. 2015). Ribosomal RNA molecules and ribosome components are named for their sedimentation velocity, which depends on their size, shape and density, as indicated by the letter S that represents Svedberg units (Taylor and Storck 1964).

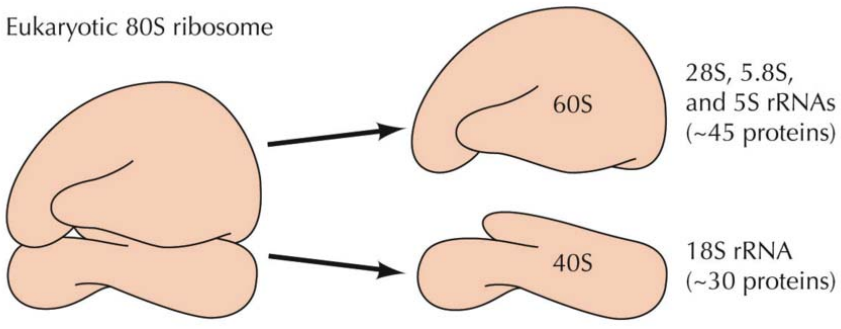

Figure 1.1. Eukaryotic ribosome. Eukaryotic ribosomes (80S) consist of small (40S) and large (60S) subunits, each associated with over 30 ribosomal proteins. Together, these subunits carry out protein synthesis: the small subunit binds and decodes mRNA to ensure correct pairing between codons and tRNA's, while the large subunit contains an active site which catalyzes peptide bond formation between amino acids to form a peptide chain (reviewed in Doudna and Rath 2002; figure from Alberts et al. 2007).

1.2.1 Ribosomal DNA organization

Ribosomal RNA (rRNA) is transcribed from a multicopy, polycistronic rRNA gene that is commonly referred to as the ribosomal DNA (rDNA). Multiple rDNA repeats are organized in one or more tandem repeat arrays in the genome of most eukaryotes (Long and Dawid 1980). However, large variations exist between the rDNA copy number (from tens to several thousands) of species and even between closely related species or different strains of the same species (Long and Dawid 1980). Interestingly, there is a positive correlation between rDNA copy number and genome size (Prokopowich et al. 2003).

The genomic location of the rDNA varies between different organisms, with the multiple rDNA copies distributed on one or more chromosomal loci, each with a tandem array of rDNA repeats (Petes et al. 1978). Differences can also be found in the region within a chromosome that contains the rDNA. For example, human chromosomes harbor the rDNA in the short arm of the five acrocentric chromosomes, and in contrast *S. cerevisiae* contains the rDNA array on the long arm of its single rDNA-containing chromosome.

rRNA gene organization is highly conserved amongst eukaryotes (Kupriyanova et al. 2015). Three rRNAs are produced from a large rRNA precursor (35S in yeast), and are post-transcriptionally processed and cleaved to remove externally transcribed spacers (ETS) and internally transcribed spacers (ITS) (Yanagida 2009), which are similar to introns from protein coding genes. This process yields mature smaller rRNA molecules (18S, 5.8S and 28S) (figure 1.2). 35S rRNA is transcribed by RNA polymerase I (Pol) I (Riggs and Nomura 1990). The 5S rRNA gene is transcribed separately by RNA Polymerase III (Pol III), and in most organisms is located in a separate locus (Bergeron and Drouin 2008; Gongadze 2011).

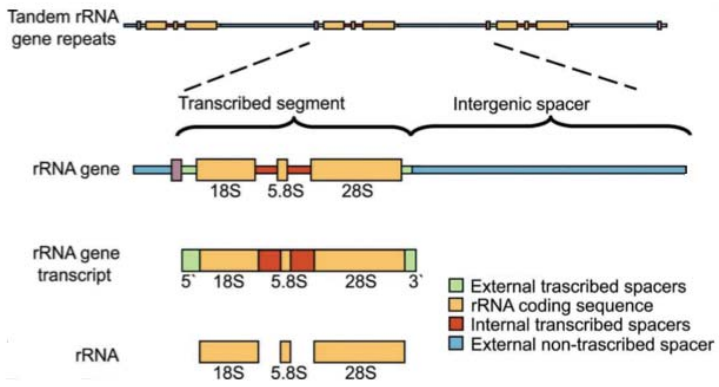

Figure 1.2. Typical eukaryote rRNA gene organization. The multicopy rRNA gene, found in tandem repeats, consists of a transcribed/coding segment (multicolored) and an intergenic spacer (blue). rRNA is transcribed by Pol I to produce a polycistronic 35S pre-rRNA precursor (rRNA gene transcript) that is post-transcriptionally processed and cleaved to remove the ETS and ITS (green and red, respectively). This generates the mature 18S, 5.8S and 28S rRNA products (shown in tan). These mature rRNAs associate with ribosomal

proteins to assemble the small (40S) and large (60S) ribosomal subunits that form the ribosome (figure from Raska et al. 2004).

1.2.1.1. Yeast rDNA

The budding yeast, *S. cerevisiae* has been used widely to study the rDNA and the molecular processes that take place at the rDNA locus (Kobayashi et al. 1998; Oakes et al. 1998; Wai et al. 2000; Tomson et al. 2006; D'Ambrosio et al. 2008a; Tsang and Carr 2008; Clemente-Blanco et al. 2009). In budding yeast, unlike other organisms, systems have been developed to genetically manipulate the rDNA, and existing strains harbor different rDNA alterations and translocations. A chromosomal rDNA deletion strain has been created by supporting its growth using a plasmid system (Wai et al. 2000), a series of *FOB1* disruption strains have been developed in which the number of rDNA repeats can be reduced and maintained without amplifications or deletions (ie. 20-copy, 40-copy and 80-copy strains) (Kobayashi et al. 1998), and a series of strains carrying ectopic rDNA arrays have been constructed (Oakes et al. 1998). Hence, yeast has become a very powerful model system for studying the rDNA.

In *S. cerevisiae* there are 150-200 rDNA repeats of 9.1 kb in a single head-to-tail tandem repeat array on chromosome XII (figure 1.3) (Petes et al. 1978). Each rDNA unit comprises a 35S rRNA coding region, and an intergenic spacer (IGS) that also contains the 5S rRNA coding region, resulting in division of the IGS into IGS1 and IGS2. The IGS also contains several non-coding functional elements (Lafontaine and Tollervey 2001), including an origin of replication (rARS), a bidirectional noncoding promoter (Brewer and Fangman 1987), and a replication fork barrier (RFB) site, which is a 100-bp sequence that has the potential to block replication fork in a unidirectional fashion (Rothstein et al. 2000). Hence, both the coding region and the IGS have functional significance.

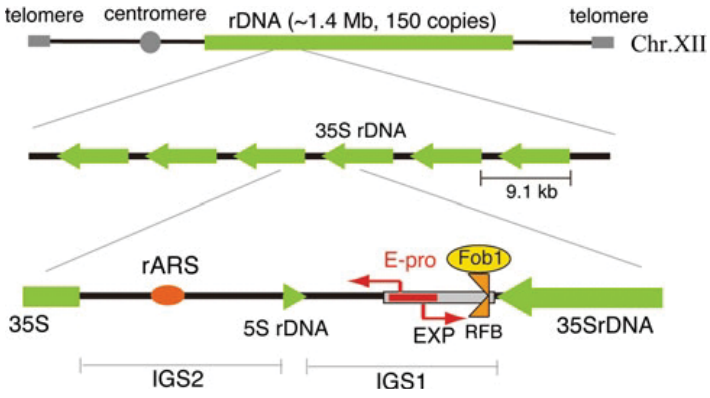

Figure 1.3. rDNA organization in yeast. *S. cerevisiae* contains 150-200 rDNA units in a head-to-tail tandem repeat array on the long arm of chromosome XII. Each unit is 9.1 kb in size and contains the 35S and 5S rRNA genes separated by intergenic spacers IGS1 and IGS2. IGS1 includes the expansion sequence (EXP) containing the replication fork barrier (RFB) that serves as a binding site for the replication fork blocking protein Fob1p, and E-pro which is a bidirectional non-coding promoter. IGS2 includes a replication origin (rARS) (Szostak and Wu 1979; Skryabin et al. 1984). Green arrows indicate direction of transcription of the 35S rRNA gene by Pol I and the 5S rRNA gene by Pol III (figure from Kobayashi 2011b).

The rDNA plays important roles in transcription control and genome stability (Saka et al. 2016); therefore, understanding its architecture and regulation is of great interest. However, its repetitive nature presents an experimental challenge because repeats have essentially the same sequence and thus are difficult to distinguish from each other. Nonetheless, the rDNA is amongst the best-characterized repeat arrays in eukaryotes, and the research contributing to this characterization is largely derived from yeast.

1.2.2. The rDNA and the nucleolus

The chromosomal regions containing the rDNA have the ability to aggregate inside the nucleus and form a sub-nuclear compartment called the nucleolus (McClintock 1934; Hadjiolov 1985). These chromosomal regions are called nucleolar organizer regions (NORs), and each NOR has the potential to produce a nucleolus, although multiple NORs often fuse at the beginning of interphase to give rise to a single or very few nucleoli (Olson and Dundr 2010). The nucleolus is not membrane-bound, instead it is demarcated by a dynamic layer of heterochromatin that can be easily visualized by microscopy (Miller and Beatty 1969; Olson et al. 2002). In *S. cerevisiae* the nucleolus is crescent shaped and is found in contact with the nuclear envelope (Smitt et al. 1973).

The main known functions of the nucleolus are rRNA transcription and ribosomal subunit assembly (Mosgoeller et al. 1998). Nucleoli typically consist of three subcompartments: a fibrillar center (FC) where the rDNA is localized, a dense fibrillar component (DFC) harboring nascent rRNA transcripts, and a granular component (GC) which consists mostly of the later stages of rRNA processing and ribosomal subunit assembly (Bernhard and Granboulan 1968; Mosgoeller et al. 1998). The nucleolar FC is present in vertebrates but is usually lacking in lower eukaryotes like yeasts (Thiry and Lafontaine 2005). The assembly of the ribosomal subunits requires many ribosomal proteins, which are transcribed by RNA polymerase II in the nucleoplasm (through the conventional protein synthesis pathway) and later transported into the nucleolus (reviewed in Raska et al. 2004). A number of unexpected proteins and RNAs have been detected in nucleoli, suggesting alternative non-traditional roles for the nucleolus besides ribosome biogenesis (Olson 2004). These proposed roles include tRNA maturation, partial assembly of telomerase complexes, cell cycle regulation through protein sequestration, viral replication, aging, epigenetic silencing, and the cellular stress response (reviewed in Boisvert et al. 2007; Sirri et al. 2008; Olson and Dundr 2010).

The nucleolus assembles following exit from mitosis and remains functional through interphase, which coincides with the highest ribosome production during the cell cycle. Pol I and the rest of the rRNA transcription factors, together with the ribosome assembly machinery, are all sequestered in the nucleolus. Before or during prophase, rRNA transcription shuts down and the nucleolus disassembles. The nucleolar components are dispersed to various parts of the cell, with only the transcription machinery remaining associated with the NORs (Raska 2004). To maintain an intact nucleolar structure, both the rDNA repeats and RNA polymerase I are necessary (Oakes et al. 1993). Yeast mutants defective in Pol I exhibit structural alterations of the nucleolus (Oakes et al. 1993), demonstrating that presence of the rDNA repeats alone is not sufficient for nucleolar localization to the nuclear periphery, and intact Pol I is required for both nucleolar structure and localization (Nogi et al. 1991b; Oakes et al. 1993). Moreover, localization of rDNA transcription factors to a region in the chromosome can induce the formation of pseudonucleoli (Mais et al. 2005; Grob et al. 2014). In addition, the rDNA facilitates structural stability of the nucleolus, as deletion of the chromosomal rDNA in yeast disrupts nucleolar structure (Oakes et al. 1998).

1.2.3 RNA polymerase I transcription of rRNA

Active rRNA genes have a high Pol I loading of up to ~50 Pol I complexes per gene at a time, resulting in a high transcriptional rate (French et al. 2003). In yeast, initiation of rDNA transcription begins with the recruitment and assembly of Pol I and other transcription factors into a pre-initiation complex (PIC) at the rRNA gene (Hontz et al. 2009). Successful PIC formation leads to promoter opening and initiation of transcription, and this is followed by elongation (Russell and Zomerdijk 2005). At least three transcription factors that form part of the PIC have been identified in yeast: upstream activation factor (UAF), core factor (CF) and Rrn3p; but Pol I is the most prominent component of the PIC (reviewed in Reeder 1999; Nomura 2001). The yeast Pol I complex consists of 14 subunits, three of which are common to all RNA polymerases (Pol I, Pol II, and Pol III), and two others are common to Pol I and Pol III only. The remaining subunits are specific to Pol I, and include the largest (A190) and the second largest (A135) subunits (Yano and Nomura 1991). Inactivation of the genes encoding for A190 and A135 has been used to create mutants defective in rRNA synthesis (Nogi et al. 1991a).

The multiple rRNA gene copies are not all actively transcribed to produce rRNA. Miller's pioneering work was the first to show that only a fraction of the rDNA repeats are transcriptionally active, while the rest are in an inactive state (Miller and Beatty 1969). The ratio of transcriptionally active and inactive rRNA genes is stable through the cell cycle (Conconi et al. 1989), and is estimated to be about 50:50 in *S. cerevisiae* (Sogo et al. 1984; Dammann et al. 1993). Despite this mixed population of active and inactive repeats, rDNA transcription occurs at a very high rate on the active copies, with Pol I being able to transcribe multiple rRNA copies from a single repeat at the same time (French et al. 2003). Distinction between active and inactive rDNA copies has been achieved through the i*n vivo* accessibility of active repeats when treated with the drug psoralen. Psoralen is only able to crosslink the transcriptionally active rDNA sites that are maintained in an open, psoralen-accessible chromatin state, while the inactive repeats shielded by nucleosomes remain inaccessible (figure 1.4) (Dammann et al. 1993; Lucchini and Sogo 1995), and these two repeat types can be distinguished electrophoretically.

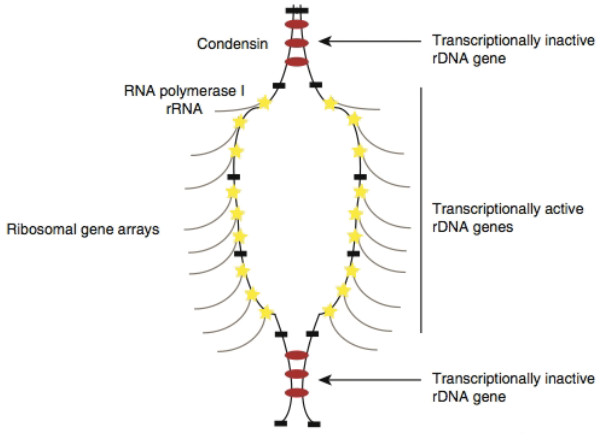

Figure 1.4. The rDNA array contains a combination of transcriptionally active and inactive rDNA copies. Yellow stars represent RNA Pol I located on transcriptionally active rDNA genes and the lines associated with each star represent pre-rRNA transcripts being synthesized. Inactive rDNA genes provide a docking platform for the association of condensin complexes (red ovals). Black boxes represent regions associated with cohesin (figure from Aragon 2010).

Pol I transcriptional silencing of the rDNA repeats is associated with its heterochromatic state. However, a number of non-rRNA transcripts are transcribed from the rDNA through the action of Pol II (Kobayashi and Ganley 2005; Li et al. 2006). There appears to be a separate silencing to that involved in differentiating active from inactive rDNA unit, in which chromatin structure limits accessibility of the Pol II transcription machinery to the rDNA (reviewed in Cioci et al. 2003). This Pol II silencing at the rDNA is mediated by Sir2 (Pasero et al. 2002), but is distinct from the Sir2 silencing at the mating type loci and telomeres, and involves formation of the regulator of nucleolar silencing and telophase exit (RENT) complex through association of Sir2 with Net1 (also called Cfi1) and Cdc14. Net1 is required for Sir2 localization to the rDNA (Straight et al. 1999), while the Cdc14 phosphatase, known to regulate exit from mitosis, is repressed through its association with Net1 (until the start of anaphase) (Shou et al. 1999). The RENT complex is recruited to the IGS, and specifically to the RFB site through interactions of Net1 with a replication fork blocking (RFB) protein called Fob1 (Huang and Moazed 2003; Wierman and Smith 2014). Pol II transcriptional silencing and its consequent RENT complex recruitment allows sequestration of Cdc14 in the nucleolus until cells are ready for mitotic exit (Shou et al. 1999).

1.2.4 rDNA replication

An rDNA origin of replication (rARS) is present in the IGS of each rDNA repeat and rDNA replication occurs during S-phase (figure 1.3) (Miller and Kowalski 1993). However, it is estimated that in yeast only about ~20% of rARSs are initiated in every cell cycle (Brewer and Fangman 1987), with activation of rARSs being suppressed by Sir2 (Pasero et al. 2002). Replication of the rDNA repeats is initially bidirectional, however, when bound by Fob1, the left replication fork arrests at the replication fork barrier (RFB) site, while the right-bound replication fork continues until it converges with another replication fork arrested at another RFB site. In this manner, rDNA replication is completed in a mostly unidirectional manner (reviewed in Torres 2015). The reason for the unidirectional replication of the rDNA is believed to be to prevent collision between the transcription and replication machineries (Takeuchi et al. 2003).

1.2.5 rDNA recombination

Recombination at the rDNA is very frequent, and this manifests as copy number fluctuations (Ganley and Kobayashi 2011 and citations within). rDNA recombination is mediated by Fob1 and Kobayashi has proposed a model, the fork block-dependent recombination model (figure 1.5) (Kobayashi et al. 1998), that outlines how the majority of rDNA recombination in yeast is believed to occur. In this model, Fob1 binds the RFB site to block replication, and this results in a double stranded break (DSB) that is repaired through homologous recombination. The repeats all have very similar DNA sequences, therefore strand invasion for repair can occur with the neighboring repeat from the sister chromatid, or with any other repeat, resulting in equal or unequal sister-chromatid recombination, respectively. The latter leads to copy number change, and the deletions and amplifications that have been observed in the rDNA (Ganley and Kobayashi 2011) are thought to result from unequal rDNA recombination, and are stimulated by noncoding transcription from the bidirectional E-pro promoter (Kobayashi and Ganley 2005). E-pro transcription displaces cohesin (from its binding site in IGS1) and biases recombination towards unequal sister chromatid recombination, resulting in rDNA copy number change. Repression of E-pro activity by Sir2 (Kobayashi et al. 2004) allows cohesin access and prevents copy number changes by restricting the recombination to equal sister chromatid recombination (figure 1.5). Despite these deletions and amplifications, the rDNA is maintained at relatively stable copy numbers within a species. Since

rDNA recombination is Fob1 dependent, deletion of *FOB1* prevents both amplifications and deletions from occurring and thus freezes rDNA copy number. This has been the basis for the creation of yeast strains that have a fixed number of rDNA copies (Takeuchi et al. 2003; Ide et al. 2010).

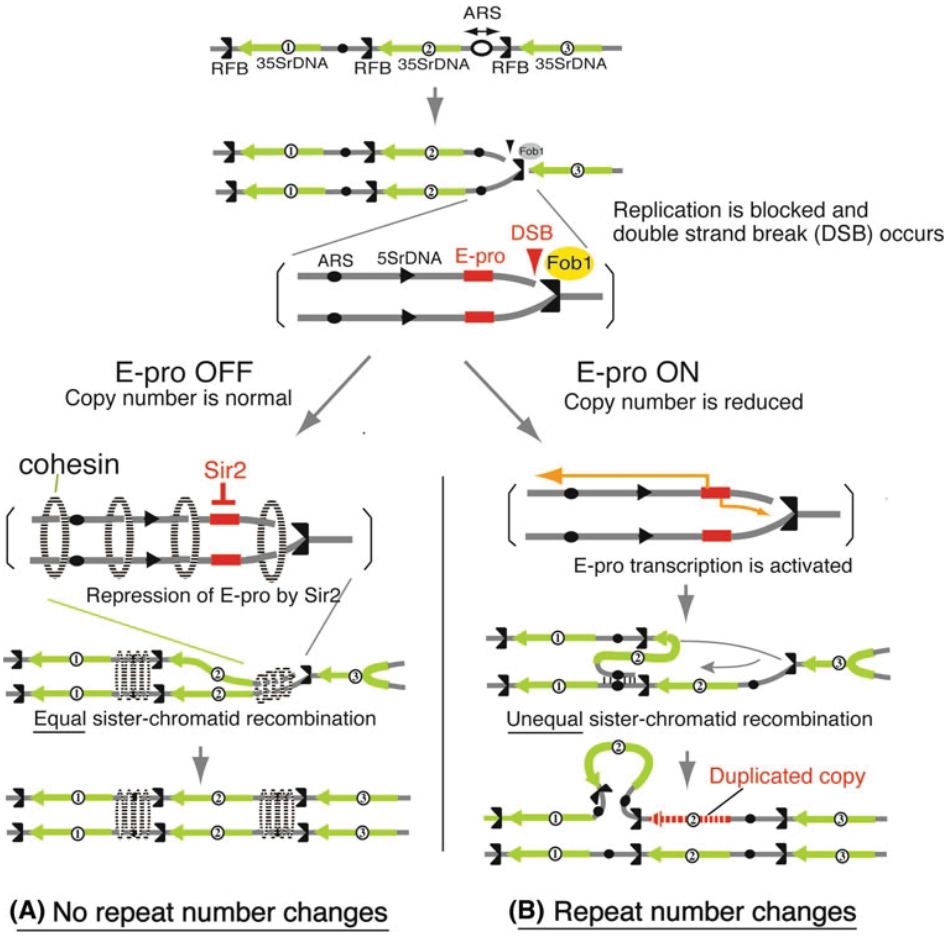

Figure 1.5. rDNA amplification model. Grey lines represent single chromatids (double stranded DNA) while each green line represents an independent 35S rRNA copy. Replication blocking by Fob1p at the RFB site induces a double stranded break, which is repaired by recombination in the presence or absence of cohesin. (A) The cohesin complex is able to associate with the rDNA only when E-pro is silenced by Sir2. This results in equal sister chromatid recombination and no rDNA repeat number change after recombination. (B) When E-pro is active, its transcription activity prevents binding of cohesin and allows the damaged rDNA copy to recombine through unequal sister chromatid recombination, resulting in repeat number change (Kobayashi et al., 1998; figure from Kobayashi 2011b).

1.2.6 Cohesin association at the rDNA

The IGS of the yeast rDNA has been shown to contain a cohesin association region (CAR) that requires several mediators for stable cohesin association. Lrs4 and Csm1 are two such mediators, and they are both part of a kinetochore associating complex called monopolin

that is important for general chromosome segregation fidelity (Huang et al. 2006). Huang *et al.* (2006) have proposed a model for cohesin association with the rDNA, in which a protein bridge forms between sister chromatids. The formation of this bridge starts with Fob1 recruiting the RENT complex (through a non-catalytic domain of Sir2 (Wu, 2011) and Tof2, which is a protein required for Lrs4/Csm1 recruitment. Lrs4/Csm1 may then form a protein bridge that clamps sister chromatids together through Csm1 association with cohesin, thus restricting the movement of sister chromatids relative to each other. This rDNA-specific recruitment of cohesin ensures that, like the rest of the genome, sister chromatids containing the rDNA array are held together until the cell is ready to proceed with their separation.

1.2.7 rDNA cohesin-independent cohesion and condensin association

Newly replicated sister chromatids are held together through cohesin linkages until cohesin cleavage by separase allows their separation in anaphase. However, after removal of cohesin, sister chromatids remain attached at the rDNA locus through cohesin-independent linkages until the end of anaphase (Tomson et al. 2006). Not much is known about these cohesin-independent linkages, but their removal has been shown to require Cdc14 activation and condensin recruitment (D'Amours et al. 2004; Sullivan et al. 2004). A model proposed by Clemente-Blanco et al. (2009) summarizes what is known about the sequence of events that leads to sister chromatid segregation at the rDNA locus (figure 1.6). Cdc14 is found in the nucleolus, inhibited by Net1 until the start of anaphase, and inhibition of Cdc14 phosphatase activity is required for efficient rRNA transcription. After cohesin removal by separase, Cdc14 is activated at the onset of anaphase and once activated, Cdc14 inhibits transcription by Pol I. Nascent rRNA transcripts are known to block condensin from binding to the rDNA, so once rDNA transcription is significantly reduced by Cdc14, condensin can access the rDNA to condense each chromatid in preparation for segregation (Strunnikov 2003). However, at this point the sister chromatids remain associated at the rDNA regions through the cohesin-independent linkages. Condensin has been proposed to mediate the removal of the cohesin-independent linkages at the rDNA, and the removal of these linkages leads to completion of chromosome XII segregation.

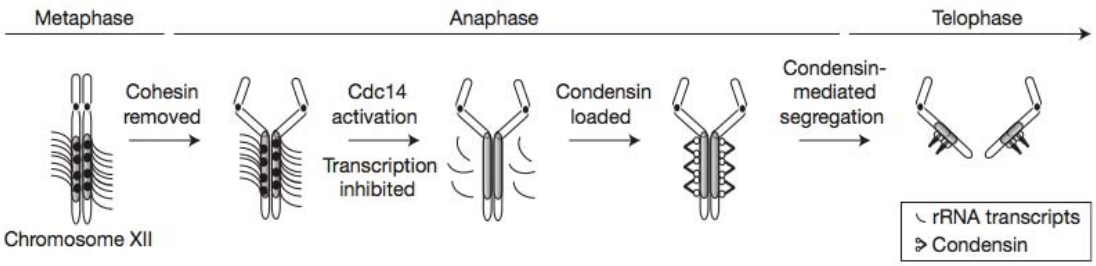

Figure 1.6. Schematic representation of *CDC14*-dependent rRNA transcription inhibition during yeast anaphase. Following removal of cohesin, transcription is inhibited by Cdc14 phosphatase through repression of Pol I (represented by the black dots). According to this model, the condensin complex cannot access chromatin until rRNA transcription is significantly reduced during anaphase. Sister chromatids remain attached at the rDNA until the end of anaphase through cohesin-independent linkages. The rDNA array is shown in darker grey on the long arm of chromosome XII (figure from Clemente-Blanco et al. 2009).

Condensin association with the rDNA has been shown to be enriched at the RFB site in a Fob1-dependent manner (Johzuka and Horiuchi 2009). Genetic screens have identified three genes, *TOF2*, *LRS4* and *CSM1* that are required for the Fob1-dependent recruitment of condensin to the RFB. ChIP experiments have revealed that Fob1 associates with the RFB site directly, followed by the orderly recruitment of Tof2, Lrs4/Csm1 and lastly condensin (Johzuka and Horiuchi 2009). Although no direct interactions have been observed between Fob1 and the subunits of condensin in co-immunoprecipitation experiments, two-hybrid analysis suggests an *in vivo* interaction between Lrs4/Csm1 and multiple subunits of condensin (Wysocka et al. 2004; Johzuka and Horiuchi 2009). Thus, condensin association to the RFB site, like cohesin, involves Fob1 mediated interactions that are unique to the rDNA.

1.3 AIMS AND OBJECTIVES

In 1985 Babu and Verma first proposed that the high frequency of Down syndrome in humans that is a consequence of nondisjunction of chromosome 21 may be a result of the presence of the rDNA on this chromosome. Although this hypothesis has never been tested and other factors have been proposed to mediate the high rate of chromosome 21 meiotic nondisjunction, a number of observations in yeast suggest a link between the rDNA and chromosome segregation. These observations include the requirement for Cdc14 activity for rDNA compaction (Machin et al. 2006), the unique cohesin-independent cohesion of the rDNA locus (Tomson et al. 2006) (section 1.2.7), and the unique ways in which the rDNA behaves

with respect to transcription (section 1.2.3), replication (section 1.2.4) and recombination (section 1.2.5). Further, studies that have monitored segregation of chromosome XII harboring the rDNA by visualization of the rDNA-binding protein Net1 fused to GFP have shown that yeast cells display a late rDNA segregation phenotype where the rDNA trails behind the rest of the genome (D'Ambrosio et al. 2008b; Miyazaki and Kobayashi 2011). Together, these observations suggest that the rDNA may be influencing the chromosome segregation in eukaryotes, therefore, the aim of this thesis is to test the hypothesis that the rDNA repeats affect chromosome segregation. Yeast is a natural diploid that is able to tolerate aneuploidy (Mulla et al. 2014; Torres 2015), and thus has been the gold standard to study eukaryotic chromosome segregation. Moreover, the range of genetic manipulations for the rDNA that are available in yeast are unparalleled in any other system (section 1.2.1.1). Therefore, I chose to explore the effect of rDNA on mitotic chromosome segregation of *S. cerevisiae.* In humans the majority of non-disjunctions arise from errors in meiosis (Hassold et al. 1996). Nonetheless I chose to explore mitosis because developing a system to measure meiotic chromosome loss conveys an added difficulty as it requires the isolation of haploid meiotic products in the absence of diploids; while developing a system to measure mitotic chromosome loss circumvents this difficult pre-requisite. I will address three specific objectives in this study:

1. To establish and optimize an assay that determines the rate of chromosome loss during yeast mitosis to quantify chromosome segregation fidelity.
2. To use the assay from (1) to determine if the rDNA repeats affect chromosome segregation by evaluating strains with different rDNA alterations.
3. To distinguish whether any rDNA-mediated effects on chromosome segregation are specific to the rDNA-containing chromosome or affect chromosome segregation generally.

[blank page]

CHAPTER TWO: MATERIALS AND METHODS

[blank page]

2.1 YEAST STRAINS, BACTERIAL STRAINS AND PLASMIDS

All yeast strains and bacterial strains used in this study are listed in table I, and plasmids in table II.

Table I. List of strains

Asterisks next to the strains name designates strains used for the chromosome loss assay (CLA)

	Strain	Features	Genotype	Origin
	S. cerevisiae			
	NOY408-1a	XII^{200} (strain W303-1b)	*MATα ade2-1 ura3-1 his3-11 trp1-1 leu2-3,112 can1-100*	(Nogi et al. 1991a)
	NOY408-1b	XII^{200} (strain W303-1a)	*MATa ade2-1 ura3-1 his3-11 trp1-1 leu2-3,112 can1-100*	(Nogi et al. 1991a)
	NOY866	*RPA135* deletion haploid	*MATα rpa135Δ::LEU2 ade2-1 ura3-1 his3-11,15 trp1-1 leu2-3,112 can1-100 fob1::HIS3, pNOY117 (CEN RPA135 TRP1) rDNA copy no. ~40*	(French et al. 2003)
	NOY984	XII^{0}+HP	MATα ade2-1 ura3-1 trp1-1 leu2-3,112 his3-11,15 can1-100 rdnΔΔ::hisG, pNOY130	(Oakes et al. 2006)
	NOY2029	WT haploid with hygromycin resistant rDNA array	*MATa ade2-1 ura3-1 trp1-1 leu2-3,112 his3-11,15 can1-100, rDNA* array substituting for RDN1*	(Oakes et al. 2006)
	NOY2030	V^{200*} XII^{0}	*MATα ade2-1 ura3-1 trp1-1 leu2-3,112 his3-11,15 can1-100 rdnΔΔ::hisG, rDNA* array near CEN5*	(Oakes et al. 2006)
	NOY2053	XII^{200} V^{200*}	*MATa ade2-1 ura3-1 trp1-1 leu2-3,112 his3-11,15 can1-100, RDN1 and rDNA* array near CEN5*	(Oakes et al. 2006)
	TAK300	XII^{20} *fob1::HIS3*	*MATα ade2-1 ura3-1 his3-11 trp1-1 leu2-3,112 can1-100 ChrXII-109,570::kanMX2 ChrXII-223,830::URA3 fob1::HIS3 RDNA1~20copies*	(Takeuchi et al. 2003)
	XII^{200KU}	NOY408-1a with marked chromosome XII	*MATα ade2-1 ura3-1 his3-11 trp1-1 leu2-3,112 can1-100 ChrXII-109,570::kanMX2 ChrXII-223,830::URA3*	This study
	XII^{200KU}	NOY408-1b with marked chromosome XII	*MATa ade2-1 ura3-1 his3-11 trp1-1 leu2-3,112 can1-100 ChrXII-109,570::kanMX2 ChrXII-223,830::URA3*	This study
*	$XII^{200/200KU}$	WT	*MATa/MATα ade2-1/ade2-1 ura3-1/ura3-1 his3-11/his3-11 trp1-1/trp1-1 leu2-3,112/leu2-3,112 can1-100/can1-100 ChrXII-109,570::kanMX2/ChrXII ChrXII-223,830::URA3/ChrXII*	Ogawa, Ganley and Kobayashi (unpublished)
*	$XII^{0/0KU}$+HP	rDNA deletion / 0-copy	*MATa/MATα ade2-1/ade2-1 ura3-1/ura3-1 his3-11/his3-11 trp1-1/trp1-1 leu2-3,112/leu2-3,112 can1-100/can1-100 ChrXII-109,570::kanMX2/ChrXII ChrXII-223,830::URA3/ChrXII rdn1ΔΔ/rdn1Δ::HIS3* +HP	Ogawa, Ganley and Kobayashi (unpublished)
*	$XII^{200/200KU}$+HP	HP control (WT with HP)	*MATa/MATα ade2-1/ade2-1 ura3-1/ura3-1 his3-11/his3-11 trp1-1/trp1-1 leu2-3,112/leu2-3,112 can1-100/can1-100 ChrXII-109,570::kanMX2/ChrXII ChrXII-223,830::URA3/ChrXII* +HP	This study
*	$XII^{200/200KU}$ *fob1*$^{-}$	*FOB1* disruption / *fob1*$^{-}$	*MATa/MATα ade2-1/ade2-1 ura3-1/ura3-1 his3-11/his3-11 trp1-1/trp1-1 leu2-3,112/leu2-3,112 can1-100/can1-100 ChrXII-109,570::kanMX2/ChrXII ChrXII-223,830::URA3/ChrXII, fob1::LEU2/fob1::LEU2*	Ogawa, Ganley and Kobayashi (unpublished)

*	XII$^{20/20KU}$ *fob1*$^{-}$	20-copy	*MATa/MATα ade2-1/ade2-1 ura3-1/ura3-1 his3-11/his3-11 trp1-1/trp1-1 leu2-3,112/leu2-3,112 can1-100/can1-100 ChrXII-109,570::kanMX2/ChrXII ChrXII-223,830::URA3/ChrXII fob1::LEU2/fob1::LEU2 RDNA1~*20copies*/RDNA1~*20copies	Ogawa, Ganley and Kobayashi (unpublished)
	XII^{20KU} *fob1*$^{-}$	spore from strain XII$^{20/20KU}$ *fob1*$^{-}$ (*fob1::LEU2*)	*MATa ade2-1 ura3-1 his3-11 trp1-1 leu2-3,112 can1-100 ChrXII-109,570::kanMX2 ChrXII-223,830::URA3 fob1::LEU2 RDNA1~*20copies	This study
	XII^{20KU} *fob1::HIS3*	*FOB1* marker replacementswap in spore XII^{20KU} *fob1*$^{-}$ (*leu2::HIS3*)	*MATa ade2-1 ura3-1 his3-11 trp1-1 leu2-3,112 can1-100 ChrXII-109,570::kanMX2 ChrXII-223,830::URA3 fob1::HIS3 RDNA1~*20copies	This study
	XII^{20} *fob1::ADE2*	*FOB1* marker replacement swap in TAK300 (*his3::ADE2*)	*MATα ade2-1 ura3-1 his3-11 trp1-1 leu2-3,112 can1-100 ChrXII-109,570::kanMX2 ChrXII-223,830::URA3 fob1::ADE2 RDNA1~20copies*	This study
*	XII$^{200/200KU}$ +pGAL-*FOB1*	WT with *FOB1* inducible plasmid	*MATa/MATα ade2-1/ade2-1 ura3-1/ura3-1 his3-11/his3-11 trp1-1/trp1-1 leu2-3,112/leu2-3,112 can1-100/can1-100 ChrXII-109,570::kanMX2/ChrXII ChrXII-223,830::URA3/ChrXII* +pGAL-*FOB1*	This study
*	XII$^{200/200KU}$ *fob1*$^{-}$ +pGAL-*FOB1*	*FOB1* disruption with *FOB1* inducible plasmid	*MATa/MATα ade2-1/ade2-1 ura3-1/ura3-1 his3-11/his3-11 trp1-1/trp1-1 leu2-3,112/leu2-3,112 can1-100/can1-100 ChrXII-109,570::kanMX2/ChrXII ChrXII-223,830::URA3/ChrXII, fob1::LEU2/fob1::LEU2* +pGAL-*FOB1*	This study
*	XII$^{20/20KU}$ *fob1*$^{-}$ +pGAL-*FOB1*	20-copy with *FOB1* inducible plasmid	*MATa/MATα ade2-1/ade2-1 ura3-1/ura3-1 his3-11/his3-11 trp1-1/trp1-1 leu2-3,112/leu2-3,112 can1-100/can1-100 ChrXII-109,570::kanMX2/ChrXII ChrXII-223,830::URA3/ChrXII fob1::LEU2/fob1::LEU2 RDNA1~*20copies/*RDNA1~*20copies +pGAL-*FOB1*	This study
*	XII$^{0/0KU}$ *fob1*$^{-}$ +HP	rDNA deletion with *FOB1* disruption	*MATa/MATα ade2-1/ade2-1 ura3-1/ura3-1 his3-11/his3-11 trp1-1/trp1-1 leu2-3,112/leu2-3,112 can1-100/can1-100 ChrXII-109,570::kanMX2/ChrXII ChrXII-223,830::URA3/ChrXII rdn1ΔΔ/rdn1Δ::HIS3* +HP, *fob1::LEU2/fob1::LEU2*	This study
	XII^{0K}+HP	spore 1A from strain XII$^{0/0KU}$+HP	*MATα ade2-1 ura3-1 his3-11 trp1-1 leu2-3,112 can1-100 ChrXII-109,570::kanMX2 rdn1Δ::HIS3* +HP	This study
	XII^{0}+HP	spore 1B from strain XII$^{0/0KU}$+HP	*MATα ade2-1 ura3-1 his3-11 trp1-1 leu2-3,112 can1-100 rdn1ΔΔ* +HP	This study
	XII^{0KU}+HP	spore 1C from strain XII$^{0/0KU}$+HP	*MATa ade2-1 ura3-1 his3-11 trp1-1 leu2-3,112 can1-100 ChrXII-109,570::kanMX2 ChrXII-223,830::URA3 rdn1ΔΔ* +HP	This study
	XII^{0KU} *fob1*$^{-}$ +HP	*FOB1* disruption in spore 1C from strain XII$^{0/0KU}$+HP	*MATa ade2-1 ura3-1 his3-11 trp1-1 leu2-3,112 can1-100 ChrXII-109,570::kanMX2 ChrXII-223,830::URA3 rdn1ΔΔ* +HP, *fob1::HIS3*	This study
	XII^{0U}+HP	spore 1D from strain XII$^{0/0KU}$+HP	*MATa ade2-1 ura3-1 his3-11 trp1-1 leu2-3,112 can1-100 ChrXII-223,830::URA3 rdn1Δ::HIS3* +HP	This study
	XII^{0}+HP	spore 2A from strain XII$^{0/0KU}$+HP	*MATa ade2-1 ura3-1 his3-11 trp1-1 leu2-3,112 can1-100 rdn1Δ::HIS3* +HP	This study
	XII^{0KU}+HP	spore 2B from strain XII$^{0/0KU}$+HP	*MATα ade2-1 ura3-1 his3-11 trp1-1 leu2-3,112 can1-100 ChrXII-109,570::kanMX2 ChrXII-223,830::URA3 rdn1Δ::HIS3* +HP	This study
	XII^{0}+HP	spore 2C from strain XII$^{0/0KU}$+HP	*MATa ade2-1 ura3-1 his3-11 trp1-1 leu2-3,112 can1-100 rdn1ΔΔ* +HP	This study
	XII^{0KU}+HP	spore 2D from strain XII$^{0/0KU}$+HP	*MATα ade2-1 ura3-1 his3-11 trp1-1 leu2-3,112 can1-100 ChrXII-109,570::kanMX2 ChrXII-223,830::URA3 rdn1ΔΔ* +HP	This study
*	XII$^{200/200KU}$ *rpa135Δ*+HP	*RPA135* deletion/ *rpa135Δ::LEU2/ rpa135Δ /rpa135*$^{-}$	*MATa/MATα ade2-1/ade2-1 ura3-1/ura3-1 his3-11/his3-11 trp1-1/trp1-1 leu2-3,112/leu2-3,112 can1-100/can1-100 ChrXII-109,570::kanMX2/ChrXII ChrXII-223,830::URA3/ChrXII rpa135::LEU2/rpa135::LEU2 +HP*	This study
	XII$^{200/200KU}$ *RPA135/rpa135Δ::LEU2*+HP	heterozygous *RPA135* deletion	*MATa/MATα ade2-1/ade2-1 ura3-1/ura3-1 his3-11/his3-11 trp1-1/trp1-1 leu2-3,112/leu2-3,112 can1-100/can1-100 ChrXII-109,570::kanMX2/ChrXII ChrXII-223,830::URA3/ChrXII RPA135/rpa135::LEU2 +HP*	Woods, Quintana and Ganley (unpublished)

	XII^{200KU} *rpa135Δ::LEU2*+HP	spore from strain XII$^{200/200KU}$ *rpa135Δ*+HP with CLA markers	*MATa ade2-1 ura3-1 his3-11 trp1-1 leu2-3,112 can1-100 ChrXII-109,570::kanMX2 ChrXII-223,830::URA3 rpa135::LEU2 +HP*	This study
	XII^{200} *rpa135Δ::LEU2*+HP	unmarked spore from strain XII$^{200/200KU}$ *rpa135Δ*+HP	*MATα ade2-1 ura3-1 his3-11 trp1-1 leu2-3,112 can1-100 rpa135::LEU2 +HP*	This study
*	XII$^{200/200KU}$ *rpa135Δ*+HP *fob1-*	*FOB1* disruption strain with a *RPA135* deletion	*MATa/MATα ade2-1/ade2-1 ura3-1/ura3-1 his3-11/his3-11 trp1-1/trp1-1 leu2-3,112/leu2-3,112 can1-100/can1-100 ChrXII-109,570::kanMX2/ChrXII ChrXII-223,830::URA3/ChrXII RPA135/rpa135::LEU2 fob1::HIS3/fob1::HIS3 +HP*	This study
	XII$^{200/200KU}$ *rpa135Δ*+HP *FOB1/fob1::HIS3*	Heterozygous *FOB1* disruption with a *RPA135* deletion	*MATa/MATα ade2-1/ade2-1 ura3-1/ura3-1 his3-11/his3-11 trp1-1/trp1-1 leu2-3,112/leu2-3,112 can1-100/can1-100 ChrXII-109,570::kanMX2/ChrXII ChrXII-223,830::URA3/ChrXII RPA135/rpa135::LEU2 FOB1/fob1::HIS3 +HP*	This study
	XII^{200KU} *rpa135Δ*+HP *fob1::HIS3*	spore from strain XII$^{200/200KU}$ *rpa135Δ*+HP *fob1::HIS3* with CLA markers	*MATa ade2-1 ura3-1 his3-11 trp1-1 leu2-3,112 can1-100 ChrXII-109,570::kanMX2 ChrXII-223,830::URA3 rpa135::LEU2 fob1::HIS3 +HP*	This study
	XII^{200} *rpa135Δ*+HP *fob1::HIS3*	unmarked spore from strain XII$^{200/200KU}$ *rpa135Δ*+HP *fob1::HIS3*	*MATα ade2-1 ura3-1 his3-11 trp1-1 leu2-3,112 can1-100 rpa135::LEU2 fob1::HIS3 +HP*	This study
	XII$^{20/20KU}$ *RPA135/rpa135Δ::LEU2*+HP *fob1-*	20-copy homozygous with *FOB1* disruption, heterozygous for *RPA135* deletion	*MATa/MATα ade2-1/ade2-1 ura3-1/ura3-1 his3-11/his3-11 trp1-1/trp1-1 leu2-3,112/leu2-3,112 can1-100/can1-100 ChrXII-109,570::kanMX2/ChrXII ChrXII-223,830::URA3/ChrXII RPA135/rpa135::LEU2 fob1::HIS3/fob1::HIS3 +HP*	This study
	XII$^{20/20KU}$ *fob1- RPA135/rpa135Δ::leu2::ADE2*+HP.	20-copy homozygous with *FOB1* disruption, heterozygous for *RPA135* deletion with replacement marker swap	*MATa/MATα ade2-1/ade2-1 ura3-1/ura3-1 his3-11/his3-11 trp1-1/trp1-1 leu2-3,112/leu2-3,112 can1-100/can1-100 ChrXII-109,570::kanMX2/ChrXII ChrXII-223,830::URA3/ChrXII RPA135/rpa135::ADE2 fob1::HIS3/fob1::HIS3 +HP*	This study
	XII$^{200/20KU}$ *fob1- RPA135/rpa135Δ::LEU2*+HP	rDNA state heterozygous with *FOB1* disruption, heterozygous for *RPA135* deletion	*MATa/MATα ade2-1/ade2-1 ura3-1/ura3-1 his3-11/his3-11 trp1-1/trp1-1 leu2-3,112/leu2-3,112 can1-100/can1-100 ChrXII-109,570::kanMX2/ChrXII ChrXII-223,830::URA3/ChrXII, fob1::HIS3, RDNA1~*20copies*/RDN1 RPA135/rpa135::LEU2 fob1::HIS3/fob1::HIS3 +HP*	This study
	XII^{20K} *fob1- rpa135Δ::LEU2* +HP	Spore 1A from strain XII$^{200/20KU}$ *fob1- RPA135/rpa135Δ::LEU2*+HP	*MATa ade2-1 ura3-1 his3-11 trp1-1 leu2-3,112 can1-100 rpa135::LEU2 fob1::HIS3 RDNA1~*20copies *ChrXII-109,570::kanMX2* +HP	This study
	XII$^{~50}$ *fob1- RPA135*+HP	Spore 1B from strain XII$^{200/20KU}$ *fob1- RPA135/rpa135Δ::LEU2*+HP	*MATα ade2-1 ura3-1 his3-11 trp1-1 leu2-3,112 can1-100 fob1::HIS3 RDNA1~*50copies +HP	This study
	XII$^{~50U}$ *fob1- RPA135*+HP	Spore 1C from strain XII$^{200/20KU}$ *fob1- RPA135/rpa135Δ::LEU2*+HP	*MATα ade2-1 ura3-1 his3-11 trp1-1 leu2-3,112 can1-100 fob1::HIS3 RDNA1~*50copies *ChrXII-223,830::URA3* +HP	This study

XII^{20KU} *fob1-rpa135Δ::LEU2* +HP	Spore 1D from strain XII$^{200/20KU}$ *fob1-RPA135/rpa135Δ::LEU2*+HP	*MATa ade2-1 ura3-1 his3-11 trp1-1 leu2-3,112 can1-100 rpa135::LEU2 fob1::HIS3 RDNA1~*20copies *ChrXII-109,570::kanMX2 ChrXII-223,830::URA3* +HP	This study
XII$^{\sim 50K}$ *fob1-RPA135*+HP	Spore 2A from strain XII$^{200/20KU}$ *fob1-RPA135/rpa135Δ::LEU2*+HP	*MATa ade2-1 ura3-1 his3-11 trp1-1 leu2-3,112 can1-100 fob1::HIS3 RDNA1~*50copies *ChrXII-109,570::kanMX2* +HP	This study
XII^{20U} *fob1-rpa135Δ::LEU2* +HP	Spore 2B from strain XII$^{200/20KU}$ *fob1-RPA135/rpa135Δ::LEU2*+HP	*MATa? ade2-1 ura3-1 his3-11 trp1-1 leu2-3,112 can1-100 rpa135::LEU2 fob1::HIS3 RDNA1~*20copies *ChrXII-223,830::URA3* +HP	This study
XII$^{\sim 50KU}$ *fob1-RPA135*+HP	Spore 2C from strain XII$^{200/20KU}$ *fob1-RPA135/rpa135Δ::LEU2*+HP	*MATα ade2-1 ura3-1 his3-11 trp1-1 leu2-3,112 can1-100 fob1::HIS3 RDNA1~*50copies *ChrXII-109,570::kanMX2 ChrXII-223,830::URA3* +HP	This study
XII^{20} *fob1-rpa135Δ::LEU2* +HP	Spore 2D from strain XII$^{200/20KU}$ *fob1-RPA135/rpa135Δ::LEU2*+HP	*MATα? ade2-1 ura3-1 his3-11 trp1-1 leu2-3,112 can1-100 rpa135::LEU2 fob1::HIS3 RDNA1~*20copies +HP	This study
XII$^{\sim 50K}$ *fob1-RPA135*+HP	Spore 3A from strain XII$^{200/20KU}$ *fob1-RPA135/rpa135Δ::LEU2*+HP	*MATα? ade2-1 ura3-1 his3-11 trp1-1 leu2-3,112 can1-100 fob1::HIS3 RDNA1~*50copies *ChrXII-109,570::kanMX2* +HP	This study
XII$^{\sim 50K}$ *fob1-RPA135*+HP	Spore 3B from strain XII$^{200/20KU}$ *fob1-RPA135/rpa135Δ::LEU2*+HP	*MATa? ade2-1 ura3-1 his3-11 trp1-1 leu2-3,112 can1-100 fob1::HIS3 RDNA1~*50copies *ChrXII-109,570::kanMX2* +HP	This study
XII^{20U} *fob1-rpa135Δ::LEU2* +HP	Spore 3C from strain XII$^{200/20KU}$ *fob1-RPA135/rpa135Δ::LEU2*+HP	*MATa? ade2-1 ura3-1 his3-11 trp1-1 leu2-3,112 can1-100 rpa135::LEU2 fob1::HIS3 RDNA1~*20copies *ChrXII-223,830::URA3* +HP	This study
XII^{20U} *fob1-rpa135Δ::LEU2* +HP	Spore 3D from strain XII$^{200/20KU}$ *fob1-RPA135/rpa135Δ::LEU2*+HP	*MATα? ade2-1 ura3-1 his3-11 trp1-1 leu2-3,112 can1-100 rpa135::LEU2 fob1::HIS3 RDNA1~*20copies *ChrXII-223,830::URA3* +HP	This study
XII^{20KU} *fob1-rpa135Δ::LEU2* +HP	Spore 4A from strain XII$^{200/20KU}$ *fob1-RPA135/rpa135Δ::LEU2*+HP	*MATa ade2-1 ura3-1 his3-11 trp1-1 leu2-3,112 can1-100 rpa135::LEU2 fob1::HIS3 RDNA1~*20copies *ChrXII-109,570::kanMX2 ChrXII-223,830::URA3* +HP	This study
XII$^{\sim 50K}$ *fob1-RPA135*+HP	Spore 4B from strain XII$^{200/20KU}$ *fob1-RPA135/rpa135Δ::LEU2*+HP	*MATα ade2-1 ura3-1 his3-11 trp1-1 leu2-3,112 can1-100 fob1::HIS3 RDNA1~*50copies *ChrXII-109,570::kanMX2* +HP	This study
XII^{20U} *fob1-rpa135Δ::LEU2* +HP	Spore 4C from strain XII$^{200/20KU}$ *fob1-RPA135/rpa135Δ::LEU2*+HP	*MATa ade2-1 ura3-1 his3-11 trp1-1 leu2-3,112 can1-100 rpa135::LEU2 fob1::HIS3 RDNA1~*20copies *ChrXII-223,830::URA3* +HP	This study

	XII$^{\sim 50}$ *fob1-RPA135*+HP	Spore 4D from strain XII$^{200/20KU}$ *fob1-RPA135/rpa135Δ::LEU2*+HP	*MATα ade2-1 ura3-1 his3-11 trp1-1 leu2-3,112 can1-100 fob1::HIS3 RDNA1*~50copies +HP	This study
	XII$^{0/0KU}$ *RPA135/rpa135Δ::LEU2* +HP	rDNA deletion, heterozygous for *RPA135* deletion	*MATa/MATα ade2-1/ade2-1 ura3-1/ura3-1 his3-11/his3-11 trp1-1/trp1-1 leu2-3,112/leu2-3,112 can1-100/can1-100 ChrXII-109,570::kanMX2/ChrXII ChrXII-223,830::URA3/ChrXII RPA135/rpa135::LEU2 rdn1ΔΔ/rdn1Δ::HIS3* +HP	This study
	XII$^{200/0KU}$ *RPA135/rpa135Δ* +HP *FOB1/fob1::HIS3*	heterozygous for a *RPA135* deletion, a rDNA deletion and a *FOB1* disruption	*MATa/MATα ade2-1/ade2-1 ura3-1/ura3-1 his3-11/his3-11 trp1-1/trp1-1 leu2-3,112/leu2-3,112 can1-100/can1-100 ChrXII-109,570::kanMX2/ChrXII ChrXII-223,830::URA3/ChrXII FOB1/fob1::HIS3 RPA135/rpa135::LEU2 RDN1/rdn1ΔΔ +HP*	This study
*	XII$^{0/200KU}$+HP	rDNA state heterozygous 0/200	*MATa/MATα ade2-1/ade2-1 ura3-1/ura3-1 his3-11/his3-11 trp1-1/trp1-1 leu2-3,112/leu2-3,112 can1-100/can1-100 ChrXII-109,570::kanMX2/ChrXII ChrXII-223,830::URA3/ChrXII, RDNA1/rdn1Δ::HIS3G* +HP	This study
	XII$^{200/0KU}$+HP	rDNA state heterozygous 200/0	*MATa/MATα ade2-1/ade2-1 ura3-1/ura3-1 his3-11/his3-11 trp1-1/trp1-1 leu2-3,112/leu2-3,112 can1-100/can1-100 ChrXII-109,570::kanMX2/ChrXII ChrXII-223,830::URA3/ChrXII, RDNA1/rdn1Δ::HIS3G* +HP	This study
*	XII$^{20/200KU}$ *fob1-*	rDNA state heterozygous 20/200	MATa/MATα *ade2-1/ade2-1 ura3-1/ura3-1 his3-11/his3-11 trp1-1/trp1-1 leu2-3,112/leu2-3,112 can1-100/can1-100 ChrXII-109,570::kanMX2/ChrXII ChrXII-223,830::URA3/ChrXII, fob1::HIS3/fob1::HIS3, RDNA1/RDNA1*~20copies	This study
*	XII$^{200/20KU}$ *fob1-*	rDNA state heterozygous 200/20	*MATa/MATα ade2-1/ade2-1 ura3-1/ura3-1 his3-11/his3-11 trp1-1/trp1-1 leu2-3,112/leu2-3,112 can1-100/can1-100 ChrXII-109,570::kanMX2/ChrXII ChrXII-223,830::URA3/ChrXII, fob1::HIS3, RDNA1*~20copies/*RDN1*	This study
*	XII$^{20/0KU}$ *fob1-* +HP	rDNA state heterozygous 20/0	*MATa/MATα ade2-1/ade2-1 ura3-1/ura3-1 his3-11/his3-11 trp1-1/trp1-1 leu2-3,112/leu2-3,112 can1-100/can1-100 ChrXII-109,570::kanMX2/ChrXII ChrXII-223,830::URA3/ChrXII, rdn1Δ::HIS3G/RDNA1* ~20 copies +HP	This study
*	XII$^{0/20KU}$ *fob1-* +HP	rDNA state heterozygous 0/20	*MATa/MATα ade2-1/ade2-1 ura3-1/ura3-1 his3-11/his3-11 trp1-1/trp1-1 leu2-3,112/leu2-3,112 can1-100/can1-100 ChrXII-109,570::kanMX2/ChrXII ChrXII-223,830::URA3/ChrXII, RDNA1* ~20 copies/*rdn1Δ::HIS3G* +HP	This study
*	V$^{0/0KU}$ XII$^{200/200}$	Chromosome V WT	*MATa/MATα ade2-1/ade2-1 ura3-1/ura3-1 his3-11/his3-11 trp1-1/trp1-1 leu2-3,112/leu2-3,112 can1-100/can1-100 ChrV-108,414::URA3/ChrV ChrV-424,837::kanMX2/ChrV*	This study
*	VI$^{0/0KU}$ XII$^{200/200}$	Chromosome VI WT	*MATa/MATα ade2-1/ade2-1 ura3-1/ura3-1 his3-11/his3-11 trp1-1/trp1-1 leu2-3,112/leu2-3,112 can1-100/can1-100 ChrVI-38,790::URA3/ChrVI ChrVI-172,381::kanMX2/ChrVI*	This study
	V^{0KU} XII^{200}	Chromosome V marked WT haploid	*MATa ade2-1 ura3-1 his3-11 trp1-1 leu2-3,112 can1-100 ChrV-108,414::URA3 ChrV-424,837::kanMX2*	This study
	VI^{0KU} XII^{200}	Chromosome VI marked WT haploid	*MATa ade2-1 ura3-1 his3-11 trp1-1 leu2-3,112 can1-100 ChrVI-38,790::URA3 ChrVI-172,381::kanMX2*	This study
*	VI$^{0/0KU}$ XII$^{0/0}$+HP	Chromosome VI marked rDNA deletion	*MATa/MATα ade2-1/ade2-1 ura3-1/ura3-1 his3-11/his3-11 trp1-1/trp1-1 leu2-3,112/leu2-3,112 can1-100/can1-100 ChrVI-38,790::URA3/ChrVI ChrVI-172,381::kanMX2/ChrVI, rdn1ΔΔ/rdn1Δ::HIS3* +HP	This study
	VI^{0KU} XII^{0}+HP	Chromosome VI marked rDNA deletion haploid	*MATα ade2-1 ura3-1 his3-11 trp1-1 leu2-3,112 can1-100 ChrVI-38,790::URA3 ChrVI-172,381::kanMX2 rdn1ΔΔ* +HP	This study

*	VI$^{0/0KU}$ XII$^{200/200}$ *fob1*$^{-}$	Chromosome VI marked *FOB1* disruption	*MATa/MATα ade2-1/ade2-1 ura3-1/ura3-1 his3-11/his3-11 trp1-1/trp1-1 leu2-3,112/leu2-3,112 can1-100/can1-100 ChrVI-38,790::URA3/ChrVI ChrVI-172,381::kanMX2/ChrVI, fob1::LEU2/fob1::HIS3*	This study
	VI^{0KU} XII^{200} *fob1::LEU2*	Chromosome VI marked *FOB1* disruption haploid	*MATa ade2-1 ura3-1 his3-11 trp1-1 leu2-3,112 can1-100 ChrVI-38,790::URA3 ChrVI-172,381::kanMX2* fob1::LEU2	This study
*	VI$^{0/0KU}$ XII$^{20/20}$ *fob1*$^{-}$	Chromosome VI marked 20-copy	*MATa/MATα ade2-1/ade2-1 ura3-1/ura3-1 his3-11/his3-11 trp1-1/trp1-1 leu2-3,112/leu2-3,112 can1-100/can1-100 ChrVI-38,790::URA3/ChrVI ChrVI-172,381::kanMX2/ChrVI,* fob1::LEU2/fob1::HIS3 *RDNA1*~20copies/*RDNA1*~20copies	This study
	VI^{0KU} XII^{20} *fob1::LEU2*	Chromosome VI marked 20-copy haploid (derived from TAK300)	*MATα ade2-1 ura3-1 his3-11 trp1-1 leu2-3,112 can1-100 ChrVI-38,790::URA3 ChrVI-172,381::kanMX2 fob1::LEU2 RDNA1*~20copies	This study
*	VI$^{0/0KU}$ XII$^{0/200}$+HP	Chromosome VI marked rDNA state heterozygote 0/200	*MATa/MATalpha ade2-1/ade2-1 ura3-1/ura3-1 his3-11/his3-11 trp1-1/trp1-1 leu2-3,112/leu2-3,112 can1-100/can1-100 ChrVI-38,790::URA3/ChrVI ChrVI-172,381::kanMX2/ChrVI, RDNA1/rdn1ΔΔ* +HP	This study
*	VI$^{0/0KU}$ XII$^{0/20}$ *fob1*$^{-}$ +HP	Chromosome VI marked rDNA state heterozygote 0/20	*MATa/MATα ade2-1/ade2-1 ura3-1/ura3-1 his3-11/his3-11 trp1-1/trp1-1 leu2-3,112/leu2-3,112 can1-100/can1-100 ChrVI-38,790/ChrVI-38,790::URA3/ChrVI ChrVI-172,381::kanMX2/ChrVI,* fob1::HIS3/fob1::HIS3 *RDNA1*~20copies/*rdn1ΔΔ* +HP	This study
*	XII$^{200/200*KU}$	Hygromycin resistant WT	*MATa/MATα ade2-1/ade2-1 ura3-1/ura3-1 his3-11/his3-11 trp1-1/trp1-1 can1-100/can1-100 ChrXII-109,570::kanMX2/ChrXII ChrXII-223,830::URA3/ChrXII rdn1Δ::rdn1-Hyg^{R}/RDN1*	This study
	XII^{200*KU}	Chromosome XII marked hygromycin resistant WT haploid. Derived from NOY2029	*MATa ade2-1 ura3-1 his3-11 trp1-1 LEU2 can1-100 ChrXII-109,570::kanMX2 ChrXII-223,830::URA3 rdn1::rdn1-Hyg^{R}* (rDNA*)	This study
*	XII$^{200/200KU}$ V$^{0/200*}$	WT with heterozygous rDNA translocation on chromosome V	*MATa/MATα ade2-1/ade2-1 ura3-1/ura3-1 his3-11/his3-11 trp1-1/trp1-1 LEU2/leu2-3,112 can1-100/can1-100 ChrXII-109,570::kanMX2/ChrXII ChrXII-223,830::URA3/ChrXII rdn1-Hyg^{R}* (rDNA*) array near *CEN5*	This study
	XII^{200KU} V^{200*}	NOY2053 with marked chromosome XII	*MATa ade2-1 ura3-1 trp1-1 leu2-3,112 his3-11,15 can1-100, RDN1 and rDNA* array near CEN5, ChrXII-109,570::kanMX2 ChrXII-223,830::URA3*	Woods, Quintana and Ganley (unpublished)
*	XII$^{0/200KU}$ V$^{0/200*}$+HP	rDNA state heterozygous for chromosome XII (marked) and V	*MATa/MATα ade2-1/ade2-1 ura3-1/ura3-1 his3-11/his3-11 trp1-1/trp1-1 leu2-3,112/leu2-3,112 can1-100/can1-100 ChrXII-109,570::kanMX2/ChrXII ChrXII-223,830::URA3/ChrXII, RDNA1/rdn1Δ::HIS3G, rdn1-Hyg^{R}* (rDNA*) array near *CEN5* +HP	This study
*	XII$^{0/200KU}$ V$^{0/200*}$ *fob1*$^{-}$ +HP	rDNA state heterozygous for chromosome XII (marked) and V, harboring a *FOB1* disruption	*MATa/MATα ade2-1/ade2-1 ura3-1/ura3-1 his3-11/his3-11 trp1-1/trp1-1 leu2-3,112/leu2-3,112 can1-100/can1-100 ChrXII-109,570::kanMX2/ChrXII ChrXII-223,830::URA3/ChrXII, RDNA1/rdn1Δ::HIS3G, rdn1-Hyg^{R}* (rDNA*) array near *CEN5, fob1::ADE2/fob1::HIS3,* +HP	This study
	XII^{200KU} V^{200*} *fob1*$^{-}$	NOY2053 with marked chromosome XII and a *FOB1* disruption	*MATa ade2-1 ura3-1 trp1-1 leu2-3,112 his3-11,15 can1-100, RDN1 and rDNA* array near CEN5, ChrXII-109,570::kanMX2 ChrXII-223,830::URA3 fob1::ADE2*	This study

*	$V^{0/200*KU}$ $XII^{200/200}$	WT with marked heterozygous rDNA translocation on chromosome V	*MATa/MATα ade2-1/ade2-1 ura3-1/ura3-1 his3-11/his3-11 trp1-1/trp1-1 LEU2/leu2-3,112 can1-100/can1-100 ChrV-108,414::URA3/ChrV ChrV-424,837::kanMX2/ChrV*, *rdn1-Hyg^R* (rDNA*) array near *CEN5*	This study
	V^{200*KU} XII^{200}	NOY2053 with marked chromosome V	*MATa ade2-1 ura3-1 trp1-1 leu2-3,112 his3-11,15 can1-100, RDN1 and rDNA* array near CEN5 ChrV-108,414::URA3 ChrV-424,837::kanMX2*	Woods, Quintana and Ganley (unpublished)
	XII^{200} V^{0}	WT haploid with *LEU2* gene repaired to use as a mating marker	*MATα ade2-1 ura3-1 his3-11 trp1-1 can1-100*	Woods, Quintana and Ganley (unpublished)
*	$V^{0/*200KU}$ $XII^{0/200}$+HP	Double rDNA state heterozygous for chromosome XII and chromsosome V (marked)	*MATa/MATα ade2-1/ade2-1 ura3-1/ura3-1 his3-11/his3-11 trp1-1/trp1-1 LEU2/leu2-3,112 can1-100/can1-100, ChrV-108,414::URA3/ChrV ChrV-424,837::kanMX2/ChrV*, rDNA* array near *CEN5, RDN1/rdnΔΔ::hisG,* +HP	Woods, Quintana and Ganley (unpublished)
	V^{200*KU} XII^{0}	NOY2030 with marked chromosome V	*MATα ade2-1 ura3-1 trp1-1 leu2-3,112 his3-11,15 can1-100 rdnΔΔ::hisG, rDNA* array near CEN5 ChrV-108,414::URA3 ChrV-424,837::kanMX2*	This study
*	$V^{0/200*KU}$ $XII^{0/200}$ *fob1*$^-$ +HP	Double rDNA state heterozygous for chromosome XII and chromsosome V (marked), harboring a *FOB1* disruption	*MATa/MATα ade2-1/ade2-1 ura3-1/ura3-1 his3-11/his3-11 trp1-1/trp1-1 leu2-3,112/leu2-3,112 can1-100/can1-100, ChrV-108,414::URA3/ChrV ChrV-424,837::kanMX2/ChrV, rdn1-Hyg^R* (rDNA*) array near *CEN5, fob1::ADE2/fob1::HIS3*, *RDN1/rdnΔΔ::hisG* +HP	This study
	V^{200*KU} XII^{200} *fob1::ADE2*	NOY2053 with marked chromosome V and a *FOB1* disruption	*MATa ade2-1 ura3-1 trp1-1 leu2-3,112 his3-11,15 can1-100, RDN1 and rDNA* array near CEN5 ChrV-108,414::URA3 ChrV-424,837::kanMX2 fob1::ADE2*	This study
	Schizosaccharomyces pombe			
	FY7950 (MY79)	Used to amplify *SpADE6*	h-leu1	M. Yanagida (Japan)
	Escherichia coli			
	TOP10	Used for cloning	F-*mcrA Δ(mrr-hsdRMS-mcrBC) φ80lacZΔM15 ΔlacX74 nupG recA1 araD139 Δ(ara-leu)7697 galE15 galK16 rpsL(StrR) endA1 λ-*	Invitrogen C4040

Table II. List of plasmids

Plasmid	Features	Origin
DAG135	pCR2.1 vector containing the *RPA135* gene and its flanking regions in the MCS. Refer to figure 4.21B for details.	This study
p*GAL-FOB1*	YCpLac22 plasmid containing a galatose promoter fused to the *FOB1* gene in the MCS. Refer to figure 4.14 for details.	This study
pCR2.1	Linear TA cloning vector with T overhangs	Invitrogen K4500-01 (Yanisch-Perron et al. 1985).
HP (helper plasmid)	pNOY353 . Refer to figure 4.5 for details.	(Wai et al. 2000) Kind gift of Takehiko Kobayashi (National Institute of Genetics).
pUC19	*E. coli* cloning vector	Invitrogen SD0061 (Yanisch-Perron et al. 1985).
YCpLac22	*S. cerevisiae* - *E. coli* shuttle vector derived from pUC19. This plasmid contains the pUC19 MCS, amp^R, *S. cerevisiae* origin of replication *ARS1*, the *S. cerevisiae CEN4* centromere, and *TRP1.*	(Gietz and Sugino 1988).
YEpLac181	*S. cerevisiae* - *E. coli* shuttle vector derived from pUC19. This plasmid contains the pUC19 MCS, amp^R, *S. cerevisiae* 2 μm DNA replicating origin and *LEU2.*	(Gietz and Sugino 1988).
YEpLac195	*S. cerevisiae* - *E. coli* shuttle vector derived from pUC19. This plasmid contains the pUC19 MCS, amp^R, *S. cerevisiae* 2 μm DNA replicating origin and *URA3.*	(Gietz and Sugino 1988).
M3939	*leu2::ADE2* marker swap plasmid	(Voth et al. 2003) Kind gift of Evelyn Sattleger (Massey University).
M2371	*his3::ADE2* marker swap plasmid	(Voth et al. 2003) Kind gift of Evelyn Sattleger (Massey University).

2.2 GROWTH CONDITIONS

All strains (yeast and bacterial) were grown on agar plates or on liquid medium while shaking at 150 rpm, and stored long term at -80 °C in 15% glycerol.

2.2.1 Yeast growth conditions

S. cerevisiae strains and the single *S. pombe* strain were grown on rich or selective media at 30 °C. To grow yeast colonies on agar plates, a sterile loop was used to streak a dash of yeast cells onto an agar plate. For liquid cultures, typically a single colony collected from an agar plate was inoculated into liquid medium using a sterile loop, and grown on a rotating wheel at 150 rpm.

2.2.2 Yeast media

All media were prepared using Milli-Q water and sterilized by autoclaving at 121 °C for 20 min.

2.2.2.1 Rich media: Yeast Peptone Dextrose (YPD) or Yeast Peptone Galactose (YPGal) Media

S. cerevisiae rich medium contains:

- 20 g/L peptone (Formedium)
- 10 g/L yeast extract (YE, Formedium)
- 20 g/L glucose (Formedium) (YPD) or galactose (Formedium) (YPGal)
- To make agar plates: 20 g/L agar (Formedium).

2.2.2.2 Synthetic Dextrose (Usdin) or Synthetic Galactose (SGal) Media

Yeast selective medium consisted of:

- 6.9 g/L yeast nitrogen base (YNB, Formedium)
- 20 g/L glucose (Formedium) (Usdin) or galactose (Formedium) (SGal)
- 200 mg/L aa mix
-160 mg/L full mix (or dropout if selection was required).

- To make agar plates: 25 g/L agar (Formedium).

2.2.2.3 Starvation Medium (SM)

Starvation medium consisted of:

- 10 mg/ml potassium acetate
- 0.05 mg/ml aa mix
- 0.04 mg/ml full mix
- 25 g/L agar.

2.2.2.4 Supplements, antibiotics and drugs

aa mix (used at a concentration of 200 mg/L): 0.4 g arginine, 0.4 g methionine, 0.6 g tyrosine, 0.6 g isoleucine, 0.6 g lysine, 1 g phenylalanine, 2 g glutamic acid, 2 g aspartic acid, 3 g valine, 4 g threonine, 8 g serine.

Full Mix (160 mg/L): 2 g adenine, 2 g uracil, 2 g tryptophan, 2 g histidine, 10 g leucine. Dropout mixes were prepared as the full mix but without the specified amino acid.

5-Fluoroorotic Acid (5FOA): To supplement agar plates, 750 mg of 5FOA (Formedium) were resuspended in 200 mL water (20% of the final volume), stirred for 1 hr while heated to 65°C, and filter sterilized into the autoclaved SD Full medium, to a final concentration of 1 g/L 5FOA .

Geneticin (G418): To supplement agar plates, 187.5 mg of G418 (Formedium) were resuspended in 50 mL of water and filter sterilized into autoclaved YPD or YPGal medium to a final concentration of 250 mg/L G418.

2.2.2.5 EMM-N medium for *S. pombe*

For *S. pombe* 23.7 g/L Edinburgh Minimal Media broth without nitrogen (EMM-N) (Formedium PMD1301) was used, supplemented with 0.925 g/L adenine dropout mix (containing equal amounts of histidine, lysine, uracil, and leucine). For plates, 20 g/L agar (Formedium) was added.

2.2.3 Bacterial media and growth conditions

All bacterial strains were grown at 37 °C on sealed agar plates or in liquid medium while shaking at 150 rpm. The bacterial medium used was Luria-Bertani (Alberts et al.) (1% NaCl, 1% bacto tryptone, 0.5% bacto yeast extract) supplemented with ampicillin 100 ug/ml.

For LB plates, 1.5% agar, 40 ug/ml XGal and 0.1 mM IPTG were added where necessary. For bacterial cell transformations, Super Optimal broth with Catabolite repression (Wysocka et al.) medium (Invitrogen 15544-034; 2% tryptone, 0.5% yeast extract, 10 mM NaCl, 2.5 mM KCl, 10 mM $MgCl_2$, 10 mM $MgSO_4$, and 20 mM glucose) was used.

2.2.4 Cell concentration from optical density (OD) measurements

To estimate cell concentration, liquid cultures were typically diluted 10-fold in sterile Mili-Q water and their optical density (OD) was measured at 600 nm (OD_{600nm}) using a Shimadzu UV Mini-1240 spectrophotometer. An OD_{600nm} of 1 is approximately $2x10^7$ cells/ml.

2.2.5 Growth curves

To compare growth between strains, growth curves were performed in 96-well plates with either rich or selective media. Cells were diluted to an OD_{600nm} of 0.1 from overnight stationary phase liquid cultures, and 100 μl of diluted culture were loaded per well. Each sample was measured in triplicate, and three biological samples were used for each strain. A FLUOstar Optima microplate reader (BMG LABTECHNOLOGIES) was used to measure the OD_{595nm} every 5 min for 21 hours. The machine was programmed to incubate the plate at 30 °C for the duration of the growth curve, with 7 mm linear shaking of the plate before every OD measurement.

2.3 MATINGS AND SPORULATIONS

2.3.1. *S. cerevisiae* matings

To create diploid *S. cerevisiae* strains, a liquid culture mating method was used. Haploids of opposite mating types were each grown overnight in 2 mL of rich medium (YPD or YPGal as required) to stationary phase. The OD_{600nm} of each cell culture was measured, the strains diluted to an $OD6_{00nm}$ of 0.2 and equal volumes (1.5 mL of each) were mixed in a round bottom glass test tube. This mixed culture was incubated at 30 °C while shaking at 150 rpm for

4 hours, and then placed at room temperature overnight without shaking. Successful matings produced a diffuse pellet at the bottom of the tube, whereas tight pellets were indicative of negative matings. If each haploid contained a unique selective marker, 100 μl from the resulting mating were plated onto double selective medium for phenotypic selection of diploids. If mating markers were not available, the resulting mating was mixed and 10 μl were smeared on the edge of a rich medium plate. Zygotes were picked from the smear on the plate and isolated onto a clear area on the plate using a Singer micromanipulation microscope MSM400 based on the "shmoo" pear-shaped phenotype. 8-16 zygotes were isolated for each diploid strain, and their diploid state was confirmed through mating type PCR.

2.3.2 *S. cerevisiae* sporulation of diploid strains

To induce sporulation, diploid strains were streaked onto starvation medium plates and incubated at room temperature. After one week, a dab of cells were inoculated into 50 μl of 20T zymolyase solution (20 mM Tris-HCl, pH 7.4, 50% glycerol, 20 mg/ml zymolyase 20T (Nacalai Tesque)) and incubated at 37 °C for approximately 5 min to digest the ascus coat, so that the four ascospores (spores) can be broken apart easily. The digestion reaction was stopped by adding 150 μl of sterile water and placing the tube on ice. 10 μl of zymolyase treated cells were applied to the edge of a rich medium plate. Using the micromanipulation microscope, tetrads were identified phenotypically (cluster of four small cells) and transferred to a clear area on the plate. The four spores were separated using the micromanipulation needle. At least 4-8 tetrads were picked for each strain, and spores were incubated as usual.

2.3.3 Determination of mating type or diploidy

The mating type of haploid and diploid strains was most commonly determined through mating type PCR using the primers from Bradbury et al. (2006) (table III). Haploid state was occasionally determined through the liquid culture method (section 2.3.1), by setting up matings with both confirmed MATa and MATα haploids, the resulting pellets (diffuse or tight) indicated whether the strain being tested was MATa or MATα. Diploid state, when possible, was determined through phenotypic selection of mating markers.

2.4 DNA PROTOCOLS

2.4.1 Yeast genomic DNA isolation

This protocol was modified from Cao et al. (1990). Yeast genomic DNA (gDNA) was extracted from 1-2 mL of liquid cultures grown overnight in rich medium until stationary phase. Cells were pelleted by centrifugation at full speed for 1 min, washed with 500 μl of 50 mM EDTA pH 8.0 and resuspended in 180 μl of 50 mM EDTA. 20 μl of 20 mg/ml 20T zymolyase solution (20 mM Tris-HCl, pH 7.4, 50% glycerol, 20 mg/ml zymolyase 20-T (Nacalai Tesque)) were added, mixed by vortexing, and incubated at 37 °C for 30 min – 1 hr. Next, 20 μl of 10% sodium dodecyl sulphate (SDS) solution was added and incubated at 65 °C for 20 min, and then 150 μl of 5 M sodium acetate were added, mixed, and incubated for 20 min on ice. An equal volume of phenol:chloroform:isoamyl alcohol (25:24:1) saturated with Tris-HCl was added followed by thorough vortexing and centrifugation at 17,000 g for 15 min at 4°C. The aqueous layer was collected, and DNA was precipitated by adding 600 μl of ice-cold isopropanol followed by centrifugation at 17,000 g for 5 min at 4 °C. The extracted DNA was washed twice with 500 μl of ice-cold 70% ethanol to remove traces of phenol, dried by incubating at 37 °C for 15 min, and resuspended in 50-100 μl of sterile water. gDNA was quantified by measuring absorbance (260 nm) using a NanoDrop (ND 1000), and its purity determined by the 260/280 ratio. gDNA was routinely stored at -20 °C.

2.4.2 Plasmid DNA from *S. cerevisiae*

To obtain plasmid DNA, total *S. cerevisiae* DNA was extracted (section 2.4.1) and linear ssDNA and dsDNA were digested with Exonuclease V (RecBCD) (NEB M0345S) following the manufacturer's instructions. The remaining plasmid DNA was precipitated using ice-cold isopropanol and washed twice with ice-cold 70% ethanol, before being resuspended in sterile water.

2.4.3 Plasmid extraction from *E. coli*

Bacterial plasmids were extracted using the E.Z.N.A. Plasmid DNA Mini Kit (D6942-01 OMEGA), following the manufacturer's instructions.

2.4.4 Polymerase Chain Reaction (PCR)

For PCR screening, TaKaRa ExTaq polymerase (TAKARA BIO INC. RR001A) was used following the manufacturer's instructions, and thermocycling was performed using a BioRad MJ Mini thermo cycler. A typical PCR reaction consisted of 2.5 μl of 10X *Ex Taq* buffer, 0.5 μl of dNTP mixture (2.5 μM each), 0.5 μl of each primer (forward and reverse, 10 μM each), 0.125 μl ExTaq polymerase, 25-100 ng DNA template and ultra pure water to a final volume of 25 μl. PCR conditions were 30 cycles of: 10 second denaturation at 98 °C, 30 second annealing at 55 °C and 1 min extension at 72 °C; followed by 5 min of final extension at 72 °C. Primers used in this thesis (table III) were resuspended to a concentration of 100 μM for long term storage and diluted to 10 μM for working stocks.

Table III. Primer sequences.

Primer	Sequence 5' to 3'	Origin
GAL1_F	TTGCGAACACCCTTGTTGTA	O'Sullivan Lab
GAL1_R	CGTGCTCGATCCTTCTTTTC	O'Sullivan Lab
M13F	GTAAAACGACGGCCAG	Invitrogen
M13R	CAGGAAACAGCTATGAC	Invitrogen
NC1094	ATGACGAGGCATTTGGCTAC	O'Sullivan Lab
NC1095	GGTACGGACAAGGGGAATCT	O'Sullivan Lab
PAG10	TTTAAGCTTATGGTACGTTTGATATCGCTG	Ganley Lab
PAG23	GCCTTAATAATGTACTTTGC	Ganley Lab
PAG24	GCAAGATCATATTATCCAAG	Ganley Lab
PAG58	TAGAACTGGTACGGACAAGGG	Ganley Lab
PAG59	AGGTAGTGGTATTTCACCGGC	Ganley Lab
PAG70	TGGATGAAAAATGGACCCGA	Ganley Lab
PAG194	TGAAGTAGCCGGACTGGATCC	Ganley Lab
PAG195	CTTTGCATAGTTGTAACTTGCGCC	Ganley Lab
PAG196	CCCGGTTGTGGTATATTTGG	This study
PAG198	GCCGCTGGCTTCCAAACCCTTTAGG	This study
PAG199	GCGCCCTTTTGAGTCTCTGCACTACC	This study
PAG200	CTGCAAGATATAAATTTGTTTACTCATACATATATATTCTATTGCGGGGCGCGGAAAGGTGAGAGGCCGGAACCGG	This study

PAG201	GCTGTCTCGTAATATTCAAGCAAGTCTTCCTCAAGAATATTGACAAATAAACGGCGGGGTATCGTATGCTTCCTTCAGCACTACCC	This study
PAG274	CAACATCACAGTCTCGAAGG	Ganley Lab
PAG275	CTGTATTTGAATATTGATGTCCAGAAGCAGAAGATTTCACATGTTGTATAAAGTATTGGATCGATCCGATGATAAGC	Ganley Lab
PAG277	AATTTTATAGGTAATATACATATATAAAAATACTTCAATCATTTTTACAATCTTGTCAGGGTTATTGTCTCATGAGCG	Ganley Lab
PAG278	TACGGCACCTTGTAAGCAGTC	Ganley Lab
PAG279	TCACAAAGTTTGTGTAAGATGCTTTCCTGGGTCGATGTGGATTGTGCCGTGGCCTTGATATCAAGCTTGCCTCGTC	Ganley Lab
PAG281	TTCAAAATACAGCCTCAGTTATTAATAGTTAAAGCACCGCTATAAAGGTGGTGAAACTGGATGGCGGCGTTAGTAT	Ganley Lab
PAG283	ACTATCGTTCGTTATTTTATAAAATATGTATTGTTACATATATATACATATATAGTGGATCGATCCGATGATAAGC	Ganley Lab
PAG285	ACTGCTATGATTTTGGATTATTCCTTCCACTCAAACCAATTGTGCACATGCATTCCCAGGGTTATTGTCTCATGAGCG	Ganley Lab
PAG286	AGAAGGATACAGCGACAGAC	Ganley Lab
PAG287	TACAGGCTGCATTTCGATTAATTAAGTAATGTAAAATTAAGACTATTAGTACATAAGATATCAAGCTTGCCTCGTC	Ganley Lab
PAG289	TCCTCACTTTCTACCTTTTTTTTTTATGCCTTAGTTGAAAAGATACGCGTATCTAACTGGATGGCGGCGTTAGTAT	Ganley Lab
PAG290	ACCGTGGATGATGTGGTCTC	Ganley Lab
PAG292	GATGTGAGAACTGTATCCTAGC	Ganley Lab
PAG293	CCATCCTATGGAACTGCCTC	Ganley Lab
PAG305	CCTCTATATGATACAATTGACCAAGCCTTCATTTACCATTCTATATCAATTTGGACCATCTCATTAAGCTGAGCTGC	This study
PAG306	GCTGTCTCGTAATATTCAAGCAAGTCTTCCTCAAGAATATTGACAAATAAACGACAGTTATGTCTATGGTCGCCTATGC	This study
PAG311	AAACCAATTCTTGGACCATCTCATTAAGCTGAGCTGC	This study
PAG312	AAATCCGGAACAGTTATGTCTATGGTCGCCTATGC	This study
PAG313	ACTTCGGAGCACTGTTGAGC	This study
PAG329	CCGTATTGGCTTGGGTTTGAAGAG	This study
PAG330	CTTGGCATTGTGACCTGGAACT	This study
PAG331	ACGACGCTCCTCGTGCTGTCTT	Ganley Lab
PAG333	GGGCAACTCTCAATTCGTTGTA	Ganley Lab
PAG344	GTGGAGTAGGTCTCAATGC	This study
PAG345	AGGACTACTGTGACGGCTTC	This study
PAG346	GTTCTGCACAAGCTGCATAC	This study
PAG352	CTAATTCGACCAGGTTAACTC	This study
PAG353	GCATTGTTGGCAATCTTATGTG	This study
PAG354	TGGATGAGCAGCTTGGAAC	This study
PAG465	CAATGATTAAAATAGCATAGTCGG	(Bradbury et al. 2006)
PAG466	CAGCACGGAATATGGGACT	(Bradbury et al. 2006)
PAG467	GGTGCATTTGTCATCCGTC	(Bradbury et al. 2006)

2.4.5 DNA cleanup

PCR products and restriction digested DNA fragments to be used for downstream applications (i.e., ligation, cloning, or transformation) were precipitated in ice-cold isopropanol. The DNA was pelleted by centrifugation at 21,100 g, washed twice with 70% ice-cold ethanol, dried by incubating at 37 °C for 15 min and resuspended in 10-20 μl of sterile water.

2.4.6 Quantitative real time PCR (qPCR)

Quantitative real time PCR (qPCR) was used to estimate rDNA copy number (relative to WT and normalized to a single copy reference gene) in haploid strains as described by Cahyani et al. (2015). qPCR was performed in The Liggins Institute (Auckland University) with the assistance of Dr. Inswasti Cahyani using primers primers from the O'Sullivan laboratory, specific for the 25S rDNA sequence (NC1094/NC1095) and the *GAL1* housekeeping (ie. single copy reference) gene (GAL1_F/GAL1_R). Each sample was analyzed in triplicate. Briefly, cross point (Cp) values for 25S rDNA were subtracted from the corresponding reference gene Cp values to obtain ΔCp values for each biological sample. The average ΔCp from four biological replicates of the WT strain was used to estimate a ΔCp control, which was then subtracted from each ΔCp to obtain ΔΔCp values. To estimate the gene copy number, $2^{-\Delta\Delta Cp}$ was calculated to obtain the rDNA copy number ratio for each sample. The obtained ratio was then multiplied by 200 (the WT copy number) to obtain the rDNA copy number relative to WT (normalized to *GAL1*) for each sample. The average relative copy number and standard deviation are presented in figure 4.30.

2.4.7 Agarose gel electrophoresis

Agarose gel electrophoresis was used to visualize gDNA, plasmid DNA, PCR products and RNA. 1% agarose gels were prepared in 1X Sodium Borate (SB) running buffer (Brody and Kern, 2004; 10 mM sodium hydroxide, pH adjusted to 8.0 with boric acid). DNA samples were mixed with 6X DNA gel loading dye (LD) (Thermo Fisher R0611) and loaded onto the wells. 100V were applied for approximately 40 min at RT. Agarose gels were stained in a solution of 5 ug/ml ethidium bromide (EtBr) in water for 15-20 min and de-stained in water for 5 min before

an image was acquired under UV light (265 nm) using a BioRad Gel Doc 2000 System. For size determination, 0.5 μg of the O'GeneRuler 1 kb DNA ladder (Thermo Scientific SM1352) were used as a marker. To recover DNA fragments from an agarose gel, the EtBr stained DNA was visualized under long wave (365 nm) UV light, and the correct size band was excised using a sterile blade. A QIAquick gel extraction kit (QIAGEN 28704) was then used to clean up the DNA following the manufacturer's instructions.

2.5 CLONING TECHNIQUES

2.5.1 Ligations

The RBC rapid ligation kit (RBC RC011) was used for joining dsDNA with cohesive termini following the manufacturer's instructions.

2.5.2 Bacterial transformations

E. coli OneShot TOP10 cells (Invitrogen C404010) from frozen stocks were grown O/N and made chemically competent using the Z-Competent *E. coli* transformation kit from Zymo Research and following the manufacture's instructions. 1 μl of plasmid DNA was mixed with 25 μl of competent cells, incubated on ice for 10 min, and heat-shocked at 42 °C for 30 sec. Immediately after, 250 μl of SOC medium were added, and the cells were incubated for 1 hr at 37 °C. 20 μl of cells were plated onto an LB plate supplemented with ampicillin and Xgal for blue/white colony screening. Plates were incubated overnight at 37 °C. The next day, potential transformants (white) were grown overnight in liquid LB medium supplemented with ampicillin for plasmid extraction (section 2.5.3). Purified plasmids were either digested using restriction enzymes to confirm the insert size, or used as template for PCR screening.

2.6 RNA PROTOCOLS

2.6.1 RNA Extraction

RNA was extracted using a modified protocol from Schmitt et al. (1990). 10 ml of cells were grown to an OD_{600nm} of 0.8, pelleted by centrifugation (2,000 g for 5 min) and resuspended in 400 μl of AE buffer (50 mM sodium acetate, 10 mM EDTA, pH 5.3) and 40 μl of 10% SDS. An equal volume of AE-equilibrated phenol was added and samples vortexed thoroughly before incubation at 65 °C for 4 min. The samples were chilled on a dry ice/ethanol bath for 1-2 min or until phenol crystals appeared, and centrifuged 20 min at 21,100 g at 4 °C. The aqueous phase was transferred to a new tube, and 500 μl of AE-equilibrated phenol were added, mixed by vortexing and the samples were again centrifuged 20 min at 21,100 g at 4 °C. The aqueous phase was collected, 40 μl of 3M sodium acetate pH 5.3 were added, and the tube was filled with 96% ethanol to precipitate the RNA. The tubes were incubated overnight at -80 °C, and the next day the RNA was pelleted by a 20 min centrifugation at 21,100 g at 4 °C, and washed twice with 80% ethanol. The pellet was dried by incubating at 37 °C for 15 min and resuspended in 10 μl of nuclease free water. The RNA samples were treated with DNase I (Invitrogen 18068-015) following the manufacturer's instructions. RNA concentration was determined using a Nanodrop (ND 1000). RNA quality was assessed by electrophoresis (section 2.4.7), with RNA samples heated for 5 min at 70 °C before loading.

2.6.2 RT-PCR conditions

Reverse transcription was performed using ThermoScript Reverse Transcriptase (Invitrogen 12236-014). For each sample, a –RT (no reverse transcriptase) control was included. The obtained cDNA was used as template for end-point PCR to determine mRNA expression of Fob1 (using primers PAG329 and PAG330), with actin used as a housekeeping control (PAG331 and PAG333).

2.7 YEAST TRANSFORMATIONS

2.7.1 Preparation of competent cells

Yeast competent cells were prepared before every transformation using 5 ml of overnight culture in rich medium. These stationary phase cells were diluted to OD_{600nm} 0.2 in a total volume of 20 ml, and grown (2-3 hrs) to OD_{600nm} 0.4. Cells were pelleted by centrifugation at room temperature (RT) at 1,500 xg for 15 sec, washed with 5 ml 1X TE 10/1 buffer (10 mM Tris-HCl pH 8.0, 1 mM EDTA pH 8.0), and resuspended in 5 ml of 0.15 M LiOAc (0.15 M Lithium Acetate, 1.5 mM Tris-HCl pH 8.0, 0.15 mM EDTA pH 8.0). Cells were incubated at 30 °C for 1 hr with gentle shaking at 50 rpm, pelleted by centrifugation and resuspended in 1 ml of 0.15 M LiOAc.

2.7.2 Transformation

Yeast transformations were performed using a modification of the protocol from Gietz and Woods (2006) by gently mixing 2 μl of carrier DNA (salmon sperm 10 μg/ml, denatured at 98 °C for 5 min and placed on ice for 5 min), 1 μg of DNA (to a maximum volume of 6 μl) and 60 μl of competent cells. This mixture was incubated at 30 °C for 30 min, with gentle mixing every 5 min. Next, 120 μl of 52% PEG (52.5% polyethylene glycol (PEG) 4000, 1 M lithium acetate, 10 mM Tris-HCl pH 8.0, 1 mM EDTA pH 8.0) were added and gently mixed, followed by a 2 hr incubation at 30 °C and a 45 min incubation at 42 °C. The cells were allowed to cool for 5 min and pelleted by centrifugation at 2,000 g for 1 min. Lastly, the cells were resuspended in 100 μl of rich medium, plated on selective medium for auxotrophic selection, and incubated at 30 °C for 2-3 days until colonies appeared.

2.7.3 Screening of transformants

Potential transformants were re-streaked onto fresh selective medium plates to confirm their ability to grow on selective medium. Following phenotypic confirmation, the gDNA from

each potential transformant was extracted and PCR was used to confirm the insertion of a selective marker, replacement of a gene, or the presence of a plasmid.

2.8 PULSE FIELD GEL ELECTROPHORESIS (PFGE)

PFGE was performed using a modified protocol from Iadonato and Gnirke (1996). To make agarose plugs containing intact, chromosome-sized DNA, cells were grown overnight in rich medium to stationary phase, and 2 ml were pelleted by centrifugation at 21,100 g for 2 min and washed twice with 350 μl of 50 mM EDTA (pH 8.0). The cells were resuspended in 4 times their volume of 50 mM EDTA and placed in a 45 °C water bath for 5 min. An equal volume of warm cells and molten 1.6% low melting point (LMP) agarose at 45 °C were gently mixed, pipetted into a plug mold, and allowed to set for 20 min at 4 °C. 2-3 plugs from the same sample were placed into a 2 ml flat bottom microfuge tube and incubated with 1 ml of freshly made spheroplasting solution (1 M Sorbitol, 20 mM EDTA pH 8, 10 mM Tris-HCl pH 7.5, 14 mM 2-mercaptoethanol, 2 mg/ml zymolyase 20-T) for 6 hrs at 37 °C, with a gentle mix by inversion after the first hr. The spheroplasting solution was then removed using a glass Pasteur pipette, and addition of an equal volume of LDS solution (1% lithium dodecyl sulphate, 100 mM EDTA pH 8, 10 mM Tris-HCl pH 8) was followed by incubation for 15 min at 37 °C. LDS solution was removed and fresh LDS solution was added for an overnight incubation at 37 °C. The next day, the plugs were washed three times for 30 min each in 1 ml of 0.2X NDS solution (0.1 M EDTA, 2 mM Tris-HCl, 0.2% sarkosyl, pH adjusted to 9.5 with NaOH) at room RT, and three times for 30 min each in 1 ml of TE 10/1. The plugs were stored in TE 10/1 at 4 °C.

A BioRad CHEF mapper XA system was used to perform PFGE. Plugs were cut in thirds or quarters and placed on a PFGE comb. The comb was placed onto the gel cast and warm 1% agarose in 0.5X TBE (40 mM Tris, 45 mM Boric Acid, 1 mM EDTA) was slowly poured ensuring the plugs remained in place. PFGE was performed in 0.5X TBE at 14 °C. The settings used were 6 V/cm, run time= 29 hr, included angle 120°, initial switch time = 4s, final switch time = 3m48s, ramping factor: a = [Linear], which are the default parameters to separate fragments sized between 2 Mb and 200 Kb using the built in autoalgorithm. The gel was stained and visualized as in section 2.4.7.

2.9 SOUTHERN BLOTTING

2.9.1 Southern blot method

PFGE and electrophoresis gels from the psoralen crosslinking assay used for Southern blotting were de-stained in water for at least 2 hrs before being washed with 0.25 M HCl for 15 min, then washed twice with 1.5 M NaCl + 0.5M NaOH for 15 min each time, and washed with 1.5 M NaCl + 1M Tris for 15 min. The gels were washed 20 min in 10X SSC (1.5 M NaCl, 150 mM sodium citrate, pH adjusted to 7 with HCl). For transfer, the gel was placed upside down on a clean bench, and a pre-cut nylon membrane (Amersham Hybond-N+ RPN119B) soaked in 10X SSC was placed on top, followed by 2 pieces of Whatman filter paper (soaked in 10X SSC). Bubbles between layers were removed before the next layer was added. Lastly, a stack of paper towels and a 300 g weight were placed on top. After 2 hrs, this was disassembled and the membrane was placed on a Whatman filter paper envelope pre-soaked in MiliQ water, and crosslinked in a UV crosslinker (UVP-CL 2000) on the 'preset' setting (approximately 8 sec).

The crosslinked membrane was rinsed with 10X SSC to remove any agarose traces, and placed into a hybridization tube, and 20 ml of PSE buffer (0.3 M sodium phosphate pH 7.2, 7% SDS, 1 mM EDTA) were added, followed by pre-hybridization for 15 min at 65 °C in a rotating oven. Next, 2-4 ng/ml of denatured Southern blot DIG-labeled was added into the hybridization tube and hybridized overnight at 65 °C. The next day, the hybridization solution was removed, and the membrane was rinsed and washed thrice with 0.1X PSE (0.03 M Sodium phosphate pH 7.2, 0.7% SDS, 0.1 mM EDTA) at 65 °C for 10 min each time. The membrane was then rinsed and washed twice with 1X TBS (20 mM Tris, 0.15 M NaCl, pH adjusted to 7.6 with HCl) 65 °C for 5 min each time. The membrane was then incubated with blocking solution (1.5% dry milk powder in 1X TBS) at RT for 60 min, and then incubated for 30 min with 10 mL of 1:10,000 anti-DIG antibody in blocking solution (Roche 11093274910). To remove excess antibody, the membrane was rinsed and washed for 10 min with blocking solution, and then rinsed and washed for 10 min with 1X TBS. Lastly, the membrane was rinsed and equilibrated for 15 min in alkaline phosphatase buffer (100 mM Tris pH 8, 100 mM NaCl, 5 mM Mg^{+2}, pH adjusted to 9.5 with NaOH), and 1 ml of CSPD-Ready to use (Roche 11655884001) was applied to the membrane for chemiluminiscent detection, spread evenly,

and the membrane sealed in a plastic folder. This was incubated at 37 °C to enhance the signal and then chemiluminiscence was detected using a Fujifilm LAS-4000 imager.

2.9.2 Southern blot probe DIG labeling

The probes used for Southern blotting were PCR amplified using the PCR DIG Probe Synthesis Kit (Roche 11636090910) following the manufacturer's instructions. A rDNA specific probe of 395 bp from a region of the 25S rDNA was constructed using primers PAG58 and PAG59, and a chromosome XII probe of 422 bp from a region of the *APC2* gene was constructed using primers PAG194 and PAG195.

2.10 CHROMOSOME LOSS ASSAY (CLA)

2.10.1 CLA execution

Typically, four samples were assayed in each CLA. A dab of yeast cells from each strain to be screened using the CLA was used to inoculate 2 ml of liquid SD/Gal-Ura medium and grown O/N at 30 °C on a rotating wheel (150 rpm). The next day, each cell culture was diluted from stationary phase to an OD_{600nm} of 0.2 in a total volume of 5 ml of SD/Gal-Ura medium, and cells were grown until their first doubling at an OD_{600nm} of 0.4 (usually 3-5 hrs). Cells were then pelleted by centrifugation at 2,000 g for 2 min at RT, washed with autoclaved water, and resuspended in the same volume of YPD/Gal. An aliquot (1 ml) of the cells was taken for the time 0 (t_0) platings, and the remainder was incubated until cell density had doubled (OD_{600nm} of 0.8; usually 2-3 hrs). An aliquot was then taken for the time 1 (t_1) platings.

The time t_0 and t_1 platings involved two steps. The first step was plating 50 μl, 100 μl and 200 μl of undiluted cell culture onto SD/Gal Full + 5FOA (5FOA) plates containing 5, 10 and 20 glass beads, respectively, for spreading. Duplicate selective 5FOA plates of each volume were used routinely. The second step involved diluting the cell cultures in YPD/Gal) 2,000 and 4,000 fold, for t_0 and t_1, respectively, for cell density estimations on YPD/Gal plates. 50 μl, 100 μl and 200 μl of each diluted cell culture was plated onto plates containing 5, 10

and 20 glass beads, respectively, for spreading. Triplicates of each plated volume were used routinely.

Plates were incubated at 30 °C for 2-3 days until colonies were visible. Colonies from YPD/Gal plates were counted and the average of the triplicates of the three different volumes were calculated (t_0 and t_1 cell densities). 5FOA plates were counted and replica plated using sterile velvets onto both fresh 5FOA plates and YPD/Gal+G418 (G418) plates. Replica plates were incubated until replica colonies were visible (usually 1-2 days), and each replica 5FOA plate and its corresponding G418 plate were overlaid with each other and counted to identify the chromosome loss colonies (able to grow on 5FOA but not G418). The number of chromosome loss colonies obtained from each duplicate and each volume was used to obtain the average chromosome losses for t_0 and t_1. The difference between the chromosome losses at t_0 and t_1 was divided by the difference between the t_0 and t_1 cell densities to obtain the chromosome loss rate (section 3.3). This calculation was performed independently for each biological replicate with at least two, but usually more than three, biological replicates for each strain (see appendix table II).

2.10.2 CLA statistical analysis

Statistical data analysis was performed using R studio version 3.0.1 (2013-05-16) -- "Good Sport" from R Core Team (2013. Vienna, Austria). Chromosome loss rates obtained were imported into R in comma separated values (csv) files. The Mann-Whitney-Wilcoxon rank sum test (Mann-Whitney) was performed for paired comparisons, while the Kruskal-Wallis one-way analysis of variance by ranks test (Kruskal-Wallis) was used to compare groups of more than two strains. Mann-Whitney p-values were corrected using a false discovery rate (fdr) adjustment. All R commands are presented in appendix scheme I.

2.11 PSORALEN CROSSLINKING

Crosslinking of DNA and determining the proportion of transcriptionally active versus inactive rDNA repeats were performed using a method adapted from Conconi et al. (1989) and Sogo et al. (1984). 50 ml of culture was grown to OD_{600nm} 1.0, 6 ml of this culture was pelleted

by centrifugation, resuspended in 1 ml of 1X TE 10/1 buffer, and used to test different crosslinking conditions. Samples were transferred to small plastic containers, and kept on ice until the end of their UV-exposure. A UV box (366 nm) was placed directly above the samples, and the distance from the UV source to the sample was adjusted to test different exposure distances. Total exposure times of 20 min, 25 min and 5 hrs were tested. 50 μl of a 200 μg/ml psoralen solution in absolute ethanol (or absolute ethanol only as a negative crosslinking control) were delivered to the cells a total of five times during the UV exposure every 4 min for 20 min, every 5 min for 25 min, or every 1 hr for 5 hrs. Samples were then collected in microfuge tubes and gDNA extracted immediately (section 2.4.1). gDNA was RNase treated (NEB M0297) and digested with *Eco*RI (NEB R3101) following the manufacturers' instructions, and separated by gel electrophoresis (section 2.4.7). The gel was transferred to a nylon membrane and subjected to Southern blotting using a rDNA probe (section 2.9.1). Slow migrating bands in the Southern blot correspond to transcriptionally active rDNA repeats, fast migrating bands correspond to transcriptionally inactive rDNA repeats.

CHAPTER THREE: THE CHROMOSOME LOSS ASSAY ESTABLISHMENT AND OPTIMIZATION

[blank page]

The goal of this project was to test the hypothesis that the rDNA gene repeats play a role in chromosome segregation. Under normal conditions chromosome segregation results in two daughter cells each inheriting one copy of every chromosome. However, if an error during chromosome segregation occurs, one of the daughter cells can inherit two copies of a chromosome (chromosome gain), and the other daughter cell will inherit none (chromosome loss). Several approaches have been used to measure these changes in the copy number of individual chromosomes (aneuploidy), including phenotypic screening of aneuploid colonies (Hartwell and Smith 1985; Surosky and Tye 1985; Runge et al. 1991), detection of changes in gene copy number (Hughes et al. 2000), and high-throughput detection of quantitative protein or mRNA expression changes (Pavelka et al. 2010). I decided to use phenotypic selection because it allows screening of millions of cells at a time and, unlike most techniques that detect population changes, phenotypic selection allows detection of single cell events. The introduction of genetic markers allows phenotypic selection of chromosome missegregation events, and these were used as a foundation to establish and optimize a chromosome loss assay (CLA) to test how the rDNA influences mitotic chromosome segregation. This section describes the establishment and optimization of the CLA and the assay conditions that are used throughout this study.

3.1 CHROMOSOME LOSS ASSAY (CLA)

The conceptual basis of the CLA is that it measures the rate of chromosome loss, which is a proxy for chromosome missegregation, by phenotypically identifying the loss of marker genes present on one of the two copies of a homologous chromosome in diploid yeast cells. This takes advantage of the fact that *S. cerevisiae* diploid cells that lose a chromosome (become aneuploid) remain viable. To ensure the CLA differentiates the presence or absence of a whole chromosome from other events that render a marker gene inactive (such as mutation and gene conversion), a double selection with CLA strains containing two different marker genes inserted on opposite arms of the same chromosome homolog.

Identification of the loss of a chromosome in the CLA is achieved using negative (counter-) selection, which facilitates selection for the absence of a marker gene. Currently available negative selection markers are few (Guthrie and Fink 1991), costly, and prone to growth of false positives. From the marker genes available, we chose to use *URA3* and

kanMX2 for positive and negative selection, respectively. Detection of *URA3* loss is performed through the addition of 5-fluoro-orotic acid (5-FOA) to the growth medium, which is converted by orotidine-5'-phosphate (OMP) decarboxylase, the enzyme encoded by *URA3,* into a toxic compound that causes cell death (Boeke et al. 1984). Loss of *kanMX2* is assayed through sensitivity to geneticin (G418), an antibiotic that blocks polypeptide synthesis and to which *kanMX2* confers resistance ($G418^R$) (Wach et al. 1994). Therefore genuine whole chromosome losses will have lost both *URA3* and *kanMX2,* resulting in cells that are able to grow on medium containing 5-FOA but not G418, unlike cells that result from normal chromosome segregation (figure 3.1).

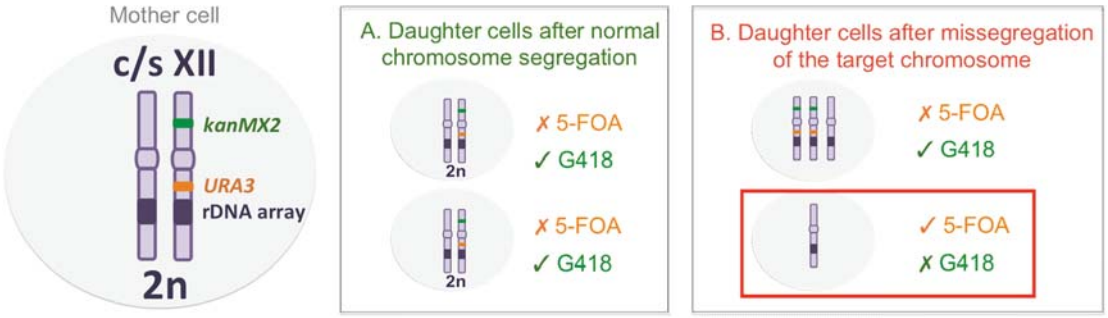

Figure 3.1. Identification of chromosome loss events during mitosis in diploid cells. Chromosome segregation of a wild type (WT) strain with a marked chromosome XII homolog is shown. The nucleus of a diploid cell (2n) undergoing mitosis is shown with only a single chromosome pair (chromosome XII). The two homologs of chromosome XII are shown in purple, both containing an rDNA array (darker purple) on the long arm, and with one homolog marked with *kanMX2* (green) and *URA3* (orange) genes. Two different segregation outcomes are illustrated. **A. Normal chromosome segregation**. Each daughter cell inherits one copy of each homolog. **B. Chromosome missegregation** of the marked chromosome. One daughter cell inherits two copies of the marked homolog and one copy of the unmarked homolog, whereas the second daughter cell inherits one copy of the unmarked homolog and none of the marked one (red box shows loss of the marked homolog). Labels on the right indicate the cells ability ( ) or inability (✗) to grow on medium containing 5FOA (orange) or G418 (green).

My aim is to measure the *rate* of chromosome loss, which is the number of chromosome loss events per cell division. However, the number of cell divisions per unit time is dependent on the growth rate of the strain being assayed. Growth rates amongst different strains can vary greatly (Ziv et al. 2013), particularly those with rDNA alterations (Ganley, unpublished results), and if not controlled for, this variation could result in inaccurate chromosome loss rate measurements. Hence, to standardize the number of cell divisions each strain goes through, the growth during the CLA is monitored in real time but is restricted to a single round of cell division. Before the start of the CLA, all strains are grown overnight to stationary phase, and then diluted to a low cell density from stationary phase for exponential

growth (pre-assay growth). The growth is then monitored during the CLA until the cell density doubles (restricting growth to a single round of cell division). The CLA involves plating cells in rich and selective media before and after one cell division to obtain cell densities and the number of chromosome loss events at those two time points, which eliminates any growth rate dependent bias on the rate of chromosome loss. Therefore, the conceptual basis for my CLA is that cells are grown for just a single round of cell division, and the cell density and numbers of chromosome losses are measured both before and after this round of cell division to calculate the rate of chromosome loss.

3.2 OPTIMIZATION OF THE CLA

Several aspects of the CLA required optimization before its establishment and implementation. First, it was necessary to choose the optimal selective growth conditions to minimize chromosome losses from arising before the start of the CLA. During the CLA, it was also important to establish a rapid method to reproducibly monitor cell density in real time. In addition, accurate post-assay cell density and chromosome loss estimations were necessary. To optimize these aspects of the CLA, we used a wild type (WT) strain in which both CLA marker genes *kanMX2* and *URA3* had been inserted into opposite arms of one chromosome XII homolog (section 4.2).

To minimize chromosome loss events from occurring before the start of the CLA, strains were grown on selective media. Liquid cultures were initially grown overnight, and then diluted and allowed to grow for a single cell division before the start of the CLA (pre-assay growth), with both of these steps carried out in selective medium. Since our CLA selection markers are *URA3* and *kanMX2*, we compared growing the cells for pre-assay growth in SD-Ura versus SD-Ura+G418 media to determine whether double selection provides greater protection against loss of the chromosome of interest than single marker selection. While the addition of G418 slightly reduced the number of chromosome loss events found at the start of the CLA (not shown) without affecting the growth rate (figure 3.2), the double selection introduced a washing step (needed to remove G418 traces) before the start of the CLA. The introduction of this washing step might convey a potential delay in the division of the exponentially growing cells (not shown). The small increase in protection was not great enough

to justify introduction of this delay, therefore SD-Ura medium was chosen for the overnight and pre-assay growth phases.

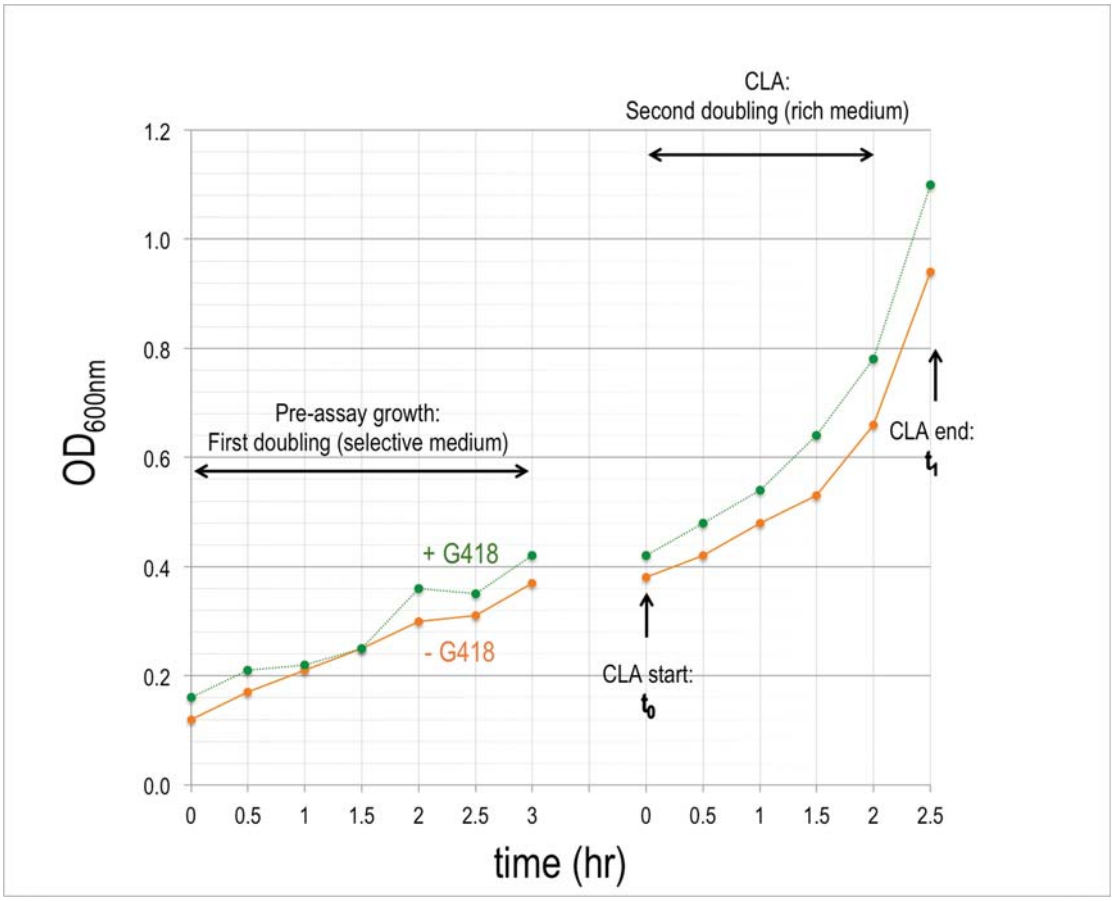

Figure 3.2. WT strain growth under selective conditions during the CLA. Stationary phase cultures of the WT strain grown in selective SD-Ura medium in the absence (solid orange lines) or presence of G418 (250 mg/ml) (dotted green lines) were diluted to an OD_{600nm} of 0.2 (approximately 4 x 10^6 cells/ml, start of first doubling), and cell densities were monitored in the same selective medium until the cells reached an OD_{600nm} of ~0.4. The cells were then pelleted and transferred into rich medium (YPD) to mimic the CLA (t_0), and cell densities were monitored by OD_{600nm} every 30 min until the cell density had doubled (t_1).

It was important to establish a method to estimate cell density in real time for pre-assay growth and during the CLA so that cell growth could be restricted to one doubling. For the CLA, accurate cell counts before and after the one round of cell division are performed by plating, but this obviously is not possible for monitoring cell density in real time. Two options for real-time monitoring were tested, with plating as the benchmark, to determine which is more accurate: OD measurements (600 nm) and hemocytometer counts. Empirically, we determined that an absorbance or optical density (OD) of 1.0 at a wavelength of 600nm (OD_{600nm}=1.0) corresponds to approximately 2x10^7 cells/ml, and this calibration was used to estimate actual cell density from OD measurements. The cell densities estimated from hemocytometer counts were the highest (figure 3.3), possibly because this technique allows each cell in a clump to be

counted, and also showed the highest variability. OD_{600nm} measurements had a much lower variability than the hemocytometer values, and, although the cell density values were higher than the ones obtained from platings, they were well correlated and closer to the plating values than the hemocytometer counts (figure 3.3). Hence, OD_{600nm} measurement was chosen as the method to monitor real time cell growth during the CLA.

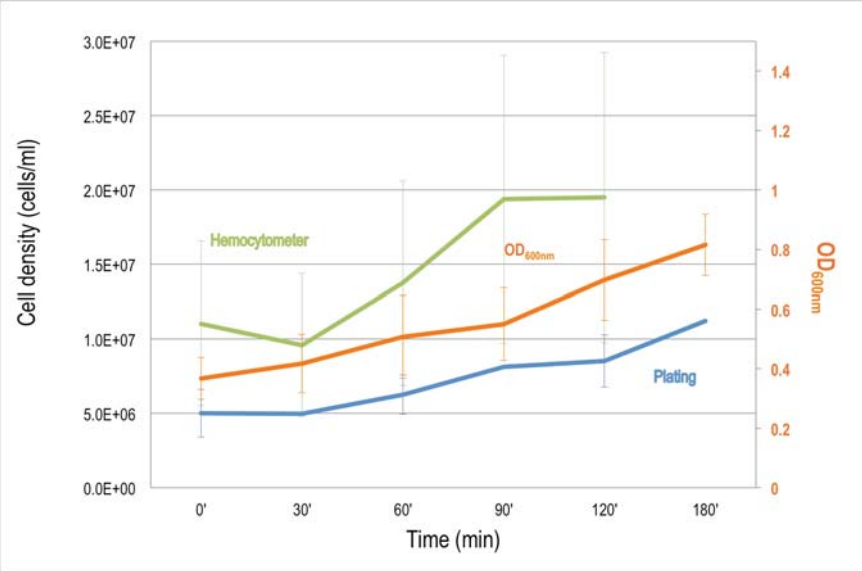

Figure 3.3. Comparison of real time cell density determination techniques. A YPD liquid culture of the WT strain was used to compare three different methods of estimating cell density: OD_{600nm} measurements (Mewborn et al.), plating colony counts from diluted and plated liquid cultures (blue), and direct counts of viable cells in a hemocytometer (green). The cell density was estimated for four biological replicates (n=4) using each of the three methods. Error bars show standard deviation.

To maintain a constant population doubling time between independent replicas from each strain during the CLA, it is important to start with exponentially growing cells and sustain their growth rate for the duration of the CLA. The pre-assay growth step (first doubling, figure 3.2), in which cells are grown for one doubling before the start of the CLA, serves to restrict chromosome loss events, and also to adjust cell populations to the same growth phase. After the pre-assay growth, cells are switched to rich medium, which is permissive for chromosome loss events, and monitored for another doubling during the CLA. Because of the two consecutive doublings (pre-assay and CLA growth) and the need for exponential growth, the OD_{600nm} at the end of the CLA should be ≤1.0 because at this OD, cell growth starts to lose its exponential nature. Hence, pre-assay growth starts with an OD_{600nm} of ~0.2, and after one doubling (in SD-Ura) the cells are transferred to rich medium and the CLA starts at an OD_{600nm} of ~0.4 and ends at an OD_{600nm} of ~0.8.

During the CLA, an aliquot of cells is diluted and plated onto rich medium to estimate cell densities through colony counts before (t_0) and after (t_1) the single cell division. At these time points, cells are also plated onto selective medium containing 5-FOA to select potential chromosome losses. After 2-3 days of incubation, colonies able to grow on 5-FOA medium (from cells that have lost the *URA3* marker or chromosome XII altogether), are replica plated onto G418 medium to determine whether these colonies have also lost the *kanMX* marker, and onto fresh 5-FOA medium to ensure that the original 5-FOA-resistant colonies are not false positives produced by a partial reversibility of 5-FOA induced growth inhibition (Boeke et al. 1984). Colonies that grow on both 5-FOA plates but not on G418 medium are counted as chromosome loss events.

The CLA requires an appropriate cell concentration for selection on 5-FOA medium because 5-FOA selection is affected by cell density (Quintana and Ganley, unpublished). In addition, an even colony distribution is necessary to allow efficient replica plating of single 5-FOA-resistant colonies. To obtain a suitable range of colonies (<200) on 5-FOA plates, different volumes of cell cultures at the t_0 and t_1 cell densities were plated onto 5-FOA. Volumes of less than 50 μl were absorbed very rapidly by the agar plates and cells could not be distributed evenly, as a result, colonies on some areas of the plates would grow too close to each other for replica plating. Volumes larger than 200 μl were absorbed very slowly and produced a smear that resulted in merged colonies. Hence three different volumes of cells that produced acceptable colony numbers (50 μl, 100 μl and 200 μl) were chosen for plating on 5-FOA medium from undiluted t_0 and t_1 cell culture aliquots, and these correspond to approximately $4x10^5$, $8x10^5$ and $1.6x10^6$ cells per plate respectively for the t_0 aliquot, and double that for the t_1 aliquot. For consistency, these same volumes were used to plate the diluted cell aliquots onto rich medium for cell density estimations, although at much higher dilutions.

3.3 OPTIMIZED CLA

The experimental design for the CLA resulting from the optimization stages is summarized in figure 3.4. For each biological replicate, a colony of the strain to be screened is taken from an SD-Ura plate and grown overnight in SD-Ura liquid medium. This liquid culture is diluted to an OD_{600nm} of ~0.2 and grown to double the cell density (OD_{600nm} of ~0.4). At this point the cells have reached log (exponential) phase and are shifted into YPD (permissive medium) for the start of the CLA (t_0). At this time, three different volumes of undiluted cells are plated onto 5-FOA medium for chromosome loss estimations (each volume in duplicate), and an aliquot is diluted 2,000 fold and three different volumes are plated onto YPD medium for cell density estimations (each volume in triplicate). The liquid culture is then allowed to grow for a further doubling until it reaches an OD_{600nm} of ~0.8 (t_1). As at t_0, three different volumes of undiluted cells are plated onto 5-FOA and an aliquot of the culture is diluted 4,000 fold and plated onto YPD medium. Following a 2-3 day incubation, 5-FOA 'resistant' colonies are replica plated onto fresh 5-FOA plates to identify false positives, and also onto YPD+G418 plates to check for loss of the G418 resistance marker. Any colony that is able to grow on both 5-FOA plates but not on the G418 plate is considered a chromosome loss event, because this growth pattern indicates they have lost both the *URA3* and *kanMX2* markers. In addition, colony counts are made for the t_0 and t_1 YPD plates to calculate total cell densities.

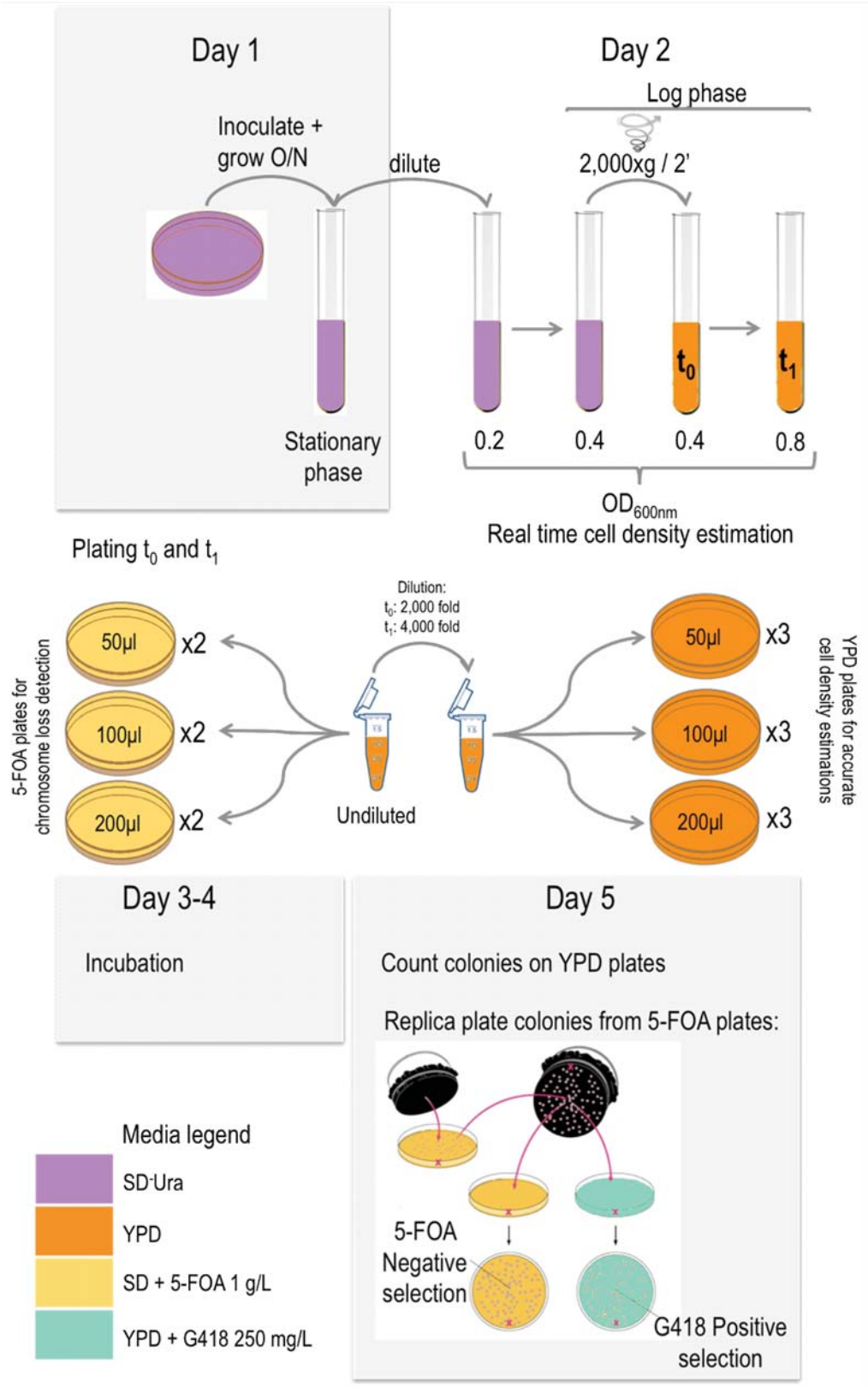

Figure 3.4. Experimental design for the chromosome loss assay. **Day 1:** Colonies are picked from SD-Ura plates, inoculated into SD-Ura liquid medium, and grown O/N until cells reach stationary phase. Day 2: The stationary phase liquid culture is diluted to an OD_{600nm} of ~0.2 in fresh SD-Ura and grown for one cell division (until it reaches an OD_{600nm} of ~0.4). Cells are then pelleted and transferred into pre-warmed YPD medium (t_0). A sample from this time point is plated onto SD+5-FOA for chromosome loss measurement and diluted and plated onto YPD for cell density estimation. Cells are grown for one more doubling until they reach an OD_{600nm} of

~0.8 (t_1). Again a sample is collected for plating onto SD+5-FOA and YPD medium plates. Three different volumes of cells at t_0 and t_1 (50 μl, 100 μl and 200 μl) are plated undiluted onto SD+5-FOA and at 2,000 and 4,000 fold dilutions onto YPD. **Day 4:** Following incubation, colonies on YPD plates are counted to estimate cell density. Colonies from SD+5-FOA plates are counted and replica plated onto fresh SD+5-FOA and YPD+G418 plates (red crosses record the orientation of each plate). After incubation, all colonies from the replica plates are counted. The different media used are color coded (bottom left corner).

To calculate the rate of chromosome loss per cell division, the number of background chromosome losses (t_0) is subtracted from the number of losses obtained at the end of the assay (t_1). This number of chromosome losses is then divided by the exact number of cell divisions that have occurred during growth in rich medium (cell density of t_1 minus cell density of t_0) to give the rate of chromosome loss. This chromosome loss calculation is shown below for one biological replicate of the WT strain.

$$\text{Rate of chromosome loss} = \frac{\text{Number of chromosome losses } (t_1 - t_0)}{\text{cell density } (t_1 - t_0)}$$

Example:

$$\text{Rate of WT chromosome XII loss} = \frac{52.50 - 5 \text{ losses/ml}}{1.30\text{x}10^7 - 5.23\text{x}10^6 \text{ cells/ml}}$$

$$= 6.14\text{x}10^{-6} \text{ chromosome losses per cell division}$$

The rate of chromosome loss is estimated independently for at least two biological replicates for every strain screened, with the average and standard error (SE) indicated. Initially, we estimated the chromosome loss rate of the WT strain ($XII^{200/200KU}$). The average WT chromosome XII loss rate from 36 independent biological replicates was found to be $6.01\text{x}10^{-6}$ chromosome losses per cell division. To determine statistical differences, nonparametric statistics were used. For differences between groups of strains, a Kruskal-Wallis one-way analysis of variance by ranks was used, and for paired comparisons, Mann-Whitney-Wilcoxon rank sum tests were performed. All p-values obtained were corrected using a false discovery rate (fdr) adjustment.

3.4 CHROMOSOME LOSS VALIDATION

In order to validate that the colonies I count as chromosome losses in the CLA really are chromosome loss events, I tried using contour-clamped homogeneous electric field (CHEF) gel electrophoresis and Southern blotting to confirm aneuploidy. CHEF gel electrophoresis can separate yeast chromosomes by size and specific chromosomes can be detected using chromosome-specific probes. To confirm chromosome losses, I isolated chromosome XII loss colonies from a CLA strain with chromosome XII homologs of different sizes. The different homolog sizes allowed detection and differentiation of each homolog on a CHEF gel, resulting in two bands; while chromosome loss colonies result in a single band, corresponding to the homolog that remains. I was able to detect loss of one homolog by the absence of the one of the bands in some of colonies, but in others I was also unable to detect the remaining homolog (not shown). These results were unreliable due to the lack of correct detection and nonspecific hybridization of the Southern blot probe. Therefore I decided to use another technique to validate the chromosome loss events detected by the CLA.

To confirm the chromosome loss colonies isolated had in fact lost one chromosome XII homolog, an independent PCR method was used. PCR primers were designed to amplify the regions around the *URA3* and *kanMX2* insertions in chromosome XII. All CLA strains have insertions of both markers on one of the two chromosome XII homologs, hence they are heterozygous for the insertions. This results in two PCR products per primer set for the parental strains. Importantly, the loss colonies show only one band, corresponding to the unmarked homolog, as expected if these really are chromosome loss events (figure 3.5). Together, these results strongly support the absence of the marked chromosome XII homolog from the chromosome loss colonies obtained via the CLA, indicating that the CLA can robustly detect chromosome losses and is not prone to false positives.

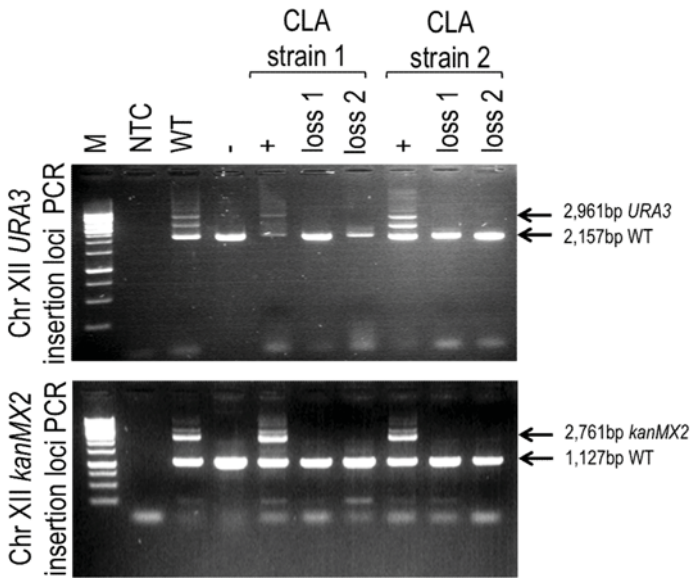

Figure 3.5. PCR confirms the absence of *URA3* and *kanMX2* in chromosome loss colonies. Chromosome loss colonies were collected from the CLA to confirm loss of chromosome XII. The *URA3* and *kanMX2* insertion loci were PCR amplified from two strains (CLA strain 1: XII$^{20/20KU}$ *fob1*$^{-}$, and CLA strain 2: XII$^{0/0KU}$+HP) and from two chromosome loss colonies for each strain (loss 1 and loss 2 for each). M (marker), NTC (no template control), WT (WT CLA diploid strain XII$^{200/200KU}$), - (haploid unmarked WT strain), + (parental CLA strain), and loss (chromosome loss colonies 1 and 2). For the Chr XII *URA3* insertion PCR (primers PAG352 and PAG353), the WT locus size is 2,157bp and the *URA3* insertion locus size is 2,961bp, a third unspecific band was also present in WT and the + control from strain 2. For the Chr XII *kanMX2* insertion PCR (primers PAG344 and PAG345), the WT locus size is 1,127bp and the *kanMX2* insertion locus size is 2,761bp.

The CLA is independent of growth rate, but poor growth of aneuploid cells could compromise detection of chromosome loss events in the CLA. Therefore I tested whether cells that have lost a copy of chromosome XII have an impaired growth rate compared to WT. No difference was observed between the growth rate of the WT CLA strain XII$^{200/200KU}$ and a chromosome XII loss colony from the same strain (figure 3.6). This shows that loss of a chromosome XII homolog does not affect growth rate, and indicates that detection of chromosome loss events is not compromised by growth selection against chromosome loss colonies.

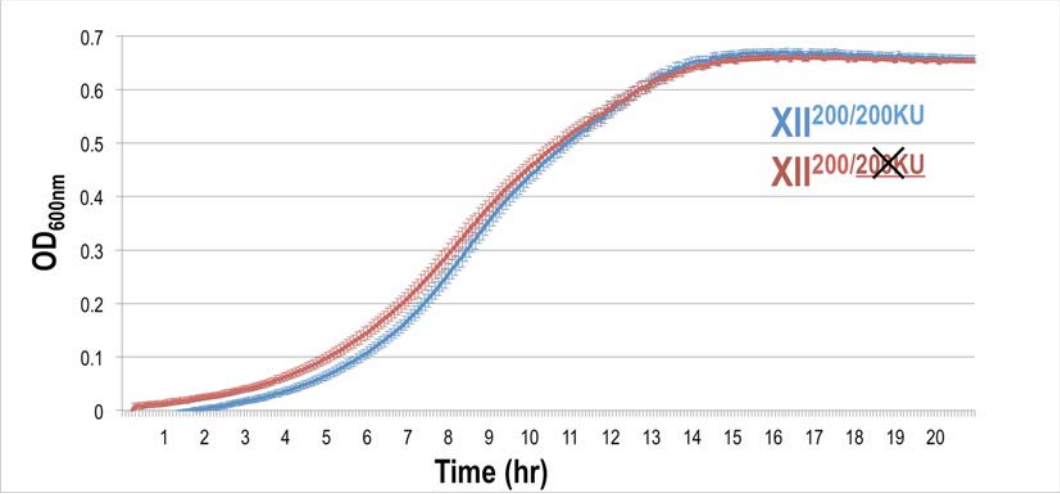

Figure 3.6. Loss of chromosome XII does not affect growth rate. Growth rates were measured using a 96 well plate reader (section 2.2.5). Growth in YPD of the WT CLA strain ($XII^{200/200KU}$; blue) was compared to its growth after loss of chromosome XII. n=3 (3 biological replicas, each with 3 technical replicas). Error bars show SE.

Finally, to test the ability of the CLA to distinguish chromosome loss in a diploid strain from other events that inactivate the markers, a haploid strain carrying the chromosome XII markers (XII^{200KU}) was used as a negative control. This strain can lose either marker gene or potentially both, but loss of its only copy of chromosome XII is not viable. As expected, no chromosome loss events were identified for the haploid strain XII^{200KU}. A few colonies were obtained on 5-FOA plates but these are all likely to be *URA3* mutations as they all grew in the G418 replica plates (data not shown). This showed that assaying for the presence of the second marker gene (*kanMX2*) is a powerful way to distinguish chromosome losses from other gene inactivation events. Taken together, these results confirm the authenticity of the chromosome loss colonies identified using the CLA, and show that the assay is robust.

CHAPTER FOUR: STRAIN CONSTRUCTION AND CHARACTERIZATION

[blank page]

To investigate the role of the rDNA in chromosome segregation, a number of diploid strains were required. These strains carry the CLA markers (section 3.1) and genetic modifications of interest. This chapter describes the strain construction and genotype confirmations of these strains. Details on the rationale for each strain and their chromosome missegregation phenotypes are presented in Chapter five.

4.1 STRAIN NOMENCLATURE

All strains used in this study have been assigned a nomenclature tailored to describe, in a simple way, the genetic modifications they harbor and the chromosome in which the CLA markers have been inserted. This nomenclature uses roman numerals to specify chromosome number, and superscripts to indicate rDNA copy number and insertion of the CLA markers. Other traits such as mutations and gene replacements are specified using conventional genetic nomenclature. Using this nomenclature, a wild type (WT) haploid strain with 200 copies of the rDNA on their native locus on chromosome XII is designated XII^{200}. *S. cerevisiae* haploid cells of opposite mating types (MATa and MATα) can be mated to create diploid cells (MATa/α). For diploid strains, a forward slash is used in the superscript to distinguish the traits of interest on each homologous chromosome. So, for a diploid WT strain carrying 200 rDNA copies on each chromosome XII homolog with the CLA markers *kanMX2* (K) and *URA3* (U) on one of these homologs, the strain designation is $XII^{200/200KU}$.

4.2 CHARACTERIZATION OF THE WT STRAIN $XII^{200/200KU}$

The WT CLA strain $XII^{200/200KU}$ used for the CLA optimization also served as a starting point to measure the rate of chromosome XII loss under normal conditions. This strain was created by Ogawa, Ganley and Kobayashi (unpublished) by insertion of *kanMX2* into the short arm of chromosome XII, and *URA3* into the long arm of chromosome XII (between *CEN12* and *RDN1*) of a haploid WT strain (figure 4.1). This haploid strain (XII^{200KU}) was mated with an untagged WT haploid strain (XII^{200}) of the opposite mating type to create strain $XII^{200/200KU}$.

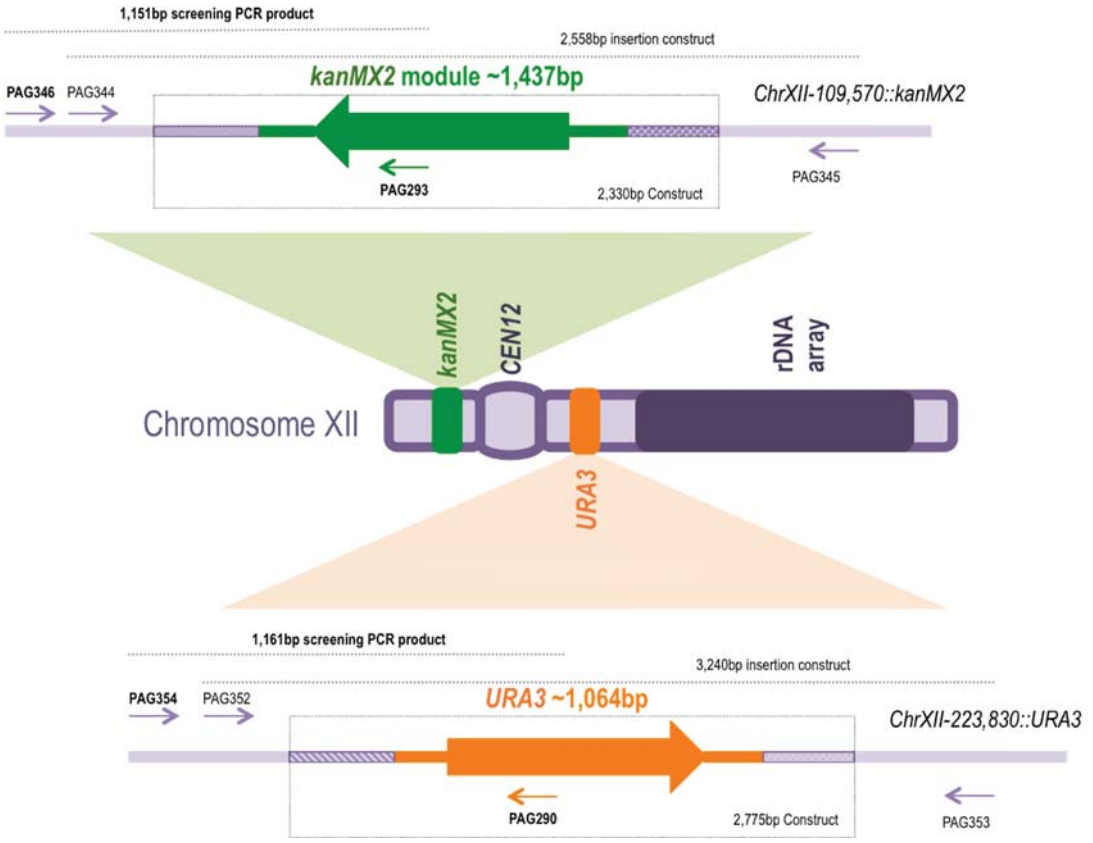

Figure 4.1. Insertion sites of the *kanMX2* and *URA3* markers in the short and long arms of chromosome XII, respectively. The *kanMX2* construct (top dotted box around green arrow) carries the 1,437 bp *kanMX2* module inserted into position 109,570 of chromosome XII. The *URA3* construct (bottom dotted box around orange arrow) carries the 1,064 bp *URA3* gene inserted into position 223,830 of chromosome XII. PCR primers for confirmation of the insertion (PAG346 and PAG293; PAG354 and PAG290) and for amplification of the whole insertion cassette (PAG344 and 345; PAG352 and PAG353) are shown for *kanMX2* and *URA3*, respectively. The positions of the insertions relative to the chromosome XII centromere (*CEN12*) and the rDNA array (purple) are indicated in the middle (not to scale). Marker insertion designed by Ogawa, Ganley and Kobayashi (unpublished).

The genotype of XII$^{200/200KU}$ was verified and is summarized in figures 4.2A and 4.2B. Chromosome XII size was evaluated through CHEF and Southern blotting (figure 4.2C), and the low mobility of chromosome XII is indicative of a WT length rDNA array (Kobayashi et al. 1998). PCR was used to confirm the presence of the CLA markers on chromosome XII (figure 4.2D), and the diploid nature of the strain (figure 4.2E). To corroborate that only one homolog chromosome carries the CLA tags, the strain was sporulated and tetrads were dissected, resulting in a 2:2 segregation of the *kanMX2* and *URA3* CLA markers (figure 4.3).

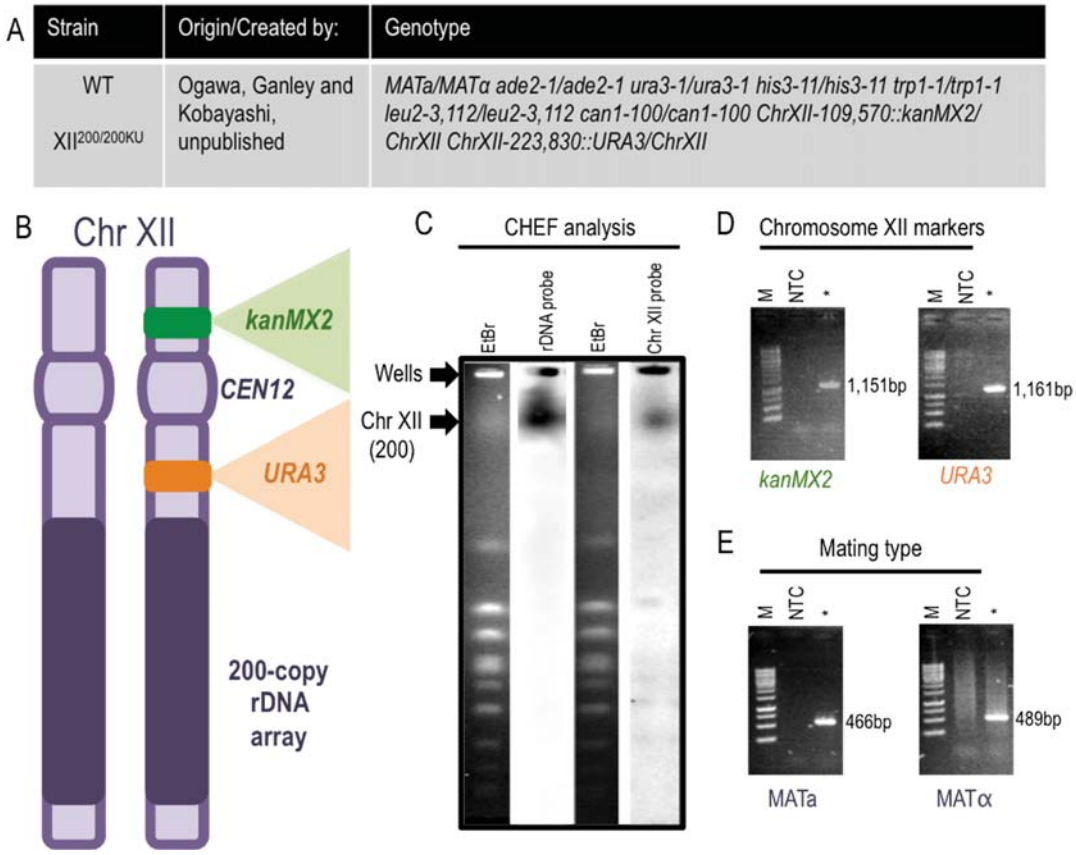

Figure 4.2. Characterization of the WT CLA strain XII$^{200/200KU}$. (**A**) Genotype of the WT strain. (**B**) Cartoon depicting the two chromosome XII homologs in the diploid WT strain. Chromosome XII is ~2.9 Mb and carries ~200 copies of the rDNA gene (dark purple) on each homolog. (**C**) Chromosome XII size was confirmed and rDNA copy number estimated by CHEF and Southern blotting with an rDNA and a chromosome XII probe. (**D**) PCR was used to confirm the insertion of the CLA selective markers *kanMX2* (PAG346 and PAG293) and *URA3* (PAG354 and PAG290) in chromosome XII at positions 109,570 and 223,830 respectively (see figure 4.1 for details). (**E**) PCR was also used to confirm diploidy by amplification of the mating type loci MATa (PAG465 and PAG467) and MATα (PAG466 and PAG467). M (Marker), NTC (no template control), and * (WT gDNA of strain XII$^{200/200KU}$).

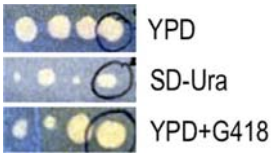

Figure 4.3. Haploid colonies from dissected tetrads of the WT CLA strain XII$^{200/200KU}$. One full tetrad dissected from strain XII$^{200/200KU}$ is shown with the 4 spores plated onto YPD, SD-Ura and YPD+G418 to confirm a 2:2 the segregation of the *URA3* and *kanMX2* CLA markers. From left to right, haploid colonies are XII^{200}, XII^{200U}, XII^{200K} and XII^{200KU}. The XII^{200KU} colony carrying both CLA markers that is prototrophic for uracil and G418 resistant is circled. There is some initial residual growth of spores on incompatible media due to the large number of cells transferred from the replica plating. However, the size difference between colonies is consistent with a 2:2 segregation of both CLA markers.

To determine whether insertion of the CLA tags into chromosome XII affects growth, the growth rate of the WT CLA strain XII$^{200/200KU}$ was compared to haploid WT strains with and

without the CLA tags on chromosome XII. An increase was observed in the slope of the growth curve of the diploid and haploid strains with the CLA tags compared to the untagged haploid WT, indicating an increased growth rate in the presence of the CLA tags (figure 4.4). This increase in growth rate can be explained by the presence of the *URA3* gene, as it has been previously shown that the growth rate of uracil auxotrophic (Ura^-) strains (such as our control haploid XII^{200}) is somewhat slower than that of uracil prototrophic (Ura^+) strains (Weng and Nickoloff 1997). Clearly, then, the CLA tags do not impair the growth rate of the WT strain, and instead provide a slight growth advantage. The CLA controls for differences in growth rates, therefore this growth advantage is not expected to affect the chromosome loss rate measurements.

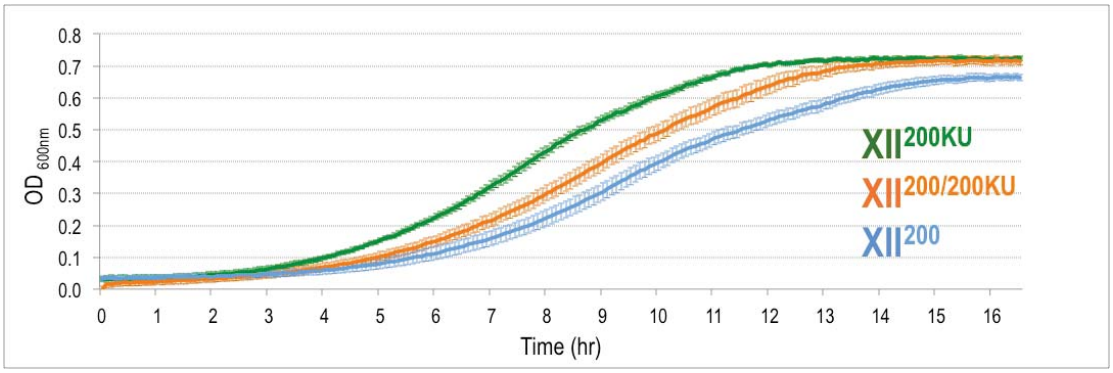

Figure 4.4. Chromosome XII tags for the CLA do not impair growth rate. Growth rates using 96 well plates (section 2.2.5) were obtained for the WT CLA strain $XII^{200/200KU}$, as well as haploid controls XII^{200KU} and XII^{200}. All strains were grown in YPD and their growth was monitored until they reached stationary phase. n=3 for each strain (3 biological replicates where each biological replicate consists of 3 technical replicates). Error bars show SE.

4.3 rDNA DELETION STRAINS

To examine the effect of the rDNA on chromosome segregation, I wanted to test the effect of removing the rDNA array from its native chromosomal location. To achieve this, a strain with the rDNA completely deleted from chromosome XII that was originally constructed by Wai et al. (2000) and that has the CLA markers inserted in one chromosome XII homolog was obtained from Ogawa, Ganley and Kobayashi (unpublished). This strain carries a 2-micron plasmid that contains a 35S rRNA gene driven by the Polymerase II Gal7 promoter and is referred to as the helper plasmid (HP) (figure 4.5). The helper plasmid also contains a 5S rRNA

gene, and a *TRP1* gene to allow auxotrophic selection. This tagged rDNA deletion strain is therefore referred to as XII$^{0/0KU}$+HP (figure 4.6A, 4.6B).

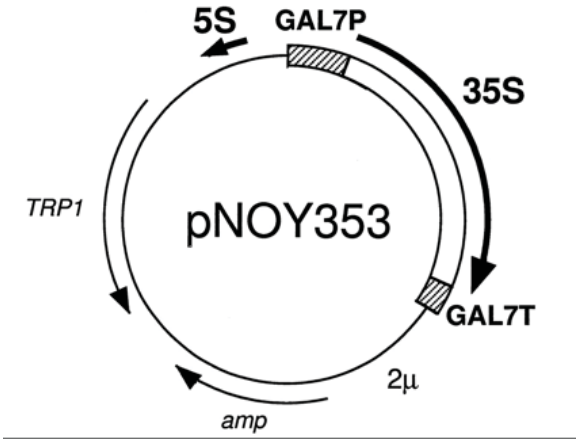

Figure 4.5. Helper plasmid (HP). The helper plasmid (HP) corresponds to pNOY353 created by Wai *et al.* (2000), and consists of a 2 micron plasmid carrying a 35S rRNA gene with a Gal7 promoter, a 5S rRNA gene, a *TRP1* gene for yeast auxotrophic selection, and an *amp* gene for selection during cloning (figure from Wai et al. 2000).

4.3.1 Characterization of the CLA strain XII$^{0/0KU}$+HP

To confirm that only one homolog carries the CLA tags, XII$^{0/0KU}$+HP was sporulated and tetrads were dissected (section 2.3.2). As anticipated, a 2:2 segregation ratio of the CLA markers *kanMX2* and *URA3* was observed (table IV). PCR was performed to confirm diploidy of this strain (figure 4.6E), insertion of the two CLA tags into chromosome XII (figure 4.6D), and the presence of the HP (figure 4.6F). Finally, CHEF and Southern blotting were performed to confirm that this strain contains no rDNA copies on chromosome XII. The chromosome XII band migrated further than the WT chromosome XII band and with a similar mobility to chromosomes VII and XV (figure 4.6C). This size of about 1 Mb corresponds to the 1,078 kb sequenced length of chromosome XII without the rDNA repeats (Goffeau et al. 1996). Additionally, chromosome XII was detected when a probe for chromosome XII was used, but could not be detected with an rDNA probe (figure 4.6C). These results confirm deletion of the rDNA array from both chromosome XII homologs, and this strain is referred to as the rDNA deletion strain in this thesis.

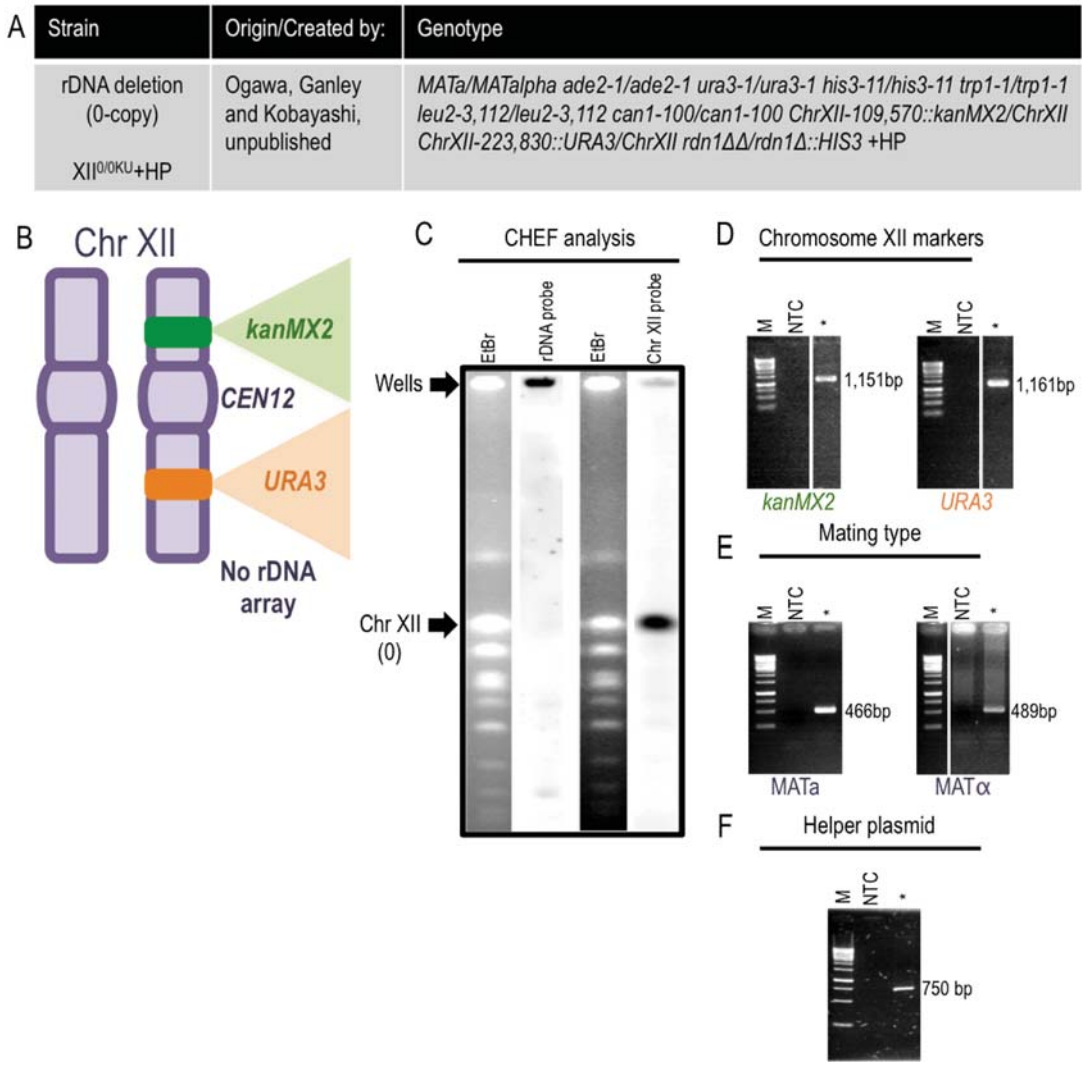

Figure 4.6. Characterization of the rDNA deletion strain XII$^{0/0KU}$+HP. (**A**) Genotype of the rDNA deletion strain. (**B**) Cartoon depicting the two chromosome XII homologs in the diploid XII$^{0/0KU}$ strain with the CLA *kanMX2* and *URA3* markers as in figure 4.2. In this strain chromosome XII is ~1.08 Mb and does not harbor any chromosomal rDNA gene copies on either homolog. (**C**) Chromosome size and rDNA copy number were confirmed using CHEF and Southern blotting. Insertion of CLA markers into chromosome XII (**D**), and diploidy of this strain (**E**) were confirmed through PCR as in figure 4.2. (**F**) PCR, using primers PAG10 and PAG313, was used to confirm the presence of the HP. M (marker), NTC (no template control), and * (gDNA of rDNA deletion strain XII$^{0/0KU}$+HP).

The rDNA deletion strain XII$^{0/0KU}$+HP is unusual in that it is able to grow in glucose, even though it should be dependent on galactose for growth because it uses a Polymerase II Gal7 promoter for rRNA transcription. The change that has enabled strain XII$^{0/0KU}$+HP to grow in glucose media is not known, but has been previously observed and may be the result of helper plasmid recombination with the 2-micron plasmid (A. Ganley personal communication). Despite this unusual growth ability, the 0-copy strain XII$^{0/0KU}$+HP was confirmed to have all rDNA copies deleted from chromosome XII using CHEF and Southern blot (figure 4.6). To determine whether growth of the 0-copy CLA strain is compromised, its growth rate was

compared to the WT strain XII$^{200/200KU}$. Deletion of the rDNA repeats from chromosome XII marginally decreases the growth rate in YPD medium when compared to WT (figure 4.7).

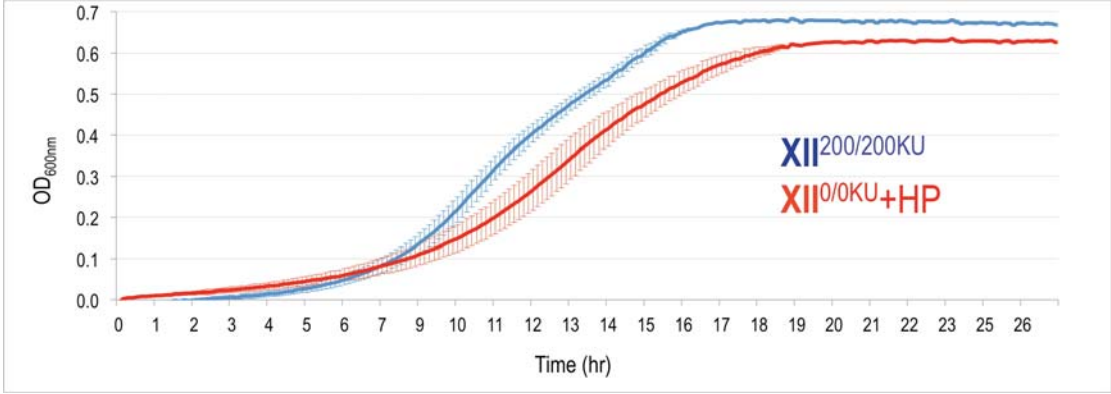

Figure 4.7. Deletion of the rDNA repeats from chromosome XII marginally decreases the growth rate. A strain with the rDNA deleted (XII$^{0/0KU}$+HP) grows slightly slower than a strain with WT rDNA copy number (XII$^{200/200KU}$). Growth rates were measured in YPD for both strains by following OD_{600nm} using a 96 well plate reader. For both strains n=2 (2 biological replicas per strain with 3 technical replicates each). Error bars show SE.

4.3.2 Creation of a helper plasmid control strain XII$^{200/200KU}$+HP

To examine whether the presence of the HP has any effect on chromosome segregation, a control strain was created by transforming the HP into the WT CLA strain XII$^{200/200KU}$. The HP was obtained by extracting total DNA from strain XII$^{0/0KU}$+HP (see section 2.4.2) and digesting it with RecBCD to degrade linear ssDNA and dsDNA while preserving circular plasmid DNA (figure 4.8).

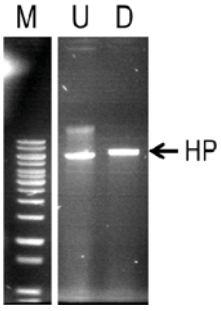

Figure 4.8. Helper plasmid from strain XII$^{0/0KU}$+HP. Ethidium bromide stained agarose gel of undigested (U) and RecBCD digested (D) XII$^{0/0KU}$+HP total DNA. M (marker). The arrow indicates HP DNA.

The HP was then transformed (section 2.7.2) into the CLA WT strain XII$^{200/200KU}$ and Trp^{+} colonies were selected. Successful transformation of the HP was confirmed through PCR

(figure 4.9) using a primer pair that amplifies a fragment between the Gal7 promoter and the 5S rRNA gene from the HP (figure 4.5).

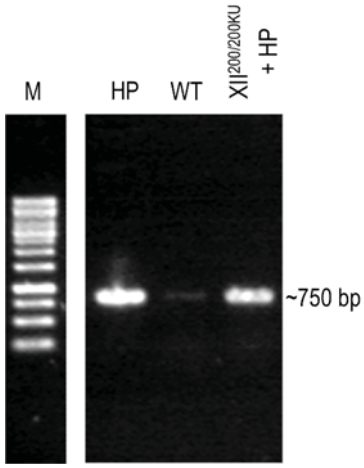

Figure 4.9. PCR confirms the presence of the HP in strain XII$^{200/200KU}$+HP. A ~750 bp fragment of the HP was amplified by PCR using primers PAG10 and PAG313 and separated by gel electrophoresis. M (marker), HP (HP purified plasmid DNA), WT (WT gDNA), and XII$^{0/0KU}$+HP (gDNA).

4.4 rDNA COPY NUMBER REDUCTION AND DISRUPTION OF *FOB1*

Strains that are disrupted for *FOB1* and that have reduced rDNA copy number were required for this study. To maintain a reduced number of rDNA copies, Fob1 must be inactivated, as its presence allows amplification of reduced rDNA copies back to the WT copy number (Kobayashi et al. 1998). Strains with the CLA markers inserted into chromosome XII and a disrupted copy of *FOB1* were obtained from Ogawa, Ganley and Kobayashi (unpublished), with either WT rDNA copy number or a reduced number of rDNA copies.

4.4.1 Characterization of strain XII$^{200/200KU}$ *fob1^{-}*

The genotype of strain XII$^{200/200KU}$ *fob1^{-}* is shown in figures 4.10A and 4.10B. This strain was confirmed to be prototrophic for uracil and G418 resistant, and it is also prototrophic for leucine as a consequence of the *FOB1* disruption. CHEF and Southern blotting confirmed that this strain contains a WT length rDNA array on chromosome XII (figure 4.10C), and a 2:2 segregation ratio of the CLA markers following sporulation confirmed that only one homolog

carries the CLA markers. PCR confirmed the insertion of the two CLA markers into chromosome XII (figure 4.10D), diploidy of the strain (figure 4.10E), and *FOB1* disruption (figure 4.10F). Disruption of *FOB1* by Ogawa, Ganley and Kobayashi was achieved by insertion of the *LEU2* gene into the middle of the *FOB1* coding sequence using a *fob1::LEU2* construct (Kobayashi and Horiuchi 1996) (figure 4.11). This strain is referred to as the *FOB1* disruption strain in this thesis.

A

Strain	Origin/Created by:	Genotype
FOB1 disruption XII$^{200/200KU}$ *fob1*$^{-}$	Ogawa, Ganley and Kobayashi, unpublished	*MATa/MATalpha ade2-1/ade2-1 ura3-1/ura3-1 his3-11/his3-11 trp1-1/ trp1-1 leu2-3,112/leu2-3,112 can1-100/can1-100 ChrXII-109,570::kanMX2/ChrXII ChrXII-223,830::URA3/ChrXII, fob1::LEU2/fob1::LEU2*

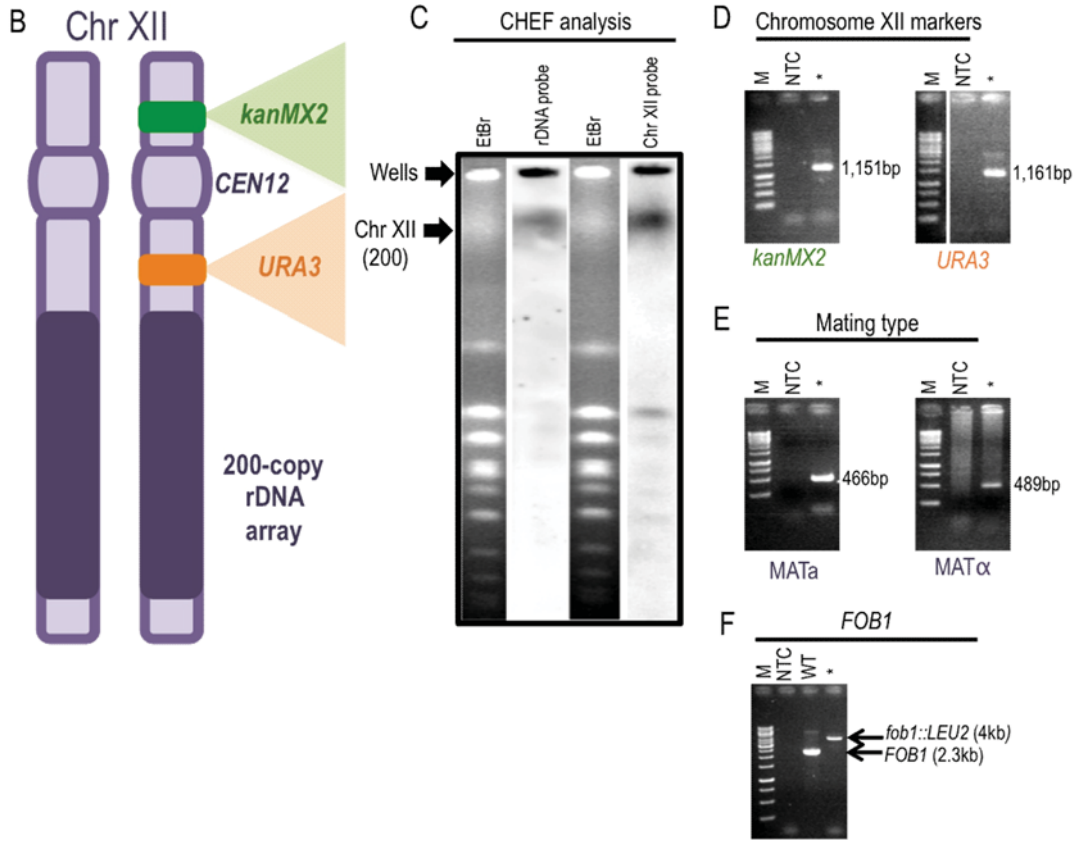

Figure 4.10. Characterization of the FOB1 disruption strain XII$^{200/200KU}$ *fob1*$^{-}$. (**A**) Genotype of the *fob1*$^{-}$ strain. (**B**) Cartoon depicting the two chromosome XII homologs in the diploid XII$^{200/200KU}$ *fob1*$^{-}$ strain. In this strain chromosome XII is ~2.9 Mb and carries ~200 copies of the rDNA gene on each chromosome arm. As in figure 4.2, chromosome XII was analyzed by CHEF and Southern blotting (**C**), and PCR was used to confirm the insertion of the CLA selective markers (**D**) and diploidy (**E**). PCR (using primers PAG23 and PAG24) was also used to confirm disruption of *FOB1* (**F**). M (marker), NTC (no template control), WT (gDNA of WT strain XII$^{200/200KU}$), and * (gDNA of strain XII$^{200/200KU}$ *fob1*$^{-}$).

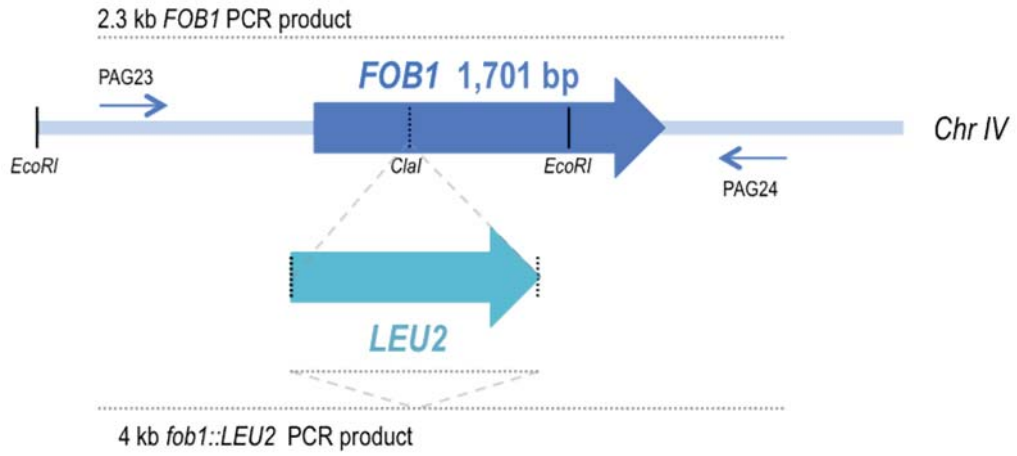

Figure 4.11. Disruption of *FOB1* using *LEU2*. Disruption of *FOB1* by insertion of *LEU2* into the *ClaI* restriction site of the *FOB1* coding region. Primers PAG23 and PAG24 are used to confirm *fob1::LEU2* by PCR amplification of a 2.3 kb product from *FOB1* versus a 4 kb product from *fob1::LEU2* .

4.4.2 Characterization of strain XII$^{20/20KU}$ *fob1*$^{-}$

We used the low rDNA copy number strain XII$^{20/20KU}$ *fob1*$^{-}$ from Ogawa, Ganley and Kobayashi (unpublished). This XII$^{20/20KU}$ *fob1*$^{-}$ strain has ~20 rDNA copies per array on both chromosome XII homologs, and sporulation confirmed a single copy of each CLA marker through 2:2 segregation. Figure 4.12A summarizes this strain's genotype and its important features are depicted in figure 4.12B. PCR confirmed its diploid state, CLA marker insertion into chromosome XII, and *FOB1* disruption (figure 4.12D,F). CHEF and Southern blotting indicates a smaller size of chromosome XII relative to WT but bigger than the rDNA deletion strain, with each homolog being a slightly different size. The homologs from this strain have been previously reported to contain ~20 rDNA gene copies each (Takeuchi et al. 2003). This strain is referred to as the 20-copy strain in this thesis. As for the rDNA deletion strain, we compared the growth rates of the *FOB1* disrupted and 20 copy strains, and both grow at a similar rate to WT (figure 4.13).

A

Strain	Origin/Created by:	Genotype
20-copy XII$^{20/20KU}$ *fob1*$^{-}$	Ogawa, Ganley and Kobayashi, unpublished	*MATa/MATalpha ade2-1/ade2-1 ura3-1/ura3-1 his3-11/his3-11 trp1-1/trp1-1 leu2-3,112/leu2-3,112 can1-100/can1-100 ChrXII-109,570::kanMX2/ChrXII ChrXII-223,830::URA3/ChrXII fob1::LEU2/fob1::LEU2 RDNA1~20copies/ RDNA1~20copies*

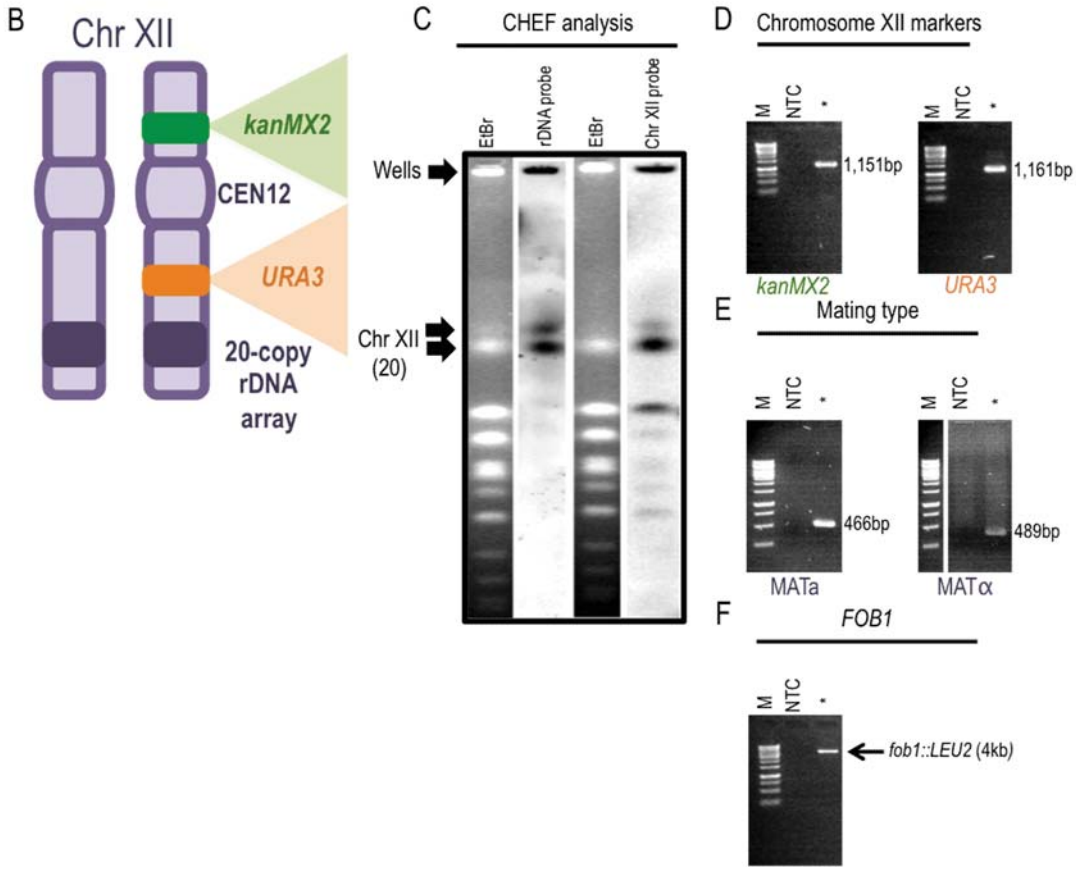

Figure 4.12. Characterization of the 20-copy strain XII$^{20/20KU}$ *fob1*$^{-}$. (**A**) Genotype of the 20-copy strain. (**B**) Cartoon depicting the two chromosome XII homologs in the diploid XII$^{20/20KU}$ *fob1*$^{-}$ 20-copy strain. In this strain chromosome XII is ~1.2 – 1.5 Mb and carries rDNA 20-30 copies on each homolog (dark purple). As in figure 4.10, chromosome XII was analyzed by CHEF and Southern blotting to confirm chromosome size and estimate rDNA copy number (**C**), and PCR was used to confirm the insertion of the CLA markers (**D**), diploid state (**E**) and disruption of *FOB1* (**F**). M (marker), NTC (no template control), and * (gDNA of strain XII$^{20/20KU}$ *fob1*$^{-}$).

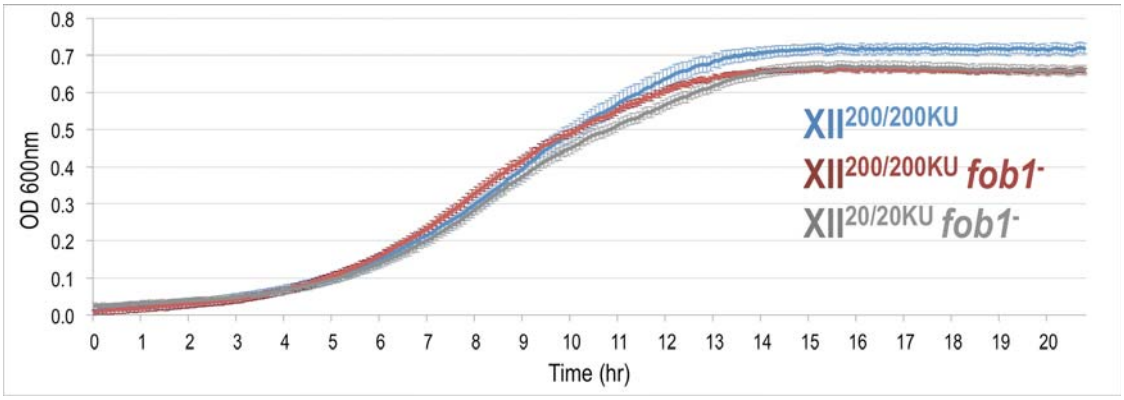

Figure 4.13. Disruption of *FOB1* and rDNA copy number reduction do not affect the growth rate of CLA strains. The *FOB1* disruption (XII$^{200/200KU}$ *fob1*$^{-}$) and 20 copy (XII$^{20/20KU}$ *fob1*$^{-}$) strains

grow at a similar rate to WT ($XII^{200/200KU}$). Growth rates for each strain were measured in YPD by following OD_{600nm} using a 96 well plate reader. For all strains strains n=2 (2 biological replicas per strain with 3 technical replicates each). Error bars show SE.

4.4.3 Creation of a Fob1p inducible plasmid: pGAL-*FOB1*

To determine the effect of complementing the *FOB1* disruption, an inducible *FOB1* system was used. I constructed a *FOB1* complementation system designed by M. Woods (Woods, Quintana and Ganley unpublished) to selectively induce expression of *FOB1* in the presence of galactose. The galactose promoter was chosen because of its reported ability to be activated in the presence of galactose and repressed in the presence of glucose (Johnston and Davis 1984; West et al. 1987).

The galactose inducible *FOB1* plasmid pGAL-*FOB1* was constructed by fusing a galatose promoter to *FOB1* and inserting the fused product into the multiple cloning site (MCS) of the yeast centromeric plasmid YCpLac22 (Gietz and Sugino 1988). To achieve this, first the GAL1-10 bidirectional promoter sequence between the *GAL1* and *GAL10* ORFs was PCR amplified, introducing novel *Sac*I and *Bam*HI restriction sites into the 5' and 3' ends by incorporating these restriction sites into the primer sequences. In parallel, *FOB1* was PCR amplified, introducing novel *Sal*I and *Bam*HI restriction sites into the 5' and 3' ends by incorporating these sites into the primer sequences. Both GAL1-10 and *FOB1* PCR products were digested with *Bam*HI. The GAL1-10 and alkaline phosphatase treated *FOB1* products were ligated to each other, and the GAL1-10-*FOB1* ligation product was amplified by PCR, adding A' overhangs. This fragment was cloned into the TA vector pCR2.1 and excised using *SalI* and *SacI* restriction endonucleases. Plasmid YCpLac22 was also digested and linearized with these restriction enzymes, and the resulting products were ligated to each other to insert the GAL1-10-*FOB1* construct into the YCpLac22 MCS, producing pGAL-*FOB1* (figure 4.14). This plasmid was confirmed by *Sal*I/*Sac*I restriction digestion to have a 4,854 bp backbone and a 2,450 bp insert (figure 4.15).

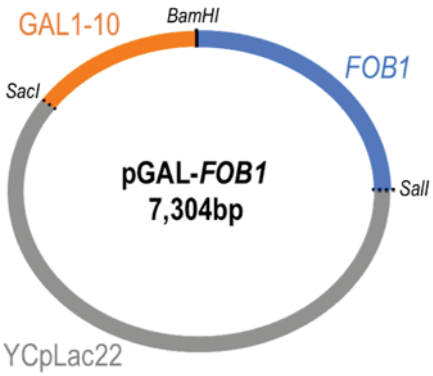

Figure 4.14. *FOB1* complementation plasmid pGAL-*FOB1*. The main features in the construction of pGAL-*FOB1* are illustrated. The *FOB1* gene was ligated to the GAL1-10 promoter sequence using *Bam*HI and the resulting ligation product was inserted into the YCpLac22 *Sac*I/*Sal*I MCS.

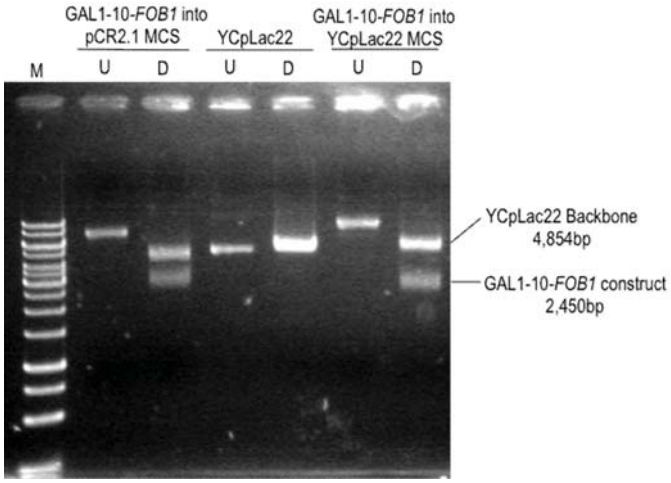

Figure 4.15. Construction of pGAL-*FOB1*. Ethidium bromide stained agarose gel of undigested (U) and *Sal*I/*Sac*I digested (D): GAL1-10-*FOB1* into pCR2.1 MCS (pCR2.1 plasmid containing the GAL1-10-*FOB1* construct), YCpLac22, and GAL1-10-*FOB1* into YCpLac22 MCS (newly constructed plasmid pGAL-*FOB1*).

Plasmid pGAL-*FOB1* was transformed into strains XII$^{200/200KU}$, XII$^{200/200KU}$ *fob1*$^{-}$, and XII$^{20/20KU}$ *fob1*$^{-}$ to allow expression of *FOB1* through growth in galactose. Transformants were selected for their ability to grow on medium lacking tryptophan. Presence of pGAL-*FOB1* was confirmed by PCR amplification of the GAL1-10-*FOB1* construct using primers M13F and M13R (which bind to the MCS in YCpLac22) (figure 4.16).

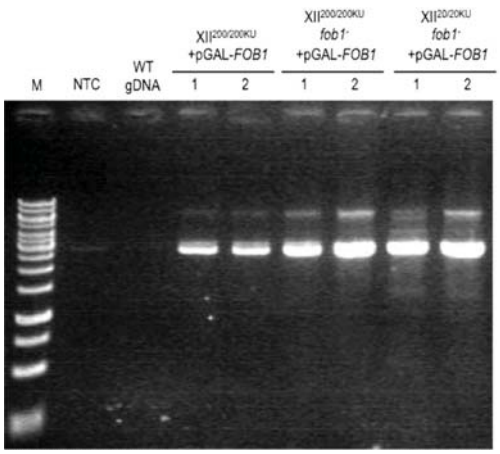

Figure 4.16. PCR confirms successful transformation of pGAL-*FOB1* into strains XII$^{200/200KU}$, XII$^{200/200KU}$ *fob1*$^{-}$, and XII$^{20/20KU}$ *fob1*$^{-}$. A ~2.5 kb product from pGAL-*FOB1* was amplified by PCR using M13F and M13R primers and separated by gel electrophoresis. M (marker), NTC (no template control), and WT gDNA (negative amplification control from XII$^{200/200KU}$). Two different isolates from each transformant were screened.

4.4.4 Creation and characterization of strain XII$^{0/0KU}$ *fob1*$^{-}$+HP

Strain XII$^{0/0KU}$ *fob1*$^{-}$+HP was created from strain XII$^{0/0KU}$+HP. First, to obtain rDNA deletion haploids of opposite mating types, one with and one without the CLA markers, strain XII$^{0/0KU}$+HP was sporulated. Spores from two sets of tetrads were streaked onto selective media to determine the presence or absence of the CLA markers and the HP. As expected, a 2:2 segregation of the markers (G418^{R} and Ura^{+}) and a 4:0 inheritance of the HP (Trp^{+}) were observed (table IV). The mating type of each spore was determined by the liquid culture method (see section 2.3.3).

Table IV. Phenotypic traits and mating types of haploid spores from strain XII$^{0/0KU}$+HP

S = Sensitive, R = Resistant, + = Prototroph, - = Auxotroph, *=Spores used to construct strain XII$^{0/0KU}$ *fob1*$^{-}$+HP

Tetrad	Spore	G418	Ura	HP (Trp)	Mating type
1	A	R	-	+	α
	B*	S	-	+	α
	C*	R	+	+	a
	D	S	+	+	a
2	A	S	-	+	a
	B	R	+	+	α
	C	S	-	+	a
	D	R	+	+	α

Spores 1B and 1C of opposite mating types and carrying the HP (table IV) were then subjected to *FOB1* disruption through insertion of *HIS3* to partially replace the 5' end of the *FOB1* coding sequence (figure 4.17), as previously performed by Kobayashi *et al*. (Kobayashi et al. 1998). PCR employing the same primers used to amplify the *FOB1* locus (figure 4.9) was used to confirm successful *fob1::HIS3* disruption in the His^+ colonies of spores 1B (Schischka and Ganley, unpublished, not shown) and 1C (figure 4.18) through a fragment size increase for *fob1::HIS3* compared to *FOB1*.

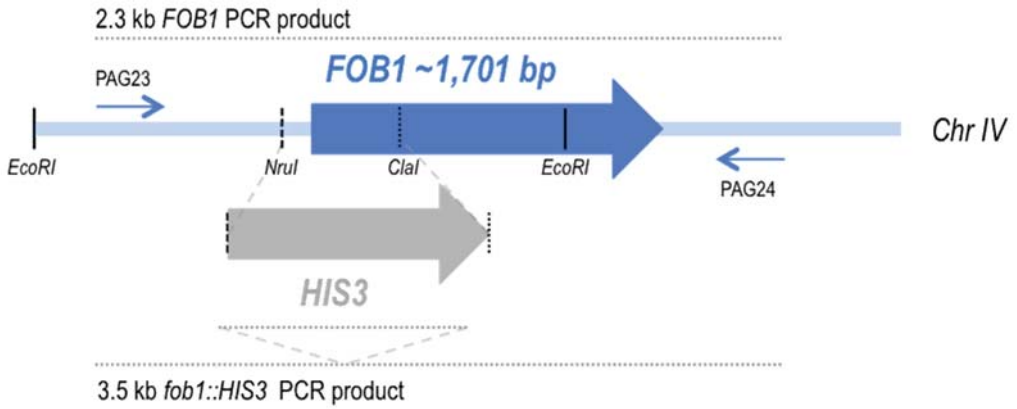

Figure 4.17. Disruption of *FOB1* by *HIS3*. Disruption of *FOB1* followed the method of Kobayashi *et al.*. (1998) who used a *NruI/Cla*I flanked *HIS3* PCR product to replace the *NruI/Cla*I fragment containing part of the *FOB1* coding region (about 750 bp encompassing ~550 bp of the 5' end of *FOB1*). Primers PAG23 and PAG24 were used to confirm *fob1::HIS3* by PCR amplification of a 2.3 kb product from *FOB1* versus a 3.5 kb product from *fob1::HIS3*. This 3.5 kb *fob1::HIS3* PCR product was used to disrupt *FOB1* in other CLA strains in this study.

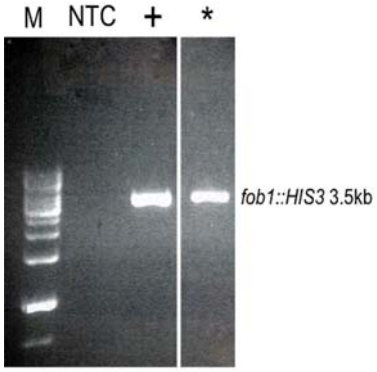

Figure 4.18. *FOB1* disruption in rDNA deletion haploid spore 1C (XII^{0KU}+HP). *FOB1* disruption in the haploid rDNA deletion strain XII^{0KU}+HP (*) is demonstrated by PCR amplification of a 3.5 kb product corresponding to *fob1::HIS3*. M (Marker), NTC (no template control) and + (positive gDNA control from *fob1::HIS3* strain $XII^{200/200KU}$ *fob1*$^-$).

The *fob1*$^-$ rDNA deletion haploids (XII^0 *fob1*$^-$+HP and XII^{0KU} *fob1*$^-$+HP) were then mated and zygotes selected using a micromanipulation microscope to obtain a diploid rDNA deletion strain with a homozygous *FOB1* disruption. The diploid nature of the new $XII^{0/0KU}$ *fob1*$^-$+HP strain was confirmed through PCR (appendix 8.1).

4.5 CREATION OF *RPA135* DELETION STRAINS

4.5.1 Construction of XII$^{200/200KU}$ *rpa135Δ*+HP strain

To evaluate the effect of rDNA transcription on chromosome XII segregation, our approach was to inactivate Pol I to abolish chromosomal rDNA transcription without altering chromosome size or removing the rDNA repeats. Since rDNA transcription by Pol I is essential for cell survival, strains were first transformed with the helper plasmid before Pol I inactivation. Pol I inactivation was achieved through deletion of the *RPA135* gene that encodes the second largest subunit of the Pol I complex. Several strategies were used to attempt to replace the *RPA135* coding sequence with a selective marker.

Our initial strategy to replace *RPA135* with the *LEU2* gene was to use a direct knockout approach that involved amplification of *LEU2* with long primers containing ~50 bp of sequence matching the *RPA135* flanking regions (figure 4.19). Following amplification, the *rpa135Δ::LEU2* PCR product was directly transformed into WT haploid yeast cells containing the HP and selection was performed on minimal medium lacking leucine. However, all the phenotypically positive screened colonies were negative for *RPA135* deletion (data not shown).

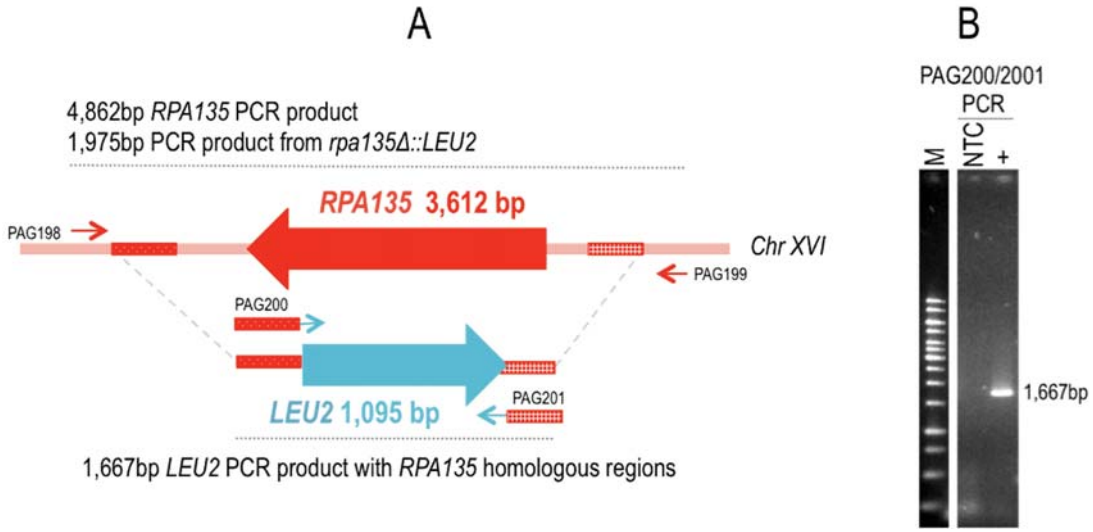

Figure 4.19. *RPA135* direct PCR replacement approach with *LEU2*. (**A**) A 1,667 bp product (using primers PAG200 and PAG201, bottom dotted line) of *LEU2 (*from YEpLac181) with *RPA135* homologous flanking regions (50 bp on the 5' end and 53 bp on the 3' end; shown in red) was used to replace *RPA135* on chromosome XVI. Primers PAG198 and PAG199 upstream and downstream of the transformation target site, respectively, were used to confirm replacement of *RPA135* by *LEU2* through amplification of a 4,862 bp product from *RPA135* or a 1,975 bp product from *rpa135Δ::LEU2* (top dotted line). (**B**) The ~1,667 bp disruption construct was PCR amplified using primers PAG200 and PAG201 and separated by gel electrophoresis. M (marker), NTC (no template control), and + (YEpLac181 was used as a positive *LEU2* amplification control).

The haploid strain is auxotrophic for leucine due to double frameshift mutations (*leu2,112* and *leu3,112*) in the native *LEU2* locus. Therefore it is possible that the *rpa135Δ::LEU2* construct integrated at the native *LEU2* locus instead of the *RPA135* locus. To circumvent this, we decided to use the same replacement strategy, but instead using a selective marker with low sequence identity to the native *S. cerevisiae* gene. The *ADE6* gene from *Schizosaccharomyces pombe* (*SpADE6*), which is a homolog of the *S. cerevisiae ADE2* gene (Forsburg 2001) with ~80% sequence similarity, was chosen as a selective marker for *RPA135* disruption. Long primers containing the same ~50 bp *RPA135* flanking regions as above were used to amplify *ADE6* (figure 4.20). Following amplification, the *rpa135Δ::ADE6* PCR product was directly transformed into WT haploid yeast cells containing the HP. However, no colonies grew on minimal medium lacking adenine, despite multiple transformation attempts.

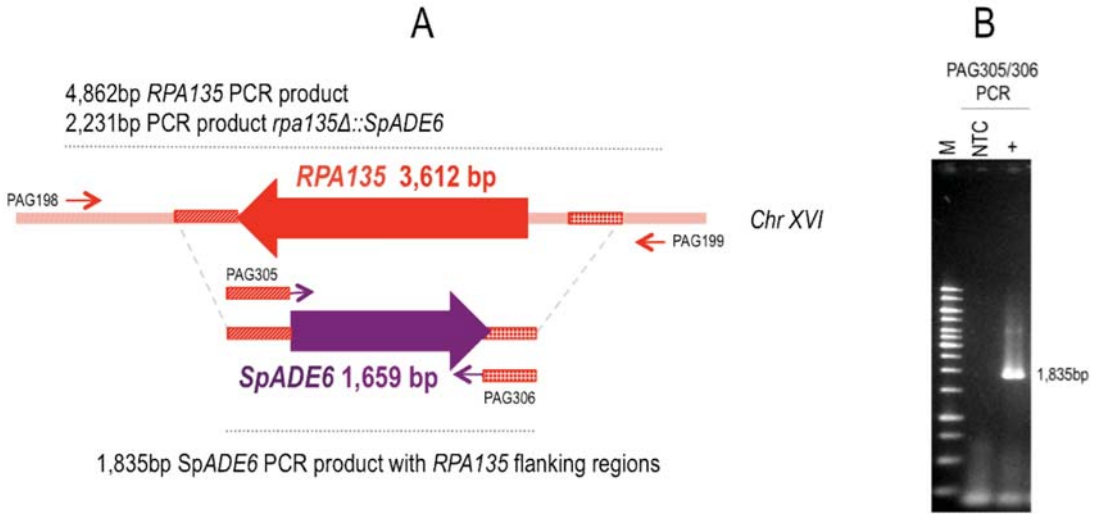

Figure 4.20. *RPA135* direct PCR replacement approach using *rpa135Δ::SpADE6*. **(A)** An *SpADE6 (*from *S. pombe)* PCR product (1,835 bp using primers PAG305 and PAG306) with *RPA135* (from *S. cerevisiae*) flanking regions (54 bp on the 5' end and 53 bp on the 3' end) was used to directly transform yeast to replace the *RPA135* locus. Primers PAG198 and PAG199 (upstream and downstream of the transformation target site) were used to confirm replacement of *RPA135* by *SpADE6* through amplification of a 4,862 bp product from *RPA135* or a 2,231 bp product from *rpa135Δ::SpADE6*. (**B**) The ~1,835 bp disruption construct was amplified using primers PAG305 and PAG306 and separated by gel electrophoresis. M (marker), NTC (no template control) and + (*S. pombe* gDNA was used as template to amplify *rpa135Δ::SpADE6).*

A third strategy that employs an increased homologous flanking region lengths using the *rpa135Δ::ADE6* construct was undertaken, in case the short flanking regions hindered transformation efficiency in the previous strategies. This strategy was chosen based on results showing that ~50 bp of homologous flanking regions is enough for targeted gene replacement, but that transformation efficiency is substantially enhanced when the length of the homologous

region is increased (Sugiyama et al. 2005). Therefore, *SpADE6* was PCR amplified, ligated into the TA vector pCR2.1, and excised using restriction enzymes to obtain a *SpADE6* fragment (figure 4.21A and 4.22A). In parallel, the *RPA135* gene and its flanking regions were amplified from WT gDNA and ligated into the pCR2.1 TA cloning vector to create plasmid DAG135 (figure 4.21B). DAG135 was then digested with the same restriction enzymes used to excise *SpADE6* from pCR2.1 (figure 4.22B), removing an internal portion of the *RPA135* coding region that was replaced by ligation of the *SpADE6* fragment. This creates the knockout construct *rpa135::SpADE6* (figure 4.21C), which was confirmed by PCR (figure 4.22C). This construct was used to transform WT haploid yeast cells. After several transformation attempts, some potential transformation colonies grew on minimal medium lacking adenine. However, all these transformant colonies were found to be negative for *RPA135* replacement by PCR screening (data not shown). This suggested that our *SpADE6* sequence might not complement *ADE2* deficiency or that *RPA135* disruption is difficult in this haploid strain.

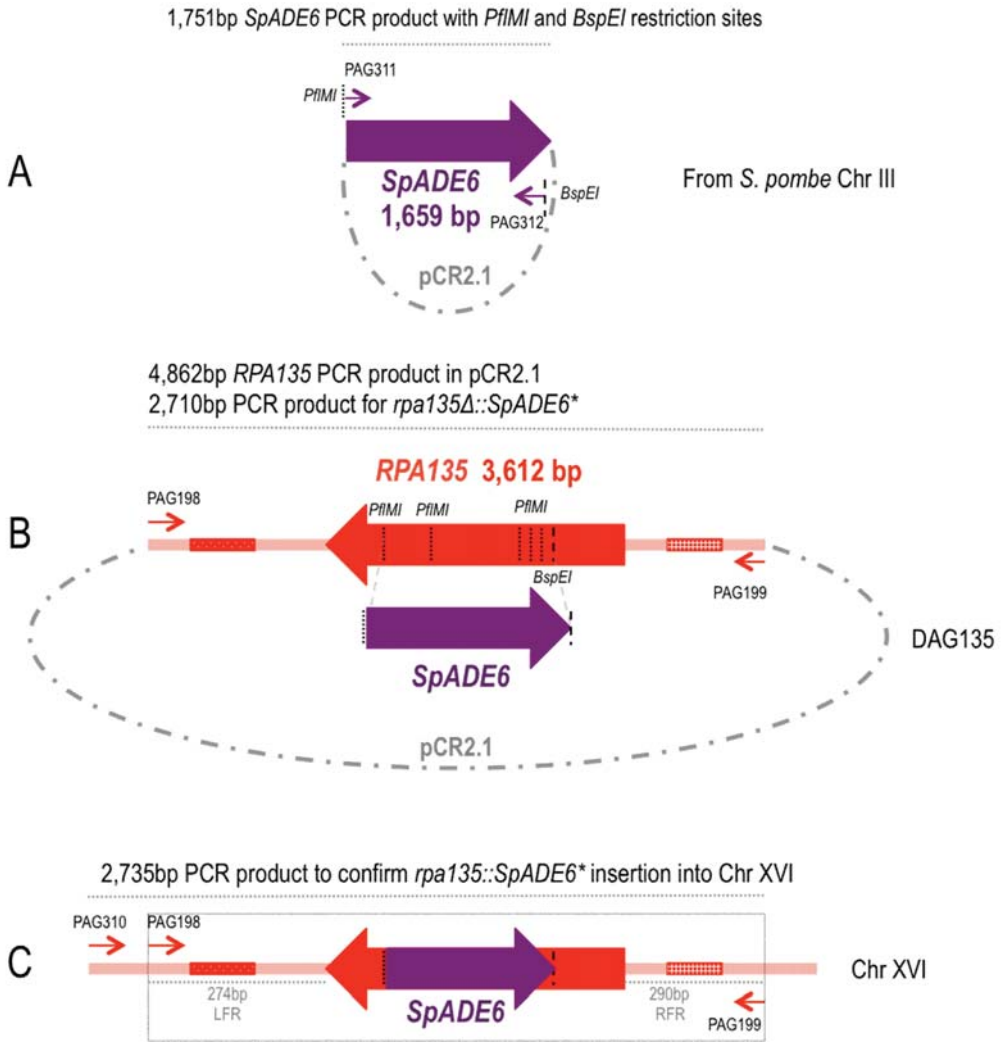

Figure 4.21. *rpa135::SpADE6* long replacement construct approach. *SpADE6* was used to partially replace the coding sequence of *RPA135*. **(A)** *SpADE6* was amplified by PCR (using primers PAG311 and PAG312 containing *Pfl*MI and *Bsp*EI restriction sites, respectively), ligated through into TA cloning plasmid pCR2.1, and excised using restriction enzymes *Pfl*MI and *Bsp*EI. **(B)** *RPA135* was PCR amplified using primers PAG198 and PAG199 (4,862 bp product) and inserted into plasmid pCR2.1 to create plasmid DAG135. The *Pfl*MI/*Bsp*EI fragment was excised from this plasmid and replaced by ligating the excised *SpADE6* product from (**A**) to create a plasmid containing the *rpa135::SpADE6* long replacement construct. Primers PAG198 and PAG199 were used to amplify this construct for transformation. (**C**) Replacement of *RPA135* by *SpADE6* was evaluated using primers PAG310 and PAG199, which amplify a 2,735 bp product from *rpa135::SpADE6.*

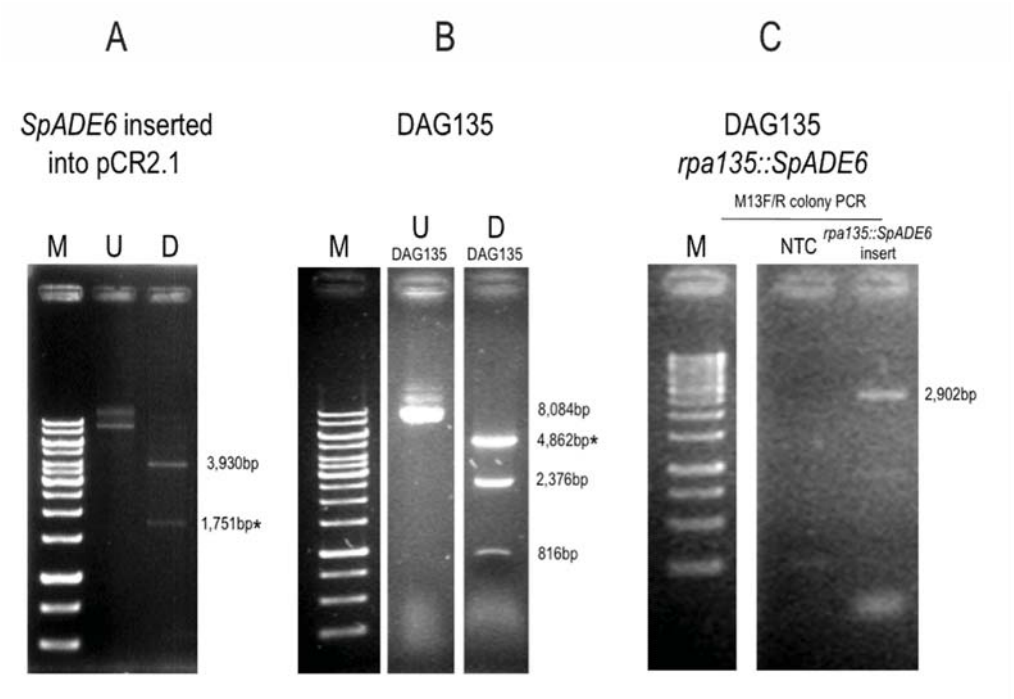

Figure 4.22. Creation of the *rpa135::SpADE6* long replacement construct. Ethidium bromide stained agarose gels show the construction of *rpa135::SpADE6.* (**A**) *SpADE6* inserted into PCR2.1 is shown before (U, undigested) and after (D, digested) *Pfl*MI and *Bsp*EI excision to obtain a 1,751 bp *SpADE6* fragment with sticky *PflMI/BspEI* ends (*). (**B**) DAG135 (U) was digested using *PflMI* and *BspEI* (D) to remove a portion of the *RPA135* coding sequence and yield the 4,862 bp DAG135 backbone with sticky *PflMI/BspEI* ends (*). (**C**) The two fragments with sticky *PflMI/BspEI* ends from A and B (*) were ligated to each other, and the newly formed plasmid was verified by PCR using M13 primers to obtain a 2,902 bp fragment encompassing the *rpa135::SpADE6* construct. M (marker), NTC (no template control).

Next, we tried using the *RPA135* deletion strategy of Nogi et al. (1991b). These authors replaced a single copy of *RPA135* with *LEU2* in a diploid strain, making it heterozygous *RPA135/rpa135Δ::LEU2,* and then sporulated this strain to obtain a haploid with a *RPA135* deletion (NOY866). Although their strain has a *RPA135* deletion, it has a different genetic background to the other strains in this study. Therefore I transformed the CLA WT diploid strain XII$^{200/200KU}$+HP with the *rpa135Δ::LEU2* construct (Woods, Quintana and Ganley, unpublished results). This yielded colonies able to grow on galactose medium lacking leucine. Replacement of one copy of *RPA135* with *LEU2* was confirmed through PCR (Figure 4.23A), and PCR of the HP (Figure 4.23B) confirmed it was still present, as it is necessary for viability of sporulated *rpa135Δ::LEU2* haploids.

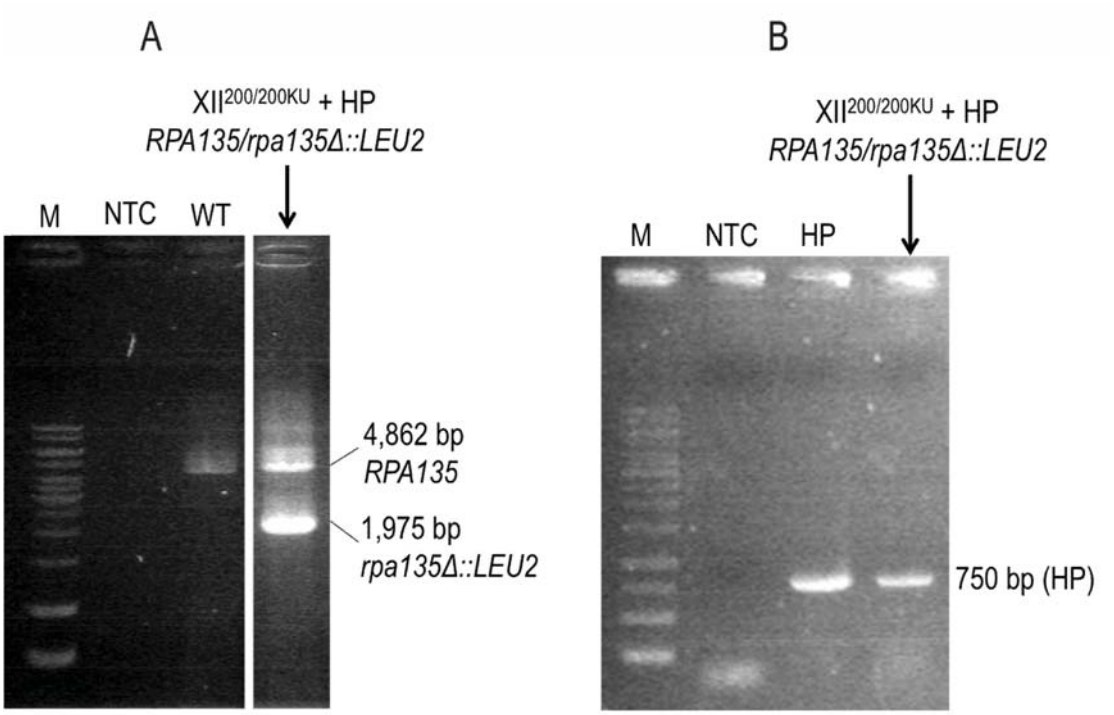

Figure 4.23. Replacement of one copy of *RPA135* with *LEU2* in a WT diploid strain. (**A**) The *RPA135* locus was PCR amplified using primers PAG198 and PAG199 to confirm replacement of one *RPA135* copy in the transformed XII$^{200/200KU}$+HP strain, as shown by one WT *RPA135* copy (4,862 bp) and one copy that has been replaced with *LEU2* (*rpa135Δ::LEU2*; 1,975 bp). M (marker), NTC (no template control), and WT (WT gDNA used as a positive *RPA135* control). (**B**) PCR (as in figure 4.8) confirming the presence of the HP in strain XII$^{200/200KU}$ *RPA135/rpa135Δ::LEU2*+HP (HP DNA was used as a positive amplification control).

Strain XII$^{200/200KU}$ *RPA135/rpa135Δ::LEU2*+HP was sporulated and tetrads dissected to obtain *rpa135Δ::LEU2* haploids. For most dissected tetrads, only two viable colonies were observed, but when a third or fourth colony was obtained from a tetrad, it exhibited an extremely small size and slow growth compared to the other two colonies. This dissimilarity in colony size is suggestive of 2:2 segregation of *rpa135Δ::LEU2* and *RPA135* (e.g. figure 4.24, colonies 1 and 3 versus 2 and 4, respectively), as the growth rate has been reported to decrease 4-5 fold in a *RPA135* deletion strain (Nogi et al. 1991b). Full sets of spores also displayed a 2:2 segregation for their ability to grow on medium lacking uracil and for G418 sensitivity (not shown), as expected for segregation of the CLA markers. Finally, only two spores from each tetrad displayed growth on glucose medium, while all four spores could grow on galactose medium, consistent with 2:2 segregation of *RPA135* and HP-dependent *rpa135Δ::LEU2.*

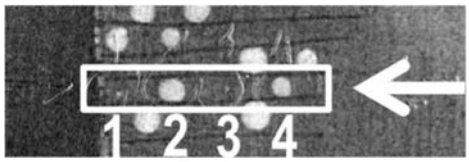

Figure 4.24. Dissected tetrads from XII$^{200/200KU}$ *RPA135/rpa135Δ::LEU2*+HP strain. Tetrads were dissected in YPGal medium using a micromanipulation microscope. Colonies obtained from one tetrad are boxed as an example, with colonies 1 and 3 being extremely small.

Haploid spores giving rise to very small colonies and unable to grow in glucose medium were screened through PCR to verify the insertion of the *rpa135Δ::LEU2* construct into the *RPA135* native locus in chromosome XVI. For specificity in detecting the construct in the correct location, we used a primer binding upstream to the *RPA135* locus and paired it with a primer binding internally to the *LEU2* coding sequence. We were able to verify successful deletion of *RPA135* in ten haploid spores. Mating type and CLA marker presence were also checked by PCR for the haploid spores XII^{200KU} *rpa135Δ::LEU2*+HP and XII^{200} *rpa135Δ::LEU2*+HP (appendix figure 8.2).

To create a CLA *rpa135Δ::LEU2* homozygous diploid strain, haploid XII^{200KU} *rpa135Δ::LEU2*+HP and XII^{200} *rpa135Δ::LEU2*+HP spores (with and without the CLA markers, respectively) of opposite mating type were mated to each other and zygotes picked using a micromanipulation microscope. The diploid state of the new strain XII$^{200/200KU}$ *rpa135Δ*+HP was confirmed through mating type PCR (appendix figure 8.3).

4.5.2 *FOB1* disruption in a *RPA135* deletion background

We also created a *RPA135* deletion strain that harbors a *FOB1* disruption. Since our *RPA135* deletion construct uses leucine selection, we used *HIS3* to disrupt *FOB1* in strain XII$^{200/200KU}$ *rpa135Δ*+HP. After transformation with the *fob1::HIS3* construct and selection for His^{+} colonies, we confirmed disruption of one of the two *FOB1* copies by the amplification of two different size products from the *FOB1* locus indicative of a *FOB1*/*fob1::HIS3* heterozygous strain (figure 4.25).

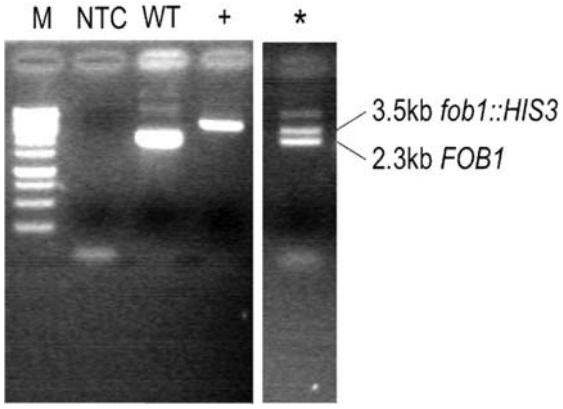

Figure 4.25. Heterozygous disruption of *FOB1* by *HIS3* in strain XII$^{200/200KU}$ *rpa135Δ*+HP.
Disruption of one *FOB1* copy in strain XII$^{200/200KU}$ *rpa135Δ*+HP *FOB1*/*fob1::HIS3* (*) was confirmed by PCR amplification (as in figure 4.10) of a 2.3 kb product from *FOB1* and a 3.5 kb product corresponding to *fob1::HIS3*. M (marker), NTC (no template control), WT (gDNA from XII$^{200/200KU}$ used as a *FOB1* control), + (the *fob1::HIS3* construct was used as a positive control).

We next sporulated strain XII$^{200/200KU}$ *rpa135Δ*+HP *FOB1*/*fob1::HIS3* to obtain haploids that were both leucine and histidine prototrophs and hence carried both the *RPA135* deletion and the *FOB1* disruption. We obtained 11 haploid spores prototrophic for leucine and histidine, and five were confirmed by PCR to harbor the *fob1::HIS3* construct and to carry the CLA markers. Following mating type determination (appendix figure 8.4), spores XII^{200KU} *rpa135Δ::LEU2*+HP *fob1::HIS3* and XII^{200} *rpa135Δ::LEU2*+HP *fob1::HIS3* of opposite mating type were mated and zygotes selected to obtain a diploid CLA strain homozygous for both the *RPA135* replacement and *FOB1* disruption. The diploid state of the new strain XII$^{200/200KU}$ *rpa135Δ*+HP *fob1*$^{-}$ was confirmed through mating type PCR (appendix figure 8.5).

4.5.3 Attempts to construct a 20-copy strain harboring a *RPA135* deletion

We next attempted to construct a 20-copy rDNA strain with a *RPA135* deletion. As disruption of *FOB1* is necessary to maintain a stably reduced rDNA copy number, we first created a 20-copy strain with *FOB1* disrupted by *HIS3* instead of *LEU2,* because the *LEU2* marker was used in the *rpa135Δ::LEU2* construct. This involved using strain TAK300 (XII^{20} fob1::HIS3 MATα, Takeuchi et al. 2003) and sporulating the diploid 20-copy strain (XII$^{20/20KU}$ *fob1::LEU2*) to obtain a XII^{20KU} *fob1::LEU2* MATa haploid and swapping the *LEU2* marker gene with *HIS3* through transformation of the *fob1::HIS3* construct. The *fob1::HIS3* disruption of

TAK300 and the successful *leu2::HIS3* marker swap of the XII^{20KU} *fob1::LEU2* haploid were confirmed by PCR (figure 4.26).

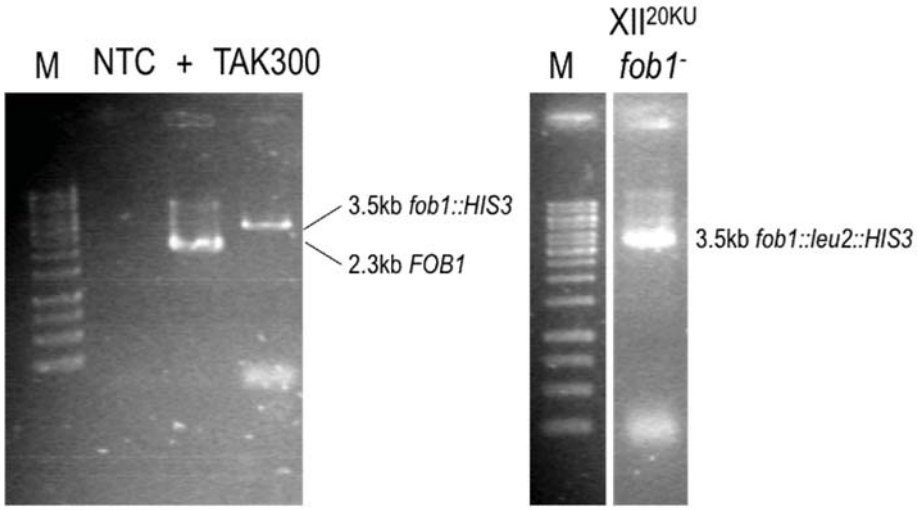

Figure 4.26. Disruption of *FOB1* with *HIS3* in the haploid strains TAK300 and XII^{20KU} *fob1::leu2::HIS3*. A 3.5 kb fragment corresponding to *fob1::HIS3* was PCR amplified and separated by gel electrophoresis in strains TAK300 and XII^{20KU} *fob1::leu2::HIS3* (*),(to confirm disruption of *FOB1* by Takeuchi *et al.*., 2003) and replacement of the *FOB1* disruption marker respectively. M (marker), NTC (no template control), + (WT gDNA from strain XII$^{200/200KU}$ used as positive amplification control of a *FOB1* (2.3 kb).

We next mated strains TAK300 and XII^{20KU} *fob1::leu2::HIS3*, and picked zygotes to obtain a 20-copy strain homozygous for *FOB1* disruption by *HIS3.* This XII$^{20/20KU}$ *fob1^{-}* (*fob1::leu2::HIS3*) strain was confirmed to be diploid through PCR (appendix figure 8.6), and was transformed with the *rpa135Δ::LEU2* construct and the HP. Five colonies were obtained from medium lacking leucine, and PCR showed replacement of one *RPA135* copy and presence of the helper plasmid (figure 4.27) in one of these colonies.

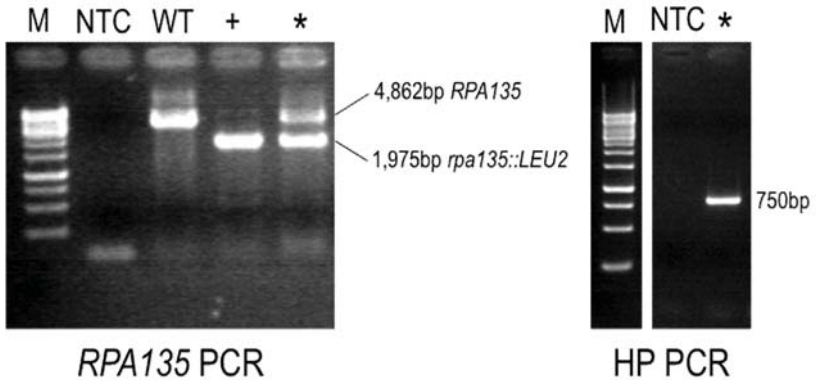

Figure 4.27. Replacement of one copy of *RPA135* with LEU2 in strain XII$^{20/20KU}$ *fob1^{-}*. The *RPA135* locus was amplified using primers PAG198 and PAG199 to confirm replacement of one *RPA135* copy in the diploid strain XII$^{20/20KU}$+HP *fob1^{-}* (*) (*RPA135* PCR**).** M (marker), NTC (no template control), WT (WT gDNA used as *RPA135* positive control producing a fragment of 4,862 bp), + (*rpa135Δ::LEU2* construct used as positive replacement control producing a fragment of 1,975 bp). HP PCR (as in figure 4.6) confirms presence of the HP.

Tetrad dissections of strain XII$^{20/20KU}$ *fob1*$^{-}$ (*fob1::leu2::HIS3*) *RPA135/rpa135Δ::LEU2*+HP never produced more than two viable spores. Every viable spore could grow in glucose medium suggesting that the two 20-copy spores inheriting the *rpa135Δ::LEU2* construct were not viable. The viable pairs of spores were not characterized further. Instead we used a marker swap cassette to replace the *LEU2* copy for the *ADE2* gene in the diploid XII$^{20/20KU}$ *fob1*$^{-}$ (*fob1::HIS3*) *RPA135/rpa135Δ::LEU2*+HP strain, so that we could re-use the *rpa135Δ::LEU2* construct to delete the second copy of *RPA135* in this strain. The *leu2::ADE2* marker swap cassette was obtained from plasmid M3939 (Voth et al. 2003), excised using *PstI/SacI* digestion, and used to transform the diploid heterozygous strain. PCR using a *RPA135* locus specific primer and an *ADE2* internal primer confirmed successful insertion of the *ADE2* marker at the *RPA135* locus, and a second PCR of the *RPA135* locus also confirmed a size increase corresponding to this insertion (figure 4.28). This strain is designated as XII$^{20/20KU}$ *fob1*$^{-}$ *RPA135/rpa135Δ::leu2::ADE2*+HP.

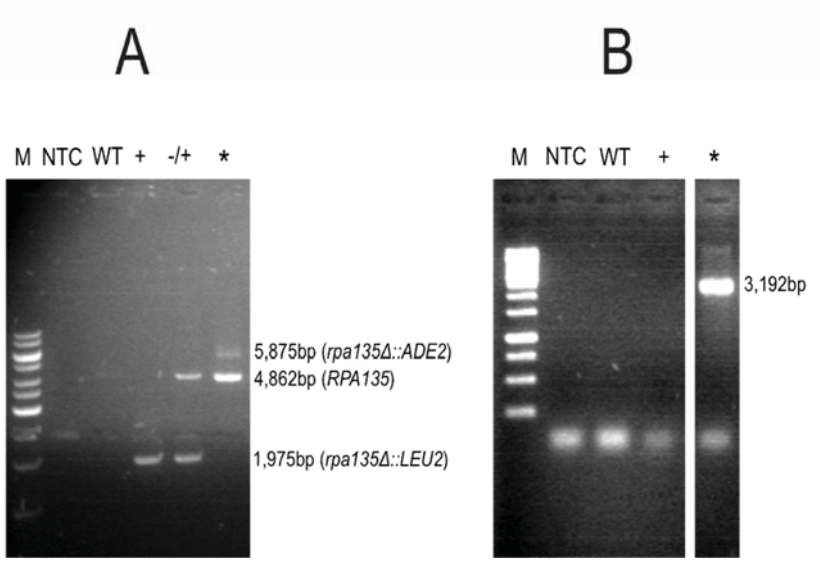

Figure 4.28. *FOB1* replacement marker swap in strain XII$^{20/20KU}$ *fob1*$^{-}$ *RPA135/rpa135Δ::LEU2*+HP. The *RPA135* locus was PCR amplified using primers PAG198 and PAG199 (**A**) to confirm replacement of the *LEU2* marker with *ADE2* in the diploid strain XII$^{20/20KU}$ *fob1*$^{-}$ *RPA135/rpa135Δ::LEU2*+HP (*)**.** M (marker), NTC (no template control), WT (WT gDNA used as *RPA135* control producing a fragment of 4,862 bp), + (*rpa135Δ::LEU2* construct used as *rpa135Δ::LEU2* control producing a fragment of 1,975 bp) and -/+ (gDNA of strain XII$^{200/20KU}$ *fob1*$^{-}$ *RPA135/rpa135Δ::LEU2*+HP used as heterozygous *RPA135/rpa135Δ::LEU2* control). (**B**) A second PCR using an internal *ADE2* primer (PAG196) in combination with PAG199 further confirms *leu2::ADE2* replacement.

Next, we transformed the original *rpa135Δ::LEU2* construct into the diploid XII$^{20/20KU}$ *fob1*$^{-}$ *RPA135/rpa135Δ::leu2::ADE2*+HP strain. 211 potential transformants were obtained

through selection in SGal-Ade-Leu-Trp medium, but none of these grew after re-streaking onto fresh selective medium. Therefore, a new strain heterozygous for both the 20-copy rDNA array and the *RPA135* deletion was created so that it could be sporulated to obtain haploids with a combination of both traits. To achieve this, the haploid strains XII^{200} *rpa135Δ*+HP *fob1::HIS3* (section 4.5.2) and XII^{20KU} *fob1::leu2::HIS3* (figure 4.26) were mated to produce strain XII$^{200/20KU}$ *fob1⁻ RPA135/rpa135Δ::LEU2*+HP. Zygotes from this mating were selected and the diploid state of the colonies obtained was confirmed through PCR (appendix figure 8.7).

The XII$^{200/20KU}$ *fob1⁻ RPA135/rpa135Δ::LEU2*+HP strain was sporulated and tetrads were dissected. All had the expected inheritance pattern: all spores were able to grow on medium lacking tryptophan and histidine, and each tetrad contained two spores able to grow on glucose medium and two able to grow on galactose medium lacking leucine. We also observed a 2:2 segregation of the CLA markers *kanMX2* and *URA3*. In addition, deletion of *RPA135* in half of the spores and segregation of the other traits (*FOB1* disruption, HP, *kanMX2* and *URA3* presence, and mating type) were confirmed through PCR (not shown).

A 2:2 segregation of the 200 and 20 copy rDNA arrays was also expected. Surprisingly, Southern blotting revealed an rDNA copy number of 20 in all spores (figure 4.29, suggesting a copy number decrease as a consequence of the deletion of *RPA135*. To corroborate this rDNA copy number decrease, we used quantitative real time PCR (qPCR) to measure the relative rDNA copy number of each haploid spore compared with a WT rDNA copy number strain. qPCR showed a 2:2 segregation of two different rDNA copy number classes (figure 4.30), neither of which corresponded to a WT length rDNA array of 200 copies. Instead, half the spores contained ~20 rDNA copies relative to WT (as did the 20-copy haploid control), while the other half contained about 50 rDNA copies. This variation in rDNA copy number was not detected by Southern blotting so qPCR, which also allows accurate quantification (Hoebeeck et al. 2007), was used as an alternative. Interestingly, all the spores with the lowest rDNA copy number also lack *RPA135*, while the spores with a relatively higher copy number harbor *RPA135*. These results suggest that a rDNA copy number reduction may have occurred in the parent heterozygous XII$^{200/20KU}$ *fob1⁻ RPA135/rpa135Δ::LEU2*+HP strain before sporulation, and that a further loss following sporulation occurs in the absence of *RPA135*. Unfortunately, due to time constraints, the mating to create a diploid 20-copy strain harboring a *RPA135* deletion could not be performed.

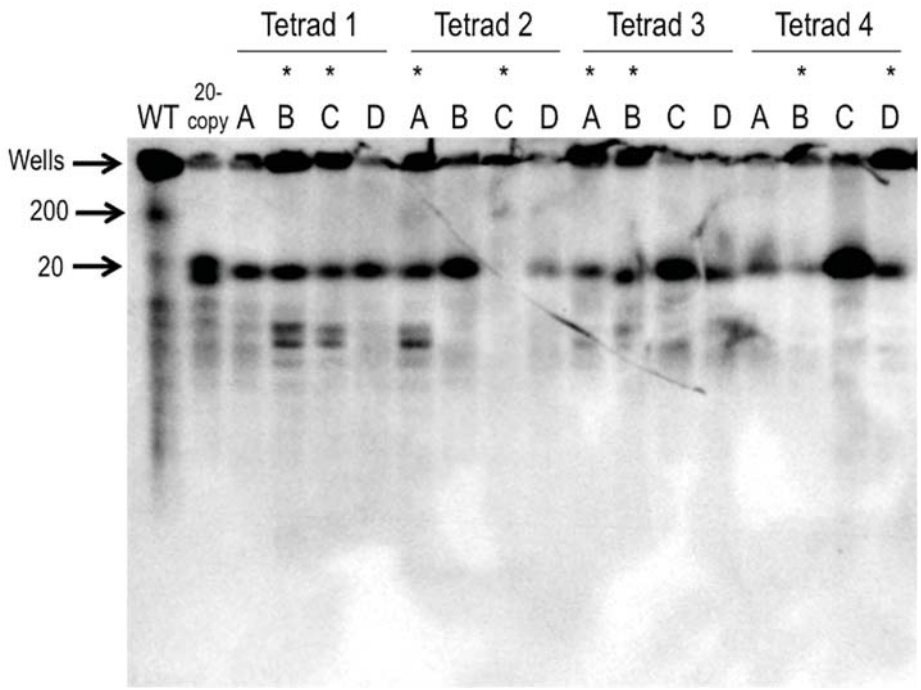

Figure 4.29. Spores dissected from XII$^{200/20KU}$ *fob1*$^{-}$ *RPA135/rpa135Δ::LEU2*+HP all have low rDNA copy numbers. Southern blot of CHEF gel using an rDNA specific DIG-labelled probe. rDNA copy number (indicated to the left) is estimated from the control strains XII$^{200/200KU}$ (WT) and XII$^{20/20KU}$ *fob1*$^{-}$ (20-copy) and is approximately 20 rDNA copies for the four spores (A-D) from the four tetrads (1-4) obtained from sporulation of the diploid heterozygous XII$^{200/20KU}$ *fob1*$^{-}$ *RPA135/rpa135Δ::LEU2*+HP strain. The asterices indicate the haploids containing the WT *RPA135*, as determined by PCR (not shown). The bands below the 20-copy chromosome are non-specific binding of the probe to other chromosomes.

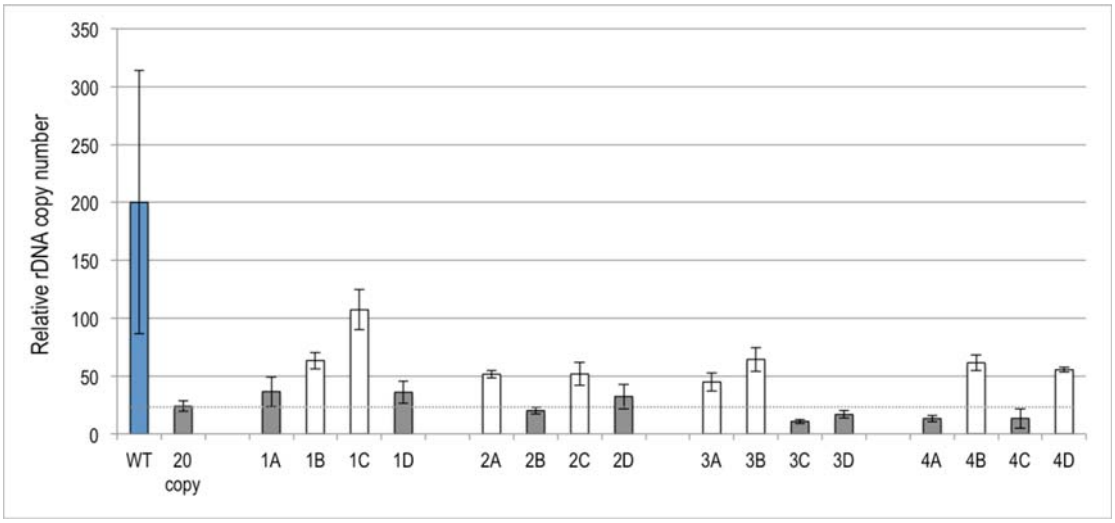

Figure 4.30. qPCR shows 2:2 segregation of different rDNA copy number classes in spores from XII$^{200/20KU}$ *fob1*$^{-}$ *RPA135/rpa135Δ::LEU2*+HP. The rDNA copy number relative to WT (n=4) and normalized to *GAL1* was estimated for four tetrads (spores A, B, C, and D from each tetrad) dissected from strain XII$^{200/20KU}$ *fob1*$^{-}$ *RPA135/rpa135Δ::LEU2*+HP using qPCR. A haploid 20-copy strain (20 copy; strain XII^{20} *fob1*$^{-}$) was used as a positive control (n=4). The results are the average of three technical replicates for each spore. Error bars show standard deviation. The two spores with the lowest rDNA copy number from each tetrad are highlighted in grey and these were all confirmed to be *rpa135Δ::LEU2*. See appendix table I for Cp values.

4.5.4 Attempts to construct an rDNA deletion strain harboring a *RPA135* deletion

To create an rDNA deletion diploid strain that also harbored a *RPA135* deletion, we first deleted one copy of *RPA135* by transforming the *rpa135Δ::LEU2* construct into the homozygous rDNA deletion strain XII$^{0/0KU}$+HP. Successful *RPA135* replacement was confirmed through PCR (appendix figure 8.8), and the heterozygous strain XII$^{0/0KU}$ *RPA135/ rpa135Δ::LEU2*+HP was sporulated to obtain rDNA and *RPA135* deletion haploids. Dissection of 30 tetrads (120 spores) yielded two or fewer viable spores in every case. No galactose dependent viable spores were obtained, suggesting that spores inheriting *rpa135Δ::LEU2* in conjunction with the rDNA deletion are not viable.

As an alternative strategy, we constructed a strain heterozygous for both *RPA135* and rDNA deletion. We used a *RPA135* deletion haploid spore with no chromosome XII markers that was confirmed to have the HP and carried a *FOB1* disruption (XII^{200} *rpa135Δ*+HP *fob1::HIS3*). This haploid was obtained by sporulating strain XII$^{200/200KU}$ *rpa135Δ*+HP *fob1*$^{-}$ and was characterized by PCR (appendix figure 8.9). This strain was mated to a haploid rDNA deletion spore (XII^{0KU}+HP), which was obtained by sporulating strain XII$^{0/0KU}$+HP and selecting for tryptophan and uracil prototrophy, G418 resistance and MATa mating type (not shown).

After successful mating of these *RPA135* deletion and rDNA deletion haploids, the diploid state of the new strain XII$^{200/0KU}$ *RPA135/rpa135Δ*+HP *FOB1/fob1::HIS3* was confirmed through PCR (appendix figure 8.10). The strain was then sporulated, and 25 tetrads were dissected. However, once again, no more than two viable spores were obtained for any of the dissected tetrads (not shown), and no galactose-dependant viable spores were obtained. Our unsuccessful attempts to create a strain harboring both a chromosomal rDNA deletion and a *RPA135* deletion suggest there may be synthetic lethality between rDNA deletion and *rpa135* deletion.

4.6 CREATION OF STRAINS WITH HETEROZYGOUS rDNA ALTERATIONS

To distinguish the chromosome missegregation rates of each chromosome XII homolog, we created a set of strains with heterozygous rDNA alterations. Each heterozygous rDNA combination examined (200/0, 200/20 and 20/0) consists of two strains, both harboring the same rDNA heterozygous alteration(s) but with the CLA markers on opposing chromosome XII homologs, to monitor segregation of each homolog.

4.6.1 Creation of 200/0 $XII^{0/200KU}$+HP and $XII^{200/0KU}$+HP heterozygous strains

First, we created a pair of strains heterozygous for the presence/absence of the rDNA array (200/0). One of these strains contains the CLA markers on the chromosome XII homolog harboring the rDNA array ($XII^{0/200KU}$+HP), and the other on the rDNA deletion homolog ($XII^{200/0KU}$+HP). Strain $XII^{0/200KU}$+HP was constructed by mating an rDNA deletion haploid strain (NOY984; XII^{0}+HP) with a WT haploid strain (NOY408-1b; XII^{200}) in which the CLA markers were inserted (Woods, Quintana and Ganley, unpublished). The two haploid strains were first confirmed for mating type by the liquid culture method, and rDNA state by Southern blotting (appendix figure 8.11). Diploid $XII^{0/200KU}$+HP colonies (figure 4.31) were selected following the mating by their ability to grow on medium lacking uracil and tryptophan.

A

Strain	Origin/Created by:	Genotype
$XII^{0/200KU}$ +HP	Quintana, Woods and Ganley	*MATa/MATalpha ade2-1/ade2-1 ura3-1/ura3-1 his3-11/his3-11 trp1-1/trp1-1 leu2-3,112/leu2-3,112 can1-100/can1-100* ***ChrXII-109,570::kanMX2****/ ChrXII* ***ChrXII-223,830::URA3****/ChrXII,* ***RDNA1****/rdn1Δ::HIS3G* +HP

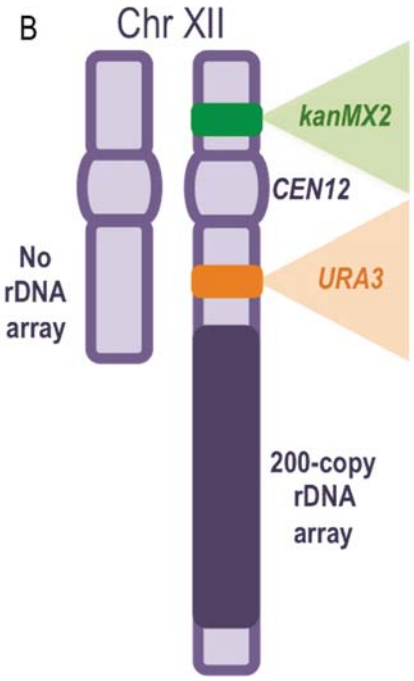

Figure 4.31. Characterization of the $XII^{0/200KU}$+HP strain. (**A**) Genotype of the $XII^{0/200KU}$+HP strain. (**B**) Cartoon depicting the two chromosome XII homologs in the diploid $XII^{0/200KU}$+HP strain with the homolog carrying the WT length rDNA array also harboring the CLA selective markers *kanMX2* and *URA3* on either side of the centromere (*CEN12*). The WT length chromosome XII homolog is ~2.9 Mb and carries ~200 copies of the rDNA gene repeats, while the other homolog is 1,078 kb and is deleted for the rDNA.

Construction of the other heterozygous strain of this set, $XII^{200/0KU}$+HP, involved mating the WT haploid strain (NOY408-1b; XII^{200}), in which the *leu2* mutation was repaired to *LEU2*+ (Woods and Ganley, unpublished), to the rDNA deletion haploid strain (NOY984; XII^{0}+HP, appendix figure 8.11) into which the CLA markers had been inserted (XII^{0KU}+HP; Woods and Ganley, unpublished). These two haploids were mated and diploid colonies were selected by their ability to grow on medium lacking uracil and leucine, and were also confirmed to be G418 resistant, giving strain $XII^{200/0KU}$+HP (figure 4.32).

A

Strain	Origin/Created by:	Genotype
XII$^{200/0KU}$ +HP	Quintana, Woods and Ganley	*MATa/MATalpha ade2-1/ade2-1 ura3-1/ura3-1 his3-11/his3-11 trp1-1/ trp1-1 leu2-3,112/leu2-3,112 can1-100/can1-100* ***ChrXII-109,570::kanMX2****/ChrXII* ***ChrXII-223,830::URA3****/ChrXII, RDNA1/* ***rdn1Δ::HIS3G*** *+HP*

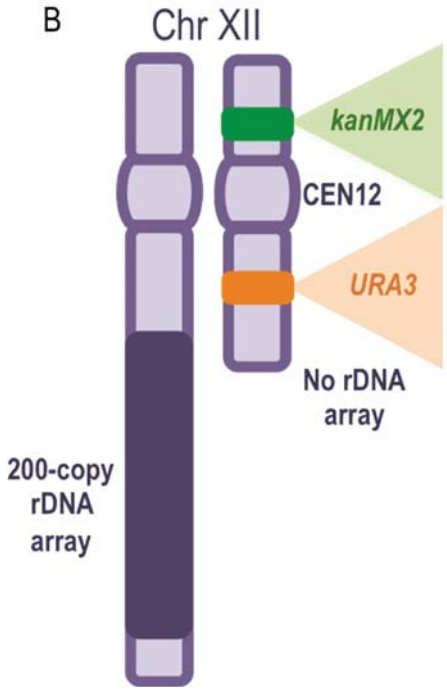

Figure 4.32. Characterization of the XII$^{200/0KU}$+HP strain. (**A**) Genotype of the XII$^{200/0KU}$+HP strain. (**B**) Cartoon depicting the two chromosome XII homologs in the diploid XII$^{200/0KU}$+HP strain, as per figure 4.31, with the 1,078 kb homolog deleted for the rDNA also harboring the CLA markers.

4.6.2 Creation of 200/20 XII$^{20/200KU}$ *fob1*$^{-}$ and XII$^{200/20KU}$ *fob1*$^{-}$ heterozygous strains

Next we created a pair of strains heterozygous for a 20-copy rDNA array and a WT length rDNA array (200/20), both of which harbor a homozygous *FOB1* disruption. The first strain, XII$^{20/200KU}$ *fob1*$^{-}$, carries the CLA markers on the chromosome XII homolog harboring the WT length rDNA array. This strain was constructed by mating the strain TAK300 (figure 4.26, section 4.5.3) to a MATa haploid strain XII^{200KU} *fob1::LEU2*. This was obtained through sporulation of the diploid XII$^{200/200KU}$ *fob1*$^{-}$ strain (section 4.4.2), followed by selection for *URA3* and *kanMX2*, and determination of MATa by the liquid culture method. These two haploids were mated and diploid XII$^{20/200KU}$ *fob1*$^{-}$ colonies were selected by their ability to grow on medium lacking histidine and leucine due to the two distinct *FOB1* disruption markers used

(*fob1::HIS3* and *fob1::LEU2*). The presence of the CLA markers and the *FOB1* disruption were confirmed through PCR (figure 4.33).

A

Strain	Origin/Created by:	Genotype
XII$^{20/200KU}$ *fob1*$^{-}$	Quintana, Woods and Ganley	*MATa/MATalpha ade2-1/ade2-1 ura3-1/ura3-1 his3-11/his3-11 trp1-1/ trp1-1 leu2-3,112/leu2-3,112 can1-100/can1-100* ***ChrXII-109,570::kanMX2****/ChrXII* ***ChrXII-223,830::URA3****/ChrXII, fob1::HIS3/fob1::HIS3,* ***RDNA1****/RDNA1~20copies*

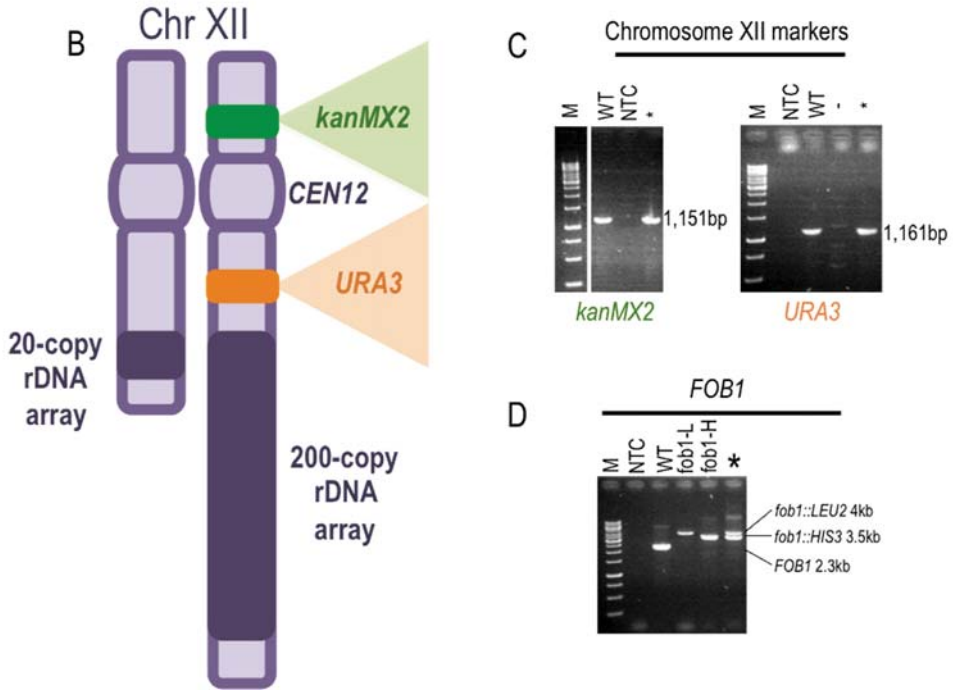

Figure 4.33. Characterization of the XII$^{20/200KU}$ *fob1*$^{-}$ strain. (**A**) Genotype of the XII$^{20/200KU}$ *fob1*$^{-}$ strain. (**B**) Cartoon depicting the two chromosome XII homologs with a 20-copy rDNA array and a WT length array that also harbors the CLA markers. (**C**) PCR was performed for the CLA markers (figure 4.2) using WT gDNA from strain XII^{200} as a negative control (-) and WT gDNA from XII$^{200/200KU}$ as a positive control (WT). (**D**) A *FOB1* PCR was performed as in figure 4.10 using positive controls for each *FOB1* replacement: gDNA from strain XII$^{200/200KU}$ *fob1*$^{-}$ produced a ~4 kb product corresponding to the *fob1::LEU2* replacement (fob1-L), and gDNA from TAK300 produced a ~3.5 kb product corresponding to the *fob1::HIS3* replacement (fob1-H). M (marker), NTC (no template control), * (gDNA of strain XII$^{20/200KU}$ *fob1*$^{-}$).

The other strain for this set is XII$^{200/20KU}$ *fob1*$^{-}$, which carries the CLA markers on the chromosome XII homolog harboring the 20-copy rDNA array. To construct this strain, a haploid 20-copy spore XII^{20KU} *fob1*$^{-}$ (*fob1::LEU2*) obtained from sporulation of strain XII$^{20/20KU}$ *fob1*$^{-}$ (figure 4.12) was mated to the WT haploid strain XII^{200} *(fob1::HIS3*) (appendix figure 8.12). The haploid 20-copy spore XII^{20KU} *fob1*$^{-}$ was confirmed to harbor the CLA markers by phenotypic selection, to be MATa using the liquid culture method, and to have a *FOB1* disruption (*fob1::HIS3*) by PCR (appendix figure 8.12). The WT haploid strain XII^{200} *fob1*$^{-}$ was also confirmed to have a *fob1::HIS3* replacement through PCR and it was determined to be MATα

through PCR (appendix figure 8.12). Mating of these haploids was followed by selection of zygotes using a micromanipulation microscope, and the resulting XII$^{200/20KU}$ *fob1*$^{-}$ colonies were confirmed by PCR to be diploid (figure 4.34).

A

Strain	Origin/Created by:	Genotype
XII$^{200/20KU}$ *fob1*$^{-}$	Quintana, Woods and Ganley	*MATa/MATalpha ade2-1/ade2-1 ura3-1/ura3-1 his3-11/his3-11 trp1-1/ trp1-1 leu2-3,112/leu2-3,112 can1-100/can1-100* ***ChrXII-109,570::kanMX2****/ChrXII* ***ChrXII-223,830::URA3****/ChrXII, fob1::HIS3,* ***RDNA1~20copies****/RDN1*

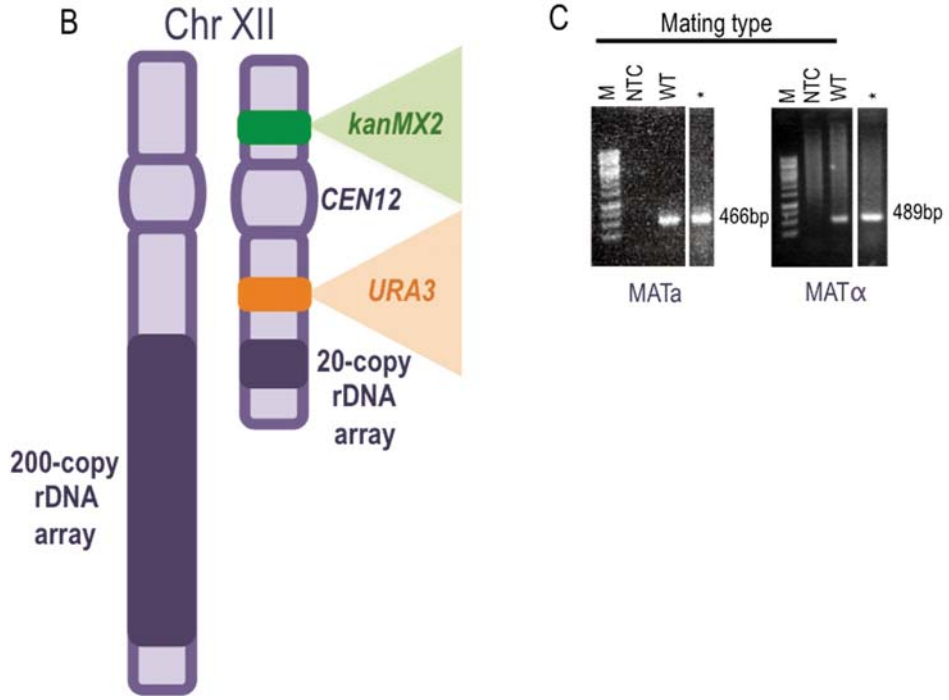

Figure 4.34. Characterization of the XII$^{200/20KU}$ *fob1*$^{-}$ strain. (**A**) Genotype of the XII$^{200/20KU}$ *fob1*$^{-}$ strain. (**B**) Cartoon depicting the two chromosome XII homologs with a WT array and a 20-copy rDNA array that harbors the CLA markers. (**C**) Mating type PCR was performed as in figure 4.2 using WT gDNA from XII$^{200/200KU}$ as positive control (WT).

4.6.3 Creation of 20/0 XII$^{20/0KU}$ *fob1*$^{-}$+HP and XII$^{0/20KU}$ *fob1*$^{-}$+HP heterozygous strains

The last heterozygous pair of strains constructed are heterozygous for a 20-copy rDNA array and an rDNA array deletion (20/0), both of which also harbor homozygous *FOB1* disruptions. The first strain, XII$^{0/20KU}$ *fob1*$^{-}$+HP, carries the CLA markers on the chromosome XII homolog harboring the 20-copy rDNA array, while the second strain, XII$^{20/0KU}$ *fob1*$^{-}$+HP, carries the CLA markers on the chromosome XII homolog harboring the rDNA deletion. Strain XII$^{0/20KU}$ *fob1*$^{-}$+HP was constructed by using an rDNA deletion haploid XII^{0}+HP (section 4.4.5, spore 2C

from table IV). *FOB1* was disrupted by transformation of the *fob1::HIS3* construct into this strain, and was confirmed through PCR (appendix figure 8.13), creating strain XII^{0} *fob1*$^{-}$+HP. This haploid strain was mated to strain XII^{20KU} *fob1*$^{-}$, a 20-copy haploid spore that contains the CLA markers and a *fob1::LEU2* replacement. This was obtained by sporulating strain XII$^{20/20KU}$ *fob1*$^{-}$ (figure 4.12), followed by confirmation of its mating type by the liquid culture method and presence of the CLA markers by phenotypic selection (not shown). Diploid XII$^{0/20KU}$ *fob1*$^{-}$+HP colonies were obtained by Leu^{+}His^{+} selection after mating these strains, and its diploid state was confirmed by PCR (figure 4.35).

A

Strain	Origin/Created by:	Genotype
XII$^{0/20KU}$ *fob1*$^{-}$ +HP	Quintana, Woods and Ganley	*MATa/MATalpha ade2-1/ade2-1 ura3-1/ura3-1 his3-1l/his3-11 trp1-1/trp1-1 leu2-3,112/leu2-3,112 can1-100/can1-100* ***ChrXII-109,570::kanMX2****/ChrXII* ***ChrXII-223,830::URA3****/ChrXII,* ***RDNA1 ~20 copies****/rdn1Δ::HIS3G* +HP

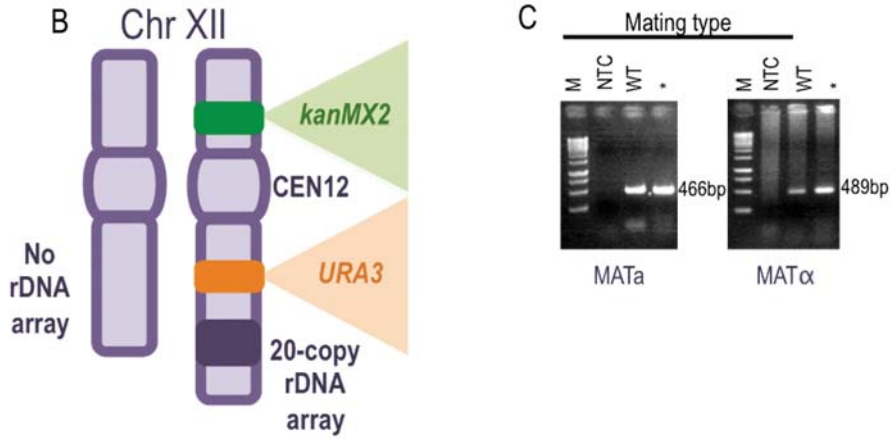

Figure 4.35. Characterization of strain XII$^{0/20KU}$ *fob1*$^{-}$+HP. (**A**) Genotype of the XII$^{0/20KU}$ *fob1*$^{-}$+HP strain. (**B**) Cartoon depicting the two chromosome XII homologs with the rDNA deleted and a 20-copy rDNA array that also harbors the CLA markers. (**C**) Mating type PCR was performed as in figure 4.2, using WT gDNA from XII$^{200/200KU}$ as a positive control (WT). The strain may carry the HP from the rDNA deletion parent strain (not tested).

Lastly, strain XII$^{20/0KU}$ *fob1*$^{-}$+HP was constructed by mating the 20-copy haploid strain TAK300 (figure 4.26, section 4.5.3) to the rDNA deletion haploid XII^{0KU} *fob1*$^{-}$+HP in which *FOB1* was previously disrupted by transformation of the *fob1::HIS3* construct (section 4.4.5, spore 1C from table IV). Mating of these haploids was followed by selection of zygotes using a micromanipulation microscope, and the colonies obtained were confirmed to be diploid by mating type PCR (figure 4.36).

A

Strain	Origin/ Created by:	Genotype
XII$^{20/0KU}$ *fob1*$^{-}$ +HP	Quintana, Woods and Ganley	*MATa/MATalpha ade2-1/ade2-1 ura3-1/ura3-1 his3-11/his3-11 trp1-1/ trp1-1 leu2-3,112/leu2-3,112 can1-100/can1-100* ***ChrXII-109,570::kanMX2****/ChrXII* ***ChrXII-223,830::URA3****/ChrXII,* ***rdn1Δ::HIS3G****/RDNA1* ~20 copies +HP

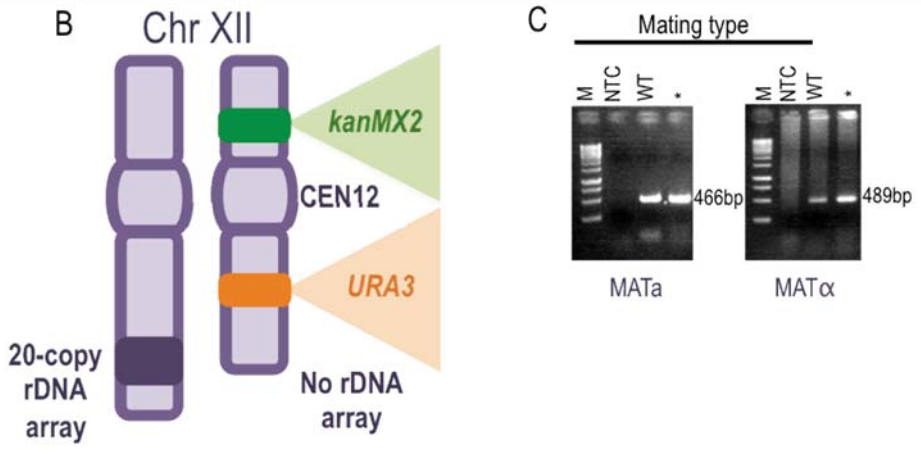

Figure 4.36. Characterization of strain XII$^{20/0KU}$ *fob1*$^{-}$+HP. (**A**) Genotype of the XII$^{0/20KU}$ *fob1*$^{-}$+HP strain. (**B**) Cartoon depicting the two homologs of chromosome XII with a 20-copy rDNA array and the rDNA deleted that also harbors the CLA markers. (**C**) Mating type PCR was performed as in figure 4.2, using WT gDNA from XII$^{200/200KU}$ as a positive control (WT). The strain may carry the HP from the rDNA deletion parent strain (not tested).

4.7 CREATION OF CHROMOSOME V AND VI MARKED STRAINS TO INVESTIGATE GLOBAL CHROMOSOME SEGREGATION

In this section, I describe the construction of a set of strains with CLA markers on chromosomes V or VI. As for the chromosome XII-tagged strains, the CLA markers *kanMX2* and *URA3* were inserted into the long and short arms of a single chromosome V or VI homolog.

4.7.1 WT V$^{0/0KU}$ XII$^{200/200}$ and VI$^{0/0KU}$ XII$^{200/200}$ CLA strains

The creation of chromosome V marked strains for the CLA involved inserting the *kanMX2* marker into the long arm of chromosome V and the *URA3* marker into the short arm of chromosome V. PCR primers, each with flanking regions that are homologous to the targeted insertion sites in chromosome V, were used to amplify each marker (figure 4.37). These PCR

products were used to transform haploid strains, and successful insertion was confirmed for both markers using a marker gene specific internal primer and a locus specific primer upstream of each insertion site (figure 4.37B, 4.37C).

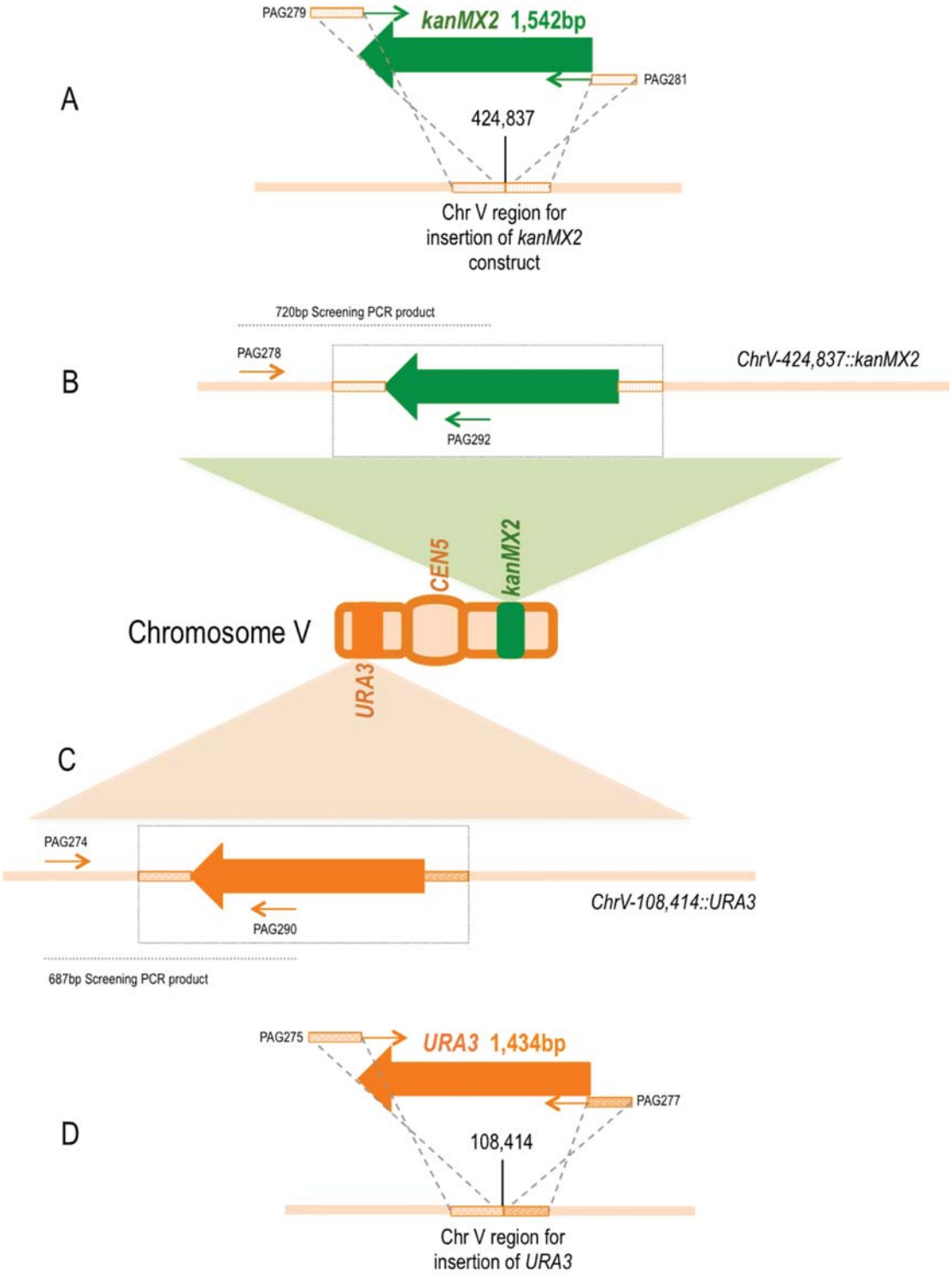

Figure 4.37. Insertion sites of the *kanMX2* and *URA3* markers into the long and short arms of chromosome V. The *kanMX2* (**A**, top green arrow) and *URA3* (**D**, bottom orange arrow) markers were PCR amplified (PAG279 and PAG281; PAG275 and PAG277) from plasmids pFA6:kanMX2 and YEpLac195, respectively. The PCR products include 56 bp flanking regions on the 5' and 3' ends homologous to

the chromosome V insertion sites at positions 424,837 and 108,414. These PCR products were transformed into the CLA strains and PCR was used to confirm the insertion of *kanMX2* (**B**, green arrow in dotted box) and *URA3* (**C**, orange arrow in dotted box) (PAG278 and PAG292; PAG274 and PAG290). The positions of the insertions relative to the chromosome V centromere (*CEN5*) are indicated (not to scale).

A WT diploid strain with chromosome V CLA markers ($V^{0/0KU}$ $XII^{200/200}$) was constructed by using the chromosome V marked haploid WT strain (V^{0KU} XII^{200}), and another WT haploid of the opposite mating type (V^{0} XII^{200}) that had the tryptophan gene repaired (Woods and Ganley, unpublished) for use as a mating marker. These strains were mated to each other and diploids were selected by their ability to grow on uracil and tryptophan double dropout medium. The diploid state and presence of the CLA markers were confirmed through PCR (figure 4.38).

A

Strain	Origin/Created by:	Genotype
$V^{0/0KU}$ $XII^{200/200}$	Quintana, Woods and Ganley	*MATa/MATalpha ade2-1/ade2-1 ura3-1/ura3-1 his3-11/his3-11 trp1-1/ trp1-1 leu2-3,112/leu2-3,112 can1-100/can1-100 ChrV-108,414::URA3/ ChrV ChrV-424,837::kanMX2/ChrV*

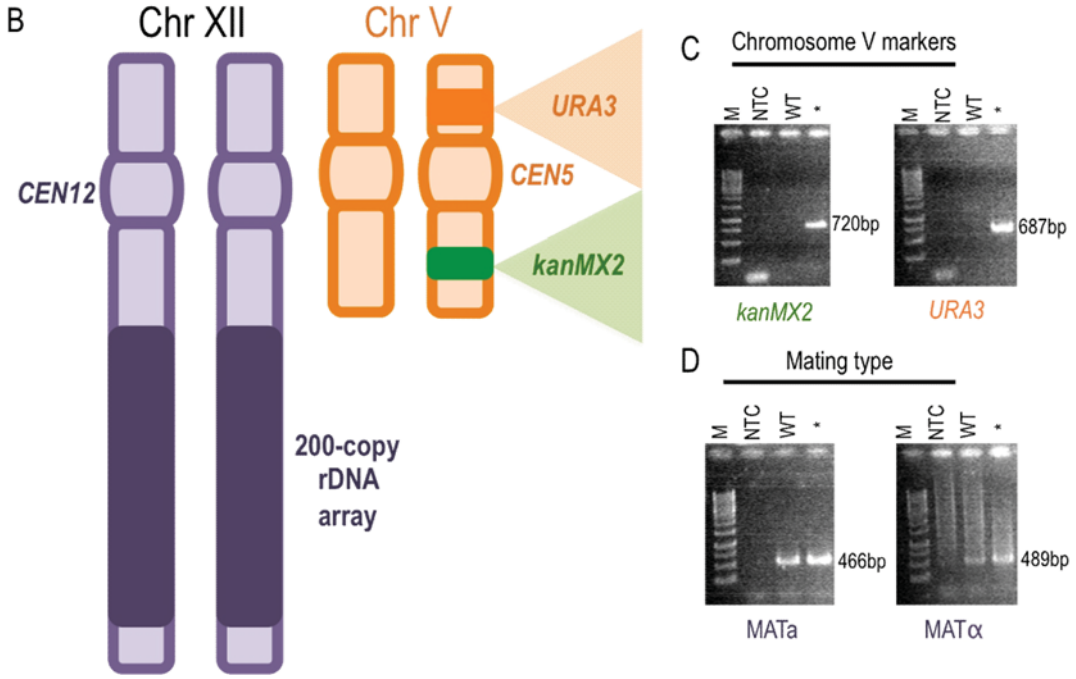

Figure 4.38. Characterization of the WT $V^{0/0KU}$ $XII^{200/200}$ strain. (**A**) Genotype of the WT **$V^{0/0KU}$ $XII^{200/200KU}$** strain. (**B**) Cartoon depicting the two WT homologs each of chromosomes XII and V, with one chromosome V homolog carrying the CLA selective markers *kanMX2* and *URA3* on either side of the centromere (*CEN5*). WT chromosome V is ~0.57 Mb. (**C, D**) PCR was used to confirm the insertion of the CLA *kanMX2* and *URA3* markers in chromosome V (see figure 4.37 for details) and to confirm diploidy as in figure 4.2, using WT gDNA from $XII^{200/200KU}$ as a positive control (WT).

The creation of chromosome VI marked strains for the CLA involved the insertion of the *kanMX2* and *URA3* markers into chromosome VI of a haploid strain as described for chromosome V (figure 4.39). This haploid was mated to a WT haploid of the opposite mating

type (VI^{0} XII^{200}), and the diploid state and presence of the CLA markers on strain $VI^{0/0KU}$ $XII^{200/200}$ were confirmed through PCR (figure 4.40).

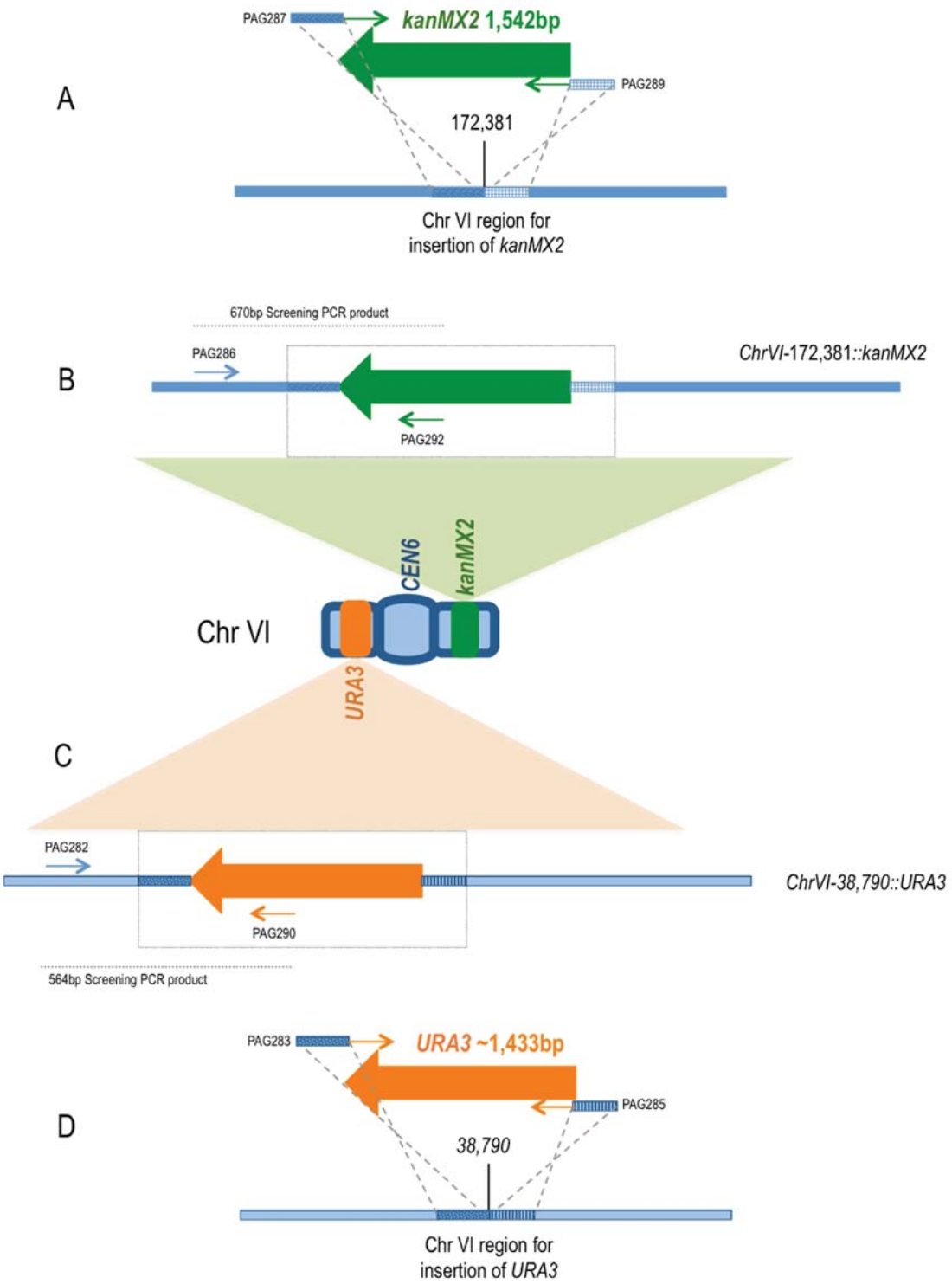

Figure 4.39. Insertion sites of the *kanMX2* and *URA3* markers into the long and short arms of chromosome VI. The *kanMX2* (**A**, top green arrow) and *URA3* (**D**, bottom orange arrow) markers were PCR amplified (PAG287 and PAG289; PAG283 and PAG285) as described in figure 4.37, but with each marker containing homologous regions to the chromosome VI insertion sites at positions 172,381 and 38,790. These products were transformed into CLA strains and PCR was used to confirm the insertion of *kanMX2* (**B**,

green arrow in dotted box) and *URA3* (**C**, orange arrow in dotted box) (PAG286 and PAG292; PAG282 and PAG290). The positions of the insertions relative to the chromosome VI centromere (*CEN6*) are indicated (not to scale).

A

Strain	Origin/Created by:	Genotype
VI$^{0/0KU}$ XII$^{200/200}$	Quintana, Woods and Ganley	*MATa/MATalpha ade2-1/ade2-1 ura3-1/ura3-1 his3-11/his3-11 trp1-1/trp1-1 leu2-3,112/leu2-3,112 can1-100/can1-100 ChrVI-38,790::URA3/ChrVI ChrVI-172,381::kanMX2/ChrVI*

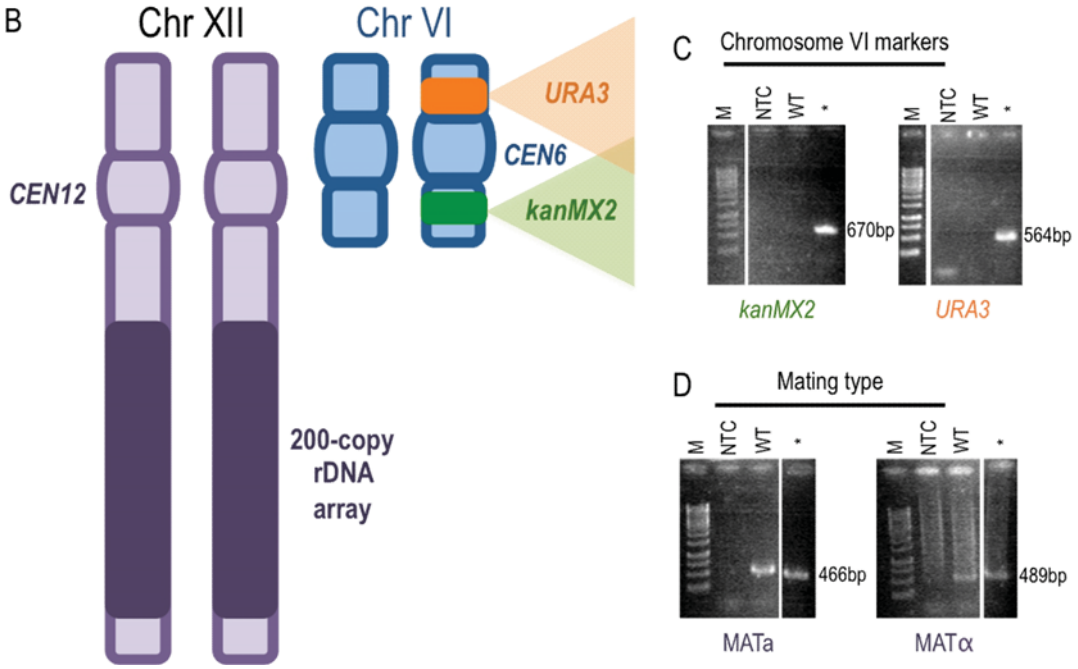

Figure 4.40. Characterization of the WT VI$^{0/0KU}$ XII$^{200/200}$ strain. (**A**) Genotype of the WT VI$^{0/0KU}$ XII$^{200/200}$ strain. (**B**) Cartoon depicts the two homologs each of chromosome XII and chromosome VI, with one chromosome VI homolog carrying the CLA selective markers *kanMX2* and *URA3* on either side of the centromere (*CEN6*). WT chromosome VI is ~0.27 Mb. (**C**, **D**) PCR was used to confirm the insertion of the CLA *kanMX2* and *URA3* markers into chromosome VI (see figure 4.39 for details) and to confirm diploidy as in figure 4.2, using WT gDNA from XII$^{200/200KU}$ as a positive control (WT).

4.7.2 Chromosome VI marked strains harboring homozygous rDNA alterations

To test the effects of homozygous rDNA alterations on global chromosome segregation, we constructed a set of strains that have the CLA markers on one WT chromosome VI homolog and that also harbor chromosome XII rDNA alterations. These rDNA alterations included an rDNA deletion strain, a *FOB1* disruption strain and a 20-copy rDNA strain. To create a homozygous rDNA deletion VI$^{0/0KU}$ XII$^{0/0}$+HP strain, the CLA markers were inserted into chromosome VI of a haploid rDNA deletion spore 1B (XII^{0}+HP), obtained by

sporulation of strain XII$^{0/0KU}$+HP (spore 1B, section 4.4.5, table IV), to create strain VI^{0KU} XII^{0}+HP. The CLA marker insertion was confirmed through PCR (appendix figure 8.14). This strain was mated with an rDNA deletion haploid strain of the opposite mating type (XII^{0}+HP) (spore 2C, section 4.4.5, table IV), and the diploid state of the new strain VI$^{0/0KU}$ XII$^{0/0}$+HP was confirmed through mating type PCR (figure 4.41).

A

Strain	Origin/Created by:	Genotype
VI$^{0/0KU}$ XII$^{0/0}$ +HP	Quintana, Woods and Ganley	*MATa/MATalpha ade2-1/ade2-1 ura3-1/ura3-1 his3-11/his3-11 trp1-1/trp1-1 leu2-3,112/leu2-3,112 can1-100/can1-100 ChrVI-38,790::URA3/ChrVI ChrVI-172,381::kanMX2/ChrVI, rdn1ΔΔ/rdn1Δ::HIS3* +HP

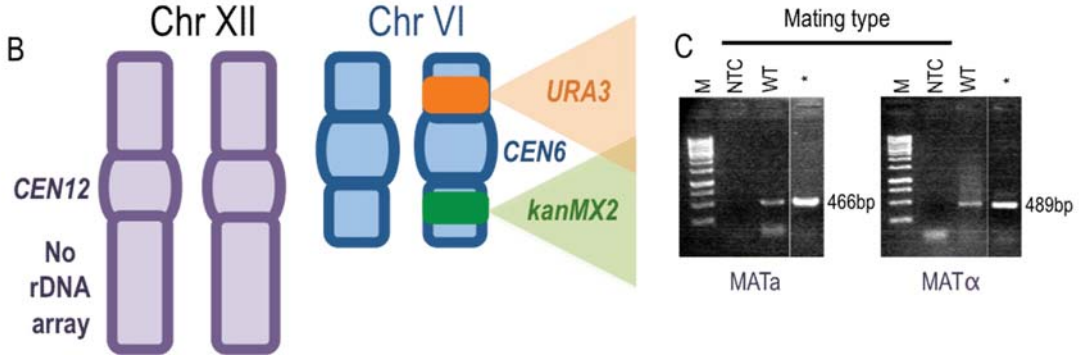

Figure 4.41. Characterization of the VI$^{0/0KU}$ XII$^{0/0}$+HP rDNA deletion strain with marked chromosome VI. (**A**) Genotype of the VI$^{0/0KU}$ XII$^{0/0}$+HP rDNA deletion strain. (**B**) Cartoon depicting the two rDNA deletion homologs of chromosome XII, and the chromosome VI homologs with one carrying the CLA *kanMX2* and *URA3* markers on either side of the centromere (*CEN6*). (**C**) PCR was used to confirm diploidy as in figure 4.2, using WT gDNA from XII$^{200/200KU}$ as a positive control (WT).

Next, we created VI$^{0/0KU}$ XII$^{200/200}$ *fob1*$^{-}$, a *FOB1* disruption strain with the CLA markers on chromosome VI. To create this strain, *FOB1* was disrupted in the haploid WT strain with chromosome VI marked (VI^{0KU} XII^{200}, section 4.7.1) using the *fob1::LEU2* construct (figures 4.11, 4.12), and was confirmed by PCR (appendix figure 8.15). This strain was mated with a *FOB1* disruption haploid strain of the opposite mating type (XII^{200} *fob1*$^{-}$, section 4.6.2), and zygotes were picked using a micromanipulation microscope. The diploid state of the new strain VI$^{0/0KU}$ XII$^{0/0}$+HP was confirmed through mating type PCR (figure 4.42).

A

Strain	Origin/Created by:	Genotype
$VI^{0/0KU}$ $XII^{200/200}$ *fob1*$^{-}$	Quintana, Woods and Ganley	*MATa/MATalpha ade2-1/ade2-1 ura3-1/ura3-1 his3-11/his3-11 trp1-1/trp1-1 leu2-3,112/leu2-3,112 can1-100/can1-100 ChrVI-38,790::URA3/ChrVI ChrVI-172,381::kanMX2/ChrVI, fob1::LEU2/fob1::HIS3*

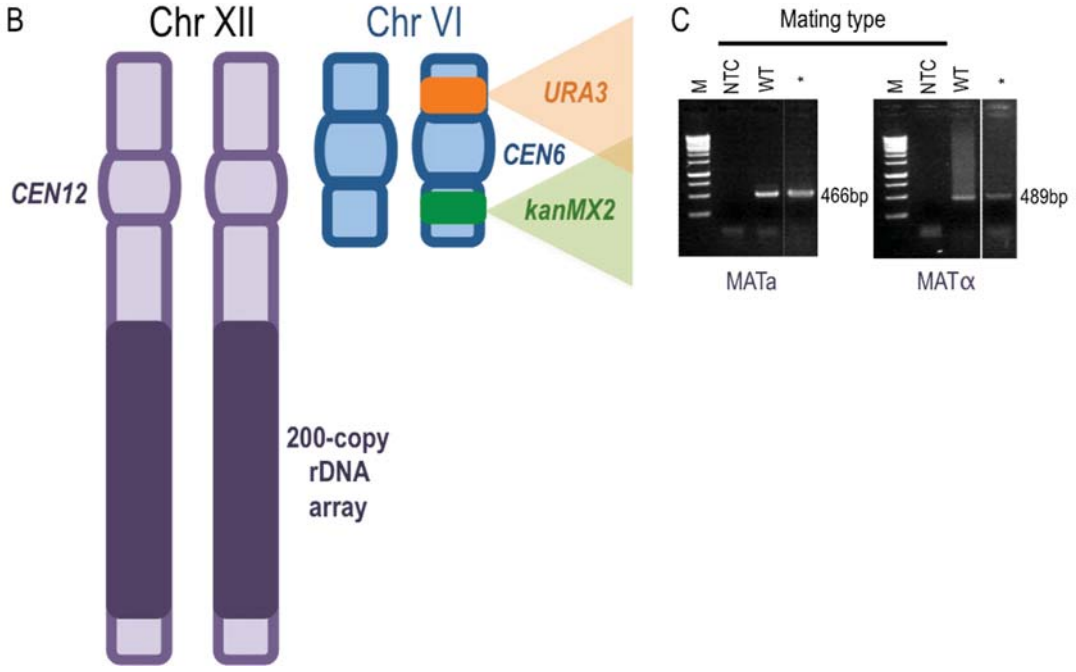

Figure 4.42. Characterization of the $VI^{0/0KU}$ $XII^{200/200}$*fob1*$^{-}$ strain with marked chromosome VI. (**A**) Genotype of the $VI^{0/0KU}$ $XII^{200/200}$ *fob1*$^{-}$ *FOB1* disruption strain. (**B**) Cartoon depicting the two WT homologs of chromosome XII, and the chromosome VI homologs with one carrying the CLA *kanMX2* and *URA3* markers on either side of the centromere (*CEN6*). (**C**) PCR was used to confirm diploidy as in figure 4.2, using WT gDNA from $XII^{200/200KU}$ as a positive control (WT).

The last of this set of strains is the 20-copy homozygous diploid with CLA markers on chromosome VI ($VI^{0/0KU}$ $XII^{20/20}$ *fob1*$^{-}$). To create this strain, the CLA markers were inserted into chromosome VI of the 20-copy haploid TAK300 strain (section 4.7.3) and their insertion was confirmed through PCR (appendix figure 8.16). The resulting strain (VI^{0KU} XII^{20} *fob1*$^{-}$) was mated with another 20-copy haploid strain of the opposite mating type (XII^{20} *fob1::LEU2*), and zygotes were picked using a micromanipulation microscope. The diploid state of the colonies was confirmed by mating type PCR (figure 4.43).

A

Strain	Origin/Created by:	Genotype
$VI^{0/0KU}$ $XII^{20/20}$ *fob1*$^{-}$	Quintana, Woods and Ganley	*MATa/MATalpha ade2-1/ade2-1 ura3-1/ura3-1 his3-11/his3-11 trp1-1/trp1-1 leu2-3,112/leu2-3,112 can1-100/can1-100 ChrVI-38,790::URA3/ChrVI ChrVI-172,381::kanMX2/ChrVI, fob1::LEU2/fob1::HIS3 RDNA1~20copies/ RDNA1~20copies*

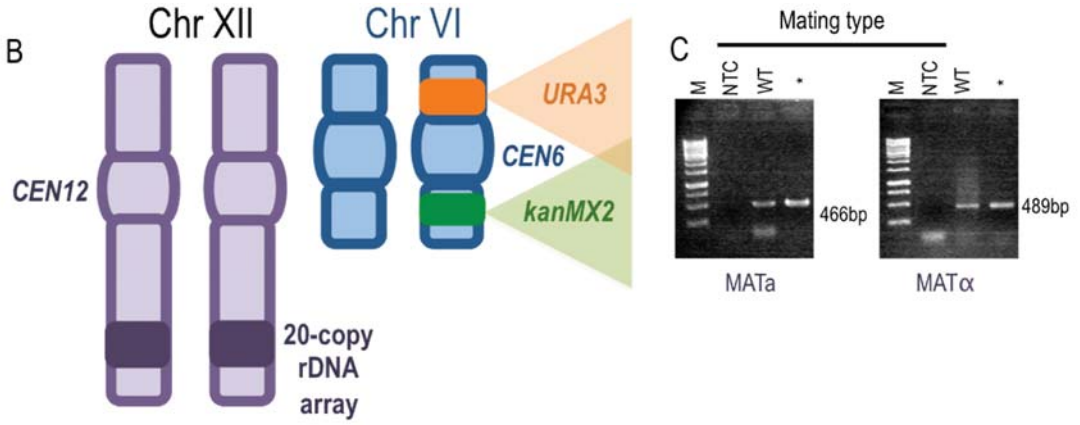

Figure 4.43. Characterization of the $VI^{0/0KU}$ $XII^{20/20}$ *fob1*$^{-}$ 20-copy strain with marked chromosome VI. (**A**) Genotype of the $VI^{0/0KU}$ $XII^{20/20}$ *fob1*$^{-}$ 20-copy strain. (**B**) Cartoon depicting the two 20-copy homologs of chromosome XII, and the two chromosome VI homologs with one carrying the CLA *kanMX2* and *URA3* markers on either side of the centromere (*CEN6*). (**C**) PCR was used to confirm diploidy as in figure 4.2, using WT gDNA from $XII^{200/200KU}$ as a positive control (WT).

4.7.3 Chromosome VI marked strains harboring heterozygous rDNA alterations

To test the effects of heterozygous rDNA alterations on global chromosome segregation we constructed strains $VI^{0/0KU}$ $XII^{0/200}$+HP and $VI^{0/0KU}$ $XII^{0/20}$ *fob1*$^{-}$+HP, which are 0/200 and 0/20 rDNA heterozygotes, respectively, and have the CLA markers on chromosome VI. Strain $VI^{0/0KU}$ $XII^{0/200}$+HP was constructed by mating the chromosome VI marked rDNA deletion haploid strain VI^{0KU} XII^{0}+HP (section 4.7.3, appendix figure 8.14) to a WT haploid strain (VI^{0KU} XII^{200}) of the opposite mating type. After the mating, zygotes were picked using a micromanipulation microscope and their diploid state was confirmed by PCR (figure 4.44).

A

Strain	Origin/Created by:	Genotype
VI$^{0/0KU}$ XII$^{0/200}$ +HP	Quintana, Woods and Ganley	*MATa/MATalpha ade2-1/ade2-1 ura3-1/ura3-1 his3-11/his3-11 trp1-1/trp1-1 leu2-3,112/leu2-3,112 can1-100/can1-100 ChrVI-38,790::URA3/ChrVI ChrVI-172,381::kanMX2/ChrVI, RDNA1/rdn1ΔΔ* +HP

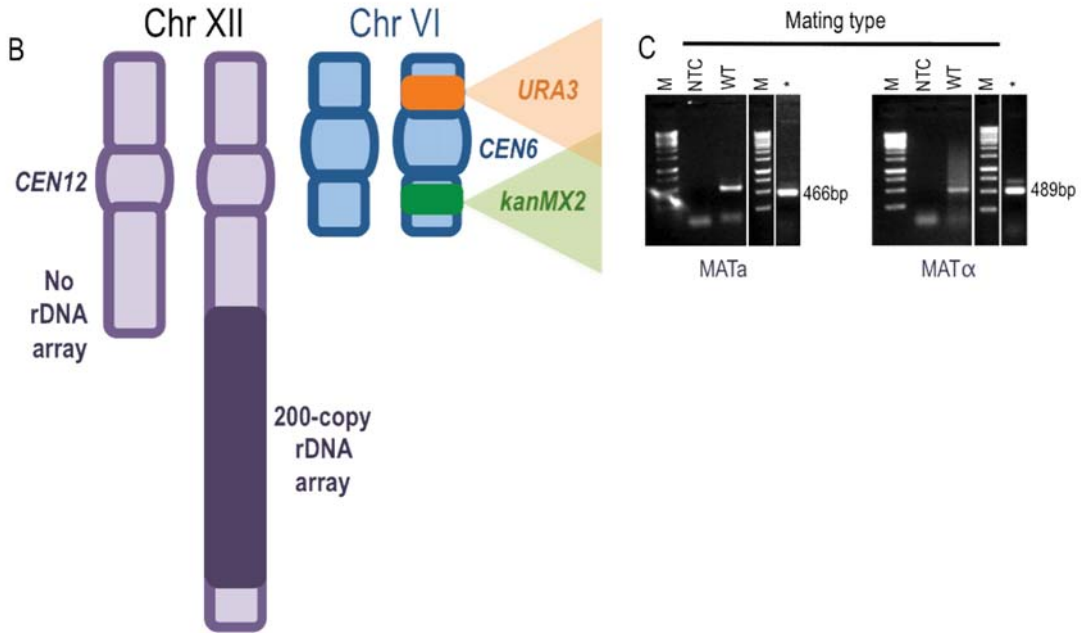

Figure 4.44. Characterization of the VI$^{0/0KU}$ XII$^{0/200}$+HP heterozygous strain with marked chromosome VI. (**A**) Genotype of the VI$^{0/0KU}$ XII$^{0/200}$+HP strain. (**B**) Cartoon depicting the two chromosome XII homologs with 0 and 200 rDNA copies, and the two chromosome VI homologs with one carrying the CLA *kanMX2* and *URA3* markers on either side of the centromere (*CEN6*). (**C**) PCR was used to confirm diploidy as in figure 4.2, using WT gDNA from XII$^{200/200KU}$ as a positive control (WT).

Strain VI$^{0/0KU}$ XII$^{0/20}$ *fob1*$^{-}$+HP, heterozygous for an rDNA deletion and a 20-copy rDNA array, and carrying CLA markers on chromosome VI, was constructed by mating the chromosome VI marked 20-copy strain TAK300 (VI^{0KU} XII$^{0/20}$ *fob1*$^{-}$, section 4.7.3, (appendix figure 8.16) to an rDNA deletion haploid strain (spore 2C, section 4.4.5, table IV) in which *FOB1* was disrupted using the *fob1::HIS3* construct. *FOB1* disruption was confirmed through PCR (appendix figure 8.17). After mating, zygotes were picked using a micromanipulation microscope and the diploid state of the strain was confirmed by PCR (figure 4.45).

A

Strain	Origin/Created by:	Genotype
VI$^{0/0KU}$ XII$^{0/20}$ *fob1*$^{-}$ +HP	Quintana, Woods and Ganley	*MATa/MATalpha ade2-1/ade2-1 ura3-1/ura3-1 his3-11/his3-11 trp1-1/trp1-1 leu2-3,112/leu2-3,112 can1-100/can1-100 ChrVI-38,790/ ChrVI-38,790::URA3/ChrVI ChrVI-172,381::kanMX2/ChrVI, fob1::HIS3/ fob1::HIS3 RDNA1~20copies/rdn1ΔΔ* +HP

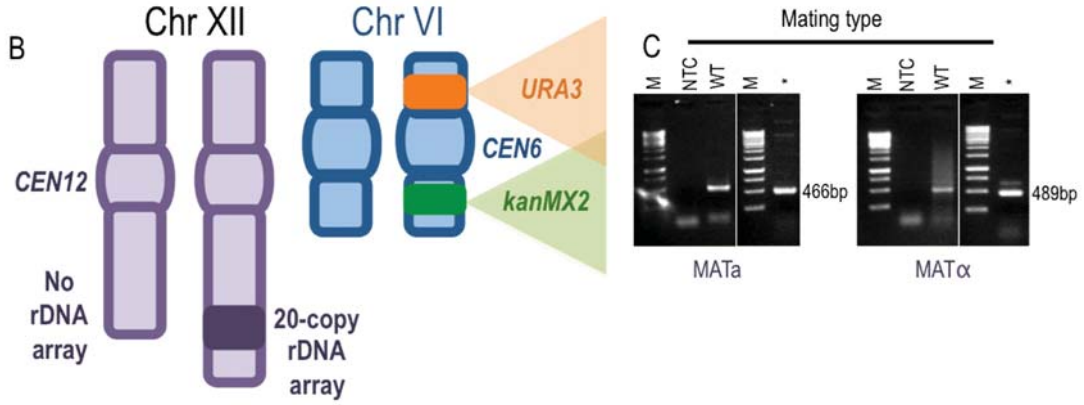

Figure 4.45. Characterization of the VI$^{0/0KU}$ XII$^{0/20}$+HP heterozygous strain with marked chromosome VI. (**A**) Genotype of the VI$^{0/0KU}$ XII$^{0/20}$+HP strain. (**B**) Cartoon depicting the two chromosome XII homologs with 20 and 0 rDNA copies, and the two chromosome VI homologs with one carrying the CLA *kanMX2* and *URA3* markers on either side of the centromere (*CEN6*). (**C**) PCR was used to confirm the diploidy as in figure 4.2, using WT gDNA from XII$^{200/200KU}$ as a positive control (WT).

4.8 CONSTRUCTION OF CLA rDNA TRANSLOCATION STRAINS

Finally, to evaluate if the rDNA effects on chromosome segregation are dependent on the chromosomal location of the rDNA repeats, we examined the effect of translocating the rDNA array to an ectopic site on another chromosome. We used the rDNA translocation strains constructed and characterized by Oakes et al. (2006). These harbor an rDNA translocation onto chromosome V in a location near *CEN5*, and were used to construct diploids in which the CLA markers are inserted into chromosome V or XII.

4.8.1 WT strain with a hygromycin resistant rDNA array (XII$^{200/200*KU}$)

The translocation rDNA arrays used by Oakes et al. (2006) carry a point mutation in the 18S rRNA coding region of each rDNA unit that confers resistance to hygromycin (Hyg^{R}) (Chernoff et al. 1994). To evaluate whether this mutation affects chromosome segregation, we created a WT diploid strain carrying the rDNA-Hyg^{R} array on the chromosome XII homolog that

carries the CLA assay markers. This strain was constructed by inserting the CLA markers into a haploid strain carrying the Hyg^R-rDNA array (NOY2029, designated by an asterisk on the strains' nomenclature; XII^{200*},Oakes et al. 2006). Successful insertion of the CLA markers was confirmed through PCR (appendix figure 8.18). This haploid strain was then mated to a WT haploid strain (XII^{200}) of the opposite mating type to create the CLA diploid strain $XII^{200/200*KU}$, and its diploid state was confirmed through PCR (figure 4.46).

A

Strain	Origin/Created by:	Genotype
rDNA-Hyg^R $XII^{200/200*KU}$	Quintana, Woods and Ganley	*MATa/MATalpha ade2-1/ade2-1 ura3-1/ura3-1 his3-11/his3-11 trp1-1/ trp1-1 leu2-3,112/leu2-3,112 can1-100/can1-100* ***ChrXII-109,570::kanMX2****/ChrXII* ***ChrXII-223,830::URA3****/ChrXII ,* ***rdn1Δ::rdn1-Hyg^R****/RDN1*

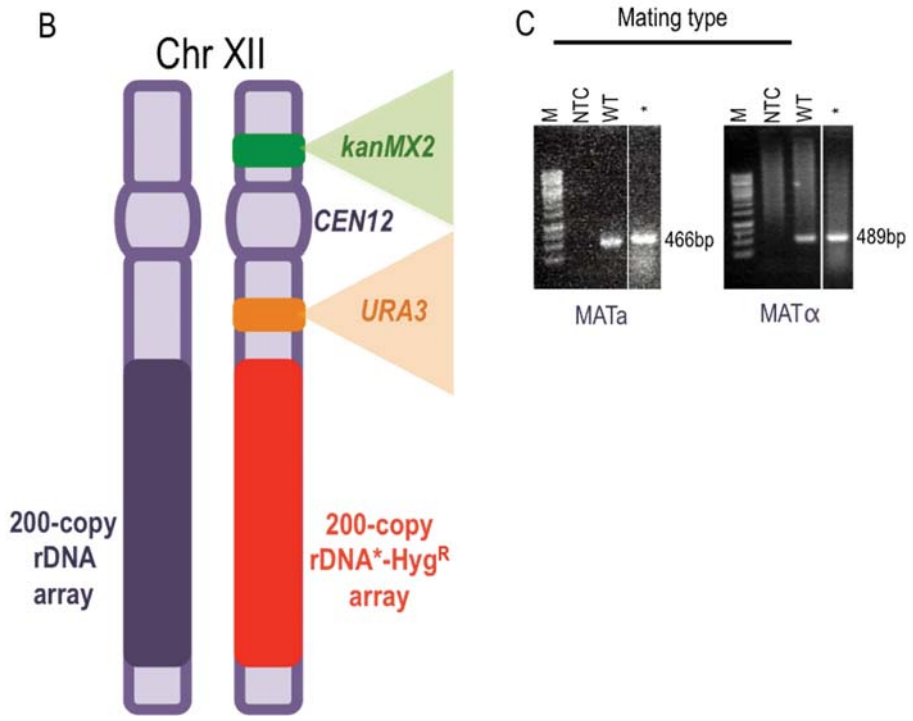

Figure 4.46. Characterization of the hygromycin-resistant rDNA array strain $XII^{200/200*KU}$. (**A**) Genotype of $XII^{200/200*KU}$ strain. (**B**) Cartoon depicting the two chromosome XII homologs with WT length rDNA arrays, one of which carries the HygR mutation and the CLA *kanMX2* and *URA3* markers on either side of the centromere (*CEN12*). (**C**) PCR was used to confirm the diploidy as in figure 4.2, using WT gDNA from $XII^{200/200KU}$ as a positive control (WT).

4.8.2 Construction of chromosome V heterozygous rDNA translocation strains with a marked chromosome XII

To evaluate if the rDNA effects on chromosome segregation are dependent on its chromosomal location, we constructed a set of strains that harbor a heterozygous rDNA

translocation onto chromosome V, in which the CLA markers are inserted into a chromosome XII homolog with a WT length rDNA array. These are a strain homozygous for the WT rDNA array on chromosome XII ($XII^{200/200KU}$ $V^{0/200*}$); a strain heterozygous for the WT rDNA array on both chromosomes XII and V ($XII^{0/200KU}$ $V^{0/200*}$+HP); and a strain heterozygous for the WT rDNA array on both chromosomes XII and V and carrying a *FOB1* disruption ($XII^{0/200KU}$ $V^{0/200*}$ *fob1*-+HP).

First, strain $XII^{200/200KU}$ $V^{0/200*}$ was constructed by inserting the CLA markers into chromosome XII of strain NOY2053 (Woods and Ganley, unpublished), a haploid that contains the native rDNA array on chromosome XII and an ectopic rDNA array with a Hyg^R mutation on chromosome V near *CEN5* (XII^{200} V^{200*}, Oakes et al. 2006). Insertion of the CLA markers into chromosome XII was confirmed by PCR (appendix figure 8.19). This haploid was mated with a WT haploid of the opposite mating type (XII^{200} V^{0}) that had the leucine gene repaired (not shown) for use as a mating marker. Diploid colonies were selected for their ability to grow on medium lacking uracil and leucine. The diploid state of this strain was confirmed by PCR (figure 4.47).

A

Strain	Origin/Created by:	Genotype
$XII^{200/200KU}$ $V^{0/200*}$	Quintana, Woods and Ganley	*MATa/MATalpha ade2-1/ade2-1 ura3-1/ura3-1 his3-11/his3-11 trp1-1/ trp1-1 LEU2/leu2-3,112 can1-100/can1-100 ChrXII-109,570::kanMX2/ ChrXII ChrXII-223,830::URA3/ChrXII* ***rdn1-Hyg^R*** *(rDNA*) array near CEN5*

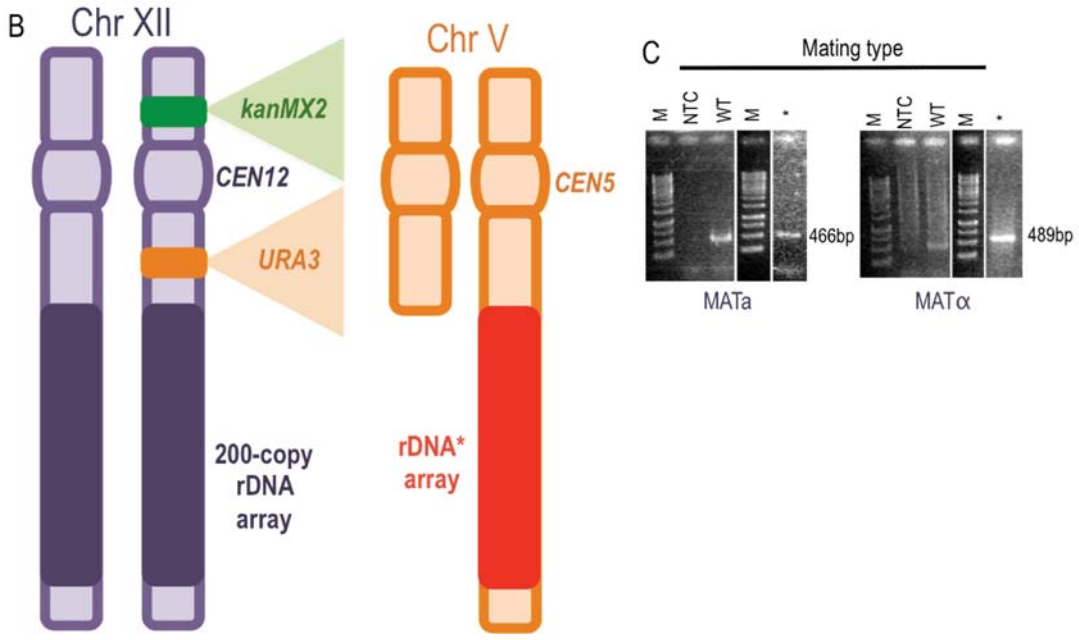

Figure 4.47. Characterization of strain $XII^{200/200KU}$ $V^{0/200*}$. (**A**) Genotype of the $XII^{200/200KU}$ $V^{0/200*}$ strain. (**B**) Cartoon depicting the two chromosome XII homologs as in figure 4.2, and chromosome V with one of the two homologs harboring a translocated rDNA array (rDNA*). (**C**) PCR was used to confirm the diploid state of this strain as in figure 4.2, using WT gDNA from $XII^{200/200KU}$ as a positive control (WT).

Next, we created a strain heterozygous for the presence of the rDNA array on both chromosomes XII and V, with CLA markers on the chromosome XII homolog harboring the WT length rDNA array ($XII^{0/200KU}$ $V^{0/200*}$+HP). Construction of this strain involved mating strain XII^{200KU} V^{200*} (section 4.8.2), to the haploid rDNA deletion strain XII^{0}+HP (spore 2C, section 4.4.5, table IV). After the mating, diploid colonies were selected by their ability to grow on medium lacking uracil and tryptophan, and their diploid state was confirmed through PCR (figure 4.48).

A

Strain	Origin/Created by:	Genotype
$XII^{0/200KU}$ $V^{0/200*}$ +HP	Quintana, Woods and Ganley	*MATa/MATalpha ade2-1/ade2-1 ura3-1/ura3-1 his3-11/his3-11 trp1-1/ trp1-1 leu2-3,112/leu2-3,112 can1-100/can1-100* ***ChrXII-109,570::kanMX2****/ChrXII* ***ChrXII-223,830::URA3****/ChrXII,* ***RDNA1****/ rdn1Δ::HIS3G,* ***rdn1-Hyg^{R}*** (rDNA*) array near *CEN5* +HP

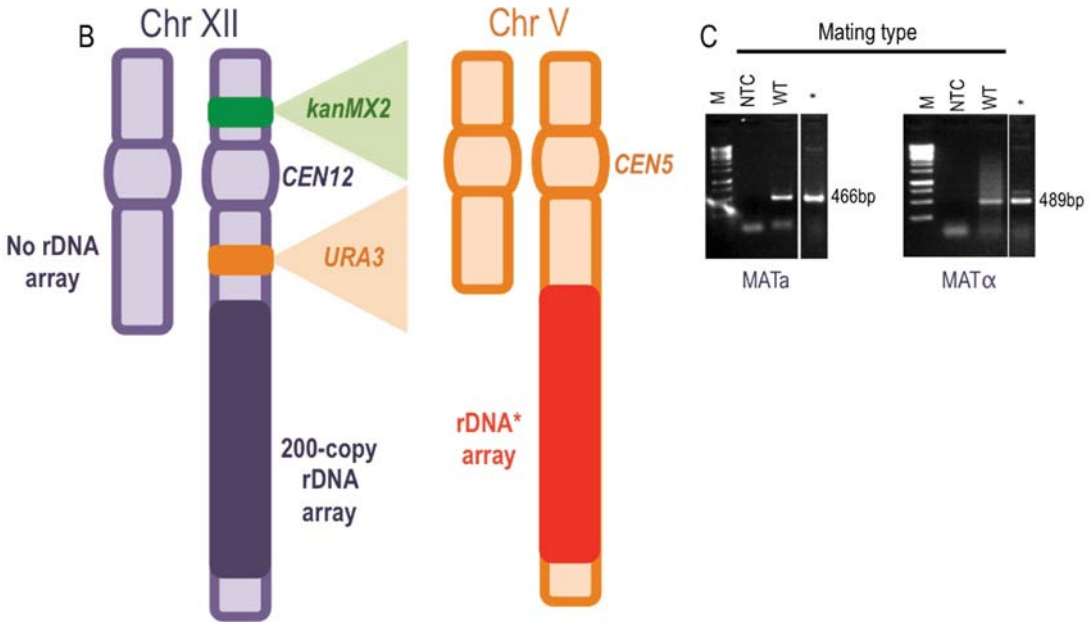

Figure 4.48. Characterization of strain $XII^{0/200KU}$ $V^{0/200*}$+HP. (**A**) Genotype of the $XII^{0/200KU}$ $V^{0/200*}$+HP strain. (**B**) Cartoon depicting the chromosome XII and chromosome V homologs, both of which are heterozygous for the presence of the rDNA array. The chromosome XII homolog harboring the rDNA array carries the CLA markers. This strain may carry the HP from the rDNA deletion parent strain (not tested). (**C**) PCR was used to confirm the diploid state of this strain as in figure 4.2, using WT gDNA from $XII^{200/200KU}$ as a positive control (WT).

Lastly, we created a strain heterozygous for the presence of the rDNA array on both chromosomes XII and V that also carried a *FOB1* disruption and CLA markers on the chromosome XII homolog that harbors the WT length rDNA array ($XII^{0/200KU}$ $V^{0/200*}$ *fob1*$^{-}$+HP). This strain was created by first replacing the *HIS3* marker used to disrupt *FOB1* in strain TAK300 with the *ADE2* marker gene using the marker swap plasmid M2371 (Voth et al. 2003). This plasmid contains a *his3::ADE2* construct that was excised using *PstI/Sac*I digestion and

transformed into TAK300. *fob1::his3::ADE2* transformants were confirmed through PCR (not shown) and a *fob1::ADE2* construct was amplified from this strain to then disrupt the *FOB1* copy of strain XII^{200KU} V^{200*}. This *fob1::ADE2* disruption was confirmed through PCR (appendix figure 8.20), and the resulting XII^{200KU} V^{200*} *fob1*$^{-}$ strain was mated to the haploid rDNA deletion, *FOB1* disruption strain XII^{0} *fob1*$^{-}$+HP (section 4.6.3, appendix figure 8.13). Diploid colonies were selected for their ability to grow on medium lacking histidine and adenine, and their diploid state was confirmed through PCR (figure 4.49).

A

Strain	Origin/Created by:	Genotype
XII$^{0/200KU}$ V$^{0/200*}$ *fob1*$^{-}$ +HP	Quintana, Woods and Ganley	*MATa/MATalpha ade2-1/ade2-1 ura3-1/ura3-1 his3-11/his3-11 trp1-1/ trp1-1 leu2-3,112/leu2-3,112 can1-100/can1-100* ***ChrXII-109,570::kanMX2****/ChrXII* ***ChrXII-223,830::URA3****/ChrXII,* ***RDNA1****/ rdn1Δ::HIS3G,* ***rdn1-Hyg^{R}*** (rDNA*) array near *CEN5, fob1::ADE2/ fob1::HIS3,* +HP

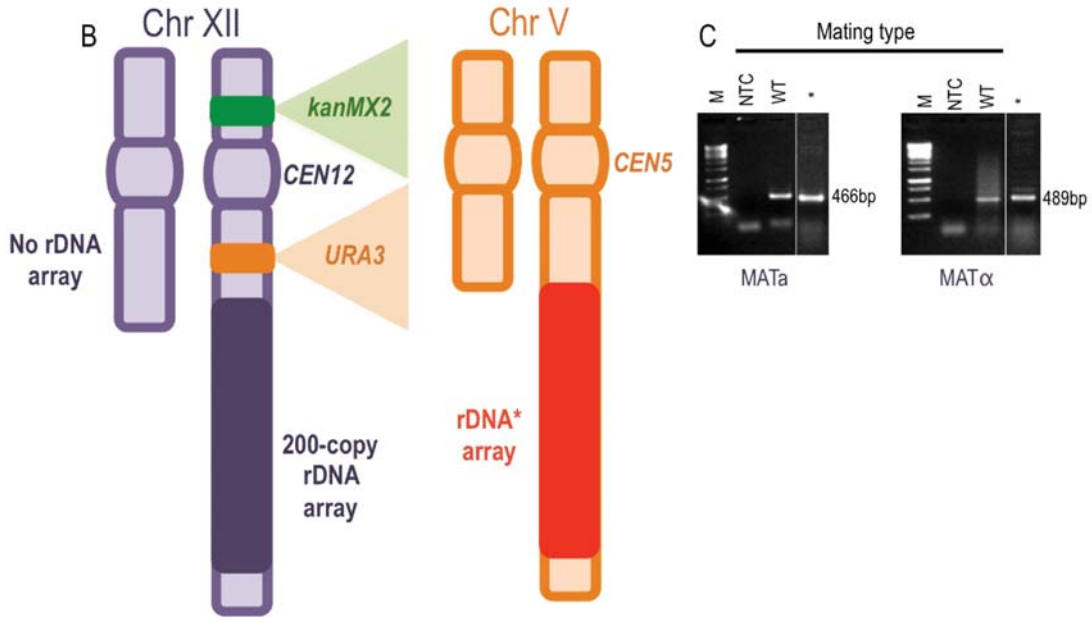

Figure 4.49. Characterization of strain XII$^{0/200KU}$ V$^{0/200*}$ *fob1*$^{-}$+HP. (**A**) Genotype of the XII$^{0/200KU}$ V$^{0/200*}$ *fob1*$^{-}$+HP strain. (**B**) Cartoon depicting the chromosome XII and chromosome V homologs, both of which are heterozygous for the presence of the rDNA array as in figure 4.48. The strain may carry the HP from the rDNA deletion parent strain (not tested). (**C**) PCR was used to confirm the diploid state of this strain as in figure 4.2, using WT gDNA from XII$^{200/200KU}$ as a positive control (WT).

4.8.3 Construction of chromosome V heterozygous rDNA translocation strains with chromosome V CLA markers

Finally, to evaluate if the rDNA effects on chromosome segregation are dependent on its chromosomal location, we constructed a set of strains that harbor a heterozygous rDNA translocation onto chromosome V in which the CLA markers are present on the chromosome V

homolog harboring the rDNA array. These are a strain homozygous for the WT rDNA array on chromosome XII ($V^{0/200*KU}$ $XII^{200/200}$); a strain heterozygous for the WT rDNA array on both chromosomes XII and V ($V^{0/*200KU}$ $XII^{0/200}$+HP); and a strain heterozygous for the WT rDNA array on both chromosomes XII and V that carries a *FOB1* disruption ($V^{0/200*KU}$ $XII^{0/200}$ *fob1-* +HP).

First, strain $V^{0/200*KU}$ $XII^{200/200}$ was constructed by inserting the CLA markers into chromosome V of strain NOY2053 (XII^{200} V^{200*}) (Oakes et al. 2006), to create the marked haploid V^{200*KU} XII^{200} (Woods and Ganley, unpublished). Insertion of the CLA markers on chromosome V was confirmed through PCR (appendix figure 8.21). This haploid was mated with a WT haploid of the opposite mating type (XII^{200} V^{0}) that had the leucine gene repaired (not shown) for use as a mating marker. Diploid colonies were selected for their ability to grow on medium lacking uracil and leucine. The diploid nature of this strain was confirmed by PCR (figure 4.50).

A

Strain	Origin/Created by:	Genotype
$V^{0/200*KU}$ $XII^{200/200}$	Quintana, Woods and Ganley	*MATa/MATalpha ade2-1/ade2-1 ura3-1/ura3-1 his3-11/his3-11 trp1-1/trp1-1 LEU2/leu2-3,112 can1-100/can1-100* ***ChrV-108,414::URA3****/ChrV* ***ChrV-424,837::kanMX2****/ChrV,* ***rdn1-Hyg^{R}*** (rDNA*) array near *CEN5*

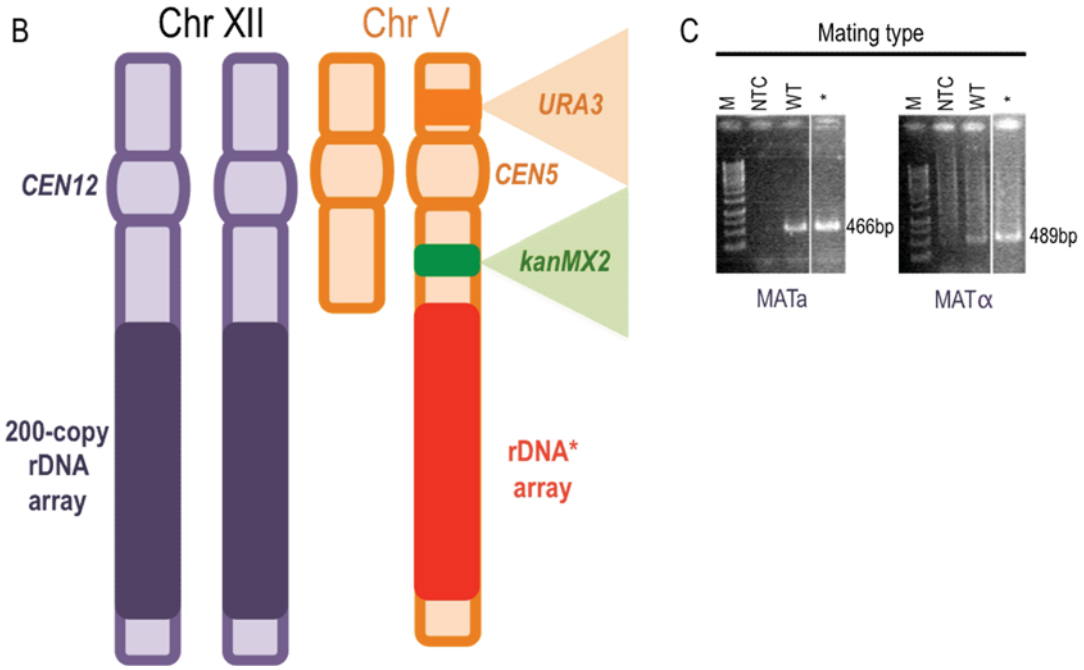

Figure 4.50. Characterization of strain $V^{0/200*KU}$ $XII^{200/200}$. (**A**) Genotype of the $V^{0/200*KU}$ $XII^{200/200}$ strain. (**B**) Cartoon depicting the WT chromosome XII homologs, and the chromosome V homologs with one carrying the translocated rDNA array (rDNA*) and the CLA *kanMX2* and *URA3* markers on either side of the centromere (*CEN5*). (**C**) PCR was used to confirm the diploidy as in figure 4.2, using WT gDNA from $XII^{200/200KU}$ as a positive control (WT).

Next, a strain heterozygous for the WT rDNA array on both chromosomes XII and V with the CLA markers on the chromosome V homolog carrying the translocated rDNA* array ($V^{0/200*KU}$ $XII^{0/200}$+HP) was constructed. Insertion of the CLA markers onto chromosome V (Woods, Quintana and Ganley, unpublished) of strain NOY2030 (V^{200*} XII^{0}, Oakes et al. 2006) created the marked haploid V^{200*KU} XII^{0}. This haploid was mated with a WT haploid of the opposite mating type (XII^{200} V^{0}) that had the leucine gene repaired (not shown) for use as a mating marker. Diploid colonies were selected for their ability to grow on medium lacking uracil and leucine. The diploid nature of this strain and the presence of the CLA markers on chromosome V were confirmed by PCR (figure 4.51).

A

Strain	Origin/Created by:	Genotype
$V^{0/200*KU}$ $XII^{0/200}$ +HP	Quintana, Woods and Ganley	*MATa/MATalpha ade2-1/ade2-1 ura3-1/ura3-1 his3-11/his3-11 trp1-1/trp1-1 LEU2/leu2-3,112 can1-100/can1-100,* ***ChrV-108,414::URA3****/ChrV* ***ChrV-424,837::kanMX2****/ChrV,* **rDNA* array near *CEN5,*** *RDN1/ rdnΔΔ::hisG,* +HP

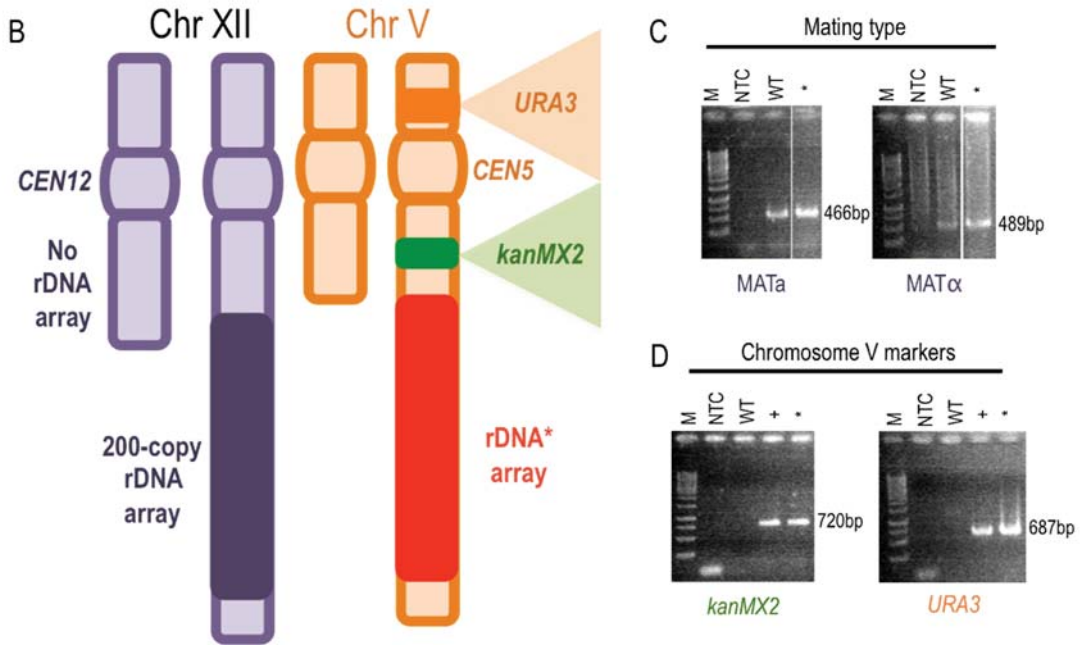

Figure 4.51. Characterization of strain $V^{0/200*KU}$ $XII^{0/200}$+HP. (**A**) Genotype of the $V^{0/200*KU}$ $XII^{0/200}$+HP strain. (**B**) Cartoon depicting the chromosome XII homologs with one carrying an rDNA deletion, and the chromosome V homologs with one carrying a translocated rDNA array (rDNA*) and the CLA *kanMX2* and *URA3* markers on either side of the centromere (*CEN5*). The strain may carry the HP from the rDNA deletion parent strain (not tested). PCR was used to confirm (**C**) diploidy as in figure 4.2, using WT gDNA from $XII^{200/200KU}$ as a positive control (WT), and (**D**) the insertion of the CLA markers (see figure 4.38 for details).

Finally, a strain that has a *FOB1* disruption and is heterozygous for the WT rDNA array on both chromosomes XII and V, and has the CLA markers on the chromosome V homolog carrying the translocation rDNA* array ($V^{0/200*KU}$ $XII^{0/200}$ *fob1*$^{-}$+HP) was constructed. This strain was created by first disrupting *FOB1* in strain V^{200*KU} XII^{200} using the *fob1::ADE2* construct and

was confirmed by PCR (appendix figure 8.22), and the resulting strain V^{200*KU} XII^{200} *fob1*$^{-}$ was mated to the haploid rDNA deletion and *FOB1* disruption strain XII^{0} *fob1*$^{-}$+HP (section 4.6.3, appendix figure 8.13). Diploid colonies were selected for their ability to grow on medium lacking histidine and adenine, and their diploid state was confirmed by PCR (figure 4.52).

A

Strain	Origin/Created by:	Genotype
$V^{0/200*KU}$ $XII^{0/200}$ *fob1*$^{-}$ +HP	Quintana, Woods and Ganley	*MATa/MATalpha ade2-1/ade2-1 ura3-1/ura3-1 his3-11/his3-11 trp1-1/trp1-1 leu2-3,112/leu2-3,112 can1-100/can1-100,* ***ChrV-108,414::URA3****/ChrV* ***ChrV-424,837::kanMX2****/ChrV,* ***rdn1-Hyg^{R}*** (rDNA*) array near *CEN5, fob1::ADE2/fob1::HIS3, RDN1/rdnΔΔ::hisG* +HP

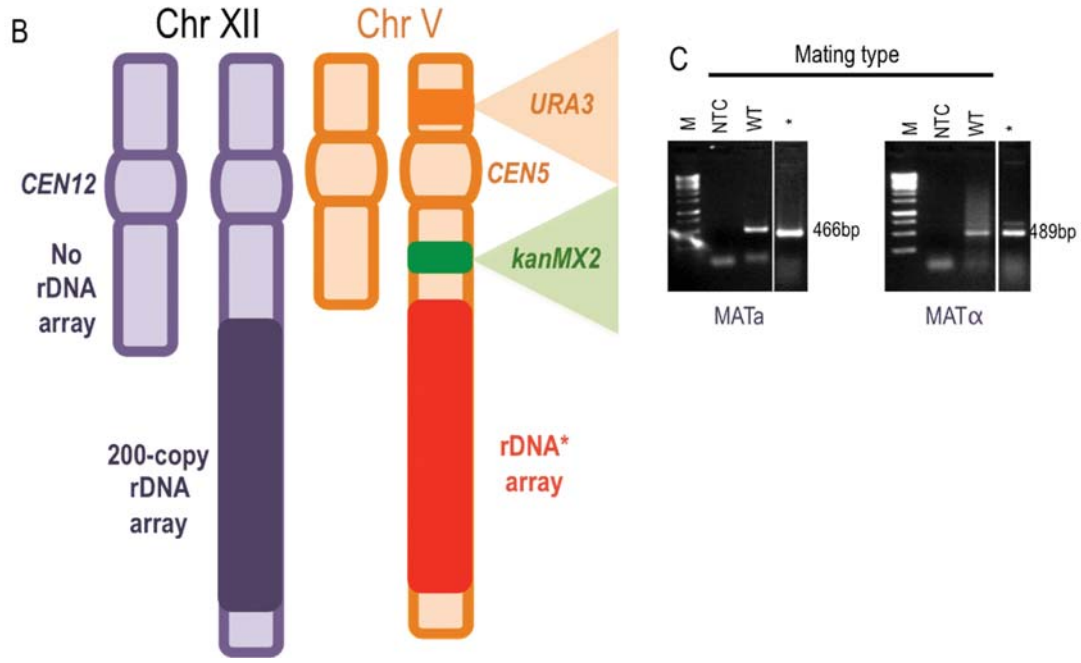

Figure 4.52. Characterization of strain $V^{0/200*KU}$ $XII^{0/200}$ *fob1*$^{-}$+HP. (**A**) Genotype of the $V^{0/200*KU}$ $XII^{0/200}$ *fob1*$^{-}$+HP strain. (**B**) Cartoon depicting the chromosome XII and V homologs as in figure 4.51, except this strain also harbors a *FOB1* disruption (not shown). The strain may carry the HP from the rDNA deletion parent strain (not tested). (**C**) PCR was used to confirm diploidy as in figure 4.2, using WT gDNA from $XII^{200/200KU}$ as a positive control (WT).

[blank page]

CHAPTER FIVE: CHROMOSOME LOSS ASSAY RESULTS

[blank page]

Previous studies led us to hypothesize that the rDNA gene repeats affect chromosome segregation. To test our hypothesis and explore how the rDNA may exert an effect on chromosome segregation, I have used the optimized CLA to measure the chromosome loss rate of strains harboring different rDNA alterations and/or disruption of certain key genes. This chapter describes my findings.

5.1 THE PRESENCE OF THE rDNA GENE REPEATS IS BENEFICIAL FOR CHROMOSOME XII SEGREGATION

The initial aim was to test whether the rDNA gene repeats have an effect on chromosome segregation by examining the chromosome XII loss rate in a strain in which all the rDNA repeats have been deleted from the chromosome ($XII^{0/0KU}$+HP; section 4.3.1). In addition, I wanted to test what effect rDNA recombination and rDNA transcription have on chromosome missegregation. To achieve the former, I measured the rate of chromosome XII loss in a *FOB1* disruption strain ($XII^{200/200KU}$ *fob1*$^-$; section 4.4.1). To assess the effect of rDNA transcription, I measured the rate of loss of chromosome XII in a strain with just 20 rDNA copies ($XII^{20/20KU}$ *fob1*$^-$; section 4.4.2) in which all the rDNA repeats are transcriptionally active.

The CLA was used to estimate the chromosome XII loss rate for the 0-copy strain $XII^{0/0KU}$+HP, the *fob1*$^-$ strain $XII^{200/200KU}$ *fob1*$^-$ and the 20-copy strain $XII^{20/20KU}$ *fob1*$^-$. I compared these rates to that found in the WT strain ($XII^{200/200KU}$; 6.01×10^{-6} chromosome losses per cell division). Deletion of the rDNA repeats resulted in a significant (~6-fold) increase in the chromosome XII loss rate relative to WT (figure 5.1), suggesting that the presence of the native chromosomal rDNA gene repeats aids faithful segregation of chromosome XII. The *fob1*$^-$ strain also showed a significant (~5-fold) increase in the rate of chromosome XII loss relative to WT (figure 5.1), suggesting that Fob1 helps mediate faithful segregation of chromosome XII. Since rDNA recombination is abolished in this *FOB1* disruption strain (Kobayashi and Horiuchi 1996; Kobayashi et al. 1998; Johzuka and Horiuchi 2002), it is possible that Fob1 mediates faithful chromosome segregation through stimulating rDNA recombination, but the other roles of Fob1 may also underlie this chromosome missegregation phenotype.

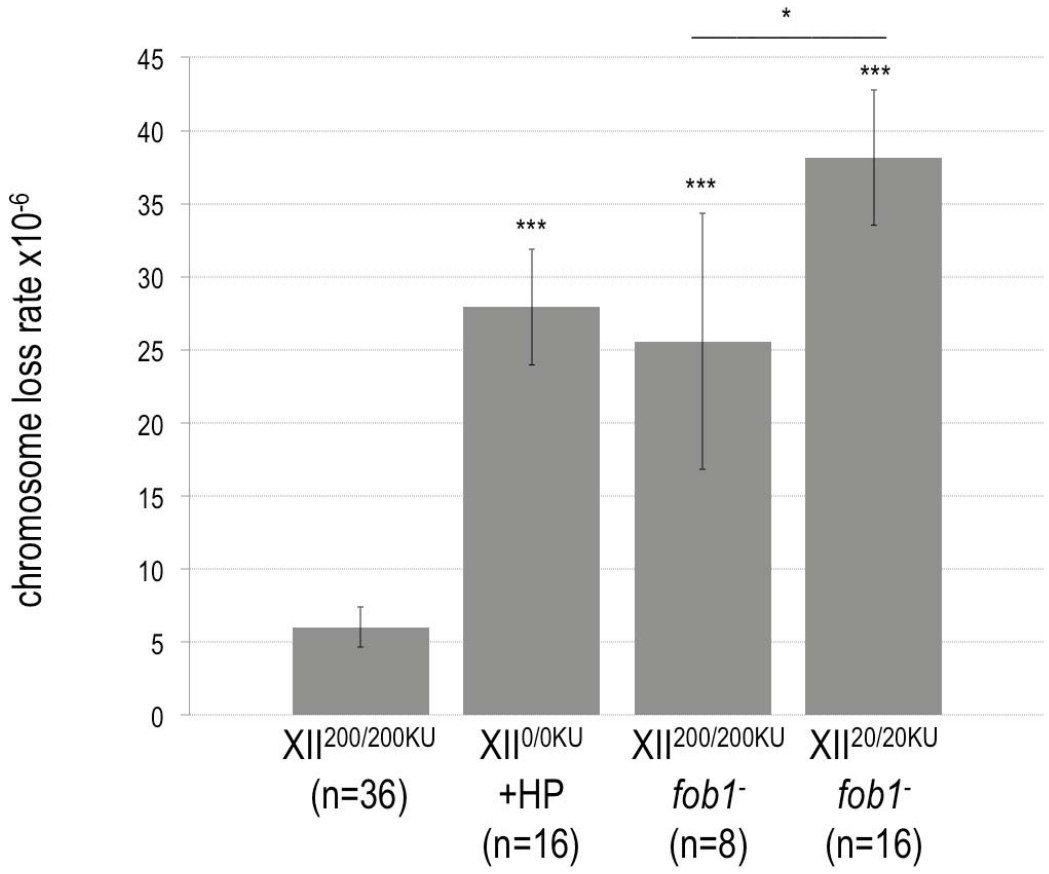

Figure 5.1. rDNA alterations result in increased rates of chromosome XII missegregation. The chromosome XII loss rate was measured using the CLA for the WT strain ($XII^{200/200KU}$), the 0-copy strain ($XII^{0/0KU}$+HP), the *fob1*$^{-}$ strain ($XII^{200/200KU}$ *fob1*$^{-}$), and the 20-copy strain ($XII^{20/20KU}$ *fob1*$^{-}$). All strains were grown in YPD. Error bars show SE. Asterisks show significant differences to the WT strain $XII^{200/200KU}$ (p-values from left to right indicate significant differences to WT: *** = $4.57x10^{-6}$, *** = $3.34x10^{-3}$, *** = $4.27x10^{-6}$; and between the *fob1*$^{-}$ and 20-copy strains: *=$6.91x10^{-2}$; no significant differences were found between the 0-copy strain and the *fob1*$^{-}$ or 20-copy strains).

The 20-copy strain also showed an increased (~7-fold) rate of chromosome XII loss compared to WT (figure 5.1). However, this strain also has a *FOB1* disruption to prevent rDNA amplification of the 20 copies back to WT. Therefore, it is possible that the elevated chromosome loss rate of the 20 copy strain is due to the lack of Fob1 rather than the change in rDNA copy number. To try and distinguish between these two possibilities, I decided to use transient *FOB1* complementation.

5.2 REDUCING THE NUMBER OF rDNA COPIES AFFECTS CHROMOSOME XII SEGREGATION INDEPENDENTLY OF Fob1

5.2.1 Growth on galactose influences the rate of chromosome XII segregation

To test whether the high missegregation rate of the 20-copy strain is a consequence of *FOB1* disruption rather than rDNA copy number reduction, I introduced Fob1 on a plasmid under the control of a galactose inducible promoter to the 20-copy rDNA strain and measured the rate of chromosome XII loss. Since *FOB1* disruption is necessary to prevent amplification of rDNA copy number in this strain, expression of *FOB1* was only induced during the CLA to limit expansion of the rDNA array.

The *FOB1* inducible plasmid pGAL-*FOB1* (section 4.4.3) was transformed into the WT ($XII^{200/200KU}$), *fob1*$^-$ ($XII^{200/200KU}$ *fob1*$^-$) and 20-copy ($XII^{20/20KU}$ *fob1*$^-$) strains, and the rate of chromosome loss was measured using the CLA in galactose media (ie. using SGal-Ura medium for initial selection and YPGal as rich medium from t_0 to t_1). As expected, introduction of Fob1 into strains lacking this protein resulted in rescue of the chromosome XII segregation defects in all strains (figure 5.2). However, these results are based on comparisons between Fob1-complemented strains grown in galactose and the original strains grown in glucose. To determine if growth in galactose has any effect on chromosome segregation independent of the Fob1 plasmid, the uncomplemented WT ($XII^{200/200KU}$), *fob1*$^-$ ($XII^{200/200KU}$ *fob1*$^-$) and 20-copy ($XII^{20/20KU}$ *fob1*$^-$) strains were screened using the CLA while grown in galactose. Strikingly, all strains exhibited a rate of chromosome XII loss significantly lower in galactose than when they were grown in glucose medium (figure 5.3). Comparison of each of the Fob1-complemented versus uncomplemented strains grown in galactose revealed no differences (data not shown). Therefore, the Fob1 complementation rescue phenotype could simply be explained by the effect of growth in galactose rather than the presence of functional Fob1. This means that I am still not able to determine whether the elevated chromosome missegregation rate observed in the 20-copy strain is the result of the reduction in rDNA copies or the disruption of *FOB1*.

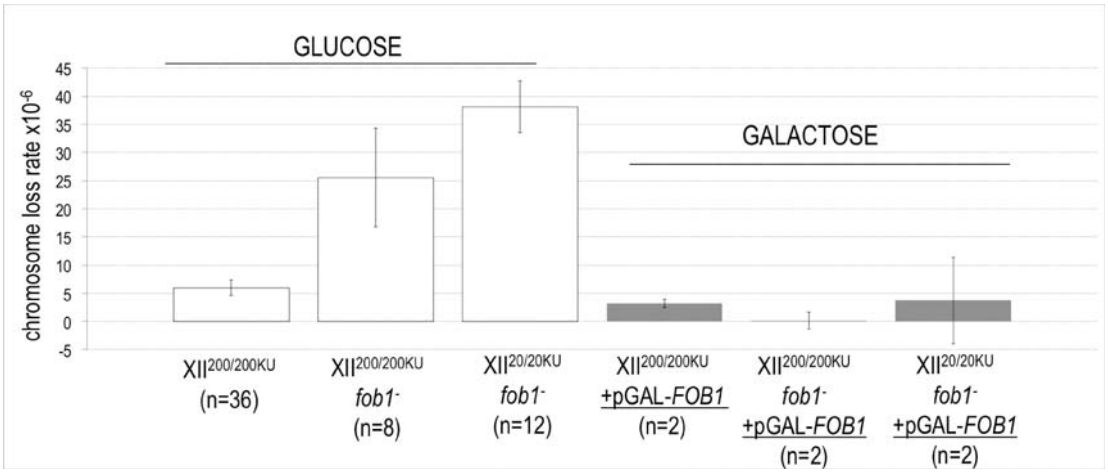

Figure 5.2. Fob1 complementation rescues chromosome XII segregation defects. The chromosome XII loss rate was measured for the WT ($XII^{200/200KU}$), *fob1-* ($XII^{200/200KU}$ *fob1-*) and 20-copy ($XII^{20/20KU}$ *fob1-*) strains in the presence of the *FOB1* inducible plasmid (+pGAL-*FOB1*) (galactose), and compared to their corresponding strain without pGAL-*FOB1* from figure 5.1 (glucose). Error bars show SE.

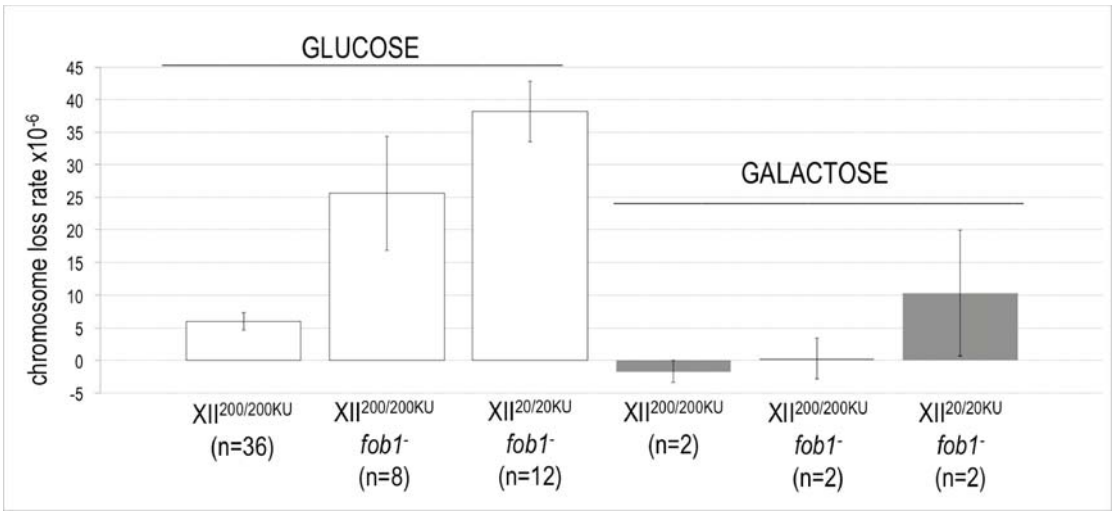

Figure 5.3. Growth in galactose results in low rates of chromosome XII missegregation. The chromosome XII segregation defects observed in the uncomplemented *fob1-* ($XII^{200/200KU}$ *fob1-*) and 20-copy ($XII^{20/20KU}$ *fob1-*) strains when compared to WT ($XII^{200/200KU}$) (from figure 5.1) when grown in glucose, are rescued by growth in galactose alone. Error bars show SE.

I noted that growth during the CLA in galactose was slower for the strains previously assayed in glucose. To determine whether there are growth rate differences between carbon sources, I performed growth curves for the WT strain in glucose and galactose, in both the absence and presence of pGAL-*FOB1*. The growth rate in galactose is much slower than in glucose irrespective of the presence of pGAL-*FOB1* (figure 5.4), and this was also found for the *fob1-* and 20-copy strains (data not shown). Yeast is known to undergo metabolic changes when grown in galactose (relative to growth in glucose) that result in growth rate differences and changes in expression of certain genes (reviewed in Timson 2001), therefore our findings

may reflect this altered metabolism when grown in galactose. If so, this effect would be expected to be global, affecting all chromosomes rather than just chromosome XII. To test if galactose causes a global effect on chromosome segregation I created WT strains carrying CLA markers on a chromosome V and VI (section 4.7.1) homolog, and compared their respective chromosome loss rates when grown in galactose vs. glucose. Surprisingly, neither chromosome V nor VI showed significantly different missegregation rates between the two carbon sources (figure 5.5). These results suggest that galactose affects the missegregation rate of chromosome XII specifically, and that this effect appears to be dominant to rDNA alterations.

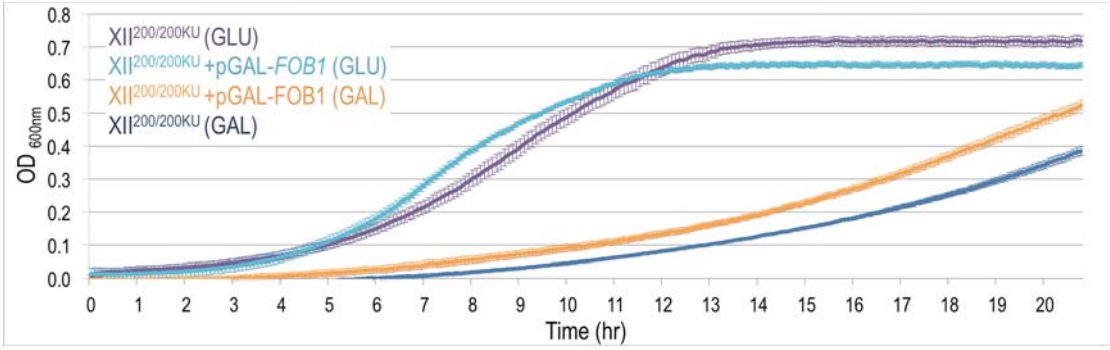

Figure 5.4. The growth rate of the WT strain is slower in galactose than in glucose. The WT strain ($XII^{200/200KU}$) was grown in galactose (GAL) and glucose (GLU) rich media, in both the presence and absence of the *FOB1* inducible plasmid (+pGAL-*FOB1*). Growth rates were measured by following OD_{600nm} using a 96 well plate reader. For every strain n=3 (3 biological replicas per strain with 3 technical replicates each). Error bars show SE.

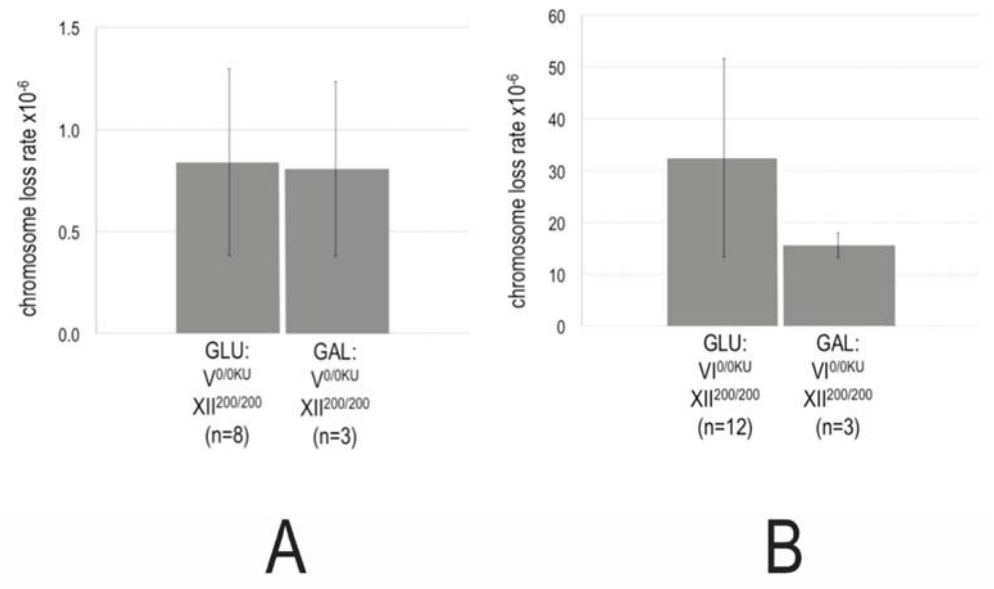

Figure 5.5. Growth in galactose does not affect the segregation rate of chromosomes V and VI. The chromosome loss rate was measured for chromosomes V and VI in WT strains $V^{0/0KU}$ $XII^{200/200}$ (**A**) and $VI^{0/0KU}$ $XII^{200/200}$ (**B**), and no significant differences were found between growth in glucose (GLU**)** and galactose (GAL) (p-values: 0.49 [A] and 0.73 [B])**.** Error bars show SE.

5.2.2 Complementation of *FOB1* in the 20-copy strain does not result in rDNA copy number change

Since re-introduction of *FOB1* expression from pGAL-*FOB1* has the potential to increase the rDNA copy number through its role in rDNA amplification (Kobayashi et al. 1998), the chromosome loss rate of the XII$^{20/20KU}$ *fob1*$^{-}$ +pGAL-*FOB1* strain may no longer reflect that of a 20-copy strain. To test whether any changes in rDNA copy number have occurred since the introduction of pGAL-*FOB1* into the XII$^{20/20KU}$ *fob1*$^{-}$ strain, the size of chromosome XII was determined through CHEF and Southern blotting using an rDNA probe. The size of chromosome XII remained unchanged in the presence of the plasmid in both glucose and galactose (figure 5.6). These results suggest that sufficient time has not yet elapsed to allow significant rDNA amplification, and that the rate of chromosome XII loss in XII$^{20/20KU}$ *fob1*$^{-}$ +pGAL-*FOB1* reflects re-introduction of *FOB1* and not an increase in rDNA copy number.

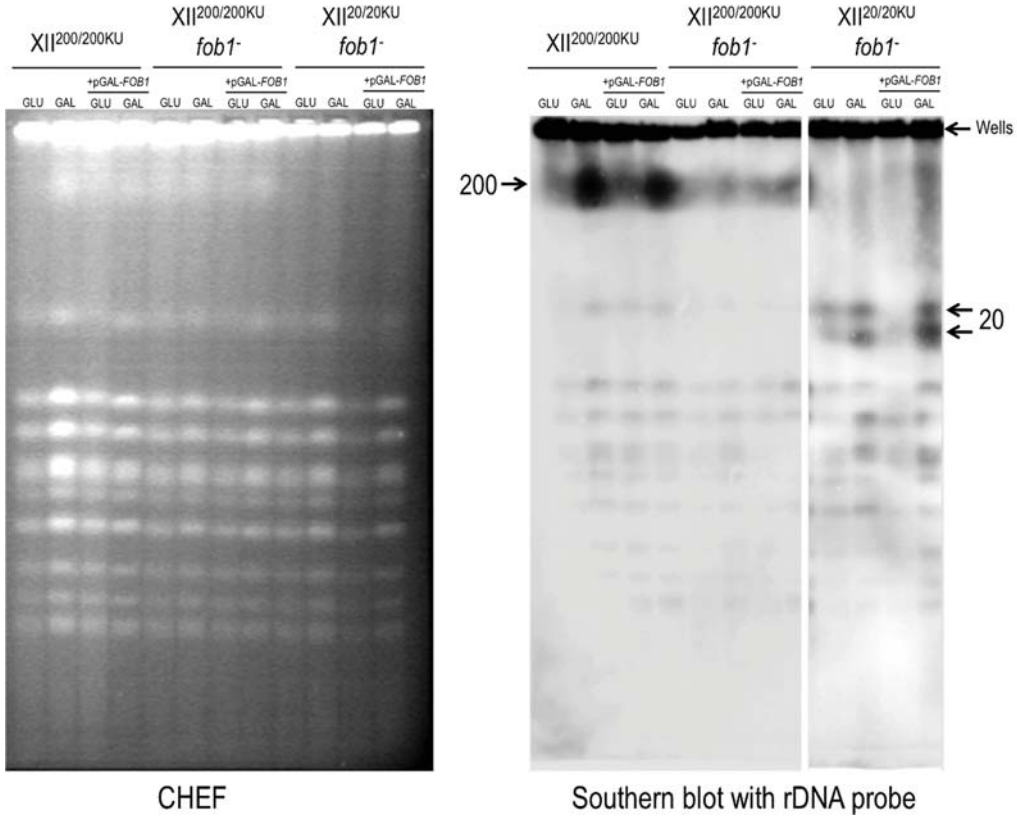

Figure 5.6. Chromosome XII size remains unchanged in strains carrying pGAL-*FOB1*. CHEF electrophoresis was used to confirm chromosome XII size. Strains XII$^{200/2000KU}$, XII$^{200/200KU}$ *fob1*$^{-}$ and XII$^{20/20KU}$ *fob1*$^{-}$ were grown in both glucose and galactose, with (+pGAL-*FOB1*) or without the *FOB1* inducible plasmid. An rDNA probe was used to detect chromosome XII. The number of rDNA copies is indicated by arrows, as are the wells. Ethidium bromide stained gel (left), Southern blot (right). The Southern blot panel on the right for strain XII$^{20/20KU}$ *fob1*$^{-}$ is a longer exposure of the same Southern blot shown on the left because of the lower signal intensity of rDNA hybridization in the 20-copy strain.

5.2.3 Leaky *FOB1* expression partially rescues 20-copy strain chromosome XII segregation defects.

The chromosome XII loss rates of strains with pGAL-*FOB1* were also measured in glucose as controls. Surprisingly, however, I saw clear differences in strains grown in glucose with and without the plasmid. The rate of chromosome XII loss of the *fob1-* strain was completely rescued by the plasmid, while that of the 20-copy strain was partially rescued (figure 5.7). In contrast, the chromosome loss rate of the WT strain increased in the presence of the plasmid. I hypothesized that these results are a consequence of leaky expression from the plasmid under glucose growth conditions.

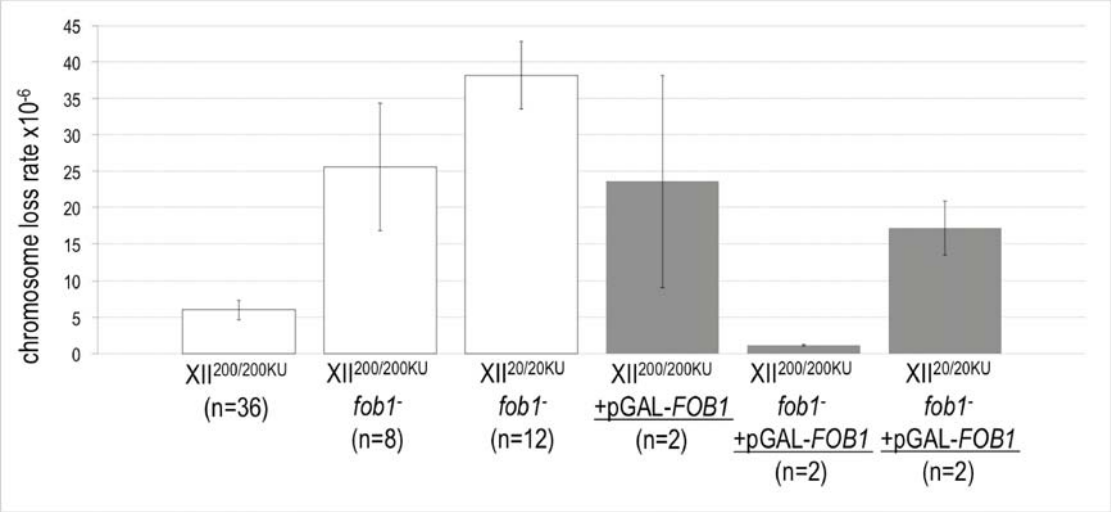

Figure 5.7 pGAL-*FOB1* alters chromosome XII segregation fidelity in glucose. The chromosome XII loss rate for the WT ($XII^{200/200KU}$), *fob1-* ($XII^{200/200KU}$ *fob1-*) and 20-copy ($XII^{20/20KU}$ *fob1-*) strains in glucose in the presence of the Fob1 plasmid (+pGAL-*FOB1*) were found to be different to those from their uncomplemented corresponding strain from figure 5.1. Error bars show SE.

To test whether there is leaky expression of pGAL-*FOB1* under glucose growth, I assayed *FOB1* expression using RT-PCR. The three strains (WT, *fob1-* and 20-copy/*fob1-*) were grown with and without pGAL-*FOB1*, and both under glucose (*FOB1* repressive) and galactose (*FOB1* inducing) conditions. Total RNA was extracted from each sample and the integrity of the 28s and 18s rRNA bands was confirmed by visualization on an agarose gel (figure 5.8). Primers PAG336 and PAG337 were designed to amplify a small *FOB1* amplicon that spans the *LEU2* insertion site. The RT-PCR elongation time was minimized to prevent amplification of the larger, *LEU2*-containing product from the *FOB1* disruption strains (figure 5.9). Another set of primers (PAG331 and PAG333) was used to amplify *ACT1* (213bp product) as a housekeeping gene control.

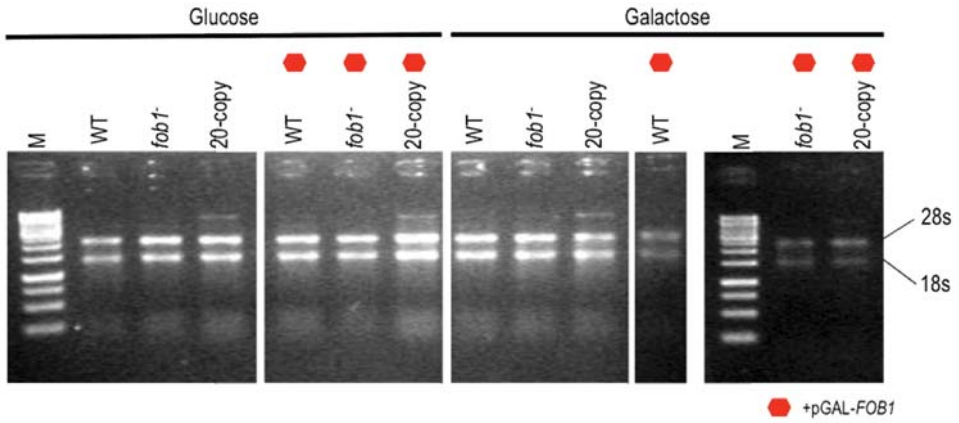

Figure 5.8. RNA extraction from WT, *fob1-* and 20-copy strains. Ethidium bromide stained agarose gel from RNA extracts from strains WT ($XII^{200/200KU}$), *fob1-* ($XII^{200/200KU}$ + *fob1-*) and 20-copy ($XII^{20/20KU}$ + *fob1-*) while grown in glucose (*FOB1* repressive) and galactose (*FOB1* inducing), both with (red hexagons) and without the pGAL-*FOB1* plasmid.

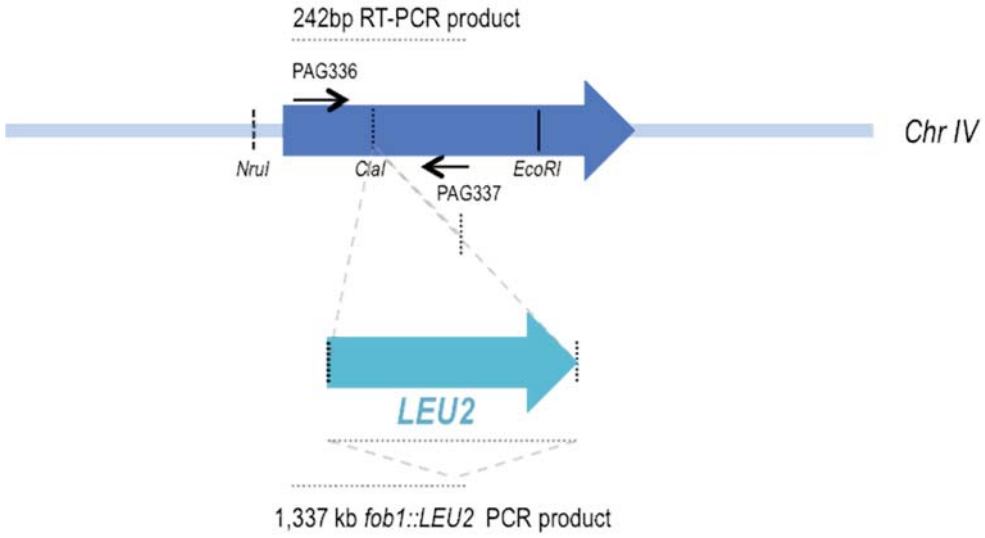

Figure 5.9. Location of primers to determine *FOB1* expression through RT-PCR. Primers PAG336 and PAG337 amplify a 242bp product from *FOB1* and a 1,337bp product from strains where *FOB1* has been disrupted by insertion of *LEU2*.

RT-PCR confirmed the absence of *FOB1* expression in the *FOB1* disruption strains and also showed that these strains express *FOB1* from pGAL-*FOB1* in both glucose and galactose (figure 5.10). These results support our hypothesis of a leaky expression of pGAL-*FOB1* in glucose. Although end point PCR was used and so is not quantitative, the *FOB1* bands are brighter in pGAL-*FOB1*-containing strains grown in galactose compared to when they are grown in glucose, suggesting there may be a difference in *FOB1* expression between inducing and non-inducing conditions. The leaky expression of *FOB1* from pGAL-*FOB1* during growth in glucose suggests that the chromosome loss rescue seen in the 20-copy and *fob1-*

strains in figure 5.6 is the result of this leaky *FOB1* expression. This further suggests that the high missegregation phenotype of the 20-copy strain (figure 5.1) may partly be consequence of *FOB1* disruption, but also partly a consequence of reduced rDNA copy number.

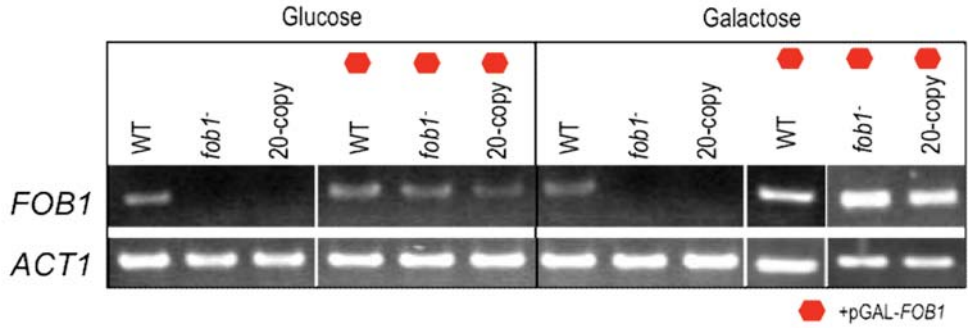

Figure 5.10. RT-PCR shows leaky *FOB1* expression in non-inducing conditions. Ethidium bromide stained agarose gel shows RT-PCR products of 242bp for *FOB1* (figure 5.8) and of 213bp for the positive control fragment from the *ACT1* gene (primers PAG331 and PAG333). RNA from figure 5.7 was used as template for RT-PCR.

5.2.4 *FOB1* mediates faithful chromosome XII segregation through the rDNA repeats

It was suspected that *FOB1* mediates faithful chromosome XII-specific segregation directly through the rDNA repeats because Fob1 binds directly to the rDNA at the RFB site. To test this, I constructed an rDNA deletion strain that also harbored a *FOB1* disruption ($XII^{0/0KU}$ *fob1-* +HP, section 4.4.4**)**. Either of these conditions (rDNA deletion/*FOB1* disruption) by itself increases chromosome XII missegregation, but if Fob1 exerts its role in chromosome segregation through the rDNA repeats, deletion of *FOB1* in the absence of rDNA should not cause a further increase. Surprisingly, I found that the absence of both Fob1 and the chromosomal rDNA repeats results in a low rate of chromosome XII missegregation, resembling that of the WT (figure 5.11). The fact that the absence of Fob1 in an rDNA deletion background restores the rate chromosome XII to WT levels indicates that Fob1 is only needed when the rDNA repeats are present. Our data so far suggests that Fob1 mediates chromosome XII segregation directly through the rDNA repeats.

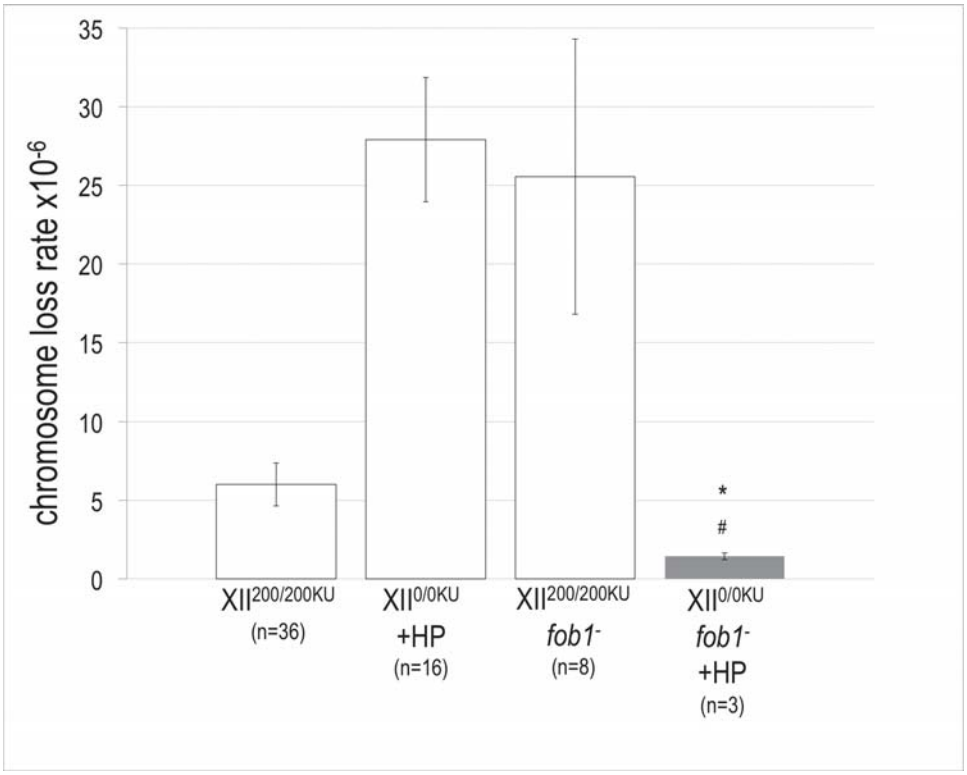

Figure 5.11. *FOB1* disruption rescues chromosome XII missegregation when the rDNA repeats are deleted. The chromosome XII loss rate was measured in the *FOB1* disrupted rDNA deleted strain $XII^{0/0KU}$ *fob1-*+HP and was compared to the WT ($XII^{200/200KU}$), the rDNA deletion ($XII^{0/0KU}$+HP) and the *FOB1* disruption ($XII^{200/200KU}$ *fob1-*) strains. Disruption of *FOB1* in an rDNA deletion background results in significantly lower chromosome missegregation than either of the two rDNA alterations alone (p-values: *= $1.81x10^{-2}$ [vs rDNA deletion], #= $1.81x10^{-2}$ [vs *FOB1* disruption]). Error bars show SE.

5.2.5 *FOB1* is required for the faithful segregation of chromosome XII but not other chromosomes.

To test whether the Fob1 effect is indeed specific to chromosome XII, I created a *FOB1* disruption strain with CLA markers on chromosome VI ($VI^{0/0KU}XII^{200/200}$ *fob1-*, section 4.7.2). No significant difference was observed in the rate of chromosome VI missegregation in the presence versus absence of *FOB1* (figure 5.12). This indicates that *FOB1* is not required for the faithful segregation of chromosome VI and suggests that the effect of *FOB1* on chromosome segregation is specific to chromosome XII.

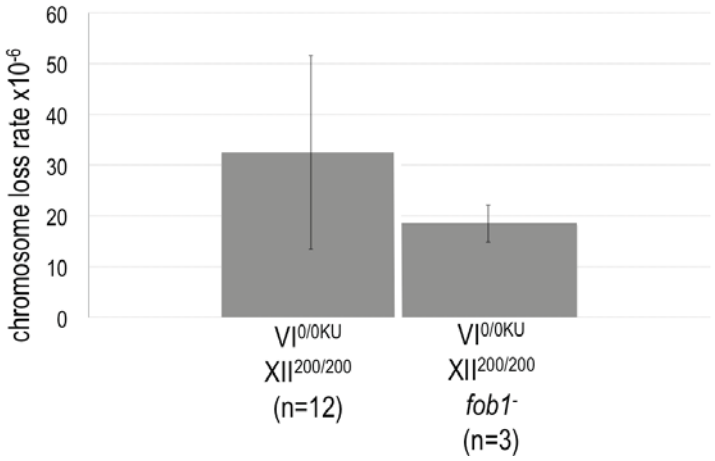

Figure 5.12. *FOB1* disruption does not alter the rate of chromosome VI loss. The chromosome VI loss rate was measured in the WT strain $VI^{0/0KU}$ $XII^{200/200}$ and in the *fob1-* strain $VI^{0/0KU}$ $XII^{200/200}$ *fob1-* (n=3). No significant difference was found between the two (p-value=0.83). Error bars show SE.

5.2.6 *FOB1* mediates faithful segregation of other chromosomes carrying the rDNA repeats.

The results from sections 5.2.4 and 5.2.5 suggest that Fob1 helps to mediate faithful segregation of the chromosome carrying the rDNA repeats (i.e. chromosome XII in a WT). To test this hypothesis, I determined the rate of loss of a chromosome V homolog that has an rDNA array translocated onto it ($V^{0/200*KU}$ $XII^{0/200}$; section 4.8.3) in the presence and absence of Fob1. The loss rate of chromosome V in a WT background is lower than that for chromosome XII, and interestingly, the rate of loss actually increases when an rDNA array is translocated onto chromosome V (strain $V^{0/200*KU}$ $XII^{0/200}$; figure 5.13). When *FOB1* is disrupted in this strain ($V^{0/200*KU}$ $XII^{0/200}$ *fob1-*), the rate of chromosome V loss further increases (figure 5.13), mirroring that seen for chromosome XII missegregation when *FOB1* is disrupted. These results, together with the results showing that disruption of *FOB1* has no effect on chromosome V missegregation when it does not carry the rDNA repeats (figure 5.12), provide strong support for the hypothesis that Fob1 facilitates faithful chromosome segregation due to its role at the rDNA repeats, regardless of which chromosome the rDNA is present on.

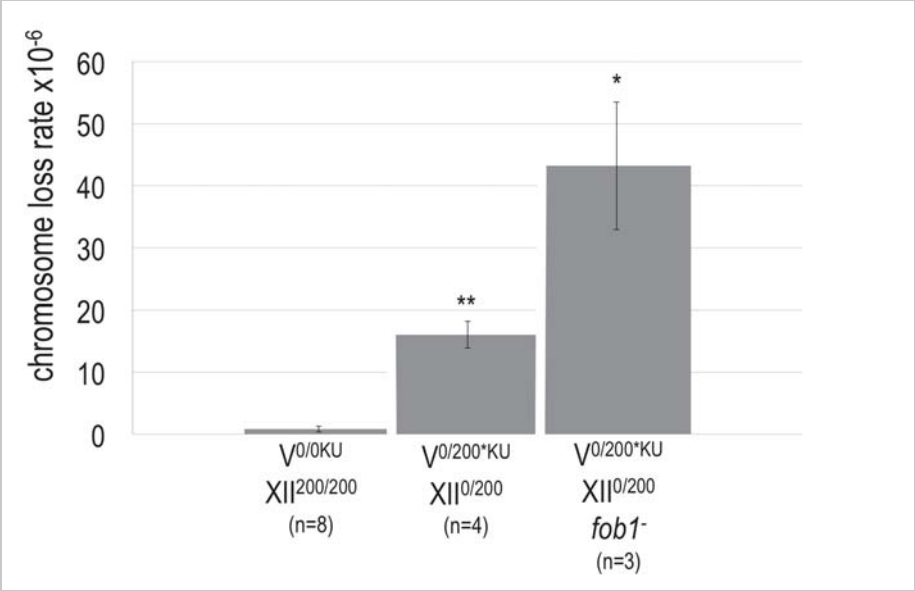

Figure 5.13. Disruption of *FOB1* increases chromosome V missegregation when it carries a translocated rDNA array. The chromosome V loss rate was measured in a strain heterozygous for the presence of the rDNA on chromosome XII and for an rDNA translocation onto the marked chromosome V homolog ($V^{0/200*KU}$ $XII^{0/200}$), before and after disruption of *FOB1* ($V^{0/200*KU}$ $XII^{0/200}$ *fob1*$^{-}$). The chromosome loss rate of the rDNA translocation strain is significantly higher than WT ($V^{0/0KU}$ $XII^{200/200}$) (p-values **= $4x10^{-3}$ and *= $1.2x10^{-2}$), and disruption of *FOB1* results in a significantly higher rate of chromosome loss again (p-value $5.7x10^{-2}$; not indicated). Error bars show SE.

5.3 INVESTIGATING THE EFFECTS OF rDNA TRANSCRIPTION ON CHROMOSOME XII SEGREGATION

I next sought to test whether it is the absence of the rDNA repeats or the loss of rDNA transcription that is responsible for the increased rate of chromosome missegregation when the rDNA repeats are removed from chromosome XII. To achieve this, I created a strain with abolished rDNA transcription. Transcription of the rDNA is carried out by RNA polymerase I (Pol I), and disruption of Pol I subunits has been used in the past to render Pol I inactive and abolish rDNA transcription (Nogi et al. 1991b). The viability of such strains is achieved by using RNA polymerase II (Pol II) transcription of rRNA from the HP, as for the $XII^{0/0KU}$+HP strain. If recruitment of Pol I to the rDNA locus or the rDNA transcription process itself mediates faithful chromosome segregation, lack of rRNA transcription would be expected to result in a segregation defect. To investigate this, Pol I activity was abolished by deleting the second largest subunit of Pol I, encoded by the *RPA135* gene (strain $XII^{200/200KU}$ *rpa135*Δ +HP, section 4.5.1).

The XII$^{200/200KU}$ *rpa135Δ* +HP strain requires growth in galactose due to its dependence on the HP for viability, and is not able to grow in glucose, unlike the rDNA deletion strain. It has a slow growth phenotype, with a doubling time of approximately 8-12 hrs (figure 5.14). This required adjustment of the CLA growth times to allow measurement of the chromosome loss rate over a single doubling.

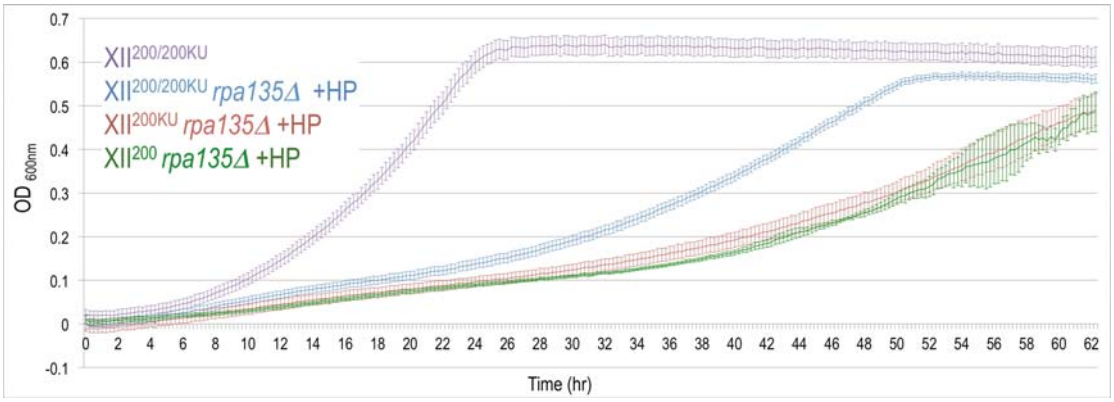

Figure 5.14. The *RPA135* deletion strain has a slower growth rate than WT. Growth rates were obtained for the XII$^{200/200KU}$ *rpa135Δ* +HP diploid strain and for haploids with (XII^{200KU} *rpa135Δ::LEU2* +HP) and without (XII^{200} *rpa135Δ::LEU2* +HP) the chromosome XII tags for the CLA. All were lower than that of the WT CLA diploid strain XII$^{200/200KU}$, with the *rpa135Δ* diploid having a somewhat faster growth rate compared to the haploids. All strains were grown in YPGal. For all strains n=3 (3 biological replicas each with 3 technical replicas). Error bars show SE.

To determine the effect of rDNA transcription on chromosome segregation, the rate of chromosome XII loss was measured in strain XII$^{200/200KU}$ *rpa135Δ* +HP when grown in galactose. Deletion of *RPA135* caused a significant reduction, of more than 6-fold, in the rate of chromosome XII loss compared to the WT strain when grown in glucose. However, no difference was observed when both strains were grown in galactose (figure 5.15).

It has been suggested that Fob1-mediated rDNA recombination is transcription-dependent (Takeuchi et al. 2003), so it is possible there is an interplay between the activities of Fob1 and Pol I at the rDNA locus that influences chromosome XII segregation. To evaluate this possibility, strain XII$^{200/200KU}$ *fob1⁻ rpa135Δ* +HP (section 4.5.2) harboring both a *FOB1* disruption and a *RPA135* deletion was assayed. No significant change in the rate of chromosome XII loss was observed when the *FOB1* disruption was incorporated onto the *RPA135* deletion strain (figure 5.15). Together these results suggest that Pol I transcription might impede faithful chromosome segregation, as deletion of *RPA135* results in a low rate of chromosome XII loss, regardless of whether *FOB1* is present or not. These results are in strong contrast to those seen when the rDNA repeats are deleted from chromosome XII (figure 5.1). However, I am unable to distinguish whether these low rates of loss are the result of

deletion of *RPA135* or growth in galactose, as the results from section 5.2.1 show decreased rates of chromosome loss following growth in galactose alone. The possibility that rDNA transcription interferes with proper chromosome XII segregation requires examination by an alternative approach that does not involve measuring the chromosome XII loss rate during growth in galactose.

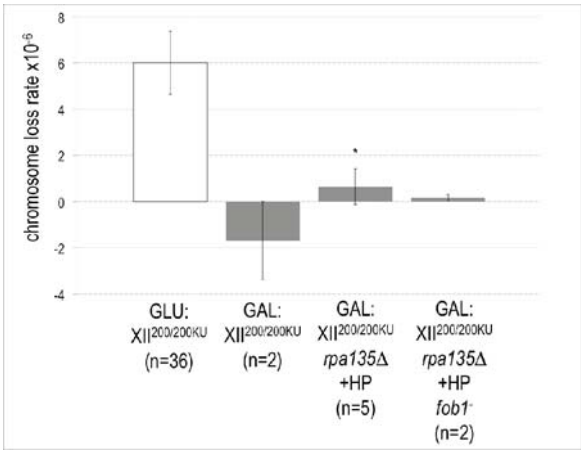

Figure 5.15. Disruption of Pol I transcription results in low rates of chromosome XII loss. The chromosome XII loss rate was measured in galactose (GAL) for strains XII$^{200/200KU}$ *rpa135*Δ +HP and XII$^{200/200KU}$ *rpa135Δ* +HP *fob1*$^{-}$, and compared to the WT strain (XII$^{200/200KU}$) grown in glucose (GLU) and galactose (GAL). The loss rate was lower in all strains grown in galactose, with strain XII$^{200/200KU}$ *rpa135*Δ +HP showing a significant difference to WT (GLU) (p-value: * = 3.96x10^{-2}). Error bars show SE.

Machin et al. (2006) have proposed that transcription of the rDNA creates linkages that can cause chromosome missegregation defects. Since, a haploid 20-copy strain has been reported to have a higher proportion of transcriptionally active rDNA repeats than WT (Dammann et al. 1993; French et al. 2003), our diploid CLA 20-copy strain is also likely to have a high proportion of transcriptionally active repeats. This raises the possibility that unresolved linkages from a high proportion of transcription intermediates in the 20-copy strain can cause the high chromosome XII missegregation rate observed when the rDNA copy number is reduced (figure 5.1). To test if deletion of *RPA135* in a 20-copy strain can restore its missegregation rate, I sought to delete *RPA135* in the 20-copy strain. However, creation of such strain proved challenging and could not be completed (section 4.5.3).

I was also interested in investigating the rate of chromosome missegregation when Pol I is inactivated in an rDNA deletion background. Since there are no chromosomal rDNA repeats in this strain, there is no active transcription by Pol I, so any effect from inactivation of Pol I in this strain would suggest a functional role of Pol I in chromosome segregation distinct from rDNA transcription. Our approach was to delete *RPA135* in an rDNA deletion strain. However, attempts to create a double deletion strain with no *RPA135* and no chromosomal rDNA repeats

were unsuccessful (section 4.5.4). Therefore, it is possible that deletion of both the chromosomal rDNA repeats and *RPA135* is synthetically lethal. Regardless, I was unable to determine whether rDNA transcription or another role of Pol I is responsible for the chromosome segregation phenotype seen in the *rpa135Δ* strain.

5.3.1 Estimating the transcription level in diploid strains

It remains a possibility that Pol I transcription linkages interfere with segregation of the rDNA locus. Potentially, the 20-copy strain with a higher proportion of transcriptionally active rDNA repeats, has more linkages to resolve to be able to achieve faithful chromosome segregation. Hence, I next wanted to examine the relative proportion of transcriptionally active and inactive rDNA repeats in our WT and 20-copy diploid strains. Previous work has estimated the proportion of actively transcribed rDNA copies for haploid yeast strains (Dammann et al. 1993; French et al. 2003), but not for diploids. I used a psoralen crosslinking assay to determine the proportion of active/inactive rDNA repeats. Psoralen is a UV-absorbing compound, able to access the transcriptionally active rDNA repeats in open chromatin structure, but not the inactive repeats in compacted chromatin state in nucleosomes. Crosslinked transcriptionally active and inactive rDNA repeats can be distinguished in a Southern blot using an rDNA specific probe because they migrate at different rates (Conconi, 1989; Dammann et al. 1993; Sanij et al. 2008). This is visualized by extracting gDNA after psoralen crosslinking and digesting the gDNA into smaller fragments to be separated by gel electrophoresis.

I first tested the WT strain XII$^{200/200KU}$ to optimize the psoralen crosslinking assay conditions. This involved using different distances from the UV light source (from 1.5 cm to 7 cm) and varying the times of continuous exposure to the UV light (from several minutes to hours). Cross-linked extracted DNA from each condition tested was subjected to a Southern blot using an rDNA probe, but the signal from bands corresponding to ‘active’ and ‘inactive’ rDNA genes was not clear on the membrane (figure 5.16A). The shortest exposure (20 min) was not sufficient to show crosslinking of active repeats, and the longest exposure (5hr) showed unspecific crosslinking even in the absence of psoralen (figure 5.16B). Several other attempts to optimize psoralen crosslinking were performed (not shown), but I was unable to establish this protocol successfully.

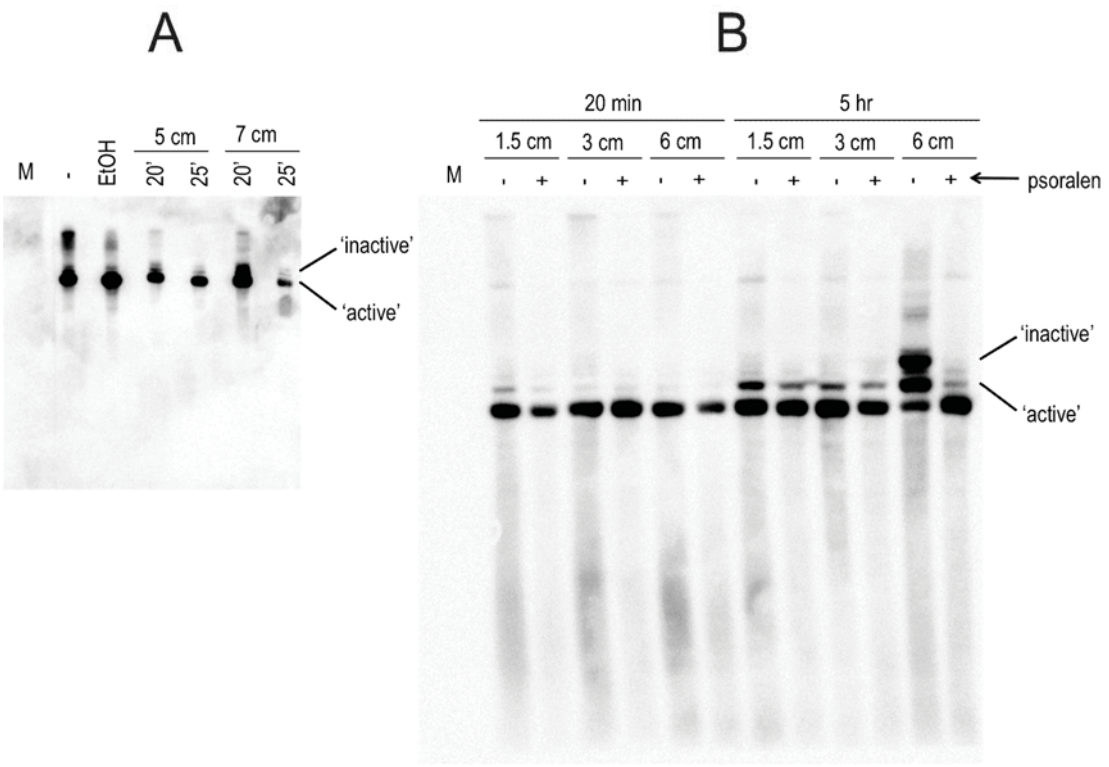

Figure 5.16. Psoralen crosslinking assay to determine the proportion of active/inactive rDNA repeats. Exponentially growing cells from the WT strain XII$^{200/200KU}$ were used to test different psoralen crosslinking conditions. After treatments using 200mg/ml psoralen and a 365nm UV light source, DNA was extracted from each sample, digested with *Eco*RI and separated by gel electrophoresis, before being subjected to Southern blotting using an rDNA probe. (**A**) – (negative control; untreated and not exposed to UV), EtOH (negative control; treated with ethanol and irradiated 5 cm away from the UV light source for 25min), and all other samples were irradiated at a distance of 5 or 7 cm (as indicated) continuously for 20 min or 25 min (as indicated) with the addition of psoralen every 5 min. (**B**) – (negative controls; treated with ethanol and irradiated 1.5, 3 or 6 cm away from the UV light source for the indicated times), + (samples were UV exposed at a distance of 1.5, 3 or 6 cm and irradiated continuously for 20 min (with the addition of psoralen every 5 min) or 5 hr (with the addition of psoralen every 1 hr). The expected positions of the bands representing transcriptionally active and inactive repeats, based on size from the marker (M), are indicated.

5.4 HETEROZYGOSITY RESCUES THE CHROMOSOME XII SEGREGATION DEFECTS

Up until now, I have only analyzed the effects of homozygous rDNA alterations on chromosome XII segregation. Homologous chromosomes are thought to segregate independently of each other in mitosis; therefore each chromosome homolog is expected to behave according to its own rDNA state. To test this, I made strains that are heterozygous for rDNA alterations. I created these strains as reciprocal pairs, where one chromosome XII

homolog is tagged in one strain, and the other homolog is tagged in the other strain. For example, strain XII$^{200/0KU}$+HP (section 4.6.1) is heterozygous for the rDNA deletion, with the CLA markers on the rDNA deletion homolog, while strain XII$^{0/200KU}$+HP (section 4.6.1) is also heterozygous for the rDNA deletion, but carries the CLA markers on the WT rDNA array homolog. When I tested these strains using the CLA, the WT homolog in strain XII$^{0/200KU}$+HP segregated with the same fidelity as it did in the WT homozygous strain, as expected (figure 5.17). Surprisingly, however, the chromosome XII loss rate in the reciprocal strain (XII$^{200/0KU}$+HP) was significantly decreased when compared to the homologous rDNA deletion strain (XII$^{0/0KU}$+HP), and is similar to the rate seen for the WT rDNA homolog in the heterozygous strain and the WT homozygous strain. This shows that the rDNA deletion homolog does not segregate with the fidelity expected from its rDNA state in a heterozygous strain, and instead the presence of a WT length rDNA array on the opposite homolog somehow confers a positive effect on chromosome XII segregation fidelity.

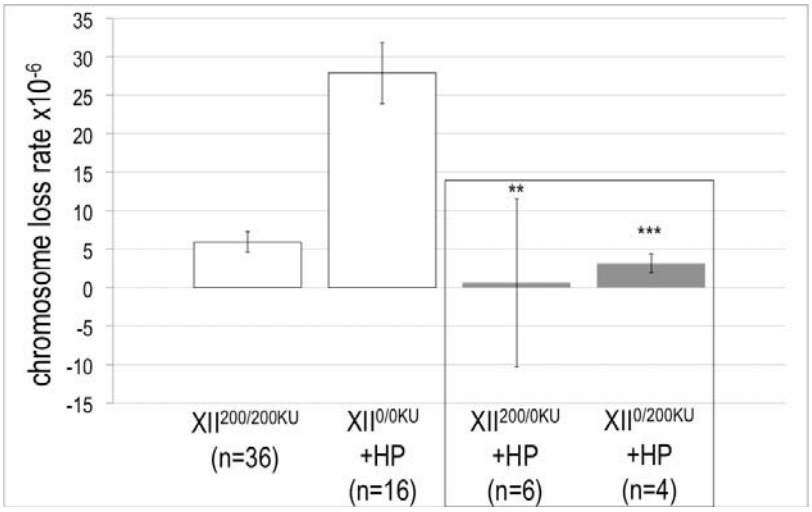

Figure 5.17. Heterozygosity of the rDNA deletion rescues the segregation defect of the rDNA deletion strain. The chromosome XII loss rate was measured in heterozygous strains XII$^{200/0KU}$+HP and XII$^{0/200KU}$+HP (boxed). The chromosome XII loss rates for both heterozygous strains are significantly lower than that seen for the homozygous rDNA deletion strain (XII$^{0/0KU}$+HP) (p-values: **=4.03x10^{-2}, ***=7.87x10^{-3}), but are not significantly different to each other or that of the WT strain (XII$^{200/200KU}$). Error bars show SE.

I next wanted to see whether the surprising rescue effect of rDNA state heterozygosity would hold true for the other rDNA alterations from section 4.6. Therefore, I examined a pair of strains heterozygous for 200 and 20 copies of the rDNA (section 4.6.2), with the CLA markers on each homolog: XII$^{20/200KU}$ *fob1*$^{-}$ and XII$^{200/20KU}$ *fob1*$^{-}$. These strains are homozygous for *FOB1* disruption to ensure maintenance of the 20-copy state on a single homolog. Interestingly, the chromosome XII segregation rate was similar for the two strains, with both

homologs segregating with similar chromosome segregation fidelities as each other and as a WT homozygous strain (figure 5.18). Both strains exhibited a significantly lower rate of chromosome loss when compared to their 20-copy homozygous counterpart and to the homozygous WT length rDNA array strain with a *FOB1* disruption (figure 5.18). Both these results support the conclusion that heterozygosity of a WT length rDNA array provides a beneficial effect for the segregation fidelity of homologs with rDNA alterations, and reveal that this protective effect extends to the absence of Fob1.

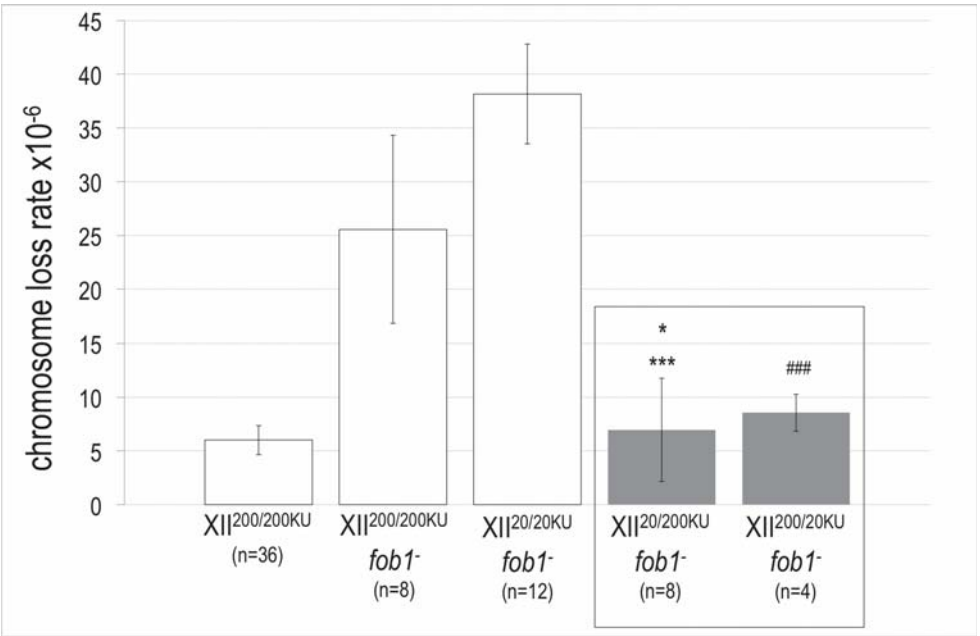

Figure 5.18. Heterozygosity of a 20-copy rDNA array rescues the segregation defect of the 20-copy strain. The chromosome XII loss rate was measured in heterozygous strains XII$^{20/200KU}$ *fob1-* and XII$^{200/20KU}$ *fob1-* (boxed). The chromosome loss rate for both heterozygous strains is significantly lower than that seen for the homozygous 20-copy (XII$^{20/20KU}$ *fob1-*) (p-values ***=2.14x10^{-3} and ###=3.29x10^{-3}) and the *fob1-* (XII$^{200/200KU}$ *fob1-*) (p-value *=9.74x10^{-2}) strains, but are not significantly different to each other or the WT strain (XII$^{200/200KU}$). Error bars show SE.

5.5 rDNA STATE AFFECTS GLOBAL CHROMOSOME SEGREGATION

Our data shows that the presence of the rDNA gene repeats aid faithful chromosome XII segregation, that absence of *FOB1* and length reduction of the rDNA array hinder it, and that rDNA heterozygosity confers a protective effect against chromosome segregation defects caused by rDNA alterations. Unexpectedly, the rate of missegregation in heterozygous strains

is independent of whether the tested homolog has an altered rDNA state or not. Given that there is no known association of homologs during mitotic segregation in yeast, these results raise the possibility that the rDNA has a global effect on chromosome segregation. To test this, I examined the missegregation rate of another chromosome in strains harboring the rDNA alterations tested with chromosome XII. I chose chromosome VI because preliminary work in our group showed that chromosome VI exhibits the highest missegregation rate of all the chromosomes tested (Seo, Quintana and Ganley, unpublished results), potentially allowing to more easily measure both increases and decreases in the missegregation rate.

5.5.1 rDNA alterations affect the segregation of chromosome VI

To test whether the deletion of the rDNA gene repeats or a reduction in their copy number affect the segregation of other chromosomes, the missegregation rate of chromosome VI was examined in rDNA deletion and 20-copy strains. Strains $VI^{0/0KU}$ $XII^{0/0}$+HP and $VI^{0/0KU}$ $XII^{20/20}$ *fob1-* (section 4.7.2) had CLA markers inserted on chromosome VI (described in section 4.7.1), and their missegregation rates were measured using the CLA. Strikingly, a significant increase in the loss of chromosome VI was observed when the rDNA array was deleted, and when it was reduced to 20-copies (figure 5.19). These effects on chromosome loss closely resemble those seen for chromosome XII: deletion of the rDNA results in a ~5-fold increase in the rate of chromosome XII loss and a ~7-fold increase in the rate of chromosome VI loss, while reduction to 20 rDNA copies results in a ~6-fold increase in the rate of chromosome XII loss and a ~5-fold increase in the rate of chromosome VI loss (figure 5.19). The similar effects of these rDNA alterations on the loss rates for both chromosome XII and VI suggests that the rDNA does not just influence the segregation of the chromosome that carries the rDNA repeats, but rather that it has a global effect on chromosome segregation.

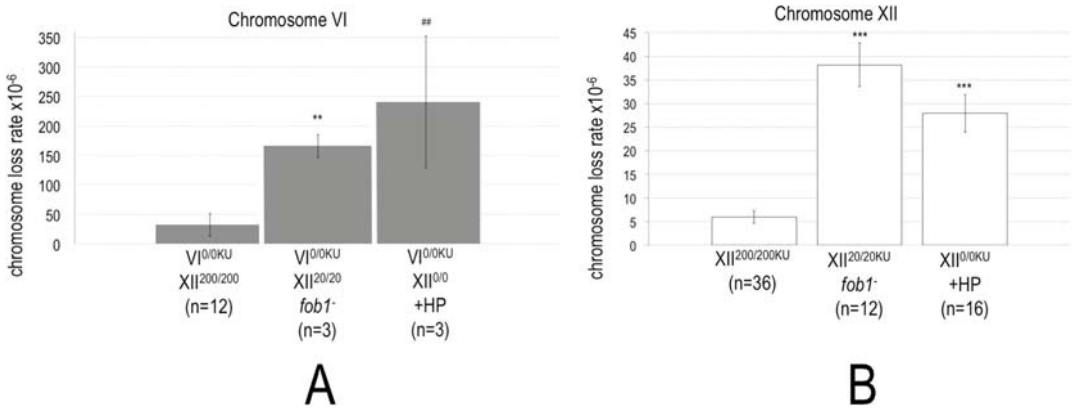

Figure 5.19. rDNA alterations affect chromosome VI segregation. (**A**) The chromosome VI loss rate was measured in the 20-copy strain ($VI^{0/0KU}$ $XII^{20/20}$ *fob1*-) and the rDNA deletion strain ($VI^{0/0KU}$ $XII^{0/0}$ +HP), and compared to the WT strain ($VI^{0/0KU}$ $XII^{200/200}$). Missegregation of chromosome VI was found to be significantly increased for both these rDNA alterations relative to WT (p-values **=$1.7x10^{-2}$ and ##=$1.7x10^{-2}$). (**B**) The results of the equivalent strains monitoring chromosome XII loss from figure 5.1 are shown for comparison. For both graphs, error bars show SE.

To investigate whether the rescue of chromosome XII segregation defects observed for heterozygosity of rDNA state extends to other chromosomes, I measured the missegregation rate of chromosome VI in strains heterozygous for rDNA alterations on chromosome XII ($VI^{0/0KU}$ $XII^{200/0}$+HP and $VI^{0/0KU}XII^{20/0}$ *fob1*-, section 4.7.3). Strikingly, the rates of chromosome VI loss in the heterozygous strains $VI^{0/0KU}$ $XII^{200/0}$+HP and $VI^{0/0KU}XII^{20/0}$ *fob1*- are similar to those seen in the WT strain (figure 5.20), and are much lower than the 20-copy and rDNA deletion strains. The small sample sizes that were used to test these heterozygous strains mean that although the average loss rate is much lower than that of the WT, the difference between the homozygous and heterozygous chromosome loss rates is not statistically significant. Nevertheless, the pattern clearly resembles that seen for the chromosome XII loss rates and suggests that heterozygosity of rDNA state is able to rescue defects in global chromosome segregation.

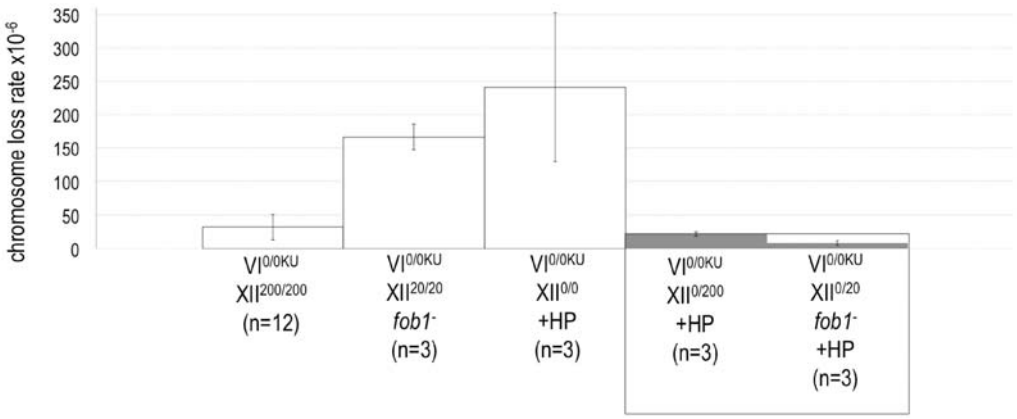

Figure 5.20. rDNA state heterozygosity rescues segregation of chromosome VI. The chromosome VI loss rate was measured in strains VI$^{0/0KU}$ XII$^{0/200}$+HP and VI$^{0/0KU}$ XII$^{0/20}$*fob1*$^{-}$+HP (boxed) that are heterozygous for rDNA alterations, and compared to the WT (VI$^{0/0KU}$ XII$^{200/200}$), the 20-copy (VI$^{0/0KU}$ XII$^{20/20}$ *fob1*$^{-}$), and the rDNA deletion (VI$^{0/0KU}$ XII$^{0/0}$+HP) strains. The rates of chromosome VI loss of the heterozygous strains (boxed) are similar to that of the WT, but not significantly different to the homozygous 20-copy and rDNA deletion strains (p-values 0.8 and 0.6 respectively). Error bars show SE.

5.5.2 Heterozygous translocation of an rDNA array onto chromosome V exerts a protective effect on chromosome XII segregation.

Heterozygous rDNA alterations on chromosome XII have a global chromosome segregation effect (section 5.5.1). However, I have shown that Fob1 influences chromosome segregation directly through the rDNA repeats regardless of their chromosomal location. Hence, it is possible that the genomic location of the rDNA array itself may influence its local and global chromosome segregation effects. To examine this, I used a set of rDNA array translocation strains created by Oakes et al. (2006), and introduced CLA markers onto chromosome XII. The translocated rDNA arrays carry a point mutation in the rRNA coding region that confers resistance to hygromycin. To verify that this point mutation has no effect on chromosome XII segregation, the chromosome loss rate of strain XII$^{200/200*KU}$ (where the asterisk indicates the array harbors the hygromycin resistance mutation, section 4.8.1) was determined. A similar missegregation rate to the WT XII$^{200/200KU}$ strain was observed (figure 5.21), indicating that the hygromycin mutation does not affect the chromosome loss rate.

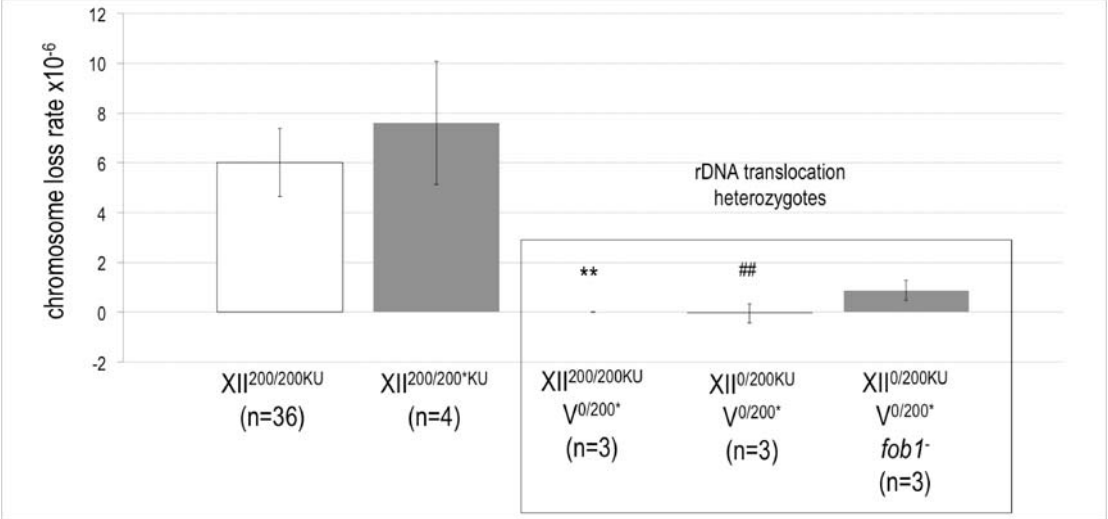

Figure 5.21. Translocation of an rDNA array onto chromosome V improves the rate of chromosome XII loss. The chromosome XII loss rate was measured in strains carrying a translocated rDNA array on one chromosome V homolog (boxed strains). A WT strain with a hygromycin resistant rDNA array ($XII^{200/200*KU}$) has a similar chromosome XII loss rate as WT ($XII^{200/200KU}$). Strains heterozygous for a translocation of the rDNA onto chromosome V show a significantly lower chromosome XII loss rate compared to WT both when chromosome XII is homozygous ($XII^{200/200KU}$ $V^{0/200*}$) or heterozygous ($XII^{0/200KU}$ $V^{0/200*}$) for the presence of the rDNA array (p-values: **= 2.51x10-2, ##= 2.86x10-2.). Disruption of *FOB1* in the double heterozygote strain ($XII^{0/200KU}$ $V^{0/200*}$ *fob1-*) results in a similar rate of chromosome XII loss, although the small sample size means the difference to WT is not statistically significant. Error bars show SE.

I next examined strain $XII^{200/200KU}$ $V^{0/200*}$ (section 4.8.2), which is heterozygous for an rDNA translocation onto chromosome V, and is homozygous for the rDNA on chromosome XII. Interestingly, this strain showed a significantly reduced chromosome XII loss rate when compared to WT (figure 5.21). This reduction might be due to the presence of a third rDNA array improving chromosome XII segregation fidelity. To test this, I evaluated the effect that translocating an rDNA array onto chromosome V has on chromosome XII missegregation in the absence of one of the arrays on chromosome XII ($XII^{0/200KU}$ $V^{0/200*}$+HP, section 4.8.2). No difference in chromosome XII loss rate was observed when compared to the translocation strain with two chromosome XII rDNA arrays (figure 5.21), suggesting that heterozygosity of the rDNA in any chromosome can exert a protective effect on the segregation of chromosome XII. Further disruption of *FOB1* from the double heterozygous strain ($XII^{0/200KU}$ $V^{0/200*}$ *fob1-* +HP, section 4.8.2) results in an additional increase in chromosome XII segregation (figure 5.21). These findings are consistent with the results from section 5.20 showing that heterozygosity of rDNA alterations on chromosome XII result in an improved rate of chromosome segregation, even in a *fob1-* background.

5.5.3 Translocation of an rDNA array onto chromosome V increases its loss rate.

I have shown that heterozygosity of rDNA alterations on an ectopic site on chromosome V (section 5.5.2) can exert a protective effect on chromosome XII segregation. Since heterozygosity of rDNA alterations on chromosome XII can affect both local and global chromosome segregation (section 5.5.1), I next wanted to examine whether the ectopic rDNA can also exert this 'protective' effect on its own segregation, ie. the chromosome it has been inserted into. To test this, I used heterozygous strains similar to the ones from section 5.2.2, but with the CLA markers on the chromosome V homolog that also carries the translocated rDNA array. First, I tested whether the translocated rDNA array had any effect on chromosome V missegregation. The chromosome V loss rate of strain $V^{0/*200KU}$ $XII^{200/200}$ (section 4.8.3) was similar to WT (figure 5.22). However, this strain has an additional rDNA array compared to WT, so to remove the influence a third rDNA array may have on chromosome segregation, I examined strains that had two rDNA arrays i.e. that are heterozygous for the presence of the rDNA array on both chromosomes V and XII (figure 5.13). The increased chromosome V loss rate of these strains (figure 5.22) suggests that heterozygosis of an ectopic rDNA array may exert a negative effect on chromosome V segregation rather than protective as in the case of chromosome XII, and this negative effect appears to be exacerbated in the absence of Fob1. Moreover, removal of the third rDNA array caused an increase in chromosome V segregation, suggesting that the presence of a third rDNA array is beneficial.

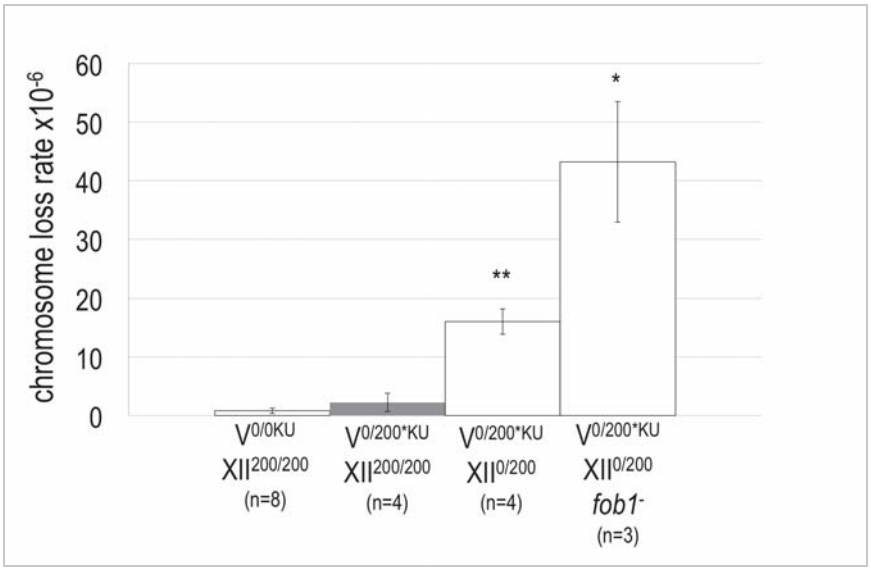

Figure 5.22. Translocation of an rDNA array onto chromosome V increases its rate of loss. The chromosome V loss rate was measured in strains heterozygous for an rDNA translocation onto chromosome V. Heterozygous chromosome V rDNA translocation strains show a similar chromosome V loss rate

to WT ($V^{0/0KU}$ $XII^{200/200}$), when chromosome XII is unaltered ($V^{0/200*KU}$ $XII^{200/200}$). However, there is a significantly higher chromosome V loss rate when the presence of the rDNA array on chromosome XII is also heterozygous ($V^{0/*200KU}$ $XII^{0/200}$), and this effect is enhanced by disruption of *FOB1* ($V^{0/*200KU}$ $XII^{0/200}$+HP *fob1*-). p-values relative to WT are **= $4x10^{-3}$ and *=$1.2x10^{-2}$. Error bars show SE.

These results are surprising, as heterozygosity of the rDNA on chromosome XII was not sufficient to confer a low missegregation rate to a strain heterozygous for the rDNA on chromosome V, despite our results showing that heterozygosity has a global effect on chromosome segregation (figures 5.20 and 5.21). Also, the fact that chromosome XII rDNA heterozygosity and *FOB1* disruption have different effects on missegregation of chromosome V versus chromosome XII suggests that this is an oversimplification.

CHAPTER SIX: DISCUSSION

[blank page]

This study aimed to determine the effects of the rDNA repeats on chromosome segregation by measuring the chromosome loss rate of strains harboring different rDNA alterations and/or disruption of candidate genes**.** This aim was achieved through the development of an optimized mitotic yeast chromosome loss assay (CLA) and the construction of CLA specifically tailored strains (chapters three and four respectively). My results (chapter five) show two beneficial effects from the rDNA on chromosome segregation. The first is a local effect, with faithful segregation of the rDNA-containing chromosome (normally chromosome XII) specifically mediated by Fob1 directly through the rDNA repeats. The second is a global effect, with rDNA alterations on chromosome XII affecting the segregation of other chromosomes, and with heterozygosis of rDNA state instigating a novel protective role on chromosome segregation.

6.1 *FOB1* MEDIATES A LOCAL EFFECT OF THE rDNA ON CHROMOSOME SEGREGATION

The main focus of this study was to test the effects of the rDNA array on mitotic chromosome segregation in *S. cerevisiae*. The unique properties of the rDNA in regards to replication, recombination and transcription, and spatial nucleolar compartmentalization, as well as the frequency of human genetic disorders arising from missegregation of the rDNA-containing chromosomes (Hassold et al. 2007), led us to propose that the rDNA locus impedes faithful chromosome segregation. My findings show that while the rDNA does influence chromosome segregation, the presence of the rDNA repeats is actually beneficial in yeast, as deletion of the rDNA array results in an increased rate of chromosome XII loss (figure 5.1). These results suggest that one or more of the unique properties of the rDNA may cooperate to maintain faithful mitotic chromosome XII segregation.

One of the major conclusions of this study is that the rDNA affects segregation fidelity of the rDNA-containing chromosome. The effect was revealed by results showing that the absence of Fob1 causes a significant increase in the rate of chromosome XII loss compared to WT (figure 5.1), similar to the effect seen when the rDNA repeats are reduced or deleted from the chromosome. However, in complete contrast to these rDNA alterations (figure 5.19), the missegregation rate of chromosome VI is not affected by the absence of Fob1 (figure 5.12).

Although this suggests that the effect observed from disruption of *FOB1* is restricted to chromosome XII and not a global chromosome segregation effect, I cannot rule out the segregation rate other chromosomes being affected by Fob1. Nevertheless, other results from our laboratory show that chromosome V segregation fidelity is also not affected by Fob1 disruption, strengthening the conclusion that the effect I observe is chromosome XII specific. In addition, my results suggest that this effect is exerted directly through the rDNA repeats, as the segregation fidelity of an independent chromosome only becomes sensitive to the absence of Fob1 when an rDNA array is translocated onto that chromosome (figure 5.13). Therefore my work has defined a new role for the rDNA in mitotic chromosome segregation. Fob1 mediates this role and works directly through the rDNA repeats to improve the segregation fidelity of the chromosome carrying the rDNA.

Fob1 is a nucleolar protein that directly binds to the rDNA replication fork block (RFB) site and is necessary for replication fork blocking and recombinational hotspot activity (Kobayashi et al. 1992; Kobayashi and Horiuchi 1996; Kobayashi et al. 2001), condensin recruitment at the rDNA locus (Johzuka et al. 2006), and recruitment of chromatin modifying factors to the rDNA (Huang and Moazed 2003; Huang et al. 2006). These Fob1 functions suggest three possible mechanisms by which Fob1 may aid faithful segregation of the rDNA repeats (figure 6.1). The first is that Fob1 may aid faithful chromosome segregation by stimulating rDNA recombination, with recombination intermediates possibly helping to maintain the structural stability of the long rDNA locus. Second, Fob1 recruits condensin to the rDNA locus and condensin association has been shown to be enriched at the rDNA during anaphase (Johzuka et al. 2006). Since condensin is known to establish intra-chromatid linkages in preparation for sister chromatid resolution (D'Ambrosio et al. 2008b), Fob1 may aid faithful chromosome segregation by promoting a timely condensation of the rDNA repeats. Third, Fob1 has been shown to mediate recruitment of chromatin modifying factors as a part of the RENT complex (Huang and Moazed 2003), including the rDNA Pol II silencing factor, Sir2 (Wierman and Smith 2014). Absence of this machinery due to the disruption of *FOB1* may alter the chromatin structure at the rDNA locus and impact its chromosome segregation fidelity. Despite these three possible mechanisms, I cannot rule out that more than one of Fob1's roles affects chromosome segregation, so the mechanism by which Fob1 mediates faithful chromosome segregation remains to be dissected.

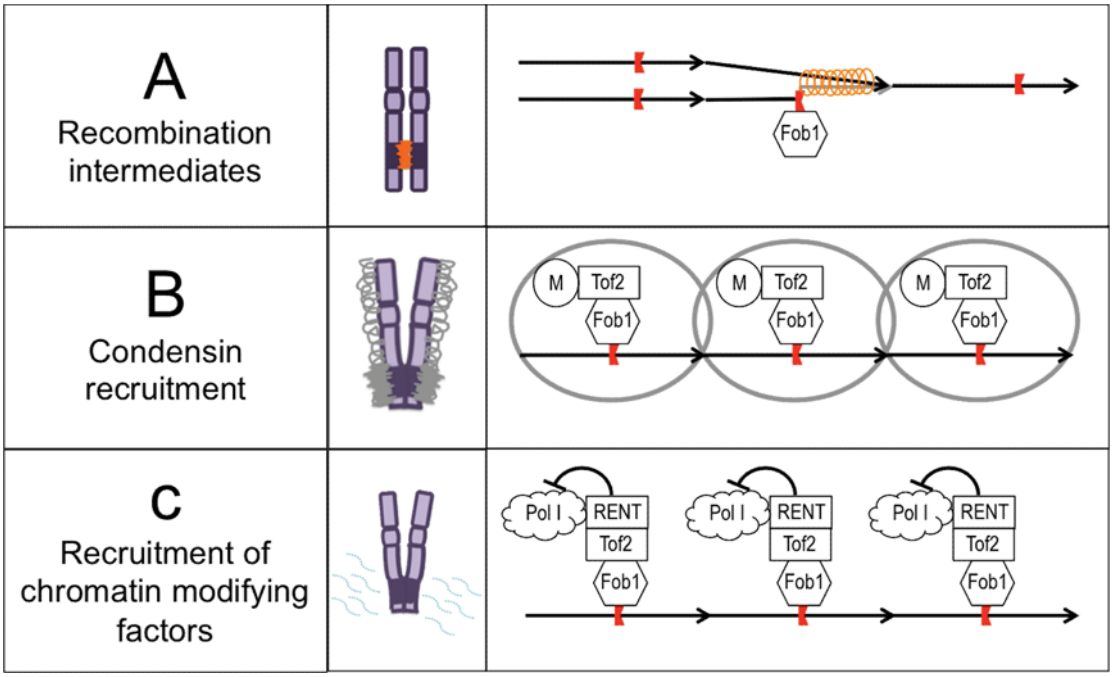

Figure 6.1. Potential mechanisms of Fob1-mediated chromosome segregation at the rDNA locus. There are three possible mechanisms by which Fob1 may aid faithful segregation of the rDNA repeats. (A) The first is through its role in rDNA recombination, where establishment of recombination intermediates (represented in orange) may help maintain the stability of the rDNA locus for faithful segregation. Recombination intermediates are a consequence of repair of Fob1-induced DSBs. (B) The second is that Fob1 may promote timely condensation of the rDNA repeats by recruiting condensin (represented in grey) to the rDNA locus. Association of condensin with the rDNA is Fob1 dependent and mediated by Tof2 and the monopolin complex (M, Lrs4 and Csm1) (Johzuka et al. 2006). (C) The third is through its role in recruiting the RENT complex (Sir2, Cdc14, and Net1) (Huang and Moazed 2003) that inhibits transcription (dotted rRNA transcripts depicted in blue indicate inhibition of transcription) by establishing a repressive chromatin state. This compact chromatin structure at the rDNA locus may facilitate faithful chromosome segregation. Cartoons (center panel) represent sister chromatids with traits mediated by Fob1. Figures on the right illustrate the association of specific factors with the rDNA repeats through Fob1 mediated interactions, with each black arrow representing a rDNA unit and the direction of transcription, and the red icon representing the RFB site.

6.1.1. An excess of Fob1 may be detrimental to chromosome segregation

A WT strain grown in glucose has an increased chromosome loss rate when it contains pGAL-*FOB1* (figure 5.7). Under these growth conditions, *FOB1* expression from the plasmid is expected to be repressed. However, RT-PCR results showed leaky expression from pGAL-*FOB1* to a level higher that WT (without the plasmid) (figure 5.10). Thus, overexpression of Fob1 may be detrimental to chromosome XII segregation. Since Fob1 is an important mediator of chromosome segregation through the rDNA repeats, and both its absence and overexpression cause an increase in chromosome XII loss rate, this suggests that there is an optimal Fob1 ratio needed for the faithful segregation of the rDNA. A better understanding of

the mechanism by which Fob1 aids faithful segregation of the rDNA repeats will help explain why the Fob1 effect may be dosage dependant. A recent study by Menzel et al. (2014) reports that strains that overexpress Fob1, which they have shown is an unstable protein with a very fast turnover, have an increased rDNA recombination frequency and potentially higher genomic instability. This suggests that Fob1 overexpression in the CLA strains carrying pGAL-*FOB1* may also have an increased rDNA recombination. Thus, one possibility is that Fob1 overexpression leads to an increase in recombination intermediates at the rDNA locus, which may create recombination linkages between sister chromatids. Removal of a surplus of recombination linkages may delay and reduce faithful chromosome segregation.

Additionally, my results show that in the absence of rDNA, the chromosome XII loss rate is significantly higher when *FOB1* is present (figure 5.11). In the rDNA deletion strain there are no chromosomal rDNA repeats, and the helper plasmid that supports the strains viability does not have an RFB site. Thus, all Fob1-dependent interactions to the RFB site in this strain must be disrupted, affecting the recruitment and distribution of other rDNA-specific epigenetic factors in the cell, such as cohesin, condensin and the RENT complex. It remains to be determined whether Fob1 is expressed at constitutive levels in the rDNA deletion strain, and where it is localized in the absence of RFB sites (in the rDNA deletion strain). Nonetheless, Fob1 presence worsening chromosome segregation when the rDNA repeats are absent, further supports the notion that Fob1 mediates beneficial chromosome segregation directly through the rDNA repeats.

6.2 THE RIBOSOMAL DNA GENE REPEATS ARE BENEFICIAL FOR GLOBAL CHROMOSOME SEGREGATION

In addition to revealing a role for the rDNA repeats in local chromosome segregation, my results reveal a beneficial effect on global mitotic chromosome segregation from the unaltered presence of the rDNA repeats at their native locus (section 5.5). I found that deleting the rDNA array or shortening the length of the rDNA array both increase the missegregation rate of chromosome XII (the rDNA containing chromosome), as well as that of a non-rDNA containing chromosome, chromosome VI. Interestingly, the magnitude of the effects these rDNA alterations have on chromosome missegregation is similar for both chromosome XII and

chromosome VI (figure 5.19), supporting the conclusion that alterations of the rDNA array influence chromosome segregation globally.

6.2.1 Heterozygosity of rDNA state maintains faithful global chromosome segregation

rDNA heterozygosity findings further support the results from the rDNA deletion and 20-copy strains showing a role for the rDNA in mediating global chromosome segregation fidelity. In rDNA heterozygous strains, the rate of chromosome loss is always low, regardless of whether the rDNA state of the specific homolog has a high or low rate of missegregation when homozygous (section 5.4). It is possible that this observation results from selection operating to bias against the loss of one homolog, thus conferring on heterozygote strains low chromosome missegregation rates despite the rDNA alterations. However, since the aneuploid strains that result from the loss of a heterozygote homolog are in some cases genotypically the same as those resulting from the loss of a homozygous homolog but yet have a different loss rate, it is unlikely that the low rates of loss in the screened heterozygote strains are a result of selection against the loss of a particular homolog. Therefore, while I cannot rule out heterozygosity imposing some general selective disadvantage to aneuploidy independent of the rDNA, I conclude that the most likely explanation of these results is that heterozygosity of rDNA state has a positive effect on global chromosome segregation.

In meiosis, homolog pairing is a fundamental feature of chromosome segregation (Bosco 2012). However association between homologs in mitosis has been identified in only a few special cases in flies and mammals (Apte and Meller 2012; Joyce et al. 2012). Since there is no evidence for mitotic chromosome pairing normally in yeast, and newly replicated sister chromatids are held together by cohesin (Haering et al. 2002) it is unexpected that one homolog can affect the segregation of its corresponding homolog. However, given that the rDNA is able to affect chromosome segregation globally, it is not surprising that the presence of rDNA on one chromosome homolog can influence the faithful segregation of the opposite homolog and of other chromosomes.

rDNA heterozygosis appears to have a protective effect on mitotic chromosome segregation. One explanation for this protective effect is that a single WT rDNA array is sufficient to sustain a normal chromosome missegregation rate. However, results from our group show that this rescue also occurs in strains heterozygous for 20 and 0 copies of the

rDNA (XII$^{0/20KU}$*fob1*$^{-}$+HP and XII$^{20/0KU}$*fob1*$^{-}$+HP, section 4.6.3) (Schischka, Quintana and Ganley, unpublished results), even though each of these rDNA alterations result in elevated chromosome missegregation rates when homozygous. Consistent with the heterozygous strains I tested, the chromosome segregation rate for 20/0 rDNA copy heterozygotes is the same regardless of which chromosome XII homolog is being assayed. These results strongly suggest that heterozygosity of the rDNA state, rather than the presence of a WT rDNA array, promotes faithful chromosome segregation.

The heterozygosis protective effect identified in chromosome XII extends to chromosome VI (figure 5.20), as heterozygosis of rDNA state on chromosome XII is able to rescue chromosome VI segregation defects that arise from chromosome XII homozygous rDNA alterations. Further, the protective effect of heterozygosity is also observed in the absence of factors such as Fob1, which I have shown to affect local chromosome segregation only. Considering that rDNA containing homologs are unlikely to be paired, I speculate that rDNA alterations produce changes in nucleolar structure that influence how chromosomes are organized within the nucleus, and that these changes in global chromosome organization affect the fidelity of chromosome segregation globally.

6.2.2. Growth in galactose affects chromosome segregation.

In this thesis, I used galactose to support growth of *RPA135* deletion mutant strains, and also to induce expression of *FOB1* from pGAL-*FOB1*. Surprisingly, I found that growth in galactose decreases the missegregation rate of chromosome XII, when compared to growth in glucose (figure 5.3). Interestingly, the effect of growth in this carbon source seems to be specific to chromosome XII, since I did not find any difference in the chromosome V or VI loss rates when WT strains were grown in glucose versus galactose. In contrast, Runge et al. (1991) report that diploid KR100 yeast cells have higher chromosome III and VII loss rates, and larger variations in the loss rates, when grown in galactose medium compared to glucose. The reasons for these discrepancies are not clear, but the influence of galactose on chromosome segregation may be chromosome-specific, or may vary between yeast strains.

My observations suggest that, because growth in galactose specifically affects chromosome XII like *FOB1* disruption, galactose may have an effect on some aspect of Fob1's function. However, unlike Fob1 disruption, the galactose-induced reduction in chromosome XII loss rate appears to be dominant over the rDNA alterations and other genetic modifications I

examined. Growth in galactose also resulted in decreased growth rates (figure 5.4), and galactose growth has been shown to activate stress response transcription factors such as Msn2 and Msn4 (Lai et al. 2005). These mediate the response of genes associated with the remodeling of reserve energy and catabolic pathways when cells are shifted to anaerobic conditions, including rRNA processing genes. It is possible that galactose-induced down-regulation of rRNA processing may lead to chromatin structure changes at the rDNA, and that these changes, possibly combined with a slower cell cycle progression, result in improved chromosome segregation fidelity. This possibility is supported by observations that the nucleolus is physically disrupted when yeast cells are grown in galactose (Harris et al. 2014). Alternatively, metabolic changes, that result from the transcription-dependent relocalization of genes within the nucleus (Berger et al. 2008) may cause changes in nuclear architecture that indirectly affect chromosome segregation. Nonetheless, it remains a possibility that a slow cell cycle progression alone, such as that observed for strains grown in galactose versus glucose, provides strains prone to chromosome missegregation with sufficient time to correct segregation errors that arise.

6.3 THE rDNA CAN INFLUENCE LOCAL AND GLOBAL CHROMOSOME SEGREGATION FROM AN ECTOPIC LOCATION

Since the rDNA has the potential to affect local and global chromosome segregation from its native locus on chromosome XII, I wanted to evaluate whether its chromosomal location can influence these effects. I used strains carrying an rDNA array translocated onto chromosome V in a heterozygous state. I found that double heterozygosity of the rDNA state in both chromosomes V and XII also exerts a protective effect on chromosome XII segregation fidelity (figure 5.21), but exerts a negative effect on chromosome V segregation fidelity (figure 5.22). However, heterozygosis of the translocated array in the presence of a homozygous WT rDNA array on chromosome XII did not affect the loss rate of chromosome V (figure 5.22). Heterozygosity of rDNA state on chromosome XII resulted in WT rates of chromosome VI loss, even when chromosome XII is heterozygosis for 20 and 0 rDNA copies (figure 5.20). This is despite the fact that each of these rDNA alterations in the homozygous state on chromosome XII increase the chromosome VI loss rate. However, the fact that heterozygosity of rDNA state

on chromosome XII did not result in normal chromosome V missegregation rates when chromosome V was also heterozygous for rDNA state suggests that the chromosome in which the rDNA is located may influence rDNA-mediated global chromosome segregation.

It is possible that when there are two native arrays on chromosome XII and one ectopic array, the ectopic translocation array may not be used (i.e. is transcriptionally inactive) and hence this ectopic array is able to segregate normally. In contrast, the strain heterozygous for the rDNA on both chromosomes V and XII, which has been reported to transcribe rRNA from both the native and ectopic arrays and to have a small shift in the position of the nucleolus but with unaffected Pol I transcription (Oakes et al. 2006), affects chromosome organization through the relocation of chromosome V into the nucleolus, resulting in changes to chromosome territories. In support of this, the haploid version of the rDNA translocation strain exhibits a chromosome V centromere closer to the nucleolus than WT (Oakes et al. 2006), indicating nuclear rearrangement as a consequence of the ectopic rDNA array. Taken together, these findings suggest that the global effect of the rDNA on nuclear structure may depend on the number and activity of rDNA arrays present in the cell and also on their location.

6.4. POTENTIAL MECHANISMS OF rDNA MEDIATED GLOBAL CHROMOSOME SEGREGATION

My work has shown that the rDNA influences faithful chromosome segregation, but the mechanism by which it mediates this is unknown. I consider three possible mechanisms for rDNA-mediated chromosome segregation: an effect of changes in ribosome biogenesis, an effect of chromosome size, and an effect of changes in nucleolar architecture. My work provides evidence to rule out the first two mechanisms, and therefore I propose that alterations in nucleolar structure lead to changes in nuclear architecture that are responsible for the influence of the rDNA on global chromosome segregation.

6.4.1 Global chromosome segregation defects are unlikely to be mediated by changes in ribosome biogenesis

The rDNA genes are essential for ribosomal biogenesis, therefore it is possible that the rDNA alterations assayed in this study might affect rRNA transcription, hence affecting ribosome biogenesis and causing an overall decrease in protein synthesis that impacts the fidelity of chromosome segregation (Shah et al. 2013). However, both the rDNA deletion and the 20-copy (with 40 rDNA gene copies in total as a diploid) homozygote strains exhibited growth rates similar to that seen for the WT (figure 4.13), in contrast to observations of a 20-copy haploid strain that grows more slowly than WT (Takeuchi et al. 2003). The lack of detectable changes in the growth rates of the CLA strains harboring rDNA alterations suggests there are no dramatic effects on protein synthesis. Critically, work subsequent to this thesis shows that a heterozygous strain harboring one chromosome XII homolog with 20 rDNA copies and the other with no rDNA copies has a WT rate of chromosome missegregation and also has WT growth rate (Schischka, Quintana, Woods and Ganley, unpublished results). Finally, the chromosome missegregation rate of the *RPA135* deletion strain, which is predicted to have similar impairment of ribosome biogenesis as an rDNA deletion strain, was indistinguishable from the rate of the WT strain grown in galactose, although this result may be confounded by the effect of growth in galactose. Nevertheless, more direct methods to assess ribosome production/protein translation could be used to rule out an effect of ribosome biogenesis. Such methods include measuring the levels of rRNA production (through quantification of 45S rRNA), or measuring the levels of overall protein synthesis (e.g. by supplying labeled amino acids to growing cell cultures for incorporation into proteins) (Selbach et al. 2008). These methods may allow the detection of translational stress that does not affect growth rate but may still affect chromosome segregation due to subtle changes in protein synthesis that result from the rDNA alterations. These potential protein synthesis changes may impact chromosome segregation by affecting the levels of proteins directly involved in chromosome segregation, such as condensin or cohesin.

6.4.2 rDNA alterations do not affect chromosome segregation through changes in chromosome size

Chromosome XII is the longest of the 16 yeast chromosomes, and in its WT state, it is almost double the length of the next largest chromosome (chromosome IV which is 1.5 Mbp). Previous work has shown that the length of chromosome III positively affects the mitotic chromosome segregation rate, with the full-length chromosome (315 kb) and a 150 kb chromosome fragment exhibiting greater segregation stability than 42 and 72 kb chromosome III fragments (Murray et al. 1986). Alterations of the rDNA copy number directly affect the length of chromosome XII, with the 20-copy and rDNA deletion strains having a much shorter chromosome XII than WT (of about a half and a third of its original size respectively). Therefore, it is possible that the effects of rDNA alterations on chromosome segregation are a simple consequence of the change in length of chromosome XII, particularly as it has been suggested that chromosome size and the frequency of mitotic chromosome loss are inversely correlated (Murray et al. 1986; Kumaran et al. 2013).

This possibility is consistent with the chromosome loss rates of the chromosomes in a WT background that were measured in this study. The chromosome loss rate of chromosome VI, the second smallest in the yeast genome (270 kb), was about 30 times higher than the loss rate of chromosome XII, which is the longest chromosome at almost 3 Mb (figure 5.5). Chromosome V, with a length of 576 kb, had the lowest loss rate, and has also been previously reported to undergo aneuploidy rarely (Zang et al. 2002; Rancati et al. 2008). Chromosome V harbors *CIN8*, a gene involved in mitotic spindle function (Dorer et al. 2005). Since an unbalanced stoichiometry of specific proteins affecting mitotic spindle function is sufficient to drive chromosome missegregation in cancer cell lines (Bakhoum et al. 2009), an unbalance of a gene such as *CIN8* could potentially promote chromosome V missegregation due to gene dosage compensation effects. Hence, the rare aneuploidy of chromosome V loss is probably due to reasons unrelated to its size.

However, my other results fail to show the inverse correlation between chromosome size and missegregation rate that is expected if rDNA alterations affect chromosome segregation through changes in chromosome size. In the homozygous strains, although not statistically significant, the 20-copy strain has a higher chromosome XII loss rate than the rDNA deletion strain, with the latter having the shorter chromosome XII (figure 5.1); while the strains heterozygous for rDNA state have different chromosome XII lengths but exhibit the same chromosome missegregation rates (figures 5.17 and 5.18). Hence, for chromosome XII,

changes in the chromosome length from rDNA alterations do not proportionally affect the loss rate. Further, translocation of the rDNA to chromosome V results in a dramatic increase in chromosome size without any significant alteration in chromosome segregation fidelity (figure 5.22). In addition, the low rate of chromosome V missegregation is dependent on the rDNA state at chromosome XII despite no change to chromosome V length (figure 5.19). Together, these observations suggest rDNA alterations do not affect chromosome segregation through changes in chromosome size.

6.4.3 Nucleolar structure changes may be responsible for the influence of the rDNA on global chromosome segregation

The organization of the genome in the nucleus, referred to as nuclear architecture, is dynamic and complex, with chromatin and multiprotein complexes organized in specific compartments (Berger et al. 2008). Nuclear architecture is important because it has been related to gene expression, and so it is considered a central determinant of genome function (Schneider and Grosschedl 2007; Burke and Stewart 2014; Pueschel et al. 2016). The nucleolus is known to localize to the nuclear periphery in *S. cerevisiae* and to have a defined crescent shape nucleolar structure (Smitt et al. 1973). Similarly, chromosomes occupy specific regions within the nucleus, which are referred to as chromosome territories (reviewed in Misteli 2008), and which are believed to be functionally significant (Weipoltshammer and Schofer 2016). Deletion of the rDNA repeats has been shown to cause structural alterations of the nucleolus (Oakes et al. 1993). It is likely that changes that disrupt nucleolar structure also result in changes to global nuclear organization, which may impact the maintenance of chromosome territories and the overall polarity of the nucleus (van Koningsbruggen et al. 2010) (figure 6.2). Changes in chromosome territories have been associated with disease and changes in gene expression (Finlan et al. 2008; Arican-Goktas et al. 2014; Sharakhov and Sharakhova 2015). Therefore, one explanation for the change in chromosome segregation fidelity in the rDNA alteration strains is that the nucleolar changes resulting from these alterations result in reorganization of the nuclear architecture that affects chromosome segregation fidelity. For example, changes in nuclear architecture could affect chromosome segregation if condensation of sister chromatids is impeded because chromosome territories or regions have been relocated to different areas within the nucleus.

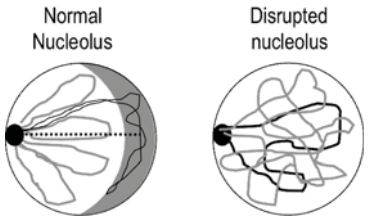

Figure 6.2. Model: Nucleolar structure may impact nuclear polarity and chromosome segregation. The nucleus is depicted with the nucleolus in dark grey, and SPB as a small black circle. Curved lines represent chromosome XII (black) and others (grey) (not to scale). **Normal nucleolus**: In WT cells, the crescent shape nucleolus is located opposite to SPB, maintains already established chromosome territories, and allows chromosome XII to segregate last. We propose that both the nucleolus and SPB serve as anchoring regions that help establish polarized chromosome territories in the nucleus and maintain chromosome segregation fidelity. Black dashed line represents the nuclear axis of polarity. **Disrupted nucleolus**: Nucleolar structure is disrupted (e.g. by rDNA deletion). Chromosome XII is not tethered opposite the SPB, and instead occupies a new territory in the nuclear center (or elsewhere in the nucleus). These chromosome distribution changes are proposed to alter nuclear polarization and lead to chromosome segregation errors.

Using immunofluorescense microscopy with antibodies against the nucleolar proteins SSB1 and fibrillarin, the haploid version of the rDNA deletion strain containing the helper plasmid has been shown to contain mininuclear bodies (MNBs) in the nucleus instead of an intact crescent shape nucleolus (Oakes et al. 1993). The MNBs are presumed to result in aggregation of several helper plasmid copies for rRNA transcription that possibly creates an rRNA processing site in the absence of an intact nucleolus in rDNA deletion strains. The CLA diploid rDNA deletion strain is likely to have a similar disruption of nucleolar structure to the haploid rDNA alteration strain. Since homozygous rDNA alterations have the ability to increase the missegregation rates of other chromosomes (figure 5.19), it may be that not only chromosome XII, but all chromosome territories are affected by nucleolar structural changes resulting from rDNA alterations. Chromosome segregation is achieved by carefully coordinated chromosome interactions, which involve the mitotic spindle, kinetochores and cohesion (reviewed in Gordon et al. 2012). These chromosome interactions may be affected by changes in nucleolar structure in strains with rDNA alterations that in turn influence chromosome segregation. In yeast, mitotic spindle polarity is determined by cues that direct microtubule attachments to be oriented along the cell axis (Segal and Bloom 2001), and the SPB is oriented opposite to the nucleolus, with telomeres maintained at the nuclear periphery (Laporte et al. 2013). The sister chromatid cohesion established during replication provides resistance to spindle microtubule forces, allowing chromatids to attach to opposite poles during metaphase through microtubule capture of kinetochores (reviewed in Marston 2014). This is necessary to ensure correct separation of sister chromatids towards opposite sides of the cell axis and correct nuclear division.

I propose that nucleolar structure is important in establishing spindle polarity along with the SPB, and therefore is a factor involved in promoting faithful chromosome segregation. However, it is possible that the effect on chromosome segregation is induced by changes in gene expression that result from rDNA alteration-mediated changes to nuclear organization, as it has been suggested previously that nuclear positions and gene expression are interlinked (O'Sullivan 2010). This premise is supported by the fact that expression-dependant nuclear topologies have been identified in the formation of muscular tissues (Neems et al. 2016) and that chromosome territories have been shown to reorganize during terminal differentiation of cancer cells (Solovei et al. 2009; Cremer and Cremer 2010), in patients with heart disease (Mewborn et al. 2010), and even during post-mitotic cell differentiation (Cvackova et al. 2009). Additionally, Berger et al. (2008) have shown that in yeast, genes induced by galactose change nuclear position upon transcriptional activation, and this is caused at least partly by carbon source-dependent nucleolar reorganization. This finding, combined with our data showing that growth in galactose sustains low levels of chromosome segregation, support the hypothesis that nucleolar structure and its influence on specific gene territories impact chromosome segregation.

The nucleolar structure in the rDNA alteration strains remains to be examined to determine their influence on global chromosome segregation. Miyazaki and Kobayashi (2011) developed a system in which each rDNA repeat unit has a *lacO* array that associates with LacI-GFP so the entire rDNA repeat can be visualized in living cells. Our research group is currently working on creating strains harboring such arrays in order to examine chromosome segregation dynamics in the homozygous and heterozygous altered rDNA strains. In particular, a variation of this system is being developed to visualize the region of chromosome XII from which the rDNA has been deleted (Schischka and Ganley, unpublished). The ability to visualize the nucleolar structure and the position of the rDNA locus relative to the SPB, will help to shed light on how the rDNA is able to influence global chromosome segregation.

6.5 CHROMOSOME SEGREGATION AND rDNA TRANSCRIPTION

Pol I transcription is a unique rDNA feature and a key factor regulating growth rate through ribosome biogenesis. The rDNA repeats are the highest transcribed genes in the

genome, with rRNA accounting for up to 80% of a yeast cell's total RNA (Warner 1999). Previous work suggests that highly transcribed loci such as the rDNA can cause non-disjunction (Machin et al. 2006), and that transcriptional linkages at the rDNA may interfere with chromosome segregation (Tomson et al. 2006). However, the increased chromosome missegregation rate in the rDNA deletion strain (figure 5.1) suggests instead that Pol I may have a beneficial effect on chromosome segregation.

Examination of the *RPA135* deletion strain revealed an improved chromosome segregation rate when compared to WT grown in glucose (figure 5.15). However, this strain, which must be grown on galactose because of the helper plasmid (HP), and the WT strain grown in galactose also have a low rate of chromosome loss (figure 5.15). Therefore I was unable to determine the effect that *RPA135* deletion has on chromosome segregation fidelity in the context of my other, glucose-grown results, although there was no significant change in the missegregation rate compared to the galactose-grown WT strain. Further testing will be required to determine whether the low rate of chromosome missegregation seen for the *RPA135* deletion strain is the result of *RPA135* deletion or growth in galactose.

I also wanted to determine whether lack of rRNA transcription (through deletion of *RPA135*) is separable from the effect of the absence of rDNA repeats by deleting both *RPA135* and the rDNA repeats in the same strain. However, I was unable to delete *RPA135* in an rDNA deletion background, despite trying several approaches (section 4.5.4). This was surprising because both *RPA135* and the rDNA repeats have been deleted independently, and it is not expected that deleting *RPA135* will have any effect additional to deletion of the rDNA repeats, given that growth is supported by the Pol II-dependent HP. My results suggest there may be synthetic lethality between these two rDNA alterations, but how the lack of Pol I could affect viability in the rDNA deletion strain is unknown.

6.6 STRENGTHS AND WEAKNESSES OF THE CLA

The basis of this study is the ability to accurately and reproducibly determine chromosome missegregation events for a variety of different strains with different growth characteristics. To achieve this, I developed and optimised a chromosome loss assay that measures the frequency of chromosome loss over a single mitotic cell division. Naturally occurring chromosome missegregation events are rare and are greatly outnumbered by normal

chromosome segregation events (Brown et al. 1991). Despite the rarity of these missegregation events, the CLA optimized for this study proved to be highly sensitive, detecting chromosome loss events as low as one event in 10^8 cell divisions (appendix table II). The CLA is a robust method because it allows chromosome loss colonies (aneuploid for a single chromosome) from diploid colonies to be distinguished from those that have lost one CLA marker but not the other. I was able to confirm aneuploidy through PCR amplification of genomic regions lacking the CLA markers from DNA of CLA-isolated chromosome loss colonies (figure 3.7). I have also shown the CLA is versatile, as it allows screening of strains with a wide range of growth rates, including some with very poor growth rates (figure 5.14). Furthermore, the assay can be performed using different carbon sources, with glucose and galactose being used in this study.

The CLA was principally used in this study to investigate the role that the rDNA repeats play in the segregation of the rDNA-containing chromosome XII, but it was also successfully used to measure the loss rate of chromosomes V and VI. The spontaneous rate of chromosome V loss is one of the few that has been studied previously, and my chromosome V loss rate ($0.39\text{-}1.29\times10^{-6}$) is consistent with that reported by Klein (2001) ($1.3\text{-}2.9\times10^{-6}$) and also comparable to that reported by Hartwell and Smith (1985) (8.3×10^{-6}). Therefore the CLA developed here can be extended to test the impact of other factors on the segregation of any yeast chromosome.

The optimized CLA protocol yielded highly reproducible chromosome loss rate values with low variability. The results were very consistent when other workers performed the assay (Quintana, Schischka, Seo and Ganley, unpublished results), providing further evidence for its accuracy and robustness. This reproducibility was critical in being able to accurately interpret the effects of the various manipulations that I performed. Some outliers were observed, including some negative chromosome loss rates (appendix table II). Negative values for chromosome loss rates can arise from stochastic fluctuations when the real chromosome loss rate is very low. Low chromosome loss rates result in very few chromosome loss events overall, and if by chance more events are found in t_0 than in t_1, the overall rate is negative. Negative rates of chromosome loss are not biologically possible, but can originate if chromosome losses occur during the transition of cells from selective (restrictive) to rich medium (chromosome loss permissive) at t_0, and hence are considered outlier values that nonetheless provide valuable information about deviations from the true mean. To circumvent a potential disproportionate effect on the mean, I used ranked parametric statistical analyses that diminish the influence of such outliers when determining differences between strains (Fay and

Gerow 2013). Together, optimization of the CLA in this thesis has resulted in a robust, versatile and reproducible method to measure chromosome loss rates, and these features make it a valuable tool to examine chromosome segregation.

A major limitation of the CLA is that it is time sensitive, requiring constant monitoring of cell densities to determine correct plating times. The CLA is also time consuming, as each strain needs several biological replicates with each biological replicate requiring multiple plates (technical replicates), and all plating must be completed while growth is being monitored in real time over a period of approximately 8-10 hrs. Furthermore, the CLA requires that any strain to be tested must have the selective markers inserted on the appropriate chromosome and that the strain is diploid. This requires considerable effort in strain construction and characterization. Despite its time limitations, the CLA developed here is a strong benchmark to test the accuracy of any alternative methods that could potentially measure chromosome losses in a shorter amount of time.

Currently the CLA colony counting strategy is performed manually and, besides being time consuming, it is subject to human error. Colony counting software is commercially available, but the difficulty in the CLA lies in the proper identification of chromosome loss colonies that are able to grow on both 5FOA plates but not on the G418 plates. This identification process involves visual comparison of plates overlaid onto each other, and such a colony comparison function is not a feature of any of the colony counting software trialed in this study. To address this issue, we have an ongoing collaboration with Dr. Andre Barczak (INMS, Massey University), who specializes in image processing, to develop a specialized colony counting software package that can perform automated comparisons between plates to determine which colonies are common between the overlaid plates and which are not. A version of this software is currently being tested in the Ganley research group.

6.7 DETERMINING THE INFLUENCE OF THE rDNA ON MEIOTIC CHROMOSOME SEGREGATION

In this thesis, I have shown that the rDNA has an effect on mitotic chromosome segregation. This raises the question of whether the rDNA also influences meiotic chromosome segregation fidelity. In mitosis, homologous chromosomes usually behave independently

during the separation of sister chromatids. In contrast, in meiosis, homologous chromosomes pair with each other and are separated during meiosis I, while in meiosis II the sister chromatids are separated. Meiosis is thought to be a modulation of mitosis with meiosis-specific factors (Hong et al. 2013). Hence, the chromosome segregation mechanisms found in mitosis can be partially extrapolated to meiosis. Specifically, it would be expected that the influence of the rDNA on meiosis II would be similar to that seen for mitosis. In contrast, whether the rDNA influences chromosome segregation during meiosis I in a similar manner is not clear because of the nature of the division is very different. Therefore, investigating the effects of the rDNA on meiotic chromosome segregation is of great value to expand the current knowledge of the mechanism behind human nondisjunction.

The CLA established in this thesis is restricted to detection of chromosome loss rates during mitotic cell divisions. However, measurement of the meiotic rate of chromosome missegregation could be achieved through a modification of the CLA. Since meiotic products that lose a chromosome are not viable, detection of meiotic chromosome missegregation is based on the ability to identify meiotic products that are haploid but disomic (harbor two copies of a single chromosome), that is, have had a chromosome gain. Detecting the gain of a chromosome requires distinction of one homolog from the other. In diploid strains that already contain the mitotic CLA markers, insertion of two additional alternative marker genes into both arms of the opposite chromosome homolog, would allow phenotypic detection of each homolog. A schematic for how this could be achieved is presented in figure 6.3. Detection of meiotic chromosome missegregation ideally involves distinction between errors arising in meiosis I versus meiosis II, which can be achieved through analysis of the markers present in the meiotic products. However, detection of meiosis II chromosome segregation errors is contingent on the occurrence of crossover events in which one of the markers is exchanged between sister chromatids of opposite homologs. The system proposed here will be beneficial to measure meiotic chromosome loss and will contribute to understand whether the effects of the mitotic rDNA-mediated chromosome segregation translate to meiotic segregation.

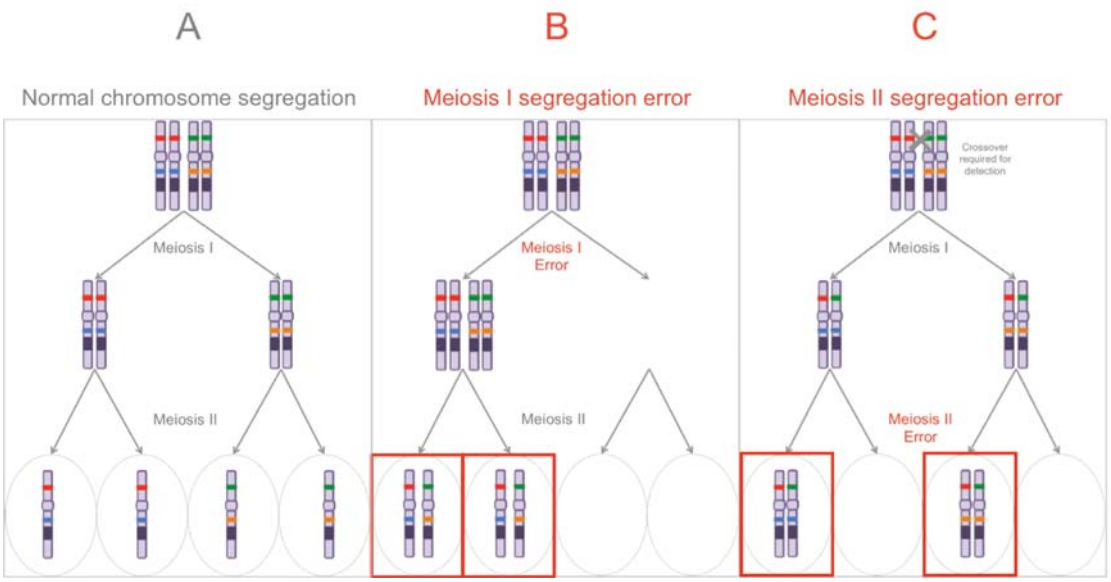

Figure 6.3. CLA adaptation for detection of meiotic chromosome missegregation. Potential meiotic chromosome missegregation assay for a diploid strain with marked chromosome XII homologs is represented. One homolog contains the same markers described for the CLA (figure 3.1), and the other contains alternative markers in the identical positions. Chromosome XII homologs are illustrated after replication, with paired sister chromatids. If normal chromosome segregation occurs (**A**), homologs are separated during meiosis I and newly replicated sister chromatids remaining together, and after meiosis II sister chromatids are separated to yield four meiotic products with only one chromosome copy each (two cells inherit a single copy of one homolog, while the other two inherit a single copy of the opposite homolog). If there is a chromosome segregation error during meiosis I (**B**), both homologs remain on the same side of the spindle apparatus, and sister chromatids from both homologs are separated during meiosis II, resulting in daughter cells that inherit one copy of each homolog. These haploids are disomic for the chromosome of interest and can be identified because they have all four markers (red boxes). The two daughter cells that do not inherit any chromosome XII copies are not viable. If there is a chromosome segregation error during meiosis II (**C**), chromosome homologs are separated during meiosis I, but sister chromatids fail to separate in meiosis II, also producing haploids disomic for the chromosome of interest. In this case however, since sister chromatids are identical, detection only occurs in cases where a crossover event has exchanged markers between the two homologs (such as the example shown), resulting in haploid products that have three out of the four markers (red boxes).

6.8 FROM YEAST TO HUMAN ANEUPLOIDY

Human chromosomes that contain rDNA (13, 14, 15, 21 and 22) are highly represented in human aneuploidies (Hall et al. 2007a). Aneuploidy accounts for almost 35% of spontaneous abortions (with monosomy of the sex chromosome X and trisomy of chromosome 16 being the most frequent) and for about 4% of stillbirths, with trisomy of chromosome 21 outnumbering other chromosomes (only chromosomes 9, 13, 18 and 22 have been reported) (Hassold et al. 1996). Approximately 0.3% of all live births are aneuploid with the most frequent (over 40%) being trisomy of chromosome 21, which results in Down syndrome (Nagaoka et al.

2012). Trisomy of chromosome 21, is the best studied case of human non-disjunction, with over 90% of cases arise from errors in oogenesis, 4% from errors in spermatogenesis and almost 3% from post-zygotic errors (during mitosis). Among the maternal errors, the vast majority (over 70%) occur during meiosis I (Freeman et al. 2007). A similar trend of increased maternal meiosis I aneuploidy has been reported for all the acrocentric chromosomes (Zaragoza et al. 1994), and evidence has emerged for acrocentric chromosome-specific patterns of nondisjunction (Hall et al. 2007b). I have shown that in yeast, the rDNA is beneficial for chromosome segregation, so it is possible that a feature different to the presence of the rDNA, but also common to all acrocentric chromosomes, is responsible for their recognized pattern of non-disjunction. My results however, are focused on mitotic chromosome segregation, so extending my research to meiosis will contribute to the proper identification of acrocentric chromosome-specific patterns of meiotic nondisjunction.

The connection between aneuploidy and human genetic disorders has been a major driver for studies in aneuploidy (Pfau and Amon 2012; Oromendia and Amon 2014). Recent work has also highlighted the recurrence of whole chromosome gains and losses in cancer (Chandhok and Pellman 2009; Durrbaum and Storchova 2016; Rutledge and Cimini 2016), identifying chromosome instability (Winey et al.) as a common feature of many human cancers (Horne et al. 2015). Aneuploidy is believed to contribute to disease pathogenesis of cancer, and to produce transcriptome and proteome effects that trigger stress responses (Hassold et al. 2007; Gordon et al. 2012). Thus, understanding the causes of aneuploidy is key. Increasing maternal age has long been considered a risk factor for non-disjunction, and this is due to the extended cell arrest (from years to decades) in prophase I that oocytes undergo until-ovulation (Oliver et al. 2008). There is evidence to suggest that loss of cohesin is a cause of human non-disjunction of maternal origin, as a result of either recombination failure or impaired sister chromatid cohesion (Nagaoka et al. 2012). There are also many environmental factors that have been linked to human aneuploidy, such as drug use and radiation, but confirmatory evidence for these has not emerged (Pacchierotti et al. 2008). Research of human aneuploidy is hampered by the unavailability of a suitable model, with only a few models having been used to date to study features of non-disjunction, including tissue samples from human individuals with aneuploidy and aneuploid mouse embryonic fibroblasts (Williams et al. 2008). Yeast is the most widely used model because it can tolerate a variety of aneuploid conditions, is highly genetically manipulable, and is easy and quick to culture. Hence, studies like this in yeast are necessary to complement findings from mammalian cells and dissect the molecular mechanisms that underlie chromosome missegregation in eukaryotes, and to support the

current focus to develop aneuploidy specific therapeutics (Mateos-Langerak et al. 2009; Gordon et al. 2012).

CHAPTER SEVEN: CONCLUSIONS AND FUTURE DIRECTIONS

[blank page]

7.1 CONCLUSIONS

CLA examination of several rDNA alterations strains in both homozygous and heterozygous state has revealed that segregation of chromosome XII and at least two other chromosomes is best when the rDNA copy number and chromosomal location is unaltered. Here, I have presented evidence for a new role of the rDNA repeats in chromosome segregation. Furthermore, I found evidence that the rDNA has two separable roles in maintaining faithful mitotic chromosome segregation:

1) A local role in which the rDNA mediates segregation of the chromosome on which it is located. This role is facilitated by Fob1. I proposed three possible mechanisms for how Fob1 may influence chromosome segregation through the rDNA: by stabilizing the rDNA array through rDNA recombination intermediates; by mediating condensin recruitment to the RFB site in a timely manner; or by recruiting the RENT silencing complex to achieve the appropriate chromatin state of the rDNA for chromosome segregation.
2) A global role in which the rDNA influences the segregation of all chromosomes. This role must be exerted through large-scale changes in the cell. I have ruled out alterations in ribosome biogenesis or chromosome length accounting for this phenomenon. The ability of heterozygosity of rDNA state to promote a wild type level of chromosome segregation suggests that this effect is mediated through the nucleolus. Therefore I propose that rDNA alterations change nucleolar structure and overall nuclear organization, and that these changes impact spindle polarity and affect the fidelity of chromosome segregation.

Strains harboring homozygous alterations of the rDNA (deletion, copy number reduction) on their native locus allowed me to show that the rDNA can influence local chromosome segregation (section 5.1). Further, I found that *FOB1* specifically mediates the local segregation of chromosomes carrying the rDNA. To support this finding I used a *FOB1* disruption strain and showed that lack of Fob1 affects the segregation rate of chromosome XII (section 5.1) and this only occurs when the rDNA repeats are present on the chromosome (section 5.2.4). I also inserted the CLA markers on an independent chromosome and showed that *FOB1* disruption does not affect the segregation of other chromosomes (section 5.2.5) unless it harbors an ectopic rDNA array (section 5.2.6).

In contrast to the *FOB1* disruption, I found that altering the rDNA array itself (deletion, copy number reduction) in homozygous strains affects the segregation rate of chromosome XII (local) (section 5.1) and also other chromosomes (global) (section 5.5.1). Since, the 20-copy strain also harbors a *FOB1* disruption, I transiently expressed Fob1 in the 20-copy strain during the CLA to show that the rDNA copy number reduction has an independent effect on chromosome segregation, independently of the *FOB1* disruption (section 5.2). Furthermore, using strains heterozygous for rDNA state, I showed that heterozygosity rescues the local (section 5.4) and global (section 5.5) chromosome segregation defects caused by homozygous state rDNA alterations.

The use of strains in which the rDNA array has been translocated to different chromosomes allowed me to show that the rDNA is able to influence local and global chromosome segregation from an ectopic location. However, this analysis is complicated by how to relate heterozygosity at native and/or ectopic locations to the situation where the rDNA is solely on chromosome XII. Notably, the rDNA-mediated chromosome segregation effects exerted from a heterozygous ectopic rDNA array differ to the effects the rDNA can exert from its native locus on chromosome XII because the ectopic rDNA array increases the chromosome loss rate of the translocation chromosome (section 5.2.3) but is able to maintain a low chromosome XII missegregation rate (section 5.2.2). Until the mechanism of how rDNA state and its heterozygosity influence chromosome segregation is understood, it is difficult to interpret the effects that ectopic rDNA arrays have on chromosome segregation fidelity.

Finally, I have provided evidence that growth in galactose affects the segregation fidelity of chromosome XII, but not other chromosomes. It is possible that a galactose-induced change in yeast metabolism may result in changes in nucleolar structure that in turn affect local chromosome segregation through alterations in nuclear architecture. This possibility is supported by observations (Harris et al. 2014) indicating that the nucleolus is physically disrupted when yeast cells are grown in galactose. However, further testing is required to determine whether galactose affects the segregation of a subset of chromosomes, including chromosome XII, or whether it is specific to chromosome XII.

I conclude that the rDNA affects mitotic chromosome segregation fidelity at a minimum of two different levels: at the rDNA-containing chromosome level; and at a global level. However, it remains possible that the second level only affects a subset of all chromosomes, with that subset including the three chromosomes tested in this study (V, VI, and XII). I further conclude that the rDNA acts in different ways at these two levels. I show that the local chromosome segregation level is mediated by Fob1, and I propose three potential mechanisms

for how Fob1 mediates this role (through rDNA recombination, condensin recruitment, or rDNA chromatin structure). In contrast, I propose that the rDNA affects global segregation through changes in nucleolar structure that impact on the accuracy of spindle polarity establishment.

My work has defined a new role for the rDNA repeats on chromosome segregation and has contributed to understanding the molecular mechanism that dictates the nature of this role. Further work is needed to dissect the mechanisms by which the rDNA mediates these two roles in chromosome segregation fidelity. The rDNA has been described as "one of the most fragile sites in the genome", with its highly repetitive nature making it highly recombinogenic and vulnerable to loss of copies from deleterious recombination events (Kobayashi 2011a). I propose that, in terms of chromosome segregation, the rDNA is instead one of the most resilient genomic sites, with an ability to positively impact chromosome segregation fidelity at a global scale.

7.2 FUTURE DIRECTIONS

7.2.1 Dissecting the role of Fob1 as a mediator of chromosome segregation at the rDNA locus.

Fob1 facilitates rDNA-mediated local chromosome segregation. I have proposed three possible mechanisms of how Fob1 may exert its role, and the candidate genes involved remain to be tested (section 6.1). The first possibility is that Fob1, through its role in rDNA recombination, may help establish recombination intermediates that maintain the structural stability of the long rDNA locus. The second possibility is that Fob1-mediated condensin recruitment (and enrichment during anaphase) to the rDNA locus, is crucial to establish intra-chromatid linkages and to promote a timely condensation of the rDNA containing sister chromatids. The third possibility is that the Fob1-mediated recruitment of chromatin modifying factors, such as the RENT complex, may be important to maintain chromatin structure at the rDNA locus. Since *TOF2* is involved in the Fob1-mediated recruitment of both condensin and the RENT complex (Huang and Moazed 2003), future work should focus on first examining the chromosome XII loss rate when *TOF2* is deleted, to test whether it is Fob1 recruitment roles (mediated by Tof2) or its role in recombination that influence chromosome segregation. If either

of Fob1 recruitment roles is involved in chromosome segregation, I expect *TOF2* deletion to increase the chromosome XII missegregation rate. *TOF2* screening should be followed by examination of *SIR2/NET1* and *CSM1/LRS4* deletions to discern between recruitment of condensin or the RENT complex respectively. If *TOF2* deletion does not affect the chromosome segregation rate, it is likely that Fob1 facilitates rDNA-mediated segregation by establishing recombination intermediates that maintain the structural stability of the long rDNA locus. It must be noted that the three proposed Fob1 mechanisms to explain its role facilitating rDNA-mediated chromosome segregation are not mutually exclusive, and so it is possible that one or more of Fob1's roles contributes to a faithful chromosome segregation.

7.2.2 Involvement of Pol I in rDNA-mediated chromosome segregation

My findings regarding the chromosome loss rate of Pol I deficient strains are not conclusive. This is due to an unanticipated effect of growth in galactose on chromosome segregation, which potentially masked the effect of Pol I inactivation, as the *RPA135* deletion strain relies on growth in galactose for rDNA transcription from the HP. To bypass the galactose-induced effect on chromosome segregation, a promoter swap for the HP to a constitutively activated promoter will allow growth of these strains on glucose, and therefore a direct test of the effect of rRNA transcription on chromosome segregation fidelity.

It has been suggested that transcription may be involved in establishing linkages between sister chromatids (Machin et al. 2006). It is likely that all the rDNA repeats in the diploid 20-copy strain XII$^{20/20KU}$ *fob1*$^{-}$ are transcriptionally active (French et al. 2003). If transcriptional linkages interfere with chromosome segregation and are responsible for the increase in the chromosome XII loss rate of the 20-copy strain, inactivating Pol I should reduce the missegregation rate. However, creating an *RPA135* deletion strain with 20 copies of the rDNA repeats proved to be difficult; and mating of *rpa135Δ* 20-copy haploids could not be performed within the timeline of this thesis. So, the possibility of Pol I affecting rDNA-mediated chromosome segregation remains to be evaluated.

7.2.3 Investigating nucleolar structure changes as a consequence of rDNA alterations

I have proposed that the rDNA alterations cause large-scale changes in nuclear architecture that affect global segregation, partly because the magnitude of the effect of these alterations is similar in chromosome XII and the other chromosomes tested in this study. An important direction to follow from this study is to test the hypothesis that rDNA alterations cause changes in nucleolar structure, and if so, to examine whether such changes affect aspects of the chromosome segregation process, such as spindle polarity, in living cells. This can be achieved by using specific fluorescent markers and time-lapse video microscopy (Miyazaki and Kobayashi 2011; Thacker et al. 2011). Such approaches should reveal the extent of nucleolar involvement in chromosome segregation and the dynamics of spindle formation, and how the different rDNA alterations, including heterozygosity of rDNA state, impact these.

7.2.4 Effects of rDNA array translocations

My results demonstrate that the rDNA is able to influence chromosome segregation regardless of its chromosomal location, but the effects on chromosome segregation of the rDNA at ectopic sites versus its native locus on chromosome XII are not easily interpretable currently. In this thesis I only tested heterozygous translocation strains. To obtain a more complete picture of the effects of rDNA translocations on chromosome segregation fidelity, a comprehensive set of strains heterozygous and homozygous for rDNA translocations and the native locations should be tested using the CLA. Information arising from these strains (heterozygous and homozygous for rDNA translocations) can be integrated with my findings from chromosome XII marked homozygous and heterozygous strains to get a clearer idea for how rDNA translocations impact rDNA-mediated chromosome segregation.

7.2.5 The CLA and development of a meiotic chromosome loss assay

The CLA is optimized for analysis of mitotic chromosome segregation, and provides a detection sensitivity advantage over other available methods, such as the use of fluorescent markers (Thacker et al. 2011). Therefore the CLA is well positioned to be employed as a tool to

examine the mitotic chromosome segregation rates of all the yeast chromosomes to produce a comprehensive picture of mitotic chromosome segregation fidelity. In addition, it can be employed to measure the impact of mutations in genes believed to play a role in chromosome segregation. Further, the CLA has provided a basis to design an assay that measures meiotic chromosome loss and this should be exploited to analyze the differences between mitotic and meiotic chromosome segregation.

In order to determine if the effects of the mitotic rDNA-mediated chromosome segregation translate to meiotic segregation, a meiotic chromosome loss assay can be developed. Development of such a meiotic assay can be achieved through a modification of the CLA (section 6.6). Detection of meiotic chromosome missegregation can be achieved through identification of meiotic products that have gained an extra chromosome copy, this requires distinction of the two chromosome homologs. Insertion of two additional marker genes into both arms of the opposite chromosome homolog of strains that already carry the CLA markers, would allow phenotypic detection of each homolog. The use of a meiotic assay would also allow comparing the meiotic chromosome loss rates of different chromosomes. The vast majority of human aneuploid conditions are a result of meiotic non-disjunction (with a higher occurrence of meiosis I errors) (Freeman et al. 2007), therefore this work is relevant to assess how the rDNA is able to impact meiotic non-disjunction.

7.2.6 Final thoughts

My work has revealed the involvement of the rDNA in local and global chromosome segregation of *S. cerevisiae*, and the high level of structural and functional similarity of the rDNA across the eukaryotes (Andersen et al. 2005; Schneider and Grosschedl 2007) means this has implications for human chromosome segregation. Firstly, I found that in yeast, the rDNA repeats are beneficial for chromosome segregation fidelity. It is possible that in humans, the location of the rDNA on multiple acrocentric chromosomes provides increased mitotic chromosomal stability, potentially reducing their missegregation rates relative to other chromosomes. However, rates of mitotic missegregation have not been measured in human chromosomes, and to date there is no method to achieve this. Second, I have shown that the rDNA has a global effect on chromosome segregation. Since humans have several rDNA loci, it is possible that the multiple loci ensure that if one rDNA alteration occurs, the other arrays can exert an effect that sustains faithful global chromosome segregation, perhaps analogous to

the heterozygosity effects of rDNA state I observed for *S. cerevisiae*. Finally, I have shown that Fob1 positively mediates segregation of chromosome XII, exerting its role directly through the rDNA repeats. Although there are no known *FOB1* mammalian homologs, there may be rDNA-specific factors that contribute to faithful chromosome segregation in an analogous manner. Therefore, my work provides a platform from which to explore the effects of the rDNA on chromosome segregation fidelity in other eukaryotes.

CHAPTER EIGHT: APPENDICES

[blank page]

Appendix Scheme I. R Commands used for statistical analysis.

- For data input from .csv file command:

```
> data <- read.csv(file.choose())
```

- To perform a Mann-Whitney-Wilcoxon rank sum test

```
> wilcox.test(data$Strain.1, data$Strain.2)
```

- To perform a Kruskal-Wallis one-way analysis of variance by ranks:

```
> kruskal.test(list(data$Strain.1, data$Strain.2,…. , data$Strain.n))
```

- To perform multiple Mann-Whitney-Wilcoxon rank sum test and group all p-values (pV)

```
> pV <-c()
> w <- wilcox.test(data$Strain.1, data$Strain.2)
> pV <- c(pV, w$p.value)
> w <- wilcox.test(data$Strain.2, data$Strain.3)
> pV <- c(pV, w$p.value)
…
> write.table(pV, quote = FALSE, sep = "\t")
```

- To correct the Mann-Whitney p-values using a false discovery rate (fdr) adjustment:

```
> pVadjusted <- p.adjust(pV, method="fdr")
> write.table(pVadjusted, quote = FALSE, sep = "\t")
```

Appendix table I. Cp values from qPCR. *GAL1* was used as a reference single copy gene to estimate rDNA copy number. The rDNA gene copy number ratio to WT was estimated for four tetrads (1 [A-D], 2 [A-D], 3 [A-D], and 4 [A-D]) obtained from sporulating strain XII$^{200/20KU}$ *fob1*$^{-}$ *RPA135/rpa135Δ::LEU2*+HP. A WT haploid strain was used as a 200-copy control, and a 20-copy haploid strain was used as a positive control. Cross point (Cp) values ± Std Dev are shown. Refer to figure 4.30.

Sample	*GAL1* Cp	25S rDNA Cp
WT1	30.13	20.57
WT1	29.74	20.42
WT1	29.63	
WT2	31.3	20.06
WT2	31.32	20.08
WT2	31.09	
WT3	29.18	19.25
WT3	29.16	19.52
WT3	29.09	19.31
WT4	30.76	19.67
WT4	30.94	19.76
WT4	30.77	19.87

20 copy 1	29.09	21.61
20 copy 1	29.24	21.99
20 copy 1	29.64	21.94
20 copy 2	29.83	22.58
20 copy 2	29.92	22.65
20 copy 2		22.49
20 copy 3	29.42	21.65
20 copy 3	29.79	21.76
20 copy 3	29.64	21.78
20 copy 4	29.29	21.64
20 copy 4	28.86	21.9
20 copy 4		21.74

1A	31.21	23.55
1A	31.87	23.26
1A	31.13	23.19
1B	28.66	19.94
1B	28.92	19.93
1B	28.81	19.78
1C	28.60	18.71
1C	28.30	18.61
1C	27.95	18.53
1D	32.12	23.66
1D	31.34	23.64
1D	32.08	24.03

Sample	*GAL1* Cp	25S rDNA Cp
2A	28.01	19.31
2A	27.67	19.03
2A	27.6	19.08
2B	29.43	22.11
2B	29.49	22.06
2B	29.16	22.15
2C	28.59	19.96
2C	28.5	19.62
2C	27.99	19.67
2D	30.15	21.91
2D	29.74	21.58
2D	29.31	22.05

3A	27.81	19.58
3A	27.93	19.62
3A	28.26	19.58
3B	29.09	20.44
3B	29.52	20.47
3B	29.67	20.58
3C	28.84	22.46
3C	29.22	22.63
3C	28.82	22.72
3D	29.97	23.34
3D	30.61	23.45
3D	30.58	23.42

4A	28.69	22.34
4A	29.27	22.33
4A	29.23	22.58
4B	28.54	19.8
4B	28.63	19.8
4B	28.82	19.78
4C	30.27	23.17
4C	28.05	23.25
4C	30.67	23.52
4D	28.19	19.52
4D	28.27	19.53
4D	28.24	19.47

Appendix table II. Chromosome loss rates for each strain. Chromosome loss rates are expressed as events per cell division *10^{-6}, and each value corresponds to an independent biological replicate. Negative (bold) and high (bold and underlined) values are indicated. CLAs performed by Schischka, Quintana and Ganley (light grey) and by Seo, Quintana and Ganley (dark grey) are highlighted. Growth in galactose (GAL) or glucose (GLU) for the CLA is indicated. The number of experiments for each strain is indicated by n.

Medium	Strain	Chromosome loss rates *10^{-6}	n
GLU	V$^{0/0KU}$ XII$^{200/200}$	2.80, 0.05, 1.05, 2.87, 0.09, **-0.27**, 0.12, 0	8
GAL	V$^{0/0KU}$ XII$^{200/200}$	1.63, 0.58, 0.20	3
GLU	V$^{0/200KU}$ XII$^{0/200}$	16.60, 16.20, 21.05, 10.46	4
GLU	V$^{0/200KU}$ XII$^{0/200}$ *fob1*$^{-}$	33.83, 63.83, 32.06	3
GLU	V$^{0/200KU}$ XII$^{200/200}$	0.87, 6.47, **-0.77**, 2.49	4
GLU	VI$^{0/0KU}$ XII$^{200/200}$	53.62, 40.75, **181.70**, 97.78, 55.29, **-95.14**, 3.89, 0.72, 1.19, **-6.69**, 33.52, 22.80	12
GAL	VI$^{0/0KU}$ XII$^{200/200}$	10.90, 18.35, 17.52	3
GLU	VI$^{0/0KU}$ XII$^{20/20}$ *fob1*$^{-}$	**131.00**, **171.00**, **197.00**	3
GLU	VI$^{0/0KU}$ XII$^{0/0}$ +HP	70.50, **202.00**, **450.00**	3
GLU	VI$^{0/0KU}$ XII$^{200/200}$ *fob1*$^{-}$	19.82, 24.02, 11.64	3
GLU	VI$^{0/0KU}$ XII$^{0/20}$ *fob1*$^{-}$	15.47, 3.28, 6.82	3
GLU	VI$^{0/0KU}$ XII$^{0/200}$ +HP	29.20, 20.21, 17.48	3
GLU	XII$^{200/200KU}$	2.31, 3.24, **-0.72**, 0.86, 1.19, **-1.68**, 2.00, **-1.35**, 3.57, 0.00, 0.61, 1.20, 3.69, 3.04, 5.31, 6.15, 2.94, 1.74, 1.11, 1.44, 7.83, 23.58, 25.72, 13.96, 18.44, 15.09, 33.04, 10.51, 0.64, 10.71, 4.72, 10.61, 1.69, 1.01, 2.09, 0.00	32
GLU	XII$^{0/0KU}$	39.43, 12.40, 15.68, 25.11, 48.07, 19.17, 14.06, 42.13, 22.46, 61.83, 37.90, 44.25, 25.10, 4.23, 19.17, 15.65	16
GLU	XII$^{200/200KU}$*fob1*$^{-}$	27.23, 15.66, 77.43, 45.84, 2.83, 14.17, 12.18, 9.17	8
GLU	XII$^{20/20KU}$*fob1*$^{-}$	60.72, 46.75, 41.03, 13.76, 68.03, 34.70, 41.52, 17.39, 29.72, 45.96, 27.71, 30.58	12
GLU	XII$^{200/0KU}$+HP	14.20, 37.09, **-16.31**, 15.62, -9.26, **-37.57**	6
GLU	XII$^{0/200KU}$+HP	6.71, 1.65, 1.61, 2.79	4
GLU	XII$^{20/200KU}$*fob1*$^{-}$	4.00, 33.61, **-11.88**, 18.43, 5.02, 2.76, **-0.71**, 4.48	8
GLU	XII$^{200/20KU}$*fob1*$^{-}$	12.55, 7.68, 4.38, 9.61	4
GLU	XII$^{200/200*KU}$	8.74, 1.17, 13.15, 7.29	4
GLU	XII$^{200/200KU}$+HP	12.52, 15.34, 15.98, 15.27	4
GAL	XII$^{200/200KU}$	0.00, **-3.38**	2
GAL	XII$^{200/200K}$ *fob1*$^{-}$	**-2.81**, 3.48	2
GAL	XII$^{20/20KU}$*fob1*$^{-}$	19.96, 0.69	2
GAL	XII$^{200/200KU}$ +pGAL-*FOB1*	2.50, 3.96	2
GAL	XII$^{200/200K}$ *fob1*$^{-}$+pGAL-*FOB1*	**-1.36**, 1.71	2
GAL	XII$^{20/20KU}$*fob1*$^{-}$+pGAL-*FOB1*	11.40, **-3.93**	2
GLU	XII$^{200/200KU}$+pGAL-*FOB1*	38.15, 9.05	2
GLU	XII$^{200/200K}$ *fob1*$^{-}$+pGAL-*FOB1*	1.25, 1.07	2
GLU	XII$^{20/20KU}$*fob1*$^{-}$+pGAL-*FOB1*	13.41, 20.92	2
GLU	XII$^{20/0KU}$*fob1*$^{-}$	1.96, 13.15, 15.66, 6.95, 2.80, 3.87	6
GLU	XII$^{0/20KU}$*fob1*$^{-}$	13.53, 9.54, 17.58, 11.41, 4.37, 2.83, 1.46, 1.38	8
GAL	XII$^{200/200KU}$*RPA135Δ*+HP	-0.76, 0.46, 3.65, -0.12, 0.00	5
GAL	XII$^{200/200KU}$*RPA135Δ fob1*$^{-}$+HP	0.00, 0.00, 0.15, 0.00, 0.74	5

GLU	XII$^{0/0KU}$ *fob1*-+HP	1.65, 1.67, 1.01	3
GLU	XII$^{0/200KU}$ VI$^{0/200}$+HP	0.59, **-0.73**, 0.00	3
GLU	XII$^{0/200KU}$ VI$^{0/200}$+HP *fob1*-	0.99, 0.13, 1.49	3
GLU	XII$^{200/200KU}$ VI$^{0/200*}$	0.00, 0.00, 0.00	3

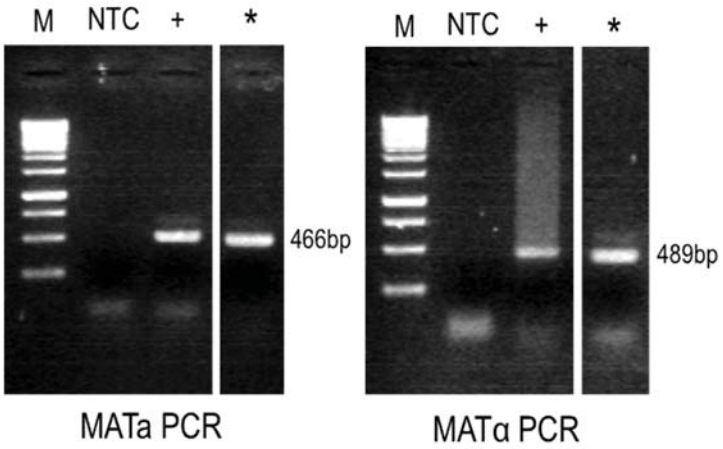

Appendix figure 8.1. Mating type PCR of CLA strain XII$^{0/0KU}$ *fob1*$^{-}$ +HP. PCR was used to confirm diploidy as in figure 4.2. Marker (M), water was used as a no template control (NTC) and WT gDNA from strain XII$^{200/200KU}$ was used as a positive control (+), while gDNA of the diploid strain XII$^{0/0KU}$ *fob1*$^{-}$ +HP was screened (*). Refer to section 4.4.5.

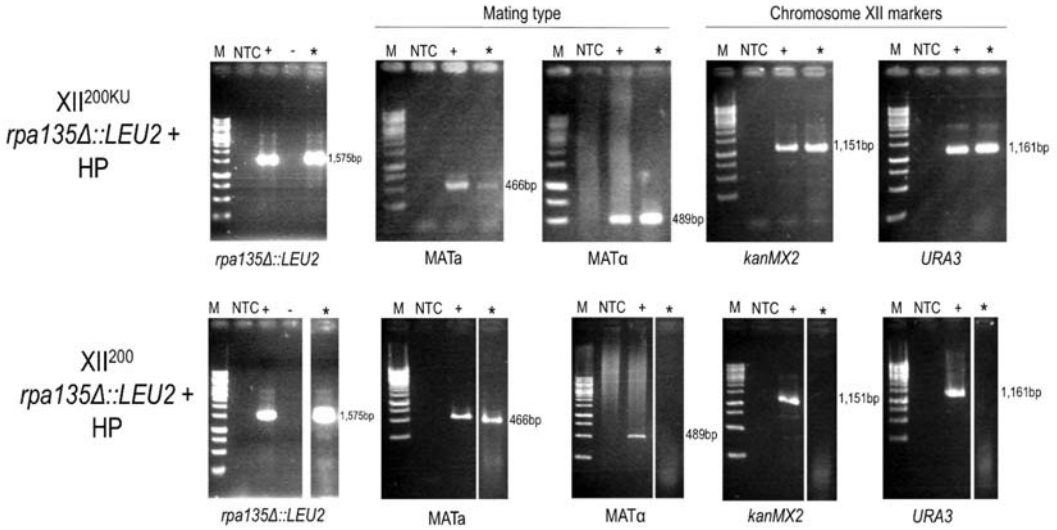

Appendix figure 8.2. PCR confirms *RPA135* replacement with *LEU2* in haploid spores, determines mating type, and confirms CLA marker presence. PCR characterization of the haploid spores XII^{200KU} *rpa135Δ::LEU2* +HP (* in top gels) and XII^{200} *rpa135Δ::LEU2* +HP (* in bottom gels). The first set of gels show amplification of the *RPA135* replacement construct with primers PAG198 and PAG135 (***rpa135Δ::LEU2* PCR**, 1,575bp fragment) using the *rpa135Δ::LEU2* construct as a positive control (+) and WT gDNA from XII$^{200/200KU}$ as a negative amplification control (-). Mating type (**MATa** and **MATα**), and CLA marker insertion (***kanMX2*** and ***URA3*)** were determined as in figure 4.2. Marker (M), water was used as a no template control (NTC) and WT gDNA from strain XII$^{200/200KU}$ was used as a positive control (+), while gDNA of both haploids was screened (*). Refer to section 4.5.1.

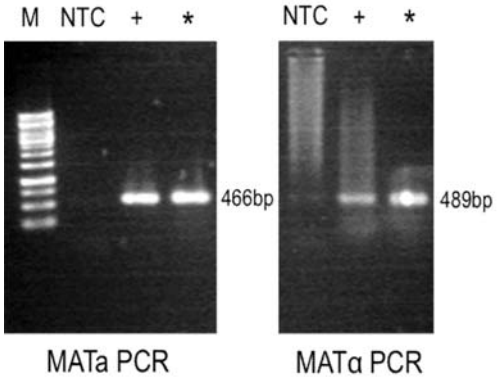

Appendix figure 8.3. PCR confirms diploid state of strain XII$^{200/200KU}$ *rpa135*Δ+HP. PCR was used to confirm diploidy as in figure 4.2. Marker (M), water was used as a no template control (NTC) and WT gDNA from strain XII$^{200/200KU}$ was used as a positive control (+), while gDNA of the diploid strain XII$^{200/200KU}$ *rpa135Δ* +HP was screened (*). Refer to section 4.5.1.

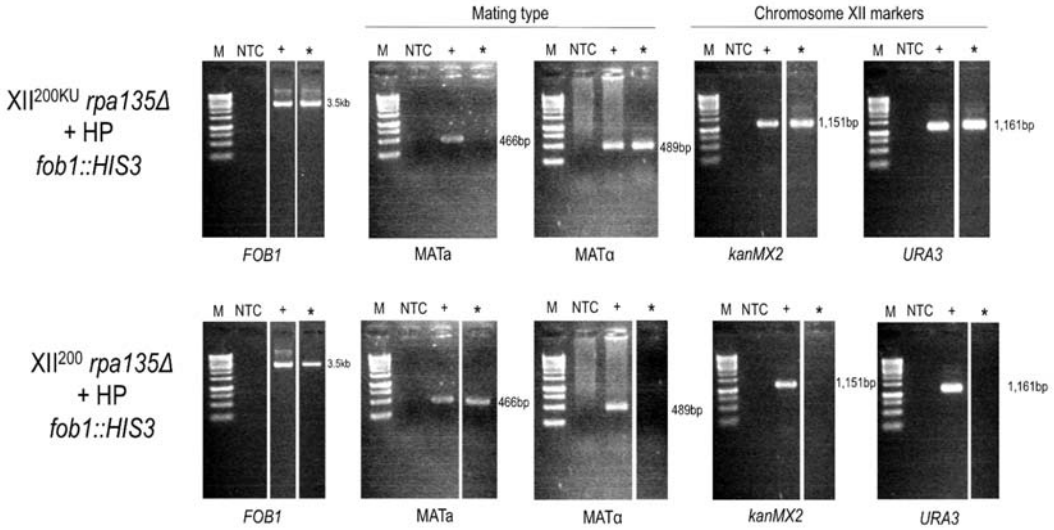

Appendix figure 8.4. PCR confirms the disruption of *FOB1* in the haploid *rpa135*Δ strains, and determines mating type and CLA marker presence. PCR characterization of the haploid spores XII^{200KU} *rpa135*$^{-}$ *fob1*$^{-}$ +HP (* in top gels) and XII^{200} *rpa135*$^{-}$ *fob1*$^{-}$ +HP (* bottom gels). The first set of gels show amplification of the *FOB1* replacement construct (***FOB1***) as in figure 4.10 using the *fob1::HIS3* construct as a positive control (+). Mating type (**MATa** and **MAT**α**)**, and CLA marker insertion (***kanMX2*** and ***URA3)*** were determined as in figure 8.2. Refer to section 4.5.2

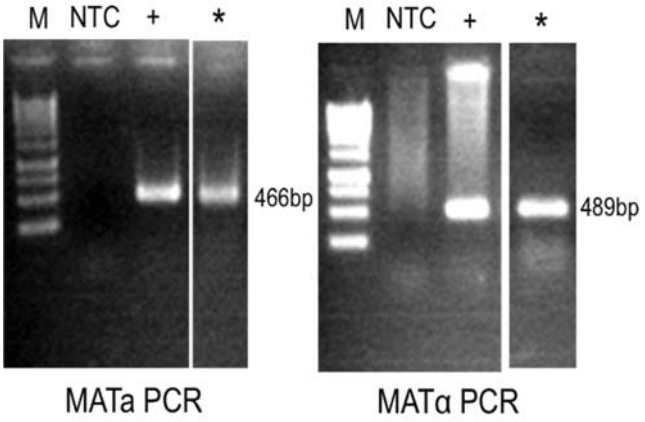

Appendix figure 8.5. PCR confirms diploid state of strain XII$^{200/200KU}$ *rpa135*Δ+HP *fob1*$^{-}$. PCR was used to confirm diploidy as in figure 4.2. Marker (M), water was used as a no template control (NTC) and WT gDNA from strain XII$^{200/200KU}$ was used as a positive control (+), while gDNA of the diploid strain XII$^{200/200KU}$ *rpa135Δ* +HP *fob1*$^{-}$ was screened (*). Refer to section 4.5.2.

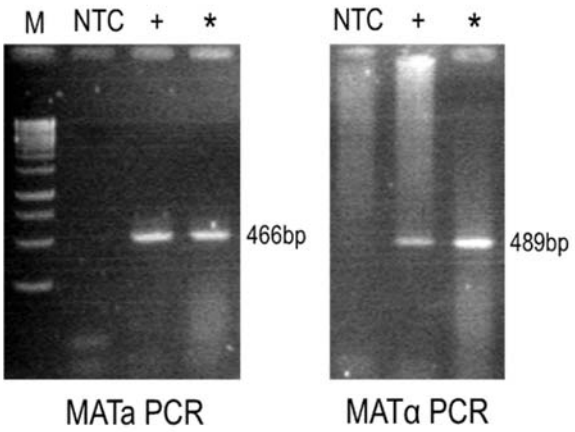

Appendix figure 8.6. PCR confirms diploid state of the new strain XII$^{20/20KU}$ *fob1*$^{-}$ (*fob1::leu2::HIS3*). PCR was used to confirm diploidy as in figure 4.2. Marker (M), water was used as a no template control (NTC) and WT gDNA from strain XII$^{200/200KU}$ was used as a positive control (+), while gDNA of the diploid strain XII$^{20/20KU}$ *fob1*$^{-}$ (*fob1::leu2::HIS3*) was screened (*). Refer to section 4.5.3.

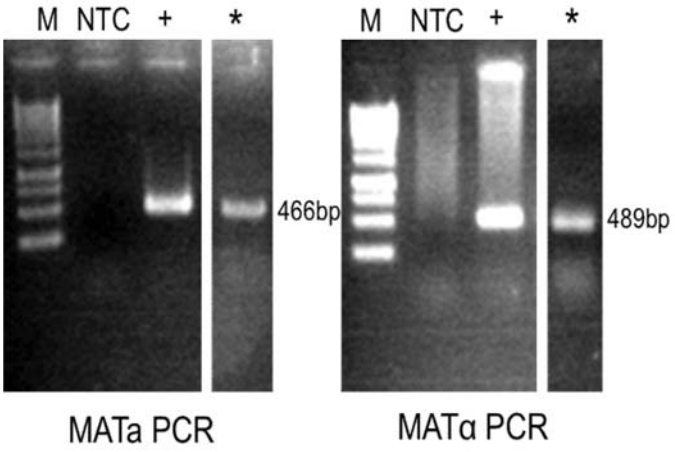

Appendix figure 8.7. PCR confirms the diploid state of strain XII$^{200/20KU}$ *fob1-RPA135/rpa135Δ::LEU2* +HP. PCR was used to confirm diploidy as in figure 4.2. Marker (M), water was used as a no template control (NTC) and WT gDNA from strain XII$^{200/200KU}$ was used as a positive control (+), while gDNA of the diploid strain XII$^{200/20KU}$ *fob1- RPA135/rpa135Δ::LEU2* +HP was screened (*). Refer to section 4.5.3.

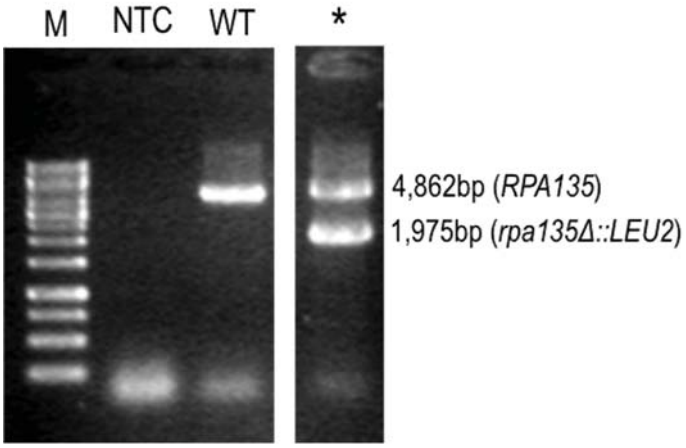

Appendix figure 8.8. PCR confirms replacement of one copy of *RPA135* with *LEU2* in the rDNA deletion strain XI$^{I0/0KU}$+HP. The *RPA135* locus was PCR amplified as in figure 4.28. Marker (M), water was used a no template control (NTC), WT gDNA (WT) was used as an *RPA135* control producing a fragment of 4,862 bp, and the transformed heterozygous strain XII$^{0/0KU}$ *RPA135/rpa135Δ::LEU2* +HP (*) exhibits one WT *RPA135* copy and a copy that has been replaced with *LEU2* (1,975 bp). Refer to section 4.5.4

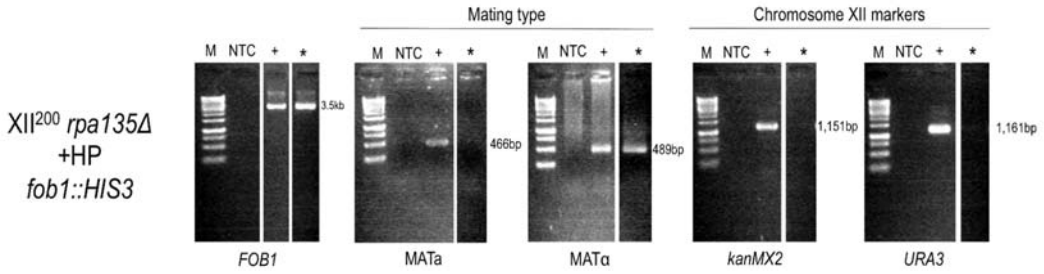

Appendix figure 8.9. PCR characterization of haploid spore XII^{200} *rpa135Δ*+HP *fob1::HIS3*. PCR characterization of the haploid spore XII^{200} *rpa135Δ* +HP *fob1::HIS3* (*). The first gel (left) shows amplification of the *fob1::HIS3* disruption (***FOB1***) as in figure 4.18 using the *fob1::HIS3* construct as a positive control (+). Mating type (**MATa** and **MATα**), and CLA marker insertion (***kanMX2*** and ***URA3)*** were determined as in figure 8.2. Refer to section 4.5.4

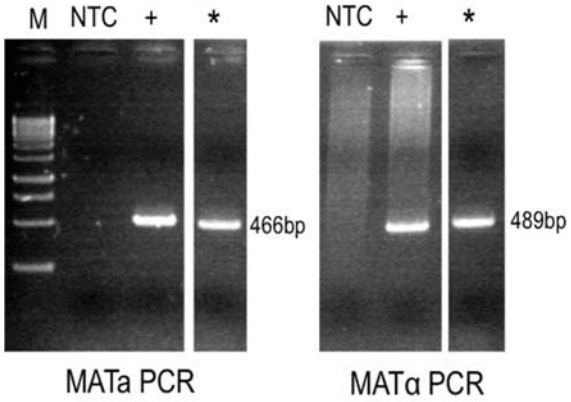

Appendix figure 8.10. PCR confirms the diploid state of strain XII$^{200/0KU}$ *RPA135/rpa135Δ*+HP *FOB1/fob1::HIS3*. PCR was used to confirm diploidy as in figure 4.2. M (Marker), water was used as a no template control (NTC) and WT gDNA from strain XII$^{200/200KU}$ was used as a positive control (+), while gDNA of the diploid strain XII$^{200/0KU}$ *RPA135/rpa135Δ* +HP *FOB1/fob1::HIS3* was screened (*). Refer to section 4.5.4.

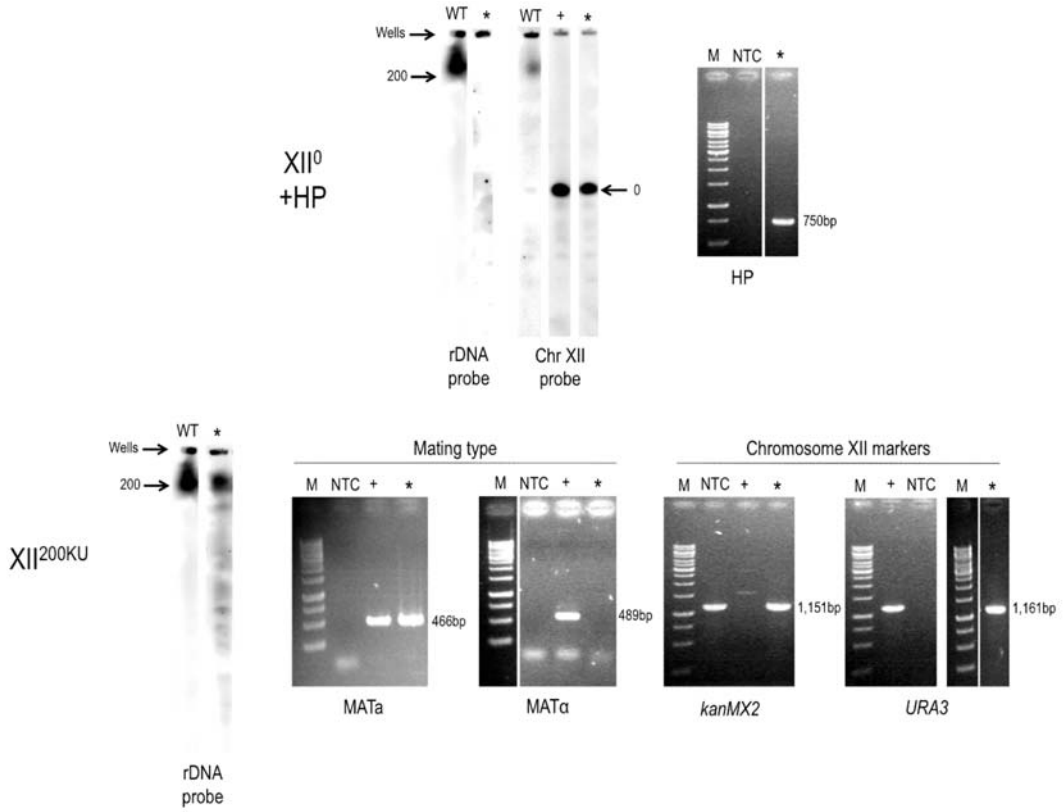

Appendix figure 8.11. Characterization of haploid strains XII^{0}+HP and XII^{200KU}. Characterization of haploid strains XII^{0} +HP (top, *) and XII^{200KU} (bottom, *) using Southern blotting with an rDNA and a chromosome XII probe (as indicated), to determine chromosome XII size and confirm the presence or absence of rDNA copies (indicated by arrows) with WT strain XII$^{200/200KU}$ (WT) and rDNA deletion strain XII$^{0/0KU}$ +HP (+) used as controls. PCR was used to confirm the presence of the HP in strain XII^{0} +HP (top) (**HP**) as in figure 4.6, for strain XII^{200KU} mating type (**MATa** and **MATα)**, and CLA marker insertion (***kanMX2*** and ***URA3)*** were determined as in figure 8.2. Marker (M), water was used as a no template control (NTC), and WT gDNA from XII$^{200/200KU}$ was used as a positive control (+), while gDNA of strains XII^{0} +HP (top, *) and XII^{200KU} (bottom, *) were assayed. Refer to section 4.6.1.

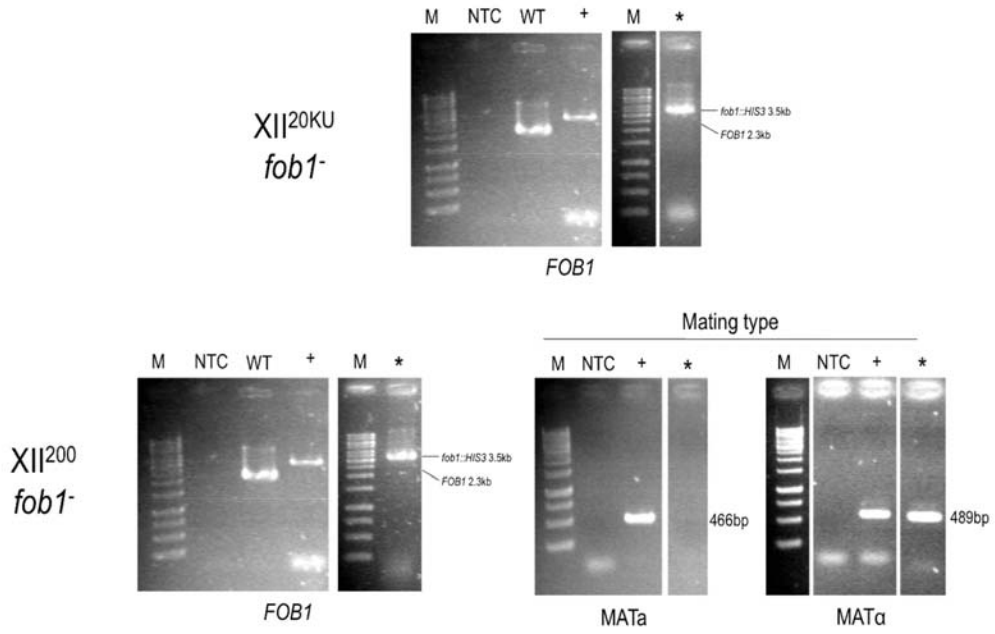

Appendix figure 8.12. Characterization of haploid strains XII^{20KU} *fob1*$^{-}$ and XII^{200} *fob1*$^{-}$. PCR characterization of the haploid spores XII^{20KU} *fob1*$^{-}$ (* in top gel) and XII^{200} *fob1*$^{-}$ (* in bottom gels). *FOB1* replacement (***FOB1***), mating type (**MATa** and **MATα**), and CLA marker insertion (***kanMX2*** and ***URA3)*** were determined as in figure 4.10. For the *FOB1* PCR, WT gDNA from XII$^{200/200KU}$ was used as a positive amplification control (WT) for *FOB1*, and gDNA from strain TAK300 was used as a positive *fob1::HIS3* replacement control (+). For the mating type PCR's, WT gDNA from XII$^{200/200KU}$ was used as a positive control (+). For all PCR's: Marker (M), and water was used as a no template control (NTC). Refer to section 4.6.2.

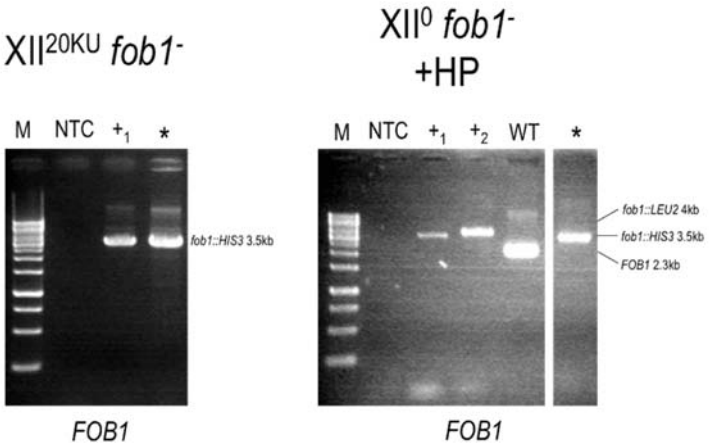

Appendix figure 8.13. PCR confirms FOB1 replacement in haploid strains XII^{20KU} *fob1*$^{-}$ and XII^{0} *fob1*$^{-}$+HP. PCR was used to confirm *FOB1* replacement in the haploid spores XII^{20KU} *fob1*$^{-}$ (* left gel) and XII^{0} *fob1*$^{-}$+HP (* right gel) as in figure 4.10. Marker (M), water was used as a no template control (NTC) and WT gDNA from XII$^{200/200KU}$ was used as a positive amplification control (WT) amplifying a 2.3 kb fragment corresponding to *FOB1*. gDNA from strain TAK300 was used as a positive control for the *fob1::HIS3* replacement (+$_1$), and gDNA from strain XII$^{200/200KU}$ *fob1*$^{-}$ was used as a positive control for the *fob1::LEU2* replacement (+$_2$; 4 kb). Refer to section 4.6.3.

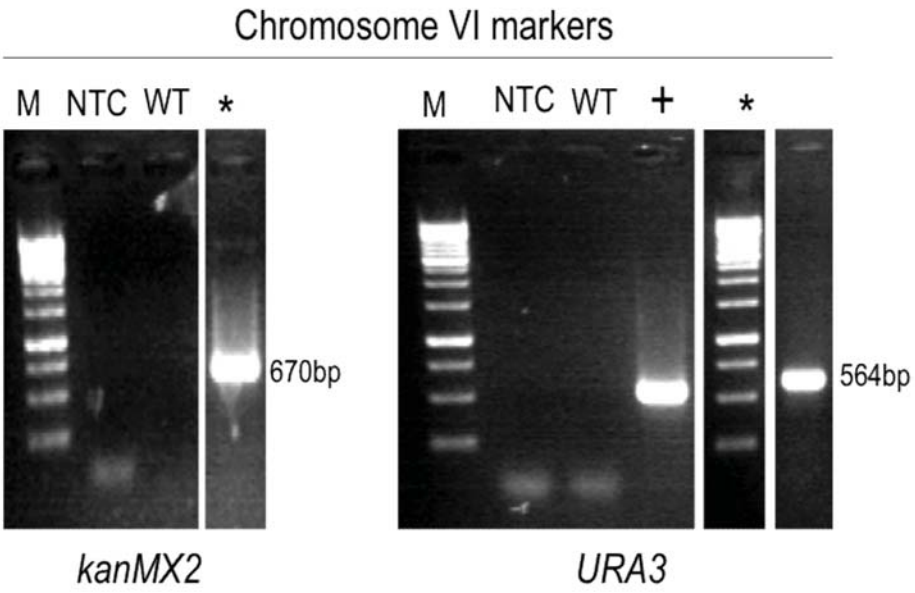

Appendix figure 8.14. PCR confirms introduction of chromosome VI CLA markers into the haploid rDNA deletion strain VI^{0KU} XII^{0}+HP. PCR was used to confirm *kanMX2* and *URA3* marker insertion into chromosome VI as in figure 4.40. Marker (M), water was used as a no template control (NTC), WT gDNA from strain XII2$^{00/200KU}$ was used as a negative control (WT), WT gDNA from strain VI$^{0/0KU}$ was used as a positive control (+), while gDNA of strain VI^{0KU} XII^{0} +HP (*) was screened. Refer to section 4.7.2

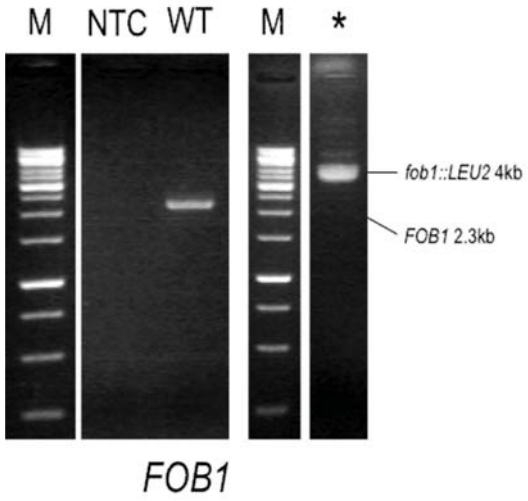

Appendix figure 8.15. PCR confirms *FOB1* replacement in haploid strain VI^{0KU} XII^{200} *fob1*$^{-}$. PCR was used to confirm *FOB1* replacement in the haploid spore VI^{0KU} XII^{200} *fob1*$^{-}$ (*) as in figure 4.10. Marker (M), water was used as a no template control (NTC) and WT gDNA from XII$^{200/200KU}$ was used as a positive amplification control (WT). gDNA from strain VI^{0KU} XII^{200} *fob1*$^{-}$ produced a 4 kb product corresponding to the *fob1::LEU2* replacement. Refer to section 4.7.2.

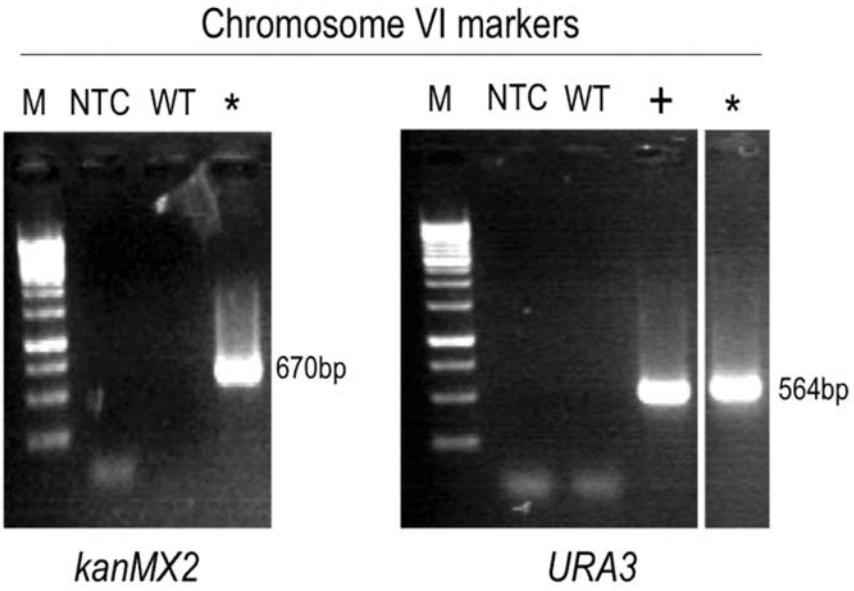

Appendix figure 8.16. PCR confirms introduction of chromosome VI CLA markers into the 20-copy haploid strain VI^{0KU} XII^{20} *fob1*$^{-}$. PCR was used to confirm *kanMX2* and *URA3* marker insertion into chromosome VI as in figure 4.40. Marker (M), water was used as a no template control (NTC), WT gDNA from strain XII2$^{00/200KU}$ was used as a negative control (WT), WT gDNA from strain VI$^{0/0KU}$ was used as a positive control (+), while gDNA of strain VI^{0KU} XII^{20} *fob1*$^{-}$ (*) was screened. Refer to section 4.7.2.

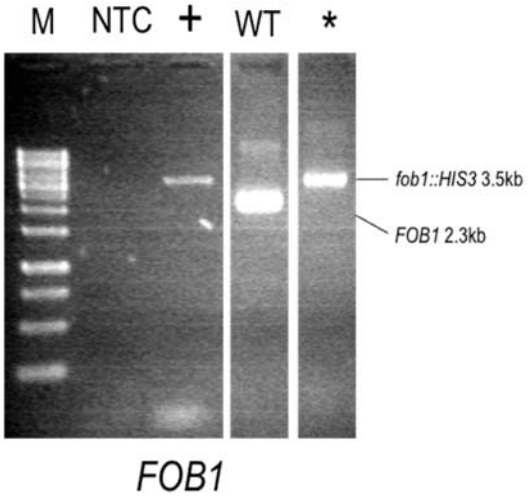

Appendix figure 8.17. PCR confirms *FOB1* replacement into the haploid rDNA deletion strain VI^{0KU} XII^{0} *fob1*$^{-}$+HP. PCR was used to confirm *FOB1* replacement in the haploid strain VI^{0KU} XII^{0} *fob1*$^{-}$ +HP (*) as in figure 4.10. Marker (M), water was used as a no template control (NTC) and WT gDNA from XII$^{200/200KU}$ was used as a positive amplification control (WT) amplifying a 2.3 kb fragment corresponding to *FOB1*. gDNA from strain VI^{0KU} XII^{0} *fob1*$^{-}$ +HP produced a 3.5 kb product corresponding to the *fob1::HIS3* replacement. Refer to section 4.7.3

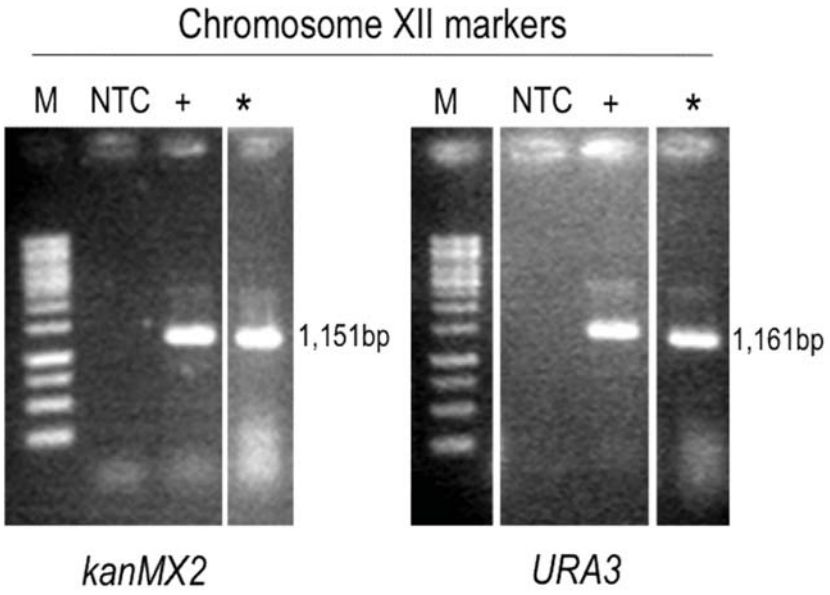

Appendix figure 8.18. PCR confirms introduction of chromosome XII CLA markers into the WT XII$^{200/200*KU}$ strain. PCR was used to confirm *kanMX2* and *URA3* marker insertion into chromosome XII as in figure 4.2. Marker (M), water was used as a no template control (NTC), WT gDNA from strain XII$^{200/200KU}$ was used as a positive control (+), while gDNA of strain XII^{200*KU} (*) was screened. Refer to section 4.8.1.

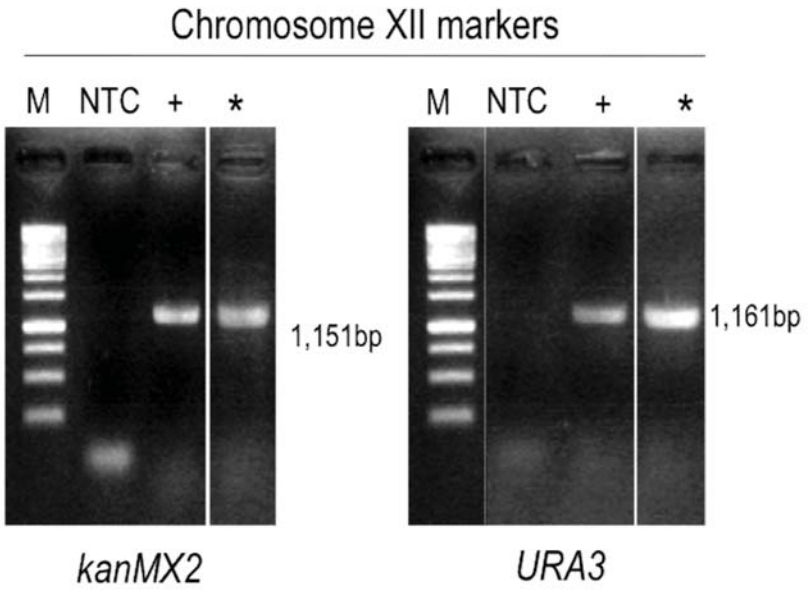

Appendix figure 8.19. PCR confirms introduction of the chromosome XII markers into strain XII^{200KU} V^{200*}. PCR was used to confirm *kanMX2* and *URA3* marker insertion into chromosome XII as in figure 4.2. Marker (M), water was used as a no template control (NTC), WT gDNA from strain XII$^{200/200KU}$ was used as a positive control (+), while gDNA of strain XII^{200KU} V^{200*} (*) was screened. Refer to section 4.8.2.

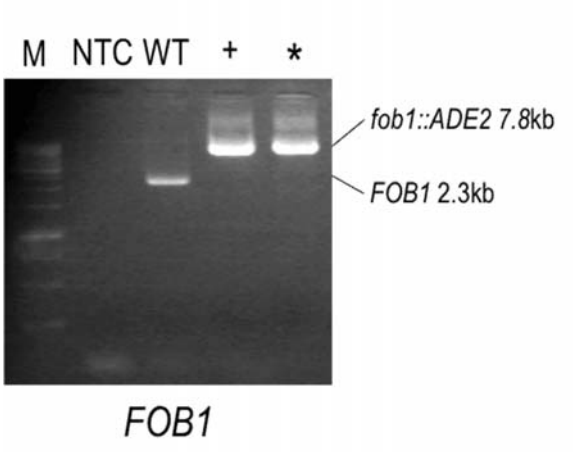

Appendix figure 8.20. PCR confirms *FOB1* disruption in strain XII^{200KU} V^{200*} *fob1^{-}*. PCR was used to confirm *FOB1* replacement in the haploid strain XII^{200KU} V^{200*} *fob1^{-}* (*) as in figure 4.10. Marker (M), water was used as a no template control (NTC) and WT gDNA from XII$^{200/200KU}$ was used as a positive amplification control (WT) amplifying a 2.3 kb fragment corresponding to *FOB1*. gDNA from TAK300 *fob1::his3::ADE2* was used as a positive *fob1::ADE2* control, and gDNA from strain XII^{200KU} V^{200*} *fob1^{-}* produced a 7.8 kb product corresponding to the *fob1::ADE2* replacement. Refer to section 4.8.2.

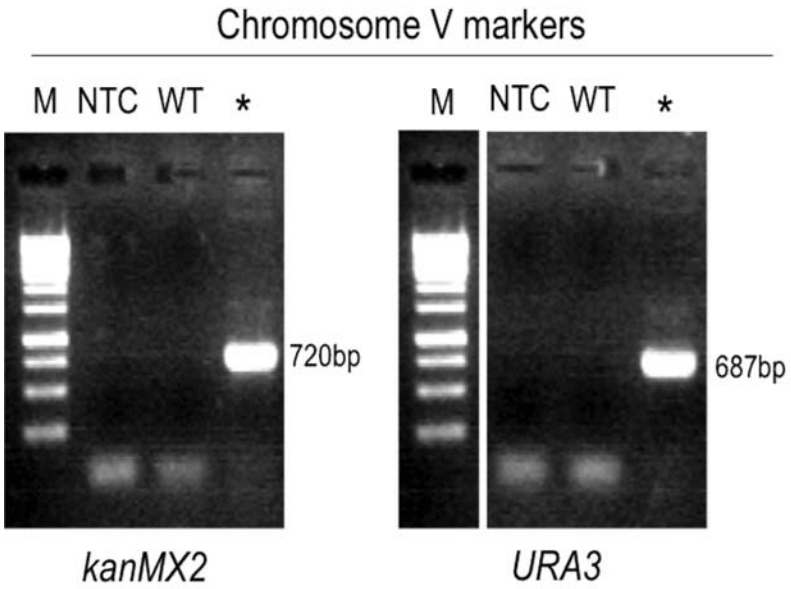

Appendix figure 8.21. PCR confirms introduction of the chromosome V markers into strain V^{200*KU} XII^{200}. PCR was used to confirm *kanMX2* and *URA3* marker insertion into chromosome V as in figure 4.38. Marker (M), water was used as a no template control (NTC), WT gDNA from strain $XII^{200/200KU}$ was used as a negative control (WT), while gDNA of strain V^{200*KU} XII^{200} (*) was screened. Refer to section 4.8.3.

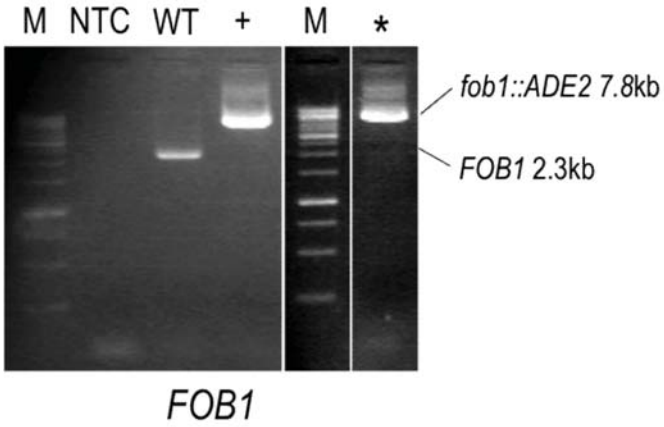

Appendix figure 8.22. PCR confirms *FOB1* disruption in strain V^{200*KU} XII^{200} *fob1*$^{-}$. PCR was used to confirm *FOB1* replacement in the haploid strain XII^{200} V^{200*KU} *fob1*$^{-}$ (*) as in figure 4.10. Marker (M), water was used as a no template control (NTC) and WT gDNA from $XII^{200/200KU}$ was used as a positive amplification control (WT) amplifying a 2.3 kb fragment corresponding to *FOB1*. gDNA from TAK300 *fob1::his3::ADE2* was used as a positive *fob1::ADE2* control. Refer to section 4.8.3.

REFERENCES

Alberts B, Johnson A, Lewis J, Raff M, Roberts K, Walter P. 2007. Molecular biology of the cell, 5th ed., by, Garland Publishing, New York. *Molecular Reproduction and Development*: 1,392.

Andersen JS, Lam YW, Leung AK, Ong SE, Lyon CE, Lamond AI, Mann M. 2005. Nucleolar proteome dynamics. *Nature* **433**: 77-83.

Apte MS, Meller VH. 2012. Homologue pairing in flies and mammals: gene regulation when two are involved. *Genetics research international* **2012**: 430587.

Aragon L. 2010. Ribosomal genes: safety in numbers. *Curr Biol* **20**: R368-370.

Arican-Goktas HD, Ittiprasert W, Bridger JM, Knight M. 2014. Differential spatial repositioning of activated genes in Biomphalaria glabrata snails infected with Schistosoma mansoni. *PLoS Negl Trop Dis* **8**: e3013.

Babu KA, Verma RS. 1985. Structural and functional aspects of nucleolar organizer regions (NORs) of human chromosomes. *International review of cytology* **94**: 151-176.

Bakhoum SF, Thompson SL, Manning AL, Compton DA. 2009. Genome stability is ensured by temporal control of kinetochore-microtubule dynamics. *Nature cell biology* **11**: 27-35.

Berger AB, Cabal GG, Fabre E, Duong T, Buc H, Nehrbass U, Olivo-Marin JC, Gadal O, Zimmer C. 2008. High-resolution statistical mapping reveals gene territories in live yeast. *Nature methods* **5**: 1031-1037.

Bergeron J, Drouin G. 2008. The evolution of 5S ribosomal RNA genes linked to the rDNA units of fungal species. *Current genetics* **54**: 123-131.

Bernhard W, Granboulan N. 1968. Electron microscopy of the nucleolus in vertebrate cells. *The Nucleus (AJ Dalton and F Haguenau, eds)*: 81-149. Academic Press, New York.

Biggins S. 2013. The composition, functions, and regulation of the budding yeast kinetochore. *Genetics* **194**: 817-846.

Boeke JD, LaCroute F, Fink GR. 1984. A positive selection for mutants lacking orotidine-5'-phosphate decarboxylase activity in yeast: 5-fluoro-orotic acid resistance. *Molecular & general genetics : MGG* **197**: 345-346.

Boisvert FM, van Koningsbruggen S, Navascues J, Lamond AI. 2007. The multifunctional nucleolus. *Nature reviews Molecular cell biology* **8**: 574-585.

Bosco G. 2012. Chromosome pairing: a hidden treasure no more. *PLoS genetics* **8**: e1002737.

Bradbury JE, Richards KD, Niederer HA, Lee SA, Rod Dunbar P, Gardner RC. 2006. A homozygous diploid subset of commercial wine yeast strains. *Antonie Van Leeuwenhoek* **89**: 27-37.

Brewer BJ, Fangman WL. 1987. The localization of replication origins on ARS plasmids in S. cerevisiae. *Cell* **51**: 463-471.

Brown M, Garvik B, Hartwell L, Kadyk L, Seeley T, Weinert T. 1991. Fidelity of mitotic chromosome transmission. *Cold Spring Harbor symposia on quantitative biology* **56**: 359-365.

Burke B, Stewart CL. 2014. Functional architecture of the cell's nucleus in development, aging, and disease. *Current topics in developmental biology* **109**: 1-52.

Cahyani I, Cridge AG, Engelke DR, Ganley AR, O'Sullivan JM. 2015. A sequence-specific interaction between the Saccharomyces cerevisiae rRNA gene repeats and a locus

encoding an RNA polymerase I subunit affects ribosomal DNA stability. *Molecular and cellular biology* **35**: 544-554.

Cao L, Alani E, Kleckner N. 1990. A pathway for generation and processing of double-strand breaks during meiotic recombination in S. cerevisiae. *Cell* **61**: 1089-1101.

Chandhok NS, Pellman D. 2009. A little CIN may cost a lot: revisiting aneuploidy and cancer. *Current opinion in genetics & development* **19**: 74-81.

Chernoff YO, Vincent A, Liebman SW. 1994. Mutations in eukaryotic 18S ribosomal RNA affect translational fidelity and resistance to aminoglycoside antibiotics. *The EMBO journal* **13**: 906-913.

Cioci F, Vu L, Eliason K, Oakes M, Siddiqi IN, Nomura M. 2003. Silencing in yeast rDNA chromatin: reciprocal relationship in gene expression between RNA polymerase I and II. *Molecular cell* **12**: 135-145.

Clemente-Blanco A, Mayan-Santos M, Schneider DA, Machin F, Jarmuz A, Tschochner H, Aragon L. 2009. Cdc14 inhibits transcription by RNA polymerase I during anaphase. *Nature* **458**: 219-222.

Conconi A, Widmer RM, Koller T, Sogo JM. 1989. Two different chromatin structures coexist in ribosomal RNA genes throughout the cell cycle. *Cell* **57**: 753-761.

Cremer T, Cremer M. 2010. Chromosome territories. *Cold Spring Harbor perspectives in biology* **2**: a003889.

Cvackova Z, Masata M, Stanek D, Fidlerova H, Raska I. 2009. Chromatin position in human HepG2 cells: although being non-random, significantly changed in daughter cells. *J Struct Biol* **165**: 107-117.

D'Ambrosio C, Kelly G, Shirahige K, Uhlmann F. 2008a. Condensin-dependent rDNA decatenation introduces a temporal pattern to chromosome segregation. *Curr Biol* **18**: 1084-1089.

D'Ambrosio C, Schmidt CK, Katou Y, Kelly G, Itoh T, Shirahige K, Uhlmann F. 2008b. Identification of cis-acting sites for condensin loading onto budding yeast chromosomes. *Genes Dev* **22**: 2215-2227.

D'Amours D, Stegmeier F, Amon A. 2004. Cdc14 and condensin control the dissolution of cohesin-independent chromosome linkages at repeated DNA. *Cell* **117**: 455-469.

Dammann R, Lucchini R, Koller T, Sogo JM. 1993. Chromatin structures and transcription of rDNA in yeast Saccharomyces cerevisiae. *Nucleic acids research* **21**: 2331-2338.

Dorer RK, Zhong S, Tallarico JA, Wong WH, Mitchison TJ, Murray AW. 2005. A small-molecule inhibitor of Mps1 blocks the spindle-checkpoint response to a lack of tension on mitotic chromosomes. *Curr Biol* **15**: 1070-1076.

Doudna JA, Rath VL. 2002. Structure and function of the eukaryotic ribosome: the next frontier. *Cell* **109**: 153-156.

Durrbaum M, Storchova Z. 2016. Effects of aneuploidy on gene expression: implications for cancer. *Febs j* **283**: 791-802.

Fay DS, Gerow K. 2013. A biologist's guide to statistical thinking and analysis. *WormBook : the online review of C elegans biology* doi:10.1895/wormbook.1.159.1: 1-54.

Finlan LE, Sproul D, Thomson I, Boyle S, Kerr E, Perry P, Ylstra B, Chubb JR, Bickmore WA. 2008. Recruitment to the nuclear periphery can alter expression of genes in human cells. *PLoS genetics* **4**: e1000039.

Forsburg SL. 2001. The art and design of genetic screens: yeast. *Nat Rev Genet* **2**: 659-668.

Freeman L, Aragon-Alcaide L, Strunnikov A. 2000. The condensin complex governs chromosome condensation and mitotic transmission of rDNA. *The Journal of cell biology* **149**: 811-824.

Freeman SB, Allen EG, Oxford-Wright CL, Tinker SW, Druschel C, Hobbs CA, O'Leary LA, Romitti PA, Royle MH, Torfs CP et al. 2007. The National Down Syndrome Project: design and implementation. *Public health reports (Washington, DC : 1974)* **122**: 62-72.

French SL, Osheim YN, Cioci F, Nomura M, Beyer AL. 2003. In exponentially growing Saccharomyces cerevisiae cells, rRNA synthesis is determined by the summed RNA polymerase I loading rate rather than by the number of active genes. *Molecular and cellular biology* **23**: 1558-1568.

Ganley AR, Kobayashi T. 2011. Monitoring the rate and dynamics of concerted evolution in the ribosomal DNA repeats of Saccharomyces cerevisiae using experimental evolution. *Molecular biology and evolution* **28**: 2883-2891.

Gietz RD, Sugino A. 1988. New yeast-Escherichia coli shuttle vectors constructed with in vitro mutagenized yeast genes lacking six-base pair restriction sites. *Gene* **74**: 527-534.

Gietz RD, Woods RA. 2006. Yeast transformation by the LiAc/SS Carrier DNA/PEG method. *Methods Mol Biol* **313**: 107-120.

Gimenez-Abian JF, Clarke DJ, Devlin J, Gimenez-Abian MI, De la Torre C, Johnson RT, Mullinger AM, Downes CS. 2000. Premitotic chromosome individualization in mammalian cells depends on topoisomerase II activity. *Chromosoma* **109**: 235-244.

Glynn EF, Megee PC, Yu HG, Mistrot C, Unal E, Koshland DE, DeRisi JL, Gerton JL. 2004. Genome-wide mapping of the cohesin complex in the yeast Saccharomyces cerevisiae. *PLoS biology* **2**: E259.

Goffeau A, Barrell BG, Bussey H, Davis RW, Dujon B, Feldmann H, Galibert F, Hoheisel JD, Jacq C, Johnston M et al. 1996. Life with 6000 genes. *Science* **274**: 546, 563-547.

Gongadze GM. 2011. 5S rRNA and ribosome. *Biochemistry Biokhimiia* **76**: 1450-1464.

Gordon DJ, Resio B, Pellman D. 2012. Causes and consequences of aneuploidy in cancer. *Nat Rev Genet* **13**: 189-203.

Grob A, Colleran C, McStay B. 2014. Construction of synthetic nucleoli in human cells reveals how a major functional nuclear domain is formed and propagated through cell division. *Genes Dev* **28**: 220-230.

Guacci V. 2007. Sister chromatid cohesion: the cohesin cleavage model does not ring true. *Genes Cells* **12**: 693-708.

Guacci V, Koshland D, Strunnikov A. 1997. A direct link between sister chromatid cohesion and chromosome condensation revealed through the analysis of MCD1 in S. cerevisiae. *Cell* **91**: 47-57.

Guthrie C, Fink GR. 1991. Guide to Yeast Genetics and Molecular and Cell Biology In *Methods in Enzymology*, Vol 194, p. 835. Academic Press.

Ha CW, Huh WK. 2011. Rapamycin increases rDNA stability by enhancing association of Sir2 with rDNA in Saccharomyces cerevisiae. *Nucleic Acids Research* **39**: 1336-1350.

Hadjiolov AA. 1985. The Nucleolus and Ribosome Biogenesis. *Springer-Verlag, Wien , New York*: 268.

Haering CH, Lowe J, Hochwagen A, Nasmyth K. 2002. Molecular architecture of SMC proteins and the yeast cohesin complex. *Molecular cell* **9**: 773-788.

Hall HE, Chan ER, Collins A, Judis L, Shirley S, Surti U, Hoffner L, Cockwell AE, Jacobs PA, Hassold TJ. 2007a. The origin of trisomy 13. *Am J Med Genet A* **143a**: 2242-2248.

Hall HE, Surti U, Hoffner L, Shirley S, Feingold E, Hassold T. 2007b. The origin of trisomy 22: evidence for acrocentric chromosome-specific patterns of nondisjunction. *Am J Med Genet A* **143a**: 2249-2255.

Harris B, Bose T, Lee KK, Wang F, Lu S, Ross RT, Zhang Y, French SL, Beyer AL, Slaughter BD et al. 2014. Cohesion promotes nucleolar structure and function. *Mol Biol Cell* **25**: 337-346.
Hartwell LH, Dutcher SK, Wood JS, Garvik B. 1982. The fidelity of mitotic chromosome reproduction in S. cerevisiae. *Rec Adv Yeast Mol Biol*: 28-38.
Hartwell LH, Smith D. 1985. Altered fidelity of mitotic chromosome transmission in cell cycle mutants of S. cerevisiae. *Genetics* **110**: 381-395.
Hassold T, Abruzzo M, Adkins K, Griffin D, Merrill M, Millie E, Saker D, Shen J, Zaragoza M. 1996. Human aneuploidy: incidence, origin, and etiology. *Environmental and molecular mutagenesis* **28**: 167-175.
Hassold T, Hall H, Hunt P. 2007. The origin of human aneuploidy: where we have been, where we are going. *Human molecular genetics* **16 Spec No. 2**: R203-208.
Henras AK, Plisson-Chastang C, O'Donohue MF, Chakraborty A, Gleizes PE. 2015. An overview of pre-ribosomal RNA processing in eukaryotes. *Wiley interdisciplinary reviews RNA* **6**: 225-242.
Hirano T. 2000. Chromosome cohesion, condensation, and separation. *Annual review of biochemistry* **69**: 115-144.
Hirano T. 2002. The ABCs of SMC proteins: two-armed ATPases for chromosome condensation, cohesion, and repair. *Genes Dev* **16**: 399-414.
Hoebeeck J, Speleman F, Vandesompele J. 2007. Real-time quantitative PCR as an alternative to Southern blot or fluorescence in situ hybridization for detection of gene copy number changes. *Methods Mol Biol* **353**: 205-226.
Hong S, Sung Y, Yu M, Lee M, Kleckner N, Kim KP. 2013. The logic and mechanism of homologous recombination partner choice. *Molecular cell* **51**: 440-453.
Hontz RD, Niederer RO, Johnson JM, Smith JS. 2009. Genetic identification of factors that modulate ribosomal DNA transcription in Saccharomyces cerevisiae. *Genetics* **182**: 105-119.
Horne SD, Pollick SA, Heng HH. 2015. Evolutionary mechanism unifies the hallmarks of cancer. *Int J Cancer* **136**: 2012-2021.
Huang J, Brito IL, Villen J, Gygi SP, Amon A, Moazed D. 2006. Inhibition of homologous recombination by a cohesin-associated clamp complex recruited to the rDNA recombination enhancer. *Genes Dev* **20**: 2887-2901.
Huang J, Moazed D. 2003. Association of the RENT complex with nontranscribed and coding regions of rDNA and a regional requirement for the replication fork block protein Fob1 in rDNA silencing. *Genes Dev* **17**: 2162-2176.
Hughes TR, Roberts CJ, Dai H, Jones AR, Meyer MR, Slade D, Burchard J, Dow S, Ward TR, Kidd MJ et al. 2000. Widespread aneuploidy revealed by DNA microarray expression profiling. *Nat Genet* **25**: 333-337.
Iadonato SP, Gnirke A. 1996. RARE-cleavage analysis of YACs. *Methods Mol Biol* **54**: 75-85.
Ide S, Miyazaki T, Maki H, Kobayashi T. 2010. Abundance of ribosomal RNA gene copies maintains genome integrity. *Science* **327**: 693-696.
Johnston M, Davis RW. 1984. Sequences that regulate the divergent GAL1-GAL10 promoter in Saccharomyces cerevisiae. *Molecular and cellular biology* **4**: 1440-1448.
Johzuka K, Horiuchi T. 2002. Replication fork block protein, Fob1, acts as an rDNA region specific recombinator in S. cerevisiae. *Genes Cells* **7**: 99-113.
Johzuka K, Horiuchi T. 2009. The cis element and factors required for condensin recruitment to chromosomes. *Molecular cell* **34**: 26-35.

Johzuka K, Terasawa M, Ogawa H, Ogawa T, Horiuchi T. 2006. Condensin loaded onto the replication fork barrier site in the rRNA gene repeats during S phase in a FOB1-dependent fashion to prevent contraction of a long repetitive array in Saccharomyces cerevisiae. *Molecular and cellular biology* **26**: 2226-2236.

Joyce EF, Williams BR, Xie T, Wu CT. 2012. Identification of genes that promote or antagonize somatic homolog pairing using a high-throughput FISH-based screen. *PLoS genetics* **8**: e1002667.

Klein F, Mahr P, Galova M, Buonomo SB, Michaelis C, Nairz K, Nasmyth K. 1999. A central role for cohesins in sister chromatid cohesion, formation of axial elements, and recombination during yeast meiosis. *Cell* **98**: 91-103.

Klein HL. 2001. Spontaneous chromosome loss in Saccharomyces cerevisiae is suppressed by DNA damage checkpoint functions. *Genetics* **159**: 1501-1509.

Kobayashi T. 2011a. How does genome instability affect lifespan?: roles of rDNA and telomeres. *Genes Cells* **16**: 617-624.

Kobayashi T. 2011b. Regulation of ribosomal RNA gene copy number and its role in modulating genome integrity and evolutionary adaptability in yeast. *Cellular and molecular life sciences : CMLS* **68**: 1395-1403.

Kobayashi T, Ganley AR. 2005. Recombination regulation by transcription-induced cohesin dissociation in rDNA repeats. *Science* **309**: 1581-1584.

Kobayashi T, Heck DJ, Nomura M, Horiuchi T. 1998. Expansion and contraction of ribosomal DNA repeats in Saccharomyces cerevisiae: requirement of replication fork blocking (Fob1) protein and the role of RNA polymerase I. *Genes Dev* **12**: 3821-3830.

Kobayashi T, Hidaka M, Nishizawa M, Horiuchi T. 1992. Identification of a site required for DNA replication fork blocking activity in the rRNA gene cluster in Saccharomyces cerevisiae. *Molecular and General Genetics MGG* **233**: 355-362.

Kobayashi T, Horiuchi T. 1996. A yeast gene product, Fob1 protein, required for both replication fork blocking and recombinational hotspot activities. *Genes Cells* **1**: 465-474.

Kobayashi T, Horiuchi T, Tongaonkar P, Vu L, Nomura M. 2004. SIR2 regulates recombination between different rDNA repeats, but not recombination within individual rRNA genes in yeast. *Cell* **117**: 441-453.

Kobayashi T, Nomura M, Horiuchi T. 2001. Identification of DNA cis elements essential for expansion of ribosomal DNA repeats in Saccharomyces cerevisiae. *Molecular and cellular biology* **21**: 136-147.

Kogut I, Wang J, Guacci V, Mistry RK, Megee PC. 2009. The Scc2/Scc4 cohesin loader determines the distribution of cohesin on budding yeast chromosomes. *Genes Dev* **23**: 2345-2357.

Kumaran R, Yang SY, Leu JY. 2013. Characterization of chromosome stability in diploid, polyploid and hybrid yeast cells. *PLoS One* **8**: e68094.

Kupriyanova NS, Netchvolodov KK, Sadova AA, Cherepanova MD, Ryskov AP. 2015. Non-canonical ribosomal DNA segments in the human genome, and nucleoli functioning. *Gene* **572**: 237-242.

Lafontaine DLJ, Tollervey D. 2001. Ribosomal RNA. In *eLS*, doi:10.1038/npg.els.0003832. John Wiley & Sons, Ltd.

Lai LC, Kosorukoff AL, Burke PV, Kwast KE. 2005. Dynamical remodeling of the transcriptome during short-term anaerobiosis in Saccharomyces cerevisiae: differential response and role of Msn2 and/or Msn4 and other factors in galactose and glucose media. *Molecular and cellular biology* **25**: 4075-4091.

Laporte D, Courtout F, Salin B, Ceschin J, Sagot I. 2013. An array of nuclear microtubules reorganizes the budding yeast nucleus during quiescence. *The Journal of cell biology* **203**: 585-594.

Li C, Mueller JE, Bryk M. 2006. Sir2 represses endogenous polymerase II transcription units in the ribosomal DNA nontranscribed spacer. *Mol Biol Cell* **17**: 3848-3859.

Long EO, Dawid IB. 1980. Repeated genes in eukaryotes. *Annual review of biochemistry* **49**: 727-764.

Lucchini R, Sogo JM. 1995. Replication of transcriptionally active chromatin. *Nature* **374**: 276-280.

Machin F, Torres-Rosell J, De Piccoli G, Carballo JA, Cha RS, Jarmuz A, Aragon L. 2006. Transcription of ribosomal genes can cause nondisjunction. *The Journal of cell biology* **173**: 893-903.

Mais C, Wright JE, Prieto JL, Raggett SL, McStay B. 2005. UBF-binding site arrays form pseudo-NORs and sequester the RNA polymerase I transcription machinery. *Genes Dev* **19**: 50-64.

Marston AL. 2014. Chromosome segregation in budding yeast: sister chromatid cohesion and related mechanisms. *Genetics* **196**: 31-63.

Mateos-Langerak J, Bohn M, de Leeuw W, Giromus O, Manders EM, Verschure PJ, Indemans MH, Gierman HJ, Heermann DW, van Driel R et al. 2009. Spatially confined folding of chromatin in the interphase nucleus. *Proc Natl Acad Sci U S A* **106**: 3812-3817.

May KM, Hardwick KG. 2006. The spindle checkpoint. *Journal of cell science* **119**: 4139-4142.

McClintock B. 1934. The relation of a particular chromosomal element to the development of the nucleoli in Zea mays. *Zeitschrift für Zellforschung und Mikroskopische Anatomie* **21**: 294-326.

Menzel J, Malo ME, Chan C, Prusinkiewicz M, Arnason TG, Harkness TA. 2014. The anaphase promoting complex regulates yeast lifespan and rDNA stability by targeting Fob1 for degradation. *Genetics* **196**: 693-709.

Mewborn SK, Puckelwartz MJ, Abuisneineh F, Fahrenbach JP, Zhang Y, MacLeod H, Dellefave L, Pytel P, Selig S, Labno CM et al. 2010. Altered chromosomal positioning, compaction, and gene expression with a lamin A/C gene mutation. *PLoS One* **5**: e14342.

Michaelis C, Ciosk R, Nasmyth K. 1997. Cohesins: chromosomal proteins that prevent premature separation of sister chromatids. *Cell* **91**: 35-45.

Miller CA, Kowalski D. 1993. cis-acting components in the replication origin from ribosomal DNA of Saccharomyces cerevisiae. *Molecular and cellular biology* **13**: 5360-5369.

Miller OL, Jr., Beatty BR. 1969. Visualization of nucleolar genes. *Science* **164**: 955-957.

Misteli T. 2008. Cell biology: Nuclear order out of chaos. *Nature* **456**: 333-334.

Miyazaki T, Kobayashi T. 2011. Visualization of the dynamic behavior of ribosomal RNA gene repeats in living yeast cells. *Genes Cells* **16**: 491-502.

Mosgoeller W, Schofer C, Wesierska-Gadek J, Steiner M, Muller M, Wachtler F. 1998. Ribosomal gene transcription is organized in foci within nucleolar components. *Histochem Cell Biol* **109**: 111-118.

Mulla W, Zhu J, Li R. 2014. Yeast: a simple model system to study complex phenomena of aneuploidy. *FEMS microbiology reviews* **38**: 201-212.

Murray AW, Schultes NP, Szostak JW. 1986. Chromosome length controls mitotic chromosome segregation in yeast. *Cell* **45**: 529-536.

Murray AW, Szostak JW. 1985. Chromosome segregation in mitosis and meiosis. *Annual review of cell biology* **1**: 289-315.

Nagaoka SI, Hassold TJ, Hunt PA. 2012. Human aneuploidy: mechanisms and new insights into an age-old problem. *Nat Rev Genet* **13**: 493-504.

Nasmyth K. 2011. Cohesin: a catenase with separate entry and exit gates? *Nat Cell Biol* **13**:1170-7.

Neems DS, Garza-Gongora AG, Smith ED, Kosak ST. 2016. Topologically associated domains enriched for lineage-specific genes reveal expression-dependent nuclear topologies during myogenesis. *Proc Natl Acad Sci U S A* **113**: E1691-1700.

Ng TM, Waples WG, Lavoie BD, Biggins S. 2009. Pericentromeric sister chromatid cohesion promotes kinetochore biorientation. *Mol Biol Cell* **20**: 3818-3827.

Nogi Y, Vu L, Nomura M. 1991a. An approach for isolation of mutants defective in 35S ribosomal RNA synthesis in Saccharomyces cerevisiae. *Proc Natl Acad Sci U S A* **88**: 7026-7030.

Nogi Y, Yano R, Nomura M. 1991b. Synthesis of large rRNAs by RNA polymerase II in mutants of Saccharomyces cerevisiae defective in RNA polymerase I. *Proc Natl Acad Sci U S A* **88**: 3962-3966.

Nomura M. 2001. Ribosomal RNA genes, RNA polymerases, nucleolar structures, and synthesis of rRNA in the yeast Saccharomyces cerevisiae. *Cold Spring Harbor symposia on quantitative biology* **66**: 555-565.

O'Sullivan JM. 2010. Yeast chromosomal interactions and nuclear architecture. *Current opinion in cell biology* **22**: 298-304.

Oakes M, Aris JP, Brockenbrough JS, Wai H, Vu L, Nomura M. 1998. Mutational analysis of the structure and localization of the nucleolus in the yeast Saccharomyces cerevisiae. *The Journal of cell biology* **143**: 23-34.

Oakes M, Nogi Y, Clark MW, Nomura M. 1993. Structural alterations of the nucleolus in mutants of Saccharomyces cerevisiae defective in RNA polymerase I. *Molecular and cellular biology* **13**: 2441-2455.

Oakes ML, Johzuka K, Vu L, Eliason K, Nomura M. 2006. Expression of rRNA genes and nucleolus formation at ectopic chromosomal sites in the yeast Saccharomyces cerevisiae. *Molecular and cellular biology* **26**: 6223-6238.

Oliver TR, Feingold E, Yu K, Cheung V, Tinker S, Yadav-Shah M, Masse N, Sherman SL. 2008. New insights into human nondisjunction of chromosome 21 in oocytes. *PLoS genetics* **4**: e1000033.

Olson MO. 2004. Sensing cellular stress: another new function for the nucleolus? *Science's STKE : signal transduction knowledge environment* **2004**: pe10.

Olson MO, Hingorani K, Szebeni A. 2002. Conventional and nonconventional roles of the nucleolus. *International review of cytology* **219**: 199-266.

Olson MOJ, Dundr M. 2010. Nucleolus: Structure and Function. In *eLS*, doi:10.1002/9780470015902.a0005975.pub3. John Wiley & Sons, Ltd.

Oromendia AB, Amon A. 2014. Aneuploidy: implications for protein homeostasis and disease. *Disease Models & Mechanisms* **7**: 15-20.

Pacchierotti F, Ranaldi R, Eichenlaub-Ritter U, Attia S, Adler ID. 2008. Evaluation of aneugenic effects of bisphenol A in somatic and germ cells of the mouse. *Mutation research* **651**: 64-70.

Pasero P, Bensimon A, Schwob E. 2002. Single-molecule analysis reveals clustering and epigenetic regulation of replication origins at the yeast rDNA locus. *Genes Dev* **16**: 2479-2484.

Pavelka N, Rancati G, Zhu J, Bradford WD, Saraf A, Florens L, Sanderson BW, Hattem GL, Li R. 2010. Aneuploidy confers quantitative proteome changes and phenotypic variation in budding yeast. *Nature* **468**: 321-325.

Petes TD, Hereford LM, Skryabin KG. 1978. Characterization of two types of yeast ribosomal DNA genes. *Journal of bacteriology* **134**: 295-305.

Pfau SJ, Amon A. 2012. Chromosomal instability and aneuploidy in cancer: from yeast to man. *EMBO Reports* **13**: 515-527.

Prokopowich CD, Gregory TR, Crease TJ. 2003. The correlation between rDNA copy number and genome size in eukaryotes. *Genome / National Research Council Canada = Genome / Conseil national de recherches Canada* **46**: 48-50.

Pueschel R, Coraggio F, Meister P. 2016. From single genes to entire genomes: the search for a function of nuclear organization. *Development (Cambridge, England)* **143**: 910-923.

Queralt E, Uhlmann F. 2005. More than a separase. *Nature cell biology* **7**: 930-932.

Rancati G, Pavelka N, Fleharty B, Noll A, Trimble R, Walton K, Perera A, Staehling-Hampton K, Seidel CW, Li R. 2008. Aneuploidy underlies rapid adaptive evolution of yeast cells deprived of a conserved cytokinesis motor. *Cell* **135**: 879-893.

Raska I. 2004. Searching for active ribosomal genes. *Progress in molecular and subcellular biology* **35**: 23-56.

Raska I, Koberna K, Malinsky J, Fidlerova H, Masata M. 2004. The nucleolus and transcription of ribosomal genes. *Biology of the cell / under the auspices of the European Cell Biology Organization* **96**: 579-594.

Reeder RH. 1999. Regulation of RNA polymerase I transcription in yeast and vertebrates. *Progress in nucleic acid research and molecular biology* **62**: 293-327.

Riggs DL, Nomura M. 1990. Specific transcription of Saccharomyces cerevisiae 35 S rDNA by RNA polymerase I in vitro. *J Biol Chem* **265**: 7596-7603.

Rothstein R, Michel B, Gangloff S. 2000. Replication fork pausing and recombination or "gimme a break". *Genes Dev* **14**: 1-10.

Runge KW, Wellinger RJ, Zakian VA. 1991. Effects of excess centromeres and excess telomeres on chromosome loss rates. *Molecular and cellular biology* **11**: 2919-2928.

Rusche LN, Kirchmaier AL, Rine J. 2003. The establishment, inheritance, and function of silenced chromatin in Saccharomyces cerevisiae. *Annual review of biochemistry* **72**: 481-516.

Russell J, Zomerdijk JC. 2005. RNA-polymerase-I-directed rDNA transcription, life and works. *Trends in biochemical sciences* **30**: 87-96.

Rutledge SD, Cimini D. 2016. Consequences of aneuploidy in sickness and in health. *Current opinion in cell biology* **40**: 41-46.

Saka K, Takahashi A, Sasaki M, Kobayashi T. 2016. More than 10% of yeast genes are related to genome stability and influence cellular senescence via rDNA maintenance. *Nucleic acids research* doi:10.1093/nar/gkw110.

Sanij E, Poortinga G, Sharkey K, Hung S, Holloway TP, Quin J, Robb E, Wong LH, Thomas WG, Stefanovsky V et al. 2008. UBF levels determine the number of active ribosomal RNA genes in mammals. *The Journal of cell biology* **183**: 1259-1274.

Schmitt ME, Brown TA, Trumpower BL. 1990. A rapid and simple method for preparation of RNA from Saccharomyces cerevisiae. *Nucleic acids research* **18**: 3091-3092.

Schneider R, Grosschedl R. 2007. Dynamics and interplay of nuclear architecture, genome organization, and gene expression. *Genes Dev* **21**: 3027-3043.

Segal M, Bloom K. 2001. Control of spindle polarity and orientation in Saccharomyces cerevisiae. *Trends Cell Biol* **11**: 160-166.

Selbach M, Schwanhausser B, Thierfelder N, Fang Z, Khanin R, Rajewsky N. 2008. Widespread changes in protein synthesis induced by microRNAs. *Nature* **455**:58-63.

Selmecki AM, Maruvka YE, Richmond PA, Guillet M, Shoresh N, Sorenson AL, De S, Kishony R, Michor F, Dowell R et al. 2015. Polyploidy can drive rapid adaptation in yeast. *Nature* **519**: 349-352.

Shah P, Ding Y, Niemczyk M, Kudla G, Plotkin JB. 2013. Rate-limiting steps in yeast protein translation. *Cell* **153**: 1589-1601.

Sharakhov IV, Sharakhova MV. 2015. Heterochromatin, histone modifications, and nuclear architecture in disease vectors. *Current opinion in insect science* **10**: 110-117.

Shou W, Seol JH, Shevchenko A, Baskerville C, Moazed D, Chen ZW, Jang J, Shevchenko A, Charbonneau H, Deshaies RJ. 1999. Exit from mitosis is triggered by Tem1-dependent release of the protein phosphatase Cdc14 from nucleolar RENT complex. *Cell* **97**: 233-244.

Siegel JJ, Amon A. 2012. New insights into the troubles of aneuploidy. *Annual review of cell and developmental biology* **28**: 189-214.

Sirri V, Urcuqui-Inchima S, Roussel P, Hernandez-Verdun D. 2008. Nucleolus: the fascinating nuclear body. *Histochem Cell Biol* **129**: 13-31.

Skryabin KG, Eldarov MA, Larionov VL, Bayev AA, Klootwijk J, de Regt VC, Veldman GM, Planta RJ, Georgiev OI, Hadjiolov AA. 1984. Structure and function of the nontranscribed spacer regions of yeast rDNA. *Nucleic acids research* **12**: 2955-2968.

Smitt WW, Vlak JM, Molenaar I, Rozijn TH. 1973. Nucleolar function of the dense crescent in the yeast nucleus. A biochemical and ultrastructural study. *Experimental cell research* **80**: 313-321.

Sogo JM, Ness PJ, Widmer RM, Parish RW, Koller T. 1984. Psoralen-crosslinking of DNA as a probe for the structure of active nucleolar chromatin. *Journal of molecular biology* **178**: 897-919.

Solovei I, Kreysing M, Lanctot C, Kosem S, Peichl L, Cremer T, Guck J, Joffe B. 2009. Nuclear architecture of rod photoreceptor cells adapts to vision in mammalian evolution. *Cell* **137**: 356-368.

Storchova Z. 2012. *The Causes and Consequences of Aneuploidy in Eukaryotic Cells, Aneuploidy in Health and Disease*.

Straight AF, Shou W, Dowd GJ, Turck CW, Deshaies RJ, Johnson AD, Moazed D. 1999. Net1, a Sir2-associated nucleolar protein required for rDNA silencing and nucleolar integrity. *Cell* **97**: 245-256.

Strunnikov AV. 2003. Condensin and biological role of chromosome condensation. *Progress in cell cycle research* **5**: 361-367.

Strunnikov AV, Hogan E, Koshland D. 1995. SMC2, a Saccharomyces cerevisiae gene essential for chromosome segregation and condensation, defines a subgroup within the SMC family. *Genes Dev* **9**: 587-599.

Strunnikov AV, Larionov VL, Koshland D. 1993. SMC1: an essential yeast gene encoding a putative head-rod-tail protein is required for nuclear division and defines a new ubiquitous protein family. *The Journal of cell biology* **123**: 1635-1648.

Sugiyama M, Ikushima S, Nakazawa T, Kaneko Y, Harashima S. 2005. PCR-mediated repeated chromosome splitting in Saccharomyces cerevisiae. *BioTechniques* **38**: 909-914.

Sullivan M, Higuchi T, Katis VL, Uhlmann F. 2004. Cdc14 phosphatase induces rDNA condensation and resolves cohesin-independent cohesion during budding yeast anaphase. *Cell* **117**: 471-482.

Sullivan M, Uhlmann F. 2003. A non-proteolytic function of separase links the onset of anaphase to mitotic exit. *Nature cell biology* **5**: 249-254.

Surosky RT, Tye BK. 1985. Resolution of dicentric chromosomes by Ty-mediated recombination in yeast. *Genetics* **110**: 397-419.

Szostak JW, Wu R. 1979. Insertion of a genetic marker into the ribosomal DNA of yeast. *Plasmid* **2**: 536-554.

Takeuchi Y, Horiuchi T, Kobayashi T. 2003. Transcription-dependent recombination and the role of fork collision in yeast rDNA. *Genes Dev* **17**: 1497-1506.

Tanaka T, Cosma MP, Wirth K, Nasmyth K. 1999. Identification of cohesin association sites at centromeres and along chromosome arms. *Cell* **98**: 847-858.

Tanaka T, Fuchs J, Loidl J, Nasmyth K. 2000. Cohesin ensures bipolar attachment of microtubules to sister centromeres and resists their precocious separation. *Nature cell biology* **2**: 492-499.

Taylor MM, Storck R. 1964. UNIQUENESS OF BACTERIAL RIBOSOMES. *Proc Natl Acad Sci U S A* **52**: 958-965.

Thacker D, Lam I, Knop M, Keeney S. 2011. Exploiting spore-autonomous fluorescent protein expression to quantify meiotic chromosome behaviors in Saccharomyces cerevisiae. *Genetics* **189**: 423-439.

Thiry M, Lafontaine DL. 2005. Birth of a nucleolus: the evolution of nucleolar compartments. *Trends Cell Biol* **15**: 194-199.

Timson D. 2001. Galactose metabolism in Saccharomyces cerevisiae. *Dynamic Biochemistry, Process Biotechnology and Molecular Biology* **1**: 63-73.

Tomson BN, D'Amours D, Adamson BS, Aragon L, Amon A. 2006. Ribosomal DNA transcription-dependent processes interfere with chromosome segregation. *Molecular and cellular biology* **26**: 6239-6247.

Torres E. 2015. Yeast as Models of Mitotic Fidelity. *Recent results in cancer research Fortschritte der Krebsforschung Progres dans les recherches sur le cancer* **200**: 143-164.

Tsang E, Carr AM. 2008. Replication fork arrest, recombination and the maintenance of ribosomal DNA stability. *DNA repair* **7**: 1613-1623.

Uhlmann F. 2003. Separase regulation during mitosis. *Biochemical Society symposium*: 243-251.

Uhlmann F, Lottspeich F, Nasmyth K. 1999. Sister-chromatid separation at anaphase onset is promoted by cleavage of the cohesin subunit Scc1. *Nature* **400**: 37-42.

Uhlmann F, Wernic D, Poupart MA, Koonin EV, Nasmyth K. 2000. Cleavage of cohesin by the CD clan protease separin triggers anaphase in yeast. *Cell* **103**: 375-386.

Usdin K. 2008. The biological effects of simple tandem repeats: lessons from the repeat expansion diseases. *Genome Res* **18**: 1011-1019.

van Koningsbruggen S, Gierlinski M, Schofield P, Martin D, Barton GJ, Ariyurek Y, den Dunnen JT, Lamond AI. 2010. High-resolution whole-genome sequencing reveals that specific chromatin domains from most human chromosomes associate with nucleoli. *Mol Biol Cell* **21**:3735-3748.

Verschoor A, Warner JR, Srivastava S, Grassucci RA, Frank J. 1998. Three-dimensional structure of the yeast ribosome. *Nucleic acids research* **26**: 655-661.

Voth WP, Jiang YW, Stillman DJ. 2003. New 'marker swap' plasmids for converting selectable markers on budding yeast gene disruptions and plasmids. *Yeast (Chichester, England)* **20**: 985-993.

Wach A, Brachat A, Pohlmann R, Philippsen P. 1994. New heterologous modules for classical or PCR-based gene disruptions in Saccharomyces cerevisiae. *Yeast (Chichester, England)* **10**: 1793-1808.

Wai HH, Vu L, Oakes M, Nomura M. 2000. Complete deletion of yeast chromosomal rDNA repeats and integration of a new rDNA repeat: use of rDNA deletion strains for functional analysis of rDNA promoter elements in vivo. *Nucleic acids research* **28**: 3524-3534.

Walczak CE, Heald R. 2008. Mechanisms of mitotic spindle assembly and function. *International review of cytology* **265**: 111-158.

Warner JR. 1999. The economics of ribosome biosynthesis in yeast. *Trends in biochemical sciences* **24**: 437-440.

Weipoltshammer K, Schofer C. 2016. Morphology of nuclear transcription. *Histochem Cell Biol* **145**: 343-358.

Weng YS, Nickoloff JA. 1997. Nonselective URA3 colony-color assay in yeast ade1 or ade2 mutants. *BioTechniques* **23**: 237-241.

West RW, Jr., Chen SM, Putz H, Butler G, Banerjee M. 1987. GAL1-GAL10 divergent promoter region of Saccharomyces cerevisiae contains negative control elements in addition to functionally separate and possibly overlapping upstream activating sequences. *Genes Dev* **1**: 1118-1131.

Westermann S, Drubin DG, Barnes G. 2007. Structures and functions of yeast kinetochore complexes. *Annual review of biochemistry* **76**: 563-591.

Wierman MB, Smith JS. 2014. Yeast sirtuins and the regulation of aging. *FEMS yeast research* **14**: 73-88.

Williams BR, Prabhu VR, Hunter KE, Glazier CM, Whittaker CA, Housman DE, Amon A. 2008. Aneuploidy affects proliferation and spontaneous immortalization in mammalian cells. *Science* **322**: 703-709.

Winey M, Bloom K. 2012. Mitotic spindle form and function. *Genetics* **190**: 1197-1224.

Winey M, Mamay CL, O'Toole ET, Mastronarde DN, Giddings TH, Jr., McDonald KL, McIntosh JR. 1995. Three-dimensional ultrastructural analysis of the Saccharomyces cerevisiae mitotic spindle. *The Journal of cell biology* **129**: 1601-1615.

Wu CS, Chen YF, Gartenberg MR. 2011. Targeted sister chromatid cohesion by Sir2. *PLoS genetics* **7**: e1002000.

Wysocka M, Rytka J, Kurlandzka A. 2004. Saccharomyces cerevisiae CSM1 gene encoding a protein influencing chromosome segregation in meiosis I interacts with elements of the DNA replication complex. *Experimental cell research* **294**: 592-602.

Yanagida M. 2009. The Basics of Chromosome Segregation. In *The Kinetochore:: From Molecular Discoveries to Cancer Therapy*, (ed. P De Wulf, CW Earnshaw), pp. 1-24. Springer New York, New York, NY.

Yanisch-Perron C, Vieira J, Messing J. 1985. Improved M13 phage cloning vectors and host strains: nucleotide sequences of the M13mp18 and pUC19 vectors. *Gene* **33**: 103-119.

Yano R, Nomura M. 1991. Suppressor analysis of temperature-sensitive mutations of the largest subunit of RNA polymerase I in Saccharomyces cerevisiae: a suppressor gene encodes the second-largest subunit of RNA polymerase I. *Molecular and cellular biology* **11**: 754-764.

Yong-Gonzalez V, Wang BD, Butylin P, Ouspenski I, Strunnikov A. 2007. Condensin function at centromere chromatin facilitates proper kinetochore tension and ensures correct mitotic segregation of sister chromatids. *Genes Cells* **12**: 1075-1090.

Zang Y, Garre M, Gjuracic K, Bruschi CV. 2002. Chromosome V loss due to centromere knockout or MAD2-deletion is immediately followed by restitution of homozygous diploidy in Saccharomyces cerevisiae. *Yeast (Chichester, England)* **19**: 553-564.

Zaragoza MV, Jacobs PA, James RS, Rogan P, Sherman S, Hassold T. 1994. Nondisjunction of human acrocentric chromosomes: studies of 432 trisomic fetuses and liveborns. *Human genetics* **94**: 411-417.

Ziv N, Siegal ML, Gresham D. 2013. Genetic and nongenetic determinants of cell growth variation assessed by high-throughput microscopy. *Molecular biology and evolution* **30**: 2568-2578.